20th Jubilee Meeting of the Central European Tectonic Studies Groups

CETEG 2024

24-27.04.2024, Srebrna Góra, Poland

Abstract Volume & Field Trips Guide

Edited by R. Sikora, M. Olkowicz & M. Adamuszek

Structural Geology & Geohazards Research Group

Uniwersytet Wrocławski

ING PAN

THE MEETING IS ORGANISED BY

Polish Geological Society (Section Structural Geology and Geohazards)

with cooperation of

Polish Geological Institute - National Research Institute
Institute Geological Science of University of Wrocław
Institute Geological Science of Polish Academy of Sciences

Organizing Committee:

Rafał Sikora (Chair, PGI-NRI)
Marta Adamuszek (Secretary, PGI-NRI)
Marta Tomaszczyk (PGI-NRI)
Kamil Bulcewicz (UWr, PGI-NRI)
Bartłomiej Grochmal (PGI-NRI)
Aleksander Kowalski (PGI-NRI)
Małgorzata Nowak (UWr, PGI-NRI)
Marcin Olkowicz (PGI-NRI)

Scientific Committee:

Jacek Szczepański (Chair, UWr)
Marta Adamuszek (PGI-NRI)
Paweł Aleksandrowski (PGI-NRI)
Marcin Dąbrowski (PGI-NRI)
Mirosław Jastrzębski (ING PAN)
Rafał Sikora (PGI-NRI)

Promotional support:

Ząbkowickie Centrum Kultury i Turystyki

Polish Geological Society
ISBN: 978-83-68112-55-9 (online PDF version)

Preface

The idea of CETEG (Central European Tectonic Studies Groups) follows up a tradition of annual meetings started by Karel Schulmann and his then students already in nearly pre-historic times (mid-1980s) and, subsequently, continued under the banner of the *Česká tektonická skupina* (Czech tectonic group). Its successive (and highly successful), 8th, reunion, held in Hrubá Skála, Czech Republic, in 2003 became the first, constitutive meeting of the Central European Tectonic Studies Groups. The idea of CETEG has been to present and share new research results and hold scientific discussions among colleagues at different career stages, representing different branches of geosciences, yet concerning topics somehow related to tectonics and structural geology. In principle, CETEG brings together geologists from Czechia, Slovakia, Hungary and Poland, but participants from other Central European countries and, also, from more distant regions of the world are always welcome. CETEG meetings are held in a different member country each year. Or, more precisely, it was so until 2020, when a yearly break happened due to the COVID-19 pandemic. The post- (or, rather, late-) COVID CETEG meeting had taken place successfully in 2021 in Terchová, Slovakia, but was followed by another yearly break, and, eventually, by the last year's extremely interesting conference in Kazincbarcika, Hungary, which, it is hoped, has re-established a regular annual cycle of the meetings.

Thus for the past 21 years, the mission of the CETEG meetings has been to enhance and strengthen interpersonal communication and scientific collaboration, as well as to facilitate formal activities of studies groups and individuals from Central Europe interested in the broadly defined tectonics and geodynamics of the lithosphere. Special attention has always been paid to the promotion of young scientists through rewarding their best oral and poster presentations and the best publications that appeared in the previous year.

The 20th Jubilee CETEG meeting is held in the Sudety Mountains (or simply in the Sudetes), in the village (former town) of Srebrna Góra (German: *Silberberg*) near the small town of Ząbkowice Śląskie (German: *Frankenstein*), ca 65 km S of Wrocław. Srebrna Góra has centuries-long ore-mining traditions, and following the Prussian-Austrian wars of 1740-1763, it developed while at service of the newly built fortress.

Our meeting is located in one of the geologically most interesting places in the Sudetes, on the Sudetic Boundary Fault and at the junction between the Góry Sowie Massif and the remains of the syn-tectonic intramontane Bardo Basin. A special focus of the field sessions is on the Variscan orogenic belt, including its orogenic and post-orogenic evolution. On the other hand, both oral and poster sessions present various topics covering the already well-established problems of the CETEG annual meetings, such as tectono-metamorphic evolution of orogenic belts, relationships between magmatism and tectonics, or basin formation and evolution, but they include also other topics investigated with methods of structural geology, petrology, geochemistry, sedimentology and geophysics.

The organizing and scientific teams that have prepared this jubilee CETEG meeting are wishing all of you a successful conference, interesting field trips and stimulating and fruitful discussions.

Organizing and Scientific Teams

Conference Programme

WEDNESDAY, April 24th

8:30 – 9:00 Registration – hotel hall

9:00 – 17:00 PRE-CONFERENCE FIELD TRIP *(Page 108)*

From Neoproterozic sedimentation on the peri-Gondwanan extended shelf to the Variscan collision of terranes - the history preserved in the Kamieniec Metamorphic Belt and the Doboszowice Metamorphic Complex
guided by Jacek Szczepański, Mirosław Jastrzębski, Sławomir Ilnicki and Robert Anczkiewicz

*Starting at **9.00 a.m.** from the Hotel Srebrna Góra* (https://maps.app.goo.gl/oWh6a31MsoHCENFW7)

18:30 – 23:00 ON THE FAULT – ICE-BREAKER PARTY

at the Karczma Micha i Chmiel in Srebrna Góra (https://maps.app.goo.gl/uGhqEZ1KR4e38X6Z7)

THURSDAY, April 25th

8:30 – 9:00 Registration – hotel hall

9:00 – 9:15 OPENING CEREMONY

9:15 – 10:15 SESSION I		**page**
9:15 – 9:45	**Keynote lecture:** Processes and mechanisms of Pangea amalgamation along Trans-Euroasian orogen (***Karel Schulmann***)	
9:45 – 10:00	Detrital zircon geochronology and the development of tectonic models for the Bohemian Massif (***Stephen Collett***)	**14**
10:00 – 10.15	Early Mississippian transpressional deformation and thermal doming at the distal foreland of the Variscan orogen (SW East European Craton, Lublin-Lviv Basin) (***Paweł Poprawa, Maciej Tomaszczyk***)	**15**

10:15 – 10:30 COFFEE BREAK

10:30 – 12:00 SESSION II		**page**
10:30 – 11:00	**Keynote lecture:** From Carboniferous convergence to Permian continental rifting – the interaction of Baltica with the Variscan belt during the assembly of Pangea (***Stanisław Mazur***)	**17**
11:00 – 11:15	Contrasting Permian plutonism in the Trans-Altai Gobi, SW Mongolia (***Pavel Hanžl, Vojtěch Janoušek, Battushig Altanbaatar, Karel Schulmann, Kristýna Hrdličková, David Buriánek***)	**18**
11:15 – 11:30	Brittle tectonics in pegmatite formation: a case study from the Bratislava granite massif, Western Carpathians (***Igor Broska, Sergii Kurylo, Ján Madarás, Pavel Uher***)	**19**
11:30 – 11:45	Tectonic evolution of the Strzegom - Sobótka Massif (***Mariusz Fiałkiewicz, Bartłomiej Grochmal, Marcin Olkowicz, Marcin Dąbrowski***)	**20**
11:45 – 12:00	"Hot vs Cold": on differences of AMS record in shear zones (***Matěj Machek, Vladimír Kusbach, Zuzana Roxerová***)	**21**

12:00 – 13:30 LUNCH

13:30 – 14.45 SESSION III		page
13:30 – 14:00	**Keynote lecture:** The effects of grain-scale melt migration process on metagranite at eclogite facies, Snieznik dome, Bohemian Massif (***Pavla Štípská, Andrew R. C. Kylander-Clark, Martin Racek, Prokop Závada, Pavlína Hasalová***)	**23**
14:00 – 14:15	Metamorphic evolution of coesite-bearing Śnieżnik eclogites (***Małgorzata Nowak, Lucie Tajčmanová, Jacek Szczepański, Marcin Dąbrowski***)	**24**
14:15 – 14:30	Timing of Variscan HP event in the Tatric Unit crystalline basement of the Western Carpathians (***Milan Kohút, Robert Anczkiewicz***)	**25**
14:30 – 14:45	New petrological and geochronological data from the Austroalpine Koralpe-Saualpe-Pohorje Complex (***Iris Wannhoff, Jan Pleuger, Xin Zhong, Timm John, Leo j. Millonig, Axel Gerdes, Richard Albert Roper***)	**26**

14:45 – 15:00 COFFEE BREAK

15:00 – 16:30 SESSION IV		page
15:00 – 15:30	**Keynote lecture:** The Caledonian Wilson Cycle from a North Atlantic perspective (***Jarosław Majka, Deta Gasser, Johannes Jakob, Christopher J. Barnes***)	**28**
15:30 – 15:45	Early Paleozoic Andean-type evolution recorded in the Dunhuang block (NW China): insights from petro-structural, geochronological and metamorphic P−T constraints (***Jérémie Soldner, Yingde Jiang, Pavla Štípská, Karel Schulmann, Chao Yuan, Robert Anczkiewicz***)	**29**
15:45 – 16:00	Unveiling Late Ediacaran Climatic and Tectonic Dynamics: Insights from Glaciogenic and Post-Glaciogenic Deposits in the Hormuz Complex, Southern Iran (***Sadegh Adineh, Prokop Závada, Jiři Bruthans, Soraya Heuss-Aßbichler, Mohammad Zare, Anke M. Friedrich***)	**30**
16:00 – 16:15	The Geochemical Data Toolkit (GCDkit) family of tools – a progress report (***Vojtěch Janoušek, Jean-François Moyen, Matthew Mayne, Colin M. Farrow, Vojtěch Erban***)	**31**

17:00 – 19:00 POSTER SESSION I (list of poster presentations on page 7)

19:00 – 00:00 GRILL PARTY with CULTURAL EVENT

FRIDAY, April 26th

	8:30 – 10:00 SESSION V	page
8:30 – 9:00	**Keynote lecture:** Sediment Deposition on Moving Salt: Minibasins or Ramp Syncline Basins? Observations from Seismic Data and Numerical Modelling (***Naiara Fernandez***)	**33**
9:00 – 9:15	The influence of passive margin geometry on lateral changes in a salt-detached fold and thrust belt: insights from southern Albania (***Márton Palotai, Balázs Törő***)	**34**
9:15 – 9.30	Step-wise inversion of a salt-bearing passive margin – the example of the central Northern Calcareous Alps (Eastern Alps, Austria) (***Oscar Fernandez, H. Ortner, W. E. H. Munday, D. Sanders, M. Moser, B. Grasemann, T. Leitner***)	**35**
9:30 – 9.45	Grain size reduction induced switch in deformation mechanisms in a salt glacier (Kuh-e-Namak, Dashti, Iran) (***Prokop Závada, Julia Schmitz, Janos Urai, Karel Schulmann***)	**36**
9:45 – 10.00	Structural characteristic of a bedded rock salt deposit in the Łeba Elevation. Implications for underground storage facility planning (***Michał Słotwiński, Marta Adamuszek, Łukasz Nowacki***)	**37**

10:00 – 10:15 COFFEE BREAK

	10:15 – 12:00 SESSION VI	
10:15 – 10:45	**Keynote lecture:** Post-Variscan tectonics in Germany: The role of inherited structures (and can we even tell?) (***Jonas Kley***)	**39**
10:45 – 11:00	Thick- versus thin-skinned thrusting within the NW Qaidam Basin, Tibet, China – insight from high-resolution 3D seismic data (***Piotr Krzywiec, Fanwei Meng, Adam Baranowski, Wenhang Liu, Stanisław Mazur***)	**40**
11:00 – 11:15	Mesozoic structural evolution of the Bükk, Darnó and Recsk areas (NE Hungary) (***Szilvia Kövér, János Haas, Ottilia Szives, Péter Ozsvárt, Ágnes Görög, Éva Oravecz, Benjamin Scherman, László Fodor***)	**41**
11:15 – 11.30	Reconstructing the tectonic movements of Adria in the Mesozoic based on quality controlled apparent polar wander path using the GPlates software package (***Máté Velki, Emő Márton, Szilvia Kövér, László Fodor***)	**42**
11:30 – 11.45	Tectonic and sedimentary mélanges in the Pieniny Klippen Belt (***Jan Golonka, Anna Waśkowska, Kamil Cichostępski, Jerzy Dec, Monika Łój, Grzegorz Bania, Włodzimierz Jerzy Mościcki, Sławomir Porzucek, Józef Chowaniec***)	**43**
11:45 – 12.00	Late Cretaceous - early Palaeogene inversion-related tectonic structures in the Sudetes and their northern foothills – short overview and new data (***Andrzej Głuszyński, Paweł Aleksandrowski***)	**44**

12:00 – 13:30 LUNCH

	13:30 – 15:00 SESSION VII	page
13:30 – 14:00	**Keynote lecture:** Are the Carpathians recently tectonically active?: new challenges and opportunities for the study of present day tectonic stress and strain (***Marek Jarosiński***)	**46**
14:00 – 14:15	Deciphering Meso-Cenozoic exhumation history of the NE Bohemian Massif using low temperature multi-thermochronometry (***Artur Sobczyk***)	**47**
14:15 – 14.30	Uncommon stress path from the coal seam to a fold hinge zone as an effect of a neotectonic deformation pattern (***Maciej J. Mendecki, Jacek Szczygieł, Grzegorz Lizurek, Lesław Teper***)	**48**

13:30 – 15:00 SESSION VII		page
14:30 – 14.45	Hidden Faults: Post-Miocene tectonics of the Northern Calcareous Alps inferred from caves deformation (***Jacek Szczygieł, Ivo Baroň, Rostislav Melichar, Lukas Plan, Ivanka Mitrović-Woodell, Eva Kaminsky, Denis Scholz, Bernhard Grasemann***)	**49**
14:45 – 15.00	Unearthing the Past: Challenges and Perspectives in Archaeoseismological Exploration Across Southern Poland (***Krzysztof Gaidzik, Miklós Kázmér***)	**50**

15:00 – 15:15 COFFEE BREAK

15:15 – 16:45 SESSION VIII		page
15:15 – 15:45	**Keynote lecture:** Depleted highly-mobile landslides and other slope deformations associated to active tectonic ruptures in the Outer Western Carpathians, Czech Republic (***Ivo Baroň, Jia-Jyun Dong, Rostislav Melichar, Martin Šuťjak, Filip Hartvich, Jan Klimeš, Chia-Han Tseng, Yi-Chin Chen, Tùng Nguyễn, Che-Ming YANG, Václav Dušek, Lenka Kociánová, Jan Černý, František BÁRTA, Régis BRAUCHER, Piotr MOSKA, Tomasz Goslar, Li-Wei Kuo, Cheng-Han Lin***)	**52**
15:45 – 16:00	Application of magnetic susceptibility anisotropy in landslide accumulations (***Vaclav Dušek, Rostislav Melichar, Jan Černý, Martin Šuťjak, František Bárta, Ivo Baroň, Yi-Chin Chen, Jia-Jyun Dong, Filip Hartvich, Jir-Ching Hu, Jan Klimeš, Lenka Kociánová, Tung Nguyễn, Matt Rowberry, Chia-Han Tseng***)	**53**
16:00 – 16.15	Formation of under-dip toppling in the Outer Western Carpathian Flysch Belt and its possible paleo seismologic implications (***Thang Tung Nguyễn, Ivo Baroň, Jia-Jyun Dong, Rostislav Melichar, Filip Hartvich, Jan Klimeš, Jan Černý, Martin Šuťjak, Lenka Kociánová, Václav Dušek, Matt Rowberry, Régis Braucher, Tomasz Goslar, Chia-Han Tseng, Yi-Chin Chen, Cheng-Han Lin***)	**54**
16:15 – 16.30	Structural and paleoseismic conditions of rockfalls and cave collapse in the Khutul Usny valley (Arts Bogd Massif, CAOB, Mongolia) (***Rafał Sikora, Antoni Wójcik, Mirosław Masojć, Grzegorz Michalec, Byamba Gunchinsuren, Marcin Szmit, Józef Szykulski)***	**55**
16:30 – 16.45	Record of superimposed late- and post-Variscan regional-scale tectonic events at the NE margin of the Bohemian Massif: structural evolution of the Kamionki Graben (SW Poland, Sudetes) (***Aleksander Kowalski, Grzegorz Pacanowski)***	**56**

17:00 – 19:00 POSTER SESSION II (list of poster presentations on page 8)

19:30 – 00:00 GALA DINNER, AWARDS CEREMONY AND DJ-PARTY

SATURDAY, April 27th

9:00 – 15:00 POST-CONFERENCE FIELD TRIP *(page 155)*

Late- to post-Variscan structural evolution of tectonic grabens on top of the Góry Sowie Massif guided by Aleksander Kowalski

*Starting at **9.00 a.m.** from the Hotel Srebrna Góra* (https://maps.app.goo.gl/oWh6a31MsoHCENFW7)

	THURSDAY, April 25th, 17:00 – 19:00 POSTER SESSION I	page
1	Stratigraphic Evolution of the Salt Stocked-Basin: The Influence of Diapirism and Compressional Tectonics on the Sedimentary Record of the Paskhand anticline (Zagros Fold-and-Thrust Belt, Southern Iran) ***(Sadegh Adineh, Prokop Závada, Jiři Bruthans, Soraya Heuss-Aßbichler, Mohammad Zare, Anke M. Friedrich)***	59
2	Record of high-pressure low-temperature metamorphism in garnet-bearing mica schists from AMINV K- borehole in Kobierzyce (Lower Silesia, SW Poland) ***(Kamil Bulcewicz, Rafał Sikora, Jacek Szczepański, Piotr Lenik, Grzegorz Zieliński)***	60
3	High-pressure metamorphism of the Micachist Zone in the Kutná hora crystalline complex ***(Pavlína Hasalová, Radmila Nahodilová, Martin Racek, Pavla Štípská)***	61
4	Oxygen isotopic record in Late Cambrian zircons from metamorphic rocks of the Sudetes ***Mirosław Jastrzębski, Ewa Krzemińska, Andrzej Żelaźniewicz, Jiří Sláma, Marek Śliwiński***	62
5	Formation of the Tsogt crustal dome in the Mongol-Altai domain during Permian orogeny ***(Petr Jeřábek, Ondrej Lexa)***	63
6	Petrological diversity of ultra-high-pressure rocks around the Saidenbach dam (Erzgebirge) ***(Martin Keseberg)***	64
7	Pressure-, temperature- and water-dependent melt productivity in felsic rocks – new parametrization and its application in models of porous melt flow ***(Petra Maierová, Pavlína Hasalová, Pavla Štípská, Karel Schulmann, Ondřej Souček)***	65
8	Does the emplacement of the East Sudetic pluton result from combined Permian hot spot and far-field extensional dynamics? ***(Karel Schulmann, Anne-Sophie Tabaud, Alexandra Guy, Stanislaw Mazur, František Hrouda, Kryštof Verner, Jitka Míková, Petr Mixa, Vratislav Pecina)***	66
9	Pervasive melt migration in large crustal-scale shear zones in southern Madagascar ***(Alice Wantz, Pavlína Hasalová, Karel Schulmann, Jean-Emmanuel Martelat, Pavla Štípská, Prokop Závada, Alfred Solofomampiely Andriamamonjy, Heninjara Narimihamina Rarivoarison)***	67
10	Challenges in the numerical fold shape analysis process ***(Weronika Wiesławska, Marta Adamuszek)***	68
11	Magma flow patterns during emplacement of the durbachite Třebíč pluton ***(Prokop Závada, Jack Percival, Pavlína Hasalová, Ondrej Lexa, Karel Schulmann)***	69
12	Sheath fold structures from the Altaussee salt mine **(Marta Adamuszek, Marcin Olkowicz, Marcin Dabrowski, Mariusz Fiałkiewicz, Bartłomiej Grochmal, Thomas Leitner, Oscar Fernandez)**	70
13	Famous tectonic phenomena in E of Bohemia (the Czech Republic) ***(Jan Juráček)***	71
14	Anisotropy of magnetic susceptibility: how to connect with microstructure? ***(Matěj Machek, Vladimír Kusbach, Zuzana Roxerová)***	72
15	Mechanical models of the ductile deformation of layered rocks ***(Marcin Dąbrowski)***	73
16	Can salt pillows form during inversion of evaporite-filled half-graben? Insights from numerical and analogue modeling ***(Marta Adamuszek, Piotr Krzywiec, Laura Filbà, Mark G. Rowan, Oriol Ferrer)***	74

	THURSDAY, April 25th, 17:00 – 19:00 POSTER SESSION I	page
17	Fault zone detecting using digital terrain model (DEM) analysis and seismic refraction tomography (SRT), Holy Cross Mountains (Poland) ***(Piotr Wilkołązki)***	**75**
18	The relationship between rock mass strength and deformation in the Bükk Mts, Hungary ***(Richard William Mcintosh, Seyed Jamal Aldin Hosseini)***	**76**
19	Tectonometamorphic history of the Erzgebirge – open questions ***(Martin B. Keseberg & Thorsten J. Nagel)***	**77**
20	Fault-related fold structures of the Moravo-Silesian fold and thrust belt ***(Mariusz Fiałkiewicz, Bartłomiej Grochmal, Marcin Dąbrowski)***	**78**
21	Leucocratic rocks at the contacts between orthogneisses and metasedimentary rocks in the Lądek-Śnieżnik Metamorphic Unit, Sudetes ***(Wojciech Stawikowski, Mirosław Jastrzębski)***	**79**
22	Photogrammetry as a tool to improve recognition of fold and fault patterns: field examples from the Northern Calcareous Alps (Austria, Hallstatt region) ***(Marcin Olkowicz, Bartłomiej Grochmal, Mariusz Fiałkiewicz, Marta Adamuszek, Marcin Dąbrowski)***	**80**

	FRIDAY, April 26th, 17:00 – 19:00 POSTER SESSION II	page
1	Quaternary tectonic activity imprinted on the river terrace in Brno ***(Benjamín Fojtík, Rostislav Melichar, Ivo Baroň, Jan Černý, Kurt Decker, Václav Dušek, Filip Hartvich, Martin Šut'jak, Dalibor Všianský, Piotr Moska, Thanh-Tùng Nguyễn)***	**82**
2	Structural analysis and paleostress investigation along Szőc Fault (Bakony Mountains, western Hungary) ***(Anwar Al Hijouj, Gábor Csillag, Melinda Fialowski, László Fodor)***	**83**
3	Tectonic environment of the Neogene magmatism in the Pieniny Klippen Belt ***(Jakub Bazarnik, Piotr Lenik)***	**84**
4	Sedimentary traces of Late Pleistocene seismic activity in glacigenic sediments in the Southern Peribalticum area (NE Germany, Lithuania, Latvia) ***(Szymon Belzyt, Małgorzata Pisarska-Jamroży, Grebal Project Team)***	**85**
5	Kinematic modelling of fault-related structures within anisotropic layered rocks of Northern Calcareous Alps (Eastern Alps, Austria) ***(Mariusz Fiałkiewicz, Bartłomiej Grochmal, Marcin Olkowicz, Marcin Dąbrowski, Bernhard Grasemann, Oscar Fernandez)***	**86**
6	Active tectonics of the Vértes Hills (Hungary) based on precise characterization of earthquakes and geological-geomorphological data ***(László Fodor, Eszter Békési, Barbara Czecze, Gábor Csillag, Dániel Kalmár, Márta Kiszely, Bálint Süle, Anna Świerczewska, Antek Tokarski)***	**87**
7	Thin-skinned vs. thick-skinned shortening of the Transdanubian Range: the switch from Neothetian obduction to the formation of the Eoalpine orogeny ***(Gábor Héja, Márton Palotai, Gyula Maros, Tamás Budai, Zsolt Kercsmár, Szilvia Kövér, Ádám Csicsek, László Fodor)***	**88**
8	New interpretation of selected tectonic structures - eastern part of the Polish Outer Carpathians ***(Adam Kozłowski, Aleksander Gąsienica, Arkadiusz Drozd, Krzysztof Pieniądz)***	**89**
9	The seismic network of the University of Silesia as a part of AdriaArray Project ***(Maciej J. Mendecki, Wojciech Czuba, Piotr Środa, Tomasz Janik, Julia Rewers, Somayeh Abdollahi, Monika Bociarska, Szymon Malinowski)***	**90**

	FRIDAY, April 26th, 17:00 – 19:00 POSTER SESSION II	page
10	Finite strain distribution in kinematic models of fault-related folding ***(Szymon Mol, Marcin Dąbrowski)***	**91**
11	Miocene volcanism in the Slanské Vrchy Mountains, eastern Slovakia ***(Jörg Ostendorf, Robert Anczkiewicz, Milan Kohút)***	**92**
12	An updated model of the Cenozoic cover of the Fore-Sudetic Block: implications for its neotectonic activity ***(Michał Słotwiński, Janusz Badura, Marcin Dąbrowski)***	**93**
13	First insights into the LiDAR-driven structural analysis of the Bystre Slice (Outer Carpathians) ***(Piotr Strzelecki, Radosław Szczęch, Jakub Andrzejak, Marta Esmund)***	**94**
14	Progressive development of an accretionary wedge margin from oblique thrust to strike-slip fault (Mikulov-Falkenstein Fault, Outer Western Carpathians) ***(Martin Šuť jak, Rostislav Melichar, Ivo Baroň, Yi-Chin Chen, Jan Černý, Jia-Jyun Dong, Václav Dušek, Filip Hartvich, Jan Klimeš, Lenka Kociánová, Tùng Nguyễn, Matt Rowberry, Chia-Han Tseng)***	**95**
15	Deformation bands in the Red River Fault Zone, Vietnam: preliminary findings ***(Piotr Strzelecki, Le Duc Anh, Anna Świerczewska, Antek K. Tokarski, Nguyen Quoc Cuong, Phan Dong Pha)***	**96**
16	Late Pleistocene surface fault rupture in slow-deforming Podhale Basin (Western Carpathians): implications for paleoseismology and geodynamics ***Jacek Szczygieł, Jerzy Zasadni, Piotr Kłapyta, Marta Woszczycka, Krzysztof Gaidzik, Maciej Mendecki, Artur Sobczyk, Christoph Grützner)***	**97**
17	Tectonic Złatne Unit in the Pieniny Klippen Belt ***(Anna Waśkowska, Jan Golonka, Kamil Cichostępski, Jerzy Dec, Monika Łój, Grzegorz Bania, Włodzimierz Jerzy Mościcki, Sławomir Porzucek, Józef Chowaniec)***	**98**
18	Deformation events of the Permian Boda Claystone recorded by tectonic veins (Tisza Mega-unit, Mecsek Mts.) ***(Ervin Hrabovszki, Péter Molnár, Félix Schubert)***	**99**
19	Reconstructing Neogene landscape and tectonic history of the NE Bohemian Massif using paleokarst sediment palynology from the Orlica-Śnieżnik Dome marbles ***(Artur Sobczyk, Elżbieta Worobiec, Marcin Olkowicz, Jacek Szczygieł)***	**100**
20	Fault patter and extension during the Miocene syn-rift phase in the central Pannonian Basin (Pilis-Buda Hills); fault geometry analysis and cross section balancing ***(Melinda Fialowski, Barbara Beke, László Fodor)***	**101**
21	Tectonics of the Silesian and Skole Nappes contact in the eastern part of the Węglówka tectonic window. ***(Rafał Nasiłowski)***	**102**
22	A pilot network of InSAR reflectors in the Śnieżnik Massive – preliminary assumptions ***(Mateusz Drożdżewski, Bartłomiej Grochmal, Marcin Olkowicz, Zbigniew Perski, Marcin Dąbrowski)***	**103**
23	Formation of the active Tabas Fold Belt as result of transpression and rotation of the tectonic blocks, Tabas block, Iran ***(Andrzej Konon, Alireza Nadimi, Mateusz Mikołajczak, Barbara Rybak-Ostrowska, Michał Wyglądała, Soheila Bouzari, Soheyla Beygi)***	**104**

Conference Contributions

Oral presentations

Session I

Chair: Milan Kohút

Thursday 9:15 – 9:45, 25th April

Late Palaeozoic paleomagnetic and tectonic constraints for amalgamation of Pangea supercontinent

Karel Schulmann[1,2], Jean Bernard Edel[†2], José Ramón Martínez Catalán[3], Stanislaw Mazur[4], Jerémie Soldner[4], Alexandra Guy[1], Igor Soejono[1], Ondrej Lexa[5], Pavla Štípská[1], Stephen Collett[1], Francis Chopin[2], Rémi Lepretre[6], Jian Zhang[7], Yingde Jiang[8]

[1]*Czech Geological Survey, Prague, Czech Republic*
[2]*Institut Terre et Environnement de Strasbourg, Université de Strasbourg, France*
[3]*Departamento de Geología, Universidad de Salamanca, Spain*
[4] *Institute of Geological Sciences, Polish Academy of Sciences, Krakow Research Centre, Poland*
[5]*Institute of Petrology and Structural Geology, Faculty of Sciences, Charles University, Prague, Czech Republic*
[6]*CY Cergy Paris Université, Département Géosciences et Environnement (GEC), France*
[7]*Department of Earth Sciences, The University of Hong Kong, China*
[8] *State Key Laboratory of Isotope Geochemistry, Guangzhou Institute of Geochemistry, Chinese, Academy of Sciences, China*
**Lead presenter e-mail: schulmann.karel@gmail.com*

Paleomagnetic, structural and geochronological data show that during late Paleozoic times the Pangea supercontinent was formed by: 1) convergence of the Gondwana mega-block with the Laurussia and European Variscan Belt (EVB) in the west and, 2) convergence of the Tarim-North China Collage (TNCC) with the Central Asian orogenic Belt (CAOB) in the east. In the west, the collision of mega-blocks led to the formation of ca. 300 – 280 Ma South-Variscan ((U)HP granulite) Belt (SVB) currently hidden in the Betic Cordillera in Spain and Mauretanides (Rif and Atlas) in Morocco and Algeria. Meanwhile, the EVB suffered formation of the Cantabrian Orocline at ca. 300 – 280 Ma and dextral shearing along the Gondwana-Laurussia boundary. At the same time, the northern Gondwana margin experienced N-S shortening of Morocco Meseta resulting in growth of ca. 325 – 300 Ma E-W trending metamorphic domes (e.g. Rehamna, Jebilet) and upright folding of late Paleozoic basins in the Anti-Atlas further south. In the East, the TNCC and CAOB collision led to the formation of ca. 320 – 260 Ma Tien-Shan – Solonker (eclogite – blue schist) Belt (TSB) considered as a suture of the Ordovician–Devonian Paleo-Asian Ocean (or one of its branch). As a response the CAOB suffered up to 1000 km shortening leading to the formation of Kazakhstan and Mongolian oroclines and development of sinistral wrench zones associated with the closure of the Mongol-Okhotsk Ocean. To the south, the TNCC basement responded by Permian N-S shortening marked by E-W upright folding of late Paleozoic basins in the Beishan and E-W upright folding and dextral shearing of Paleozoic units north of the Tarim block. Altogether, The SVB and the TSB constitute an axis of a ca. 13 000 km long and up to 1000 km wide late Carboniferous - Permian Trans-Euroasian orogenic belt involving the deformed northern margin of the Gondwana and TNCC in the south and massively shortened EVB and CAOB in the north.

Detrital zircon geochronology and the development of tectonic models for the Bohemian Massif

Stephen COLLETT[1]*

[1]*Czech Geological Survey, Prague, Czech Republic*
**Lead presenter e-mail:stephen.collett@geology.cz*

Access to relatively rapid data acquisition techniques has led to detrital zircon geochronology becoming a routine and widely applied tool in provenance studies. These data, and their correlation, are applied both to paleographic reconstructions and the development of tectonic models. Nonetheless, the increasing proliferation of detrital zircon geochronological datasets and their haphazard integration into larger-scale correlations has led to a complex web of competing hypotheses and counter-hypotheses.

In order to formulate and test coherent hypotheses it is important to first establish a consistent framework in which these data can be properly assessed in both a temporal and geographical context. To this end, a database of U-Pb and Lu-Hf zircon isotopic data has been established from late Mesoproterozoic to late Paleozoic strata from Pangea-forming orogenic belts spanning from Atlantic North America through Europe, Northern Africa, the Middle East, and Central Asia to the Pacific Ocean. The original purpose of this database was to test correlations and various paleogeographical reconstructions in these regions during the transition from the Rodinia to Pangea supercontinent.

As a case study, an extract from this database will be used to test several competing models on the pre-orogenic evolution of European Variscan Belt with specific focus on the Bohemian Massif. The Bohemian Massif is composed of four principal units, Saxothuringia, Teplá-Barrandia, Moldanubia, and Brunovistulia, which have in some tectonic models been considered to represent four distinct crustal blocks separated from one another by oceanic domains. Nonetheless, since oceanic domains should in theory act as barriers to the transportation of detritus and there are superficial similarities in detrital zircon spectra across these units; alternative models discarding one, or even all, of these oceanic domains have subsequently been proposed. However, the significance of these interpretations are hampered by either an incomplete or improper handling of the available data. In this presentation it will be demonstrated that detrital zircon data are actually supportive for, rather than an argument against, potential oceanic separation(s). This will be demonstrated by discussion of three key points: 1) The significance of Mesoproterozoic zircons in Brunovistulia, 2) the widespread occurrence of Stenian-Tonian age zircons in northern Gondwana and their distribution in the units of the Bohemian Massif, and 3) the relative abundance of Early Paleozoic zircons in northern Gondwana and the Bohemian Massif.

Early Mississippian transpressional deformation and thermal doming at the distal foreland of the Variscan orogen (SW East European Craton, Lublin-Lviv Basin)

Paweł POPRAWA[1*], Maciej TOMASZCZYK[2]

[1]*Faculty of Geology, Geophysics and Environmental Protection, AGH University of Krakow, Poland*
[2]*PKN ORLEN S.A., Department of Geology and Exploration PGNiG, Warsaw, Poland*
**Lead presenter e-mail: ppop.ecr@gmail.com*

Variscan orogeny in Europe impacted the development of the foreland plate, affecting subsidence and uplift histories and/or imposing tectonic deformations. An example of the Variscan distal foreland deformation is the early Mississippian major unconformity (referred to as the Bretonian) in the Lublin-Lviv Basin, located at the SW slope of the East European Craton. The unconformity divides the pre-Carboniferous rock complexes, being the subject to laterally differentiated uplift and erosion, from the post-tectonic sedimentary cover of the upper Visean to Westphalian age. The early Mississippian uplift separated the Lublin-Lviv Basin into several tectonic blocks, which differ in terms of stratigraphic extent of erosion cutting the sedimentary cover down to the different levels of the Devonian, the lower Paleozoic or the Precambrian basement. The thickness of eroded sediments was assessed using the palaeothickness data of Modliński et al. (2010) juxtaposed with the geological map for the sub-Carboniferous surface. It varies between individual blocks ranging from a few hundred to c. 2500 m at maximum. The early Mississippian uplift was associated with the development of a grid of faults, offsets of which usually range between a few hundred meters to c. 2000 m at maximum. Their structural style, revealed by seismic data, is mostly transpressive (comp. Tomaszczyk and Jarosiński, 2017). This is additionally confirmed by an echelon pattern of some faults, which indicate a dextral strike-slip component. South and NE of the Lublin Synclinorium, the transpression-driven uplift was assisted by thermal doming, indicated by the oval shape of the zones with maximum thickness of eroded section, as well as by their coincidence with the location of Mississippian igneous intrusions and effusive rocks. An incipient latest Famennian phase of uplift and erosion is expressed by composition of sandstones and conglomerates of the Hulcze Formation (Lublin Synclinorium, SE Poland) and conglomerates and olistoliths of the Tumin Series (south of the Volodymyr Volynskyi Fault, W Ukraine), containing lithoclasts, pebbles and blocks of the local Ediacaran, lower Paleozoic and Devonian rocks. The SW part of the Lublin-Lviv Basin is distinguished as the Radom-Kraśnik Zone, generally considered devoid of Carboniferous. However, within this zone, seismic data locally also indicate the presence of angular unconformity between Devonian and Carboniferous. This is confirmed by legacy data of a few deep boreholes, revealing Carboniferous deposits resting on various stratigraphic units of the Devonian. Therefore, we postulate that the Mississippian tectonic deformation, uplift, and erosion also affected the Radom-Kraśnik Zone. A hiatus related to the Mississippian uplift and deformations covers time span of at least 15 My, i.e. (latest Famennian-?) Tournaissian to early Visean. It coincides in time with the major tectonic events within Variscan orogeny, such as the termination of convergence and continent-continent collision, as well as high-grade metamorphism. Having no other potential source of tectonic stress, the gid of transpressive faults and the uplift in the Lublin-Lviv Basin are interpreted here as the intraplate deformations imposed by the Variscan orogeny in its distal foreland.

This study was supported by grant of NCN UMO-2021/41/B/ST10/03550.

Tomaszczyk, M., Jarosiński, M., 2017. The Kock Fault Zone as an indicator of tectonic stress regime changes at the margin of the East European Craton (Poland). Geological Quarterly, 61 (4): 908–925.

Modliński, Z. (ed.), 2010. Paleogeological Atlas of the sub-Permian Paleozoic of the East European Craton in Poland and neighbouring areas, 1:2 000 000. Polish Geological Institute – NRI, Warsaw.

Session II

Chair: Vojtěch Janoušek

Thursday 10:30 – 12:00, 25th April

From Carboniferous convergence to Permian continental rifting – the interaction of Baltica with the Variscan belt during the assembly of Pangea

Stanisław MAZUR[1]*

[1]*Institute of Geological Sciences, Polish Academy of Sciences, Krakow Research Centre, Poland*
**Lead presenter e-mail: ndmazur@cyf_kr.edu.pl*

In Western Europe, the Variscan belt contacts Avalonia along the Rhenohercynian Suture, a result of Early Carboniferous continental collision. Moving east of the Harz Mts., the Rhenohercynian suture disappears beneath a thick sedimentary sequence of the Permian-Mesozoic basin. Its extension is either truncated by major NW-SE strike-slip faults like the Elbe, Odra, or Dolsk faults or bends under the cover of a thick sedimentary succession. The extension of Avalonia into Poland is challenging to determine, with the thinned margin of Baltica considered the substratum of the Permian-Mesozoic basin. Deep seismic soundings show that the thinned margin of Baltica reaches the NW-SE oriented Dolsk or Odra fault, potentially bringing the crust of Baltica into direct contact with the crust of the Variscan internides of the Bohemian Massif. Along the Dolsk fault, there is the two-layered, low-velocity Variscan crust in the SW that contacts the three-layered Baltica crust. The geometry of this contact remains unknown, but the lower, high-velocity crust of Baltica may extend southwest to the Odra fault. In the basement of the sedimentary sequence between the Dolsk and Odra faults, low-grade metamorphosed phyllites with a metamorphic age of approximately 360 Ma are found. They apparently represent a fragment of Variscan metamorphic nappes.

The Variscan front is oriented NE-SW in Western Europe, but in Poland, it bends by 90° to the NW-SE direction, continuing to the border of Ukraine. In southeastern Poland, the front enters the slope of the East European Platform, constituting an undisputed example of a direct contact between the Variscan belt and Baltica. If the geometry of the Variscan front reflects the structure of the orogen, the edge of Baltica must have been overthrust by Variscan orogenic wedge from the south to north. This accretion event resulted in polyphase N-S to NE-SW shortening, either thin-skinned, leading to folding of the external fold-and-thrust belt, or thick-skinned, resulting in the emplacement of the Variscan nappe stack on the Baltica margin.

The last folding of external Variscides in Poland occurred around 305 Ma and was immediately followed by the emplacement of a large igneous province at the Carboniferous to Permian transition. The centre of magmatism was in NE Germany, the area of greatest crustal thinning. The origin of the igneous province was linked to plate boundary forces leading to extension and continental rifting. The latter produced the Mid-Polish Trough, an elongated continental rift running NW-SE parallel to the Teisseyre-Tornquist zone. Permian rifting further attenuated the Baltica margin and, jointly with coeval magmatism, reshaped the margin of Baltica masking its contact with the Variscan belt. Toward the east, the continuity of the Variscan internides was disrupted by early Mesozoic rifting in the area of the present-day Carpathians.

Contrasting Permian plutonism in the Trans-Altai Gobi, SW Mongolia

Pavel HANŽL[1]*, Vojtěch JANOUŠEK[1], Battushig ALTANBAATAR[2], Karel SCHULMANN[1], Kristýna HRDLIČKOVÁ[1], David BURIÁNEK[1]

[1]Czech Geological Survey, Prague, Czech Republic
[2]Takhi resources LLC, Ulaanbaatar, Mongolia
**Lead presenter e-mail: pavel.hanzl@geology.cz*

The Trans-Altai Zone (TAZ) in the southern tract of the Central Asian Orogenic Belt (CAOB) is formed by the Early Paleozoic oceanic crust covered by Carboniferous volcanosedimentary complexes and intruded by numerous Carboniferous to Permian plutons. Two contrasting belts of the Early Permian plutons stand out among them: (1) Gobi Tien Shan Intrusive Complex (GTSIC) in the south and (2) late- to post-tectonic plutons of noticeably oval shape distributed along the central and northern parts of the TAZ.

Petrologic and geochemical characteristics of the 310–290 Ma old GTSIC correlate with westerly magmatic belts in the Eastern Tien Shan and point to an active continental margin setting. Voluminous arc-related granodiorites–diorites with well-preserved magma mingling textures come from deeper parts of the GTSIC, while granites with subvolcanic features represent relatively shallow intrusion levels of the Late Carboniferous–Early Permian volcanic arc.

The Aaj Bogd Pluton (ABP) is the largest among the Early Permian (300–280 Ma) plutons distributed as beads on a necklace in a belt spanning from the Dulate Arc in the Eastern Junggar through the Trans-Altai Zone to the Khan Bogd Pluton in the Central Gobi. Whole-rock chemistry of the ABP points to an intra-plate geotectonic setting. The mafic (monzogabbroic–quartz monzodioritic) rocks in the center of ABP are interpreted as having crystallized from melts derived from asthenospheric mantle domains unmodified by previous subduction-related metasomatism. These parental magmas further evolved by assimilation of pre-existing, arc-related metaigneous crust and fractional crystallization processes to yield the prevailing syenitic–granitic members of the Aaj Bogd Pluton.

The A-type magmatic activity in the Trans-Altai Zone and I-type, subduction-related magmatism in the southerly Gobi Tien Shan were temporally and spatially connected with the Late Carboniferous–Early Permian amalgamation of the Trans-Altai Zone to the northern parts of CAOB. During this process, GTSIC is thought to have originated in a continental arc developed over a retreating oceanic subduction zone. The back-arc rifting scenario for the contemporaneous A-type magmatism in TAZ assumes asthenosphere upwelling triggered by the collisional zone probably related to the same subduction zone on which the GTSIC evolved far to the south. The linear arrangement of the A-type plutons over a distance of more than 1600 km can be explained through their association with major Permian strike-slip zones likely controlling the granite emplacement.

The research was supported by the project GAČR EXPRO 19-27682X.

Brittle tectonics in pegmatite formation: an example from the Bratislava granite massif, Western Carpathians

Igor BROSKA[1]*, Sergii KURYLO[1], Ján MADARÁS[1], Pavel UHER[2]

[1]Earth Science Institute, Slovak Academy of Sciences, Bratislava, Slovakia
[2]Comenius University, Bratislava, Slovakia
**Lead presenter e-mail: igor.broska@savba.sk*

In the crystalline core mountain of the Malé Karpaty Mts., which is a Tertiary horst structure, pegmatite swarms are developed mostly in the southern part from the Variscan Bratislava granitoid massifs and here their mineralogy, composition and fabric were explored in more detail. Pegmatite dykes are here many meters wide and are located either directly in the parental granitic rocks or in the adjacent host rocks, or they also cut diorite bodies included in the granites. The larger pegmatites commonly show zoned internal structure with border aplitic and/or coarse border zone, further from granite contact a unit of coarse-grained graphic alkali feldspar–quartz–muscovite ± biotite, blocky K-feldspar–quartz (in the most central part) and finally quartz core. Locally, the late muscovite formation and albite–quartz–muscovite–garnet zones occur too.

Pegmatites often form networks of many dykes, over many meters long distance, and their mutual crossing is mainly in north-southward and east-westward directions. This pegmatite often rectangular network formed by emplacing of residual overpressure melt into cracks of cooling granite where during granite contraction two vertical joint sets were created. The perpendicular cut to foliation of roof metapelite rocks is other evidence for high pressure emplacement process. The fluid overpressure in emplaced pegmatites caused features of brittle tectonics of crystallized minerals (ca. fragmentation, bending, fracturing, and kinking) forming locally spectacular mosaic mineral fabrics, especially in alkali feldspars. However, some pegmatite emplacement was also into ductile environment of the cooled granites. The time of pegmatite formation was close to the emplacement of parental granite dated by SHRIMP in time span of ca. 358 - 355 Ma. Pegmatite ages have been obtained from monazite, columbite and garnet. The pegmatite network in granites, mosaic disintegrated fabric of feldspars developed during fluid overpressure regime in pegmatite dykes are features indicating Tournaisian extensional tectonics during consolidation of Variscan granites.

Acknowledgement: This research was supported by project ERANET-MIN PEGMAT JTC-2021_174.

Tectonic evolution of the Strzegom - Sobótka Massif

Mariusz FIAŁKIEWICZ[1]*, Bartłomiej GROCHMAL[1], Marcin OLKOWICZ[1], Marcin DĄBROWSKI[1]

[1]*Computational Geology Laboratory, Polish Geological Institute - National Research Institute, Wrocław, Poland*
**Lead presenter e-mail: mfia@pgi.gov.pl*

The Strzegom-Sobótka Massif (SSM), a large composite granitic body located in central part of the Fore-Sudectic Block, has been subject of brittle tectonic studies for more than a century. The classical model of jointing in plutonic rocks was established here by H. Cloos. Four sets of vertical joints have been distinguished within the SSM: a dominant NW-SE striking set (Q), a NE-SW striking set (S) longitudinal to mineral fabric, and two supposedly younger sets of the so-called diagonal joints, which are striking N-S and W-E. Due to an ongoing extensive mining activity, numerous good exposures occur in a relatively small area, especially in the western part of the massif. Here, we present results of fieldwork conducted within both active and abandoned quarries of granites aimed at deciphering tectonic evolution of the SSM.

In view of our observations and in agreement with previous research, the NW-SE joint set dominates in most of the studied sites, while the NE-SW set is less pronounced. We have analyzed the relationship between the characteristics of the studied joint systems and the local petrographic variation. Aforementioned trend was observed in the hornblende-biotite granite in the western part and in biotite granodiorite in the eastern part. In the two-mica granite this trend was less pronounced due to presence of N-S and E-W striking sets and lower quality of outcrops. A significant deviation from the typical joint pattern was observed in the biotite granites near Graniczna that exhibit a dominant N-S striking set. The Łażany quarry is also characterized by an atypical joint pattern, but the close vicinity of the metamorphic cover may play an important role in this case. In detail joint pattern change significantly within mentioned petrographic varieties. For example, in the region of Kostrza, the joints are sparsely spaced allowing for block extraction, while well developed densely-spaced fracture corridors are observed in the nearby Rogoźnica quarry.

Evidence for both normal and strike-slip movements were observed along faults with slickensides. Initial paleostress analysis results showed normal faulting regime with least compressive stress oriented in the NNE-SSW to NE-SW direction. This is consistent with cartographic works of previous authors which depicts Cenozoic normal faults striking in WNW-ESE to NW-SE direction. In some fault zones, a dark material resembling pseudotachyllite is present, although no injection veins were found. The pseudotachyllite-like faults tend to be oriented in the NW-SE or less commonly N-S direction. They occur most abundantly in the area of Rogoźnica, where they are densely spaced and their thickness reaches up to few centimeters. A set of parallel faults showing horizontal slickensides can be interpreted as their prolongation in the Strzegom area.

"Hot vs Cold": on differences of AMS record in shear zones

Zuzana ROXEROVÁ[1], Vladimír KUSBACH[1]*, Matěj MACHEK[1], Monika KUČERÁKOVÁ[2], Stanislav VRATISLAV[2]

[1]*Institute of Geophysics, Czech Academy of Sciences, , Prague, Czech Republic*
[2]*Department of Solid State Engineering, FNSPE CTU, Prague, Czech Republic*
**Lead presenter e-mail: kusbach@ig.cas.cz*

There has been a comprehensive discussion around the origin of magnetic fabric and its correlation with the overall deformation and strain history of rocks. Exploring various shear zones magnetic fabric studies aimed to connect the temporal and spatial associations between finite strain and the anisotropy of magnetic susceptibility (AMS). The AMS as a dimensionless material parameter describes the degree of magnetization of a material in response to an applied magnetic field in different directions. AMS measurements combine the collective magnetic signals arising from both shape-preferred and crystallographic orientations of all constituent mineral grains, making it a widely used technique in geology for rapid quantifying of internal rock fabric.

In this study, contrasting shear zones types from low and high temperature conditions with differences in rock structure were investigated.. In both cases, different deformational mechanisms were identified. We established the correlation between AMS and strain within the shear zones in marble by integrating rock magnetic investigations, qualitative and quantitative microstructural analyses, and computational modeling of AMS based on crystallographic preferred orientations (CPOs).

Significant variations in resulting AMS cannot be explained only by slightly different strain values. The cause of the observed differences in AMS is a combination of several factors, the main ones being the chemical composition of the constituent phases and the activity of different deformation mechanisms. Also, this integrated approach to the study of rock fabric and its constituents provides significant improvements in understanding the complex interplay between deformation, strain, and magnetic fabric in rocks.

Session III

Chair: Mirosław Jastrzębski

Thursday 13:30 – 14:45, 25th April

The effects of grain-scale melt migration process on metagranite at eclogite facies, Snieznik dome, Bohemian Massif

Pavla ŠTÍPSKÁ[1]*, Andrew R. C. KYLANDER-CLARK[2], Martin RACEK[3], Prokop ZÁVADA[1], Pavlína HASALOVÁ[1]

[1] *Czech Geological Survey, Prague, Czech Republic*
[2] *Department of Earth Science, University of California, Santa Barbara, United States*
[3] *Institute of Petrology and Structural Geology, Charles University in Prague, Czech Republic*
**Lead presenter*

Augen to banded metagranite from the Snieznik dome have been modified locally to have stromatic, schlieren, nebulitic and granite-looking textures typical of migmatites. Former presence, and increasing role of melt in transformation towards nebulite is inferred from interstitial phases along grain boundaries in the dynamically recrystallized monomineralic feldspar and quartz aggregates, and from textures of fine-grained plagioclase and quartz replacing K-feldspar. These features are interpreted as resulting from dissolution-reprecipitation along grain boundaries due to grain-scale melt migration, being pervasive at the grain-scale, but localized at hand-specimen to outcrop scales. The new minerals crystallized from melt are in textural equilibrium with phengite. All the rock types have the same mineral assemblage of Grt−Ph−Bt−Ttn−Kfs−Pl−Qz±Rt±Ilm, with similar garnet, phengite and biotite composition, leading to modelled equilibration conditions of 15−17 kbar and 690–740 °C. Because the mineral compositions in the assemblage of interest are independent of the amount of melt, the modelling did not allow to estimate melt quantities in individual rock types. However, migmatite textures suggest that increasing degree of melt-rock interaction occurred from the banded to the schlieren and nebulitic types. The initiation of melt migration is related to gently dipping structures related to continental subduction to eclogite-facies conditions, and more pronounced melt migration is related with vertical fabrics leading to exhumation of the continental subduction wedge from eclogite-facies to mid-crustal conditions.

The effects of melt migration had impact on partial recrystallization of zircon. Zircon in augen to banded types shows oscillatory zoning and gives Cambro-Ordovician age of the protolith. In schlieren to nebulite types, zircon shows domains of blurred oscillatory zoning to structure-less textures. These metamorphic domains are located along grain boundaries, form embayments, form straight or curved linear structures cutting through the oscillatory zoned domains, or are affecting the whole grains. The domains with sharp oscillatory zoning tend to give Cambro-Oridovician ages, while the metamorphic domains tend to give Carboniferous age. Zircon shows numerous apparent “inclusions” of phengite, K-feldspar, quartz, plagioclase, rare garnet, rutile and biotite. However, the “inclusions” of phengite, garnet and rutile are located in the metamorphic domains of the zircon grains. In places, the inclusions are aligned, and these structures are interpreted as former cracks, along which the metamorphic phases crystallized and zircon (re)crystallized. As the assemblage of phengite-garnet-rutile is compatible with previously inferred eclogite-facies conditions, we interpret the Carboniferous zircon (re)crystallization as dating the eclogite-facies grain-scale melt migration process.

Metamorphic evolution of coesite-bearing Śnieżnik eclogites

Małgorzata NOWAK[1,2]*, Lucie TAJČMANOVÁ[2], Jacek SZCZEPAŃSKI[1], Marcin DĄBROWSKI[3]

[1]*Institute of Geological Sciences, University of Wrocław, Poland*
[2]*Institute of Earth Sciences, Heidelberg University, Heidelberg, Germany*
[3]*Computational Geology Laboratory, Polish Geological Institut - National Research Institute, Wrocław, Poland*
**Lead presenter e-mail: malgno93@gmail.com*

The Orlica-Śnieżnik Dome (OSD) is exposed in the northeastern part of the Bohemian Massif. The dome is interpreted as a fragment of the Moldanubian zone of the Variscan orogen, constituting the Variscan orogenic root. The OSD predominantly comprises orthogneisses alternating with metamorphosed volcano-sedimentary sequences. In the eastern part of the OSD, in the Śnieżnik Massif, lenses of high- and ultrahigh-pressure rocks (granulites and eclogites) occur in the orthogneisses. This study focuses on deciphering the metamorphic evolution of the eclogites outcropping in two locations in the Śnieżnik Massif: Nowa Wieś and Bielice.

The studied eclogites exhibit a rather typical metamorphic history for ultrahigh-pressure (UHP) rocks. It covers a UHP metamorphic event followed by isothermal decompression and amphibolite-facies retrogression. The studied samples are characterized by steeply-dipping, subvertical foliation. It is defined by alternating garnet- and omphacite-rich layers and parallel alignment of elongated phengite, kyanite and rutile grains. The mineral assemblage connected to isothermal decompression is present in the form of small amphibole grains and diopside-amphibole-plagioclase symplectites locally occurring along grain boundaries. The last metamorphic event, characterized by amphibole-plagioclase-zoisite/clinozoisite-margarite, can be observed in the fractures crosscutting the main foliation. This event is connected with retrogression under amphibolite-facies conditions.

The UHP metamorphic event in the studied samples is reconstructed based on the discovery of coesite, which occurs as tiny (~10-20 μm) inclusions present in omphacite and garnet. The well-preserved mineral assemblage associated with the UHP metamorphism comprises garnet-omphacite-phengite-kyanite-rutile-coesite. Based on the phase diagram modelling combined with the isopleth geothermobarometry we estimate the peak pressure metamorphic conditions at ~3.0 GPa and ~750°C. These results are consistent with the results obtained using conventional geothermobarometry (Grt-Cpx-Ph-Ky-Coe geothermobarometer) and Zr-in-rutile thermometer. The onset of isothermal decompression is marked by the occurrence of small amphibole grains, which points out to conditions of ~2.3 GPa at ~750°C in amphibole stability field.

Timing of Variscan HP event in the Tatric Unit crystalline basement of the Western Carpathians

Milan KOHÚT[1]*, Robert ANCZKIEWICZ[2]

[1]Earth Science Institute, Slovak Academy of Sciences, Bratislava, Slovakia
[2]Institute of Geological Sciences, Polish Academy of Sciences, Krakow Research Centre, Poland
**Lead presenter e-mail: milan.kohut@savba.sk*

The European Variscan and Alpine Mountain chains are typical collisional orogens. One of the crucial questions for understanding the Variscan orogeny is - when did the HP (UHP) metamorphism take place? The pre-Alpine basement of the Western Carpathians represents the eastern exposure of the Variscan orogen in Europe. The Tatra Mts. (TM) are located in the northernmost sector of the Western Carpathians, and are typical so-called core mountains within the Tatric Unit. The crystalline basement of the TM is composed of pre-Mesozoic metamorphic and granitic rocks. Metamorphic rocks are abundant in the western part (Western Tatra), whereas in the eastern part (the High Tatra) they occur as minor bodies within granites. Two superimposed tectonic units – lower unit (LU) and upper (UU), differing in lithology and metamorphic grade, have been distinguished (Janák, 1994; Janák et al., 1999, 2022). The LU in the Western Tatra is composed of metapelitic micaschists together with quartz-rich metapsammites, resembling flysch sediments, and its metamorphic conditions reached 0.6–0.8 GPa and 620–660°C. The UU is composed of para- and orthogneisses, amphibolites with retrogressed eclogites, migmatites, calc-silicates and granitoids with maximum P–T conditions at ca. 1.6–1.7 GPa and 675–695°C. Overall, metamorphic zonation in the Tatra Mts. displays an inverted sequence of high-grade metamorphic rocks and granitoids in the hangingwall, and lower-grade metamorphic rocks in the footwall. This is interpreted as a consequence of crustal thickening and mid-crustal thrusting in the course of Variscan orogeny.

Lu–Hf garnet geochronology shows the potential for dating HP and UHP episodes. Our new Lu–Hf garnet dating from the Bryšno retrogressed eclogite yielded WR–garnet isochron age ca. 355 Ma, whereas sillimanite and garnet-bearing metapelitic gneisses (MP/HT) from Gerlach peak and Velická Valley gave an age ca. 346 Ma (Lu–Hf and Sm–Nd WR–garnet isochrons). Noteworthy, the Lu–Hf and Sm–Nd age data indicate that the time span between the HP and MP metamorphism was ~10 Myr in the Tatra Mts. Earlier metamorphism in the eclogite (Tournaisian at ca. 355 Ma) can be the expression of a deeper position within the subducting slab and thus, eclogite garnet started to grow ca. 10 Myr earlier than garnets in the sillimanite-bearing gneiss (Visean ca. 346 Ma) at shallower level. The continuous return of deep crustal material from the subduction channel after maximum of the crustal-stacking was associated consequently with the extension and crustal thinning.

Acknowledgments: Support from VEGA-02/0002/24, VEGA-01/0028/24 and funding from the internal IGS PAS grant are greatly appreciated.

New petrological and geochronological data from the Austroalpine Koralpe-Saualpe-Pohorje Complex

Iris WANNHOFF[1], Jan PLEUGER[1]*, Xin ZHONG[1], Timm JOHN[1], Leo j. MILLONIG[2], Axel GERDES[2], Richard Albert ROPER[2]

[1]Freie Universität, Berlin, Germany
[2]Goethe-Universität, Frankfurt, Germany
**Lead presenter e-mail: jan.pleuger@fu-berlin.de*

The Austroalpine Koralpe-Saualpe-Pohorje Complex (KSPC) stretches from SE Austria to NE Slovenia and consists mainly of gneisses and metasediments, with abundant eclogite lenses embedded. Following a temperature-dominated Permian-Triassic tectonometamorphic event, the KSCP experienced eclogite-facies conditions during the Cretaceous Eo-Alpine tectono-metamorphic cycle. A metamorphic field gradient with an increase in peak pressure-temperature (PT) conditions from NW to SE, and UHP conditions for Pohorje, can be inferred based on thermodynamic modelling, geothermobarometry and the discovery of diamond in fluid inclusions in garnet reported in previous studies.

Here, we present new constraints for metamorphic peak PT conditions along a NW-SE transect through the KSCP applying Raman spectroscopy of quartz inclusions in garnet, Zr-in-rutile thermometry and in-situ U-Pb dating of garnet and rutile from eclogite and metasediment samples. The eclogite samples yielded maximum pressures of 1.9 GPa across the KSPC, indicating no pressure increase from the NW to SE. The metasediments and gneisses show overall lower pressures with a maximum of ca. 1.4 GPa. Zr-in-rutile thermometry yielded uniform T of 640 (±30)°C, indicating no temperature gradient. In-situ garnet U-Pb dating was conducted to identify potentially different metamorphic events. Garnet from the Koralpe, Saualpe and Pohorje metasediments yielded Early Cretaceous data ranging from ~95-105 Ma, similar to eclogitic garnet from the Koralpe with ~112 Ma. Additionally, garnet from a Saualpe micaschist yielded Late Triassic cores (~224 Ma) and Early Cretaceous rims (~115 Ma). Rutile throughout the KSPC yielded Late Cretaceous U-Pb data of ~98–83 Ma (eclogites) and ~87–80 Ma (metasediments).

The results suggest that the KSPC represents a coherent nappe. The recorded maximum pressures and temperatures are identical throughout the KSPC. The lower pressure for the metasediments is interpreted result from viscous relaxtion in garnet due to the presence of free fluid during metamorphism. Furthermore, the data obtained from both eclogites and metasediments are interpreted to represent Late Cretaceous bulk crystallization ages of garnet grown during prograde to peak metamorphic conditions. The Late Triassic event is recorded in garnet cores from the Saualpe corroborating existing literature data. The rutile data are interpreted as cooling ages. The lack of a metamorphic field gradient may imply shallow subduction of the KSPC during Eo-Alpine orogeny.

Session IV

Chair: László Fodor

Thursday 15:00 – 16:30, 25th April

The Caledonian Wilson Cycle from a North Atlantic perspective

Jarosław MAJKA[1,2]*, Deta GASSER[3,4], Johannes JAKOB[3,4], Christopher J. BARNES[5]

[1]*Faculty of Geology, Geophysics and Environmental Protection, AGH University of Krakow, Poland*
[2]*Department of Earth Sciences, Uppsala University, Uppsala, Sweden*
[3]*Department of Civil Engineering and Environmental Sciences, Western Norway University of Applied Sciences, Sogndal, Norway*
[4]*Geological Survey of Norway, Trondheim, Norway*
[5]*Institute of Geological Sciences, Polish Academy of Sciences, Krakow Research Centre, Poland*
**Lead presentere-mail: jaroslaw.majka@geo.uu.se*

One of the prime examples of a Wilson Cycle in the Earth's history is the Caledonian Wilson cycle comprising opening and closure of the Iapetus Ocean, accretion of various arcs and continents, and the collision of Laurentia and Baltica leading to the formation of the Caledonian orogen. In this talk, a 5-stage framework of the Caledonian Wilson cycle from a North Atlantic perspective will be briefly summarized. Stage 1 includes Neoproterozoic rifting of the continental margins of Baltica and Laurentia; Stage 2 covers sea-floor spreading and birth of the Iapetus Ocean, formation of several oceanic basins, and shaping of rifted margins; Stage 3 corresponds to maturation of the Iapetus Ocean, initiation of its contraction and narrowing of the ocean along several subduction zones; Stage 4 comprises the main Scandian Baltica-Laurentia collision, during which one of the largest and most spectacular (U)HP terranes formed, namely the Western Gneiss Region; finally, Stage 5 covers orogenic collapse and massive extension, formation of large post-orogenic basins, giving a foundation to the stage 1 of the subsequent Atlantic Wilson cycle.

JM was funded by the National Science Centre (Poland) project no. 2019/33/B/ST10/01728.

Early Paleozoic Andean-type evolution recorded in the Dunhuang block (NW China): insights from petro-structural, geochronological and metamorphic P−T constraints

Jérémie SODLNER[1]*, Yingde JIANG[2,3], Pavla ŠTÍPSKÁ[5], Karel SCHULMANN[4,5], Chao YUAN[2,3], Robert ANCZKIEWICZ[1]

[1]*Institute of Geological Sciences, Polish Academy of Sciences, Krakow Research Centre, Poland*
[2]*State Key Laboratory of Isotope Geochemistry, Guangzhou Institute of Geochemistry, Chinese Academy of Sciences, Guangzhou, China*
[3]*CAS Center for Excellence in Deep Earth Science, Guangzhou, China*
[4]*Institut Terre et Environnement de Strasbourg, Université de Strasbourg, France*
[5]*Centre of Lithospheric Research, Czech Geological Survey; Prague, Czech Republic*
**Lead presenter*

The Dunhuang block connecting the Central Asian Orogenic Belt to the Proto-Tethyan orogenic system was affected by multiple Paleozoic crustal reworking events. However, relationships between metamorphic ages, P−T evolution and deformational history characterizing these events remain ambiguous. In order to address this issue, P−T−t−D paths of paragneisses from the basement of the southern Dunhuang block were investigated. Inclusions in garnet and kyanite are considered as vestiges of M1 metamorphism corresponding to initiation of the prograde evolution. The earliest continuous metamorphic fabric is an originally steep N-S striking foliation S2. This fabric was further reworked by vertical folds F3 associated with development of a ubiquitous steep E-W striking axial planar foliation S3. The foliation S2 is mainly associated with the Grt–St–Ky–Sil–Bt–Ms–Pl–Qz–Rt and Grt–Ky–Sil–Bt–Kfs–Pl–Qz–Rt assemblages, whereas the S3 foliation is associated with the Grt–Sil–Bt–Ms–Pl–Qz–Kfs–Ilm assemblage. Early prograde (M1) to peak (M2a) metamorphic stages are constrained from 4.0–6.5 kbar and 540–560°C to 9–10 kbar and ~650–675°C. Subsequent decompression is initially accompanied by heating (M2b) up to 6–6.5 kbar and ~730°C, followed by cooling (M3) through 4–6.5 kbar and 550–650°C. In-situ U–Pb dating of monazite combined with monazite trace-element compositions suggest that prograde evolution (M1) most likely started at ca. 406 Ma, peak-P conditions (M2a) were reached at 400–394 Ma, decompressional heating (M2b) took place at 393–391 Ma, and cooling (M3) during exhumation probably occurred at 380 Ma. The prograde metamorphism probably reflects burial during underthrusting of neighboring continental basement below the Dunhuang block. This event culminated in pure shear thickening (D2a) of the whole supra-subduction margin followed by minor heating and exhumation (D2b). The D3-M3 event is interpreted as reflecting exhumation during orthogonal shortening of the system. Combined with the available regional data, this study reveals the existence of a complex tectono-metamorphic evolution for the Dunhuang block characterized by (i) the thickening of a previously thinned arc–back-arc crust recorded at 420–410 Ma in the pro-wedge side of the active margin, followed by (ii) the 410–390 Ma thickening in the retro-wedge side. Such a tectonic evolution resembles Andean-type migration of crustal thickening from the convergent front to hinterlands. The D3-M3 event potentially responsible for the juxtaposition of rocks from different geological occurrences and depths is seemingly independent from this Andean-type orogenic cycle.

Unveiling Late Ediacaran Climatic and Tectonic Dynamics: Insights from Glaciogenic and Post-Glaciogenic Deposits in the Hormuz Complex, Southern Iran

Sadegh ADINEH[1,2,3]*, Prokop ZÁVADA[2], Jiři BRUTHANS[2], Soraya HEUSS-AßBICHLER[3], Mohammad ZARE[4], Anke M. FRIEDRICH[3]

[1]*Institute of Geophysics ASCR, Prague, Czech Republic*
[2]*Faculty of Science, Charles University in Prague, Czech Republic*
[3]*Department of Earth and Environmental Sciences, Ludwig-Maximilians-Universität München, Munich, Germany*
[4]*Department of Earth Sciences, Shiraz University, Iran*
**Lead presenter*

The Ediacaran Period, a pivotal era in Earth's history, witnessed monumental shifts in global climate, atmospheric oxygenation, and biotic innovation, setting the stage for the Cambrian explosion of complex life. This study focuses on the Hormuz Complex within the Zagros Mountains' salt diapir caprock mélange in southern Iran, offering fresh insights into the Late Ediacaran (circa 560 Ma) climatic and tectonic dynamics. Our research unveils a comprehensive sedimentary succession, marked by dolomitic diamictites, cap carbonates, stromatolitic and oolitic dolomites, minor siliciclastics, and evaporites, signifying a period of glacial activity followed by post-glacial marine sedimentation along the eastern margin of Gondwana bordering the ProtoTethys/Panthalassic Ocean.

The identification of dropstone-bearing dolomitic diamictites overlain by cap carbonates, displaying a spectral range of $\delta^{13}C_{VPDB}$ values from -5.5 to +2‰, parallels global Late Ediacaran cap carbonate signatures indicative of post-glacial warming. Notably, the presence of tepee-like structures, crack sheets, and giant ooids within these cap carbonates diverges from conventional Late Ediacaran cap carbonates, aligning more closely with Marinoan post-glacial sedimentation patterns. This unique sedimentary architecture underscores the influence of 'Snowball Earth' conditions on shallow marine environments during the post-Shuram glaciation.

Radiogenic strontium isotopes and εNd(t) analyses of the cap carbonates point to a significant terrestrial input, likely tied to the assembly of Gondwana and resultant tectonic activities. This terrestrial influx, coupled with post-glacial global warming, may have fostered nutrient-rich ocean conditions conducive to microbial carbonate deposition. Our findings suggest a nuanced interplay between climatic shifts and tectonic movements during the Late Ediacaran, contributing to a conducive environment for the development of complex multicellular life forms.

This study not only expands our understanding of the Hormuz Complex's geological significance but also highlights the intricate connections between climate, tectonics, and biotic evolution at a critical juncture in Earth's history. By integrating sedimentological, geochemical, and isotopic data, we offer a comprehensive perspective on the environmental and geological conditions preceding the Cambrian explosion, thereby contributing to the broader discourse on the factors driving the emergence of complex life on Earth.

The Geochemical Data Toolkit (GCDkit) family of tools – a progress report

Vojtěch JANOUŠEK[1]*, Jean-François MOYEN[2], Matthew MAYNE[3], Colin M. FARROW[4], Vojtěch ERBAN[5]

[1]*Czech Geological Survey, Prague, Czech Republic*
[2]*Université Jean-Monnet, Saint-Etienne, France*
[3]*University of Stellenbosch, South Africa*
[4]*Department of Geology, University of Glasgow, Scotland*
[5]*Pragolab Ltd., Prague, Czech Republic*
**Lead presenter email: vojtech.janousek@geology.cz*

During more than 20 years of its existence, our R-language (https://www.r-project.org) software Geochemical Data Toolkit (GCDkit; https://gcdkit.org) became an established standard in recalculation and plotting of whole-rock geochemical data from igneous and metamorphic rocks.

Only recently, however, was unleashed GCDkit.Mineral (https://mineral.gcdkit.org), a much needed package for handling mineral analyses acquired by electron-probe microanalysis. Apart from recalculation to atoms per formula unit (apfu) by a number of methods (with, or without, the Fe2+/Fe3+ estimation), it yields structural formulae, end-member proportions and, for some mineral groups, provides IMA classification. The calculation options, stored externally, can be easily customized, and new calculation schemes/minerals introduced. Both the raw and recalculated data can be subsequently treated by assorted graphical and statistical tools, complemented by those of the standard GCDkit and R.

But even the aging GCDkit continues to be developed. In January was released version 6.2.0, bringing, among other features, new plugin escoRt implementing the expert system of Pearce (1987) to identify the geodynamic setting of ancient igneous rock suites, and functions to calculate ideal mineral compositions based on extensive database of mineral formulae (Le Maitre 1982). The newest addition represents HafAn, a GCDkit plugin for recalculation, visualization and statistical treatment of in-situ U–Pb ages and Hf isotopic data from igneous and detrital zircons. The debugging and writing documentation are coming to the close, and thus the plugin is due to be released soon.

Underway is also preparation of the second edition of our monograph on numerical modelling of geochemical data in R (Janoušek et al. 2016 – Springer) with envisaged publication in late 2025. The volume will be substantially updated and expanded, including brand new chapters on thermodynamically-based models based on established programs MELTS, Perple_X and Rcrust (Mayne et al. 2016). Among other developments, the text shall introduce also our new package for seamless interaction with the MELTS thermodynamic software (https://melts.ofm-research.org), using GCDkit for editing the modelling parameters, as well as plotting and computing complementary trace-element data. Most of the code is ready, and it is currently being optimized for speed, using, inter alia, the powerful tools for parallel R computing.

The development of the GCDkit family tools is supported by the GACR project 22-34175S.

Session V

Chair: Marta Adamuszek

Friday 08:30 – 10:00, 26th April

Sediment Deposition on Moving Salt: Minibasins or Ramp Syncline Basins? Observations from Seismic Data and Numerical Modelling

Naiara FERNANDEZ[1]*

[1]*Helmholtz Centre Potsdam, GFZ German Research Centre for Geosciences, Potsdam, Germany*
**Lead presentere-mail: naiara@gfz-potsdam.de*

Minibasin are small synkinematic basins formed by subsidence into a relatively thick salt layer. On salt-detached slopes, where minibasins experience both subsidence and downslope translation, the base-of-salt geometry strongly influences the mobility and deformation styles of the supra-salt sequence. As gravity drives downslope salt flow, the overlying sedimentary cover (including minibasins) translates along with it. If the base-of-salt is smoothly dipping, the main outcome of the downslope salt flow is the partitioning of continental slope into three different domains: an up-dip extensional domain and a down-dip compressional domain, separated by a translational domain. However, the base-of-salt often exhibits topographic irregularities such as basement steps. Salt is sensitive to the geometry of the basal surface it flows across, and sediments depositing on top of this moving salt can result in characteristic stratal geometries that reflect the salt flow over basal steps. Salt-detached ramp-syncline basins (RSBs) exemplify such characteristic geometries. RSBs are growth synclines formed by translation of the sedimentary cover above a stepped salt detachment and are commonly used to indirectly determine translation magnitudes on salt-detached slopes. While conceptual models of RSBs formation include a pre-kinematic layer, this contribution will show that equivalent geometries result from numerical models of sediments depositing directly on top of the moving salt (i.e., without a pre-kinematic layer). I will also illustrate how a single basement configuration can produce distinct stratal geometries (minibasins and ramp-syncline basins) and will explore the parameters responsible for this variation. Finally, I will discuss how the base-of-salt relief might play a crucial role in the initiation and localization of minibasins.

The influence of passive margin geometry on lateral changes in a salt-detached fold and thrust belt: insights from southern Albania

Márton PALOTAI[1,2]*, Balázs TÖRŐ[1,3]

[1]*CASP, United Kingdom*
[2]*SZTFH Geological Survey, Hungary*
[3]*Eötvös Loránd University, Department of Geology, Hungary*
**Lead presenter e-mail: marton.palotai@sztfh.hu*

The Hellenic fold and thrust belt (FTB) is affected by transverse zones where structures deviate from the regional NW-SE trends. One of these zones, the Borshi–Kardhiqi Transverse Zone (BKTZ) potentially coincides with the onshore termination of the subthrust Sazani Unit. The Sazani Unit is a carbonate platform that constitutes the parautochthonous foreland of the orogen in the NW. In the SE, the external FTB only affects the pelagic Ionian basin.

Two field-constrained cross-sections were constructed and balanced on either side of the BKTZ to quantify the amount of shortening and establish the timing of structures in the two tectonic domains. XS1 runs in the NW from the Sazani coast to the internal nappes. XS2 runs further SE where the Sazani Unit is absent. Field work was also undertaken to describe the structural geology of the BKTZ and to define the former passive margin architecture by identifying pre-orogenic structures.

Regional deformation is thin-skinned and has propagated in a mostly in-sequence manner from Oligocene times. An exception is the likely post-Miocene out-of-sequence reactivation of the Berati thrust in XS1. The amount of shortening along XS1 exceeds that along XS2.

Abrupt thickness variations around the orogen-perpendicular Kardhiqi diapir imply pre-orogenic salt tectonics. Thrust sheets are partly discontinuous across the BKTZ, with evidence for primary welding, backthrusting and rotations. In the lowermost Ionian thrust sheet, thrusting probably originated with a curved trace around the margin of the Sazani carbonate platform. While thrusts in the SE of the BKTZ propagated unhindered towards the SW into the offshore region during the Neogene, in the NW, thrusting has been restricted to the NE of the Sazani platform.

The BKTZ most likely had its origin as a Late Triassic facies boundary between the Sazani carbonates and the Ionian evaporites in the NW and SE, respectively. In the Middle Jurassic, rifting resulted in a NE-SW trending discontinuity between the Apulian/Sazani platform and the Ionian basin. This trend was also present within the Ionian basin to the NE, where the Kardhiqi diapir formed prior to being incorporated into the FTB. The morphology of the carbonate platform and the diapir influenced the location and orientation of the curve in the orogen. The changes in FTB architecture across the BKTZ reflect the buttressing effect of the parautochthonous Sazani platform in the NW and the absence of such a buttress in the SE where the pre-orogenic Ionian basin was wider.

Step-wise inversion of a salt-bearing passive margin – the example of the central Northern Calcareous Alps (Eastern Alps, Austria)

Oscar. FERNANDEZ[1]*, Hugo. ORTNER[2], William E. H. MUNDAY[1], Diethard SANDERS[2], Michael MOSER[1], Bernhard GRASEMANN[1], Thomas. LEITNER[3]

[1]*Department of Geology, Uniersity of Vienna, Austria*
[2]*Deartment of Geology, University of Innsbruck, Austria*
[3]*Salinen AG, Altaussee, Austria*
**Lead presenter*

The Northern Calcareous Alps (NCA) developed initially a salt-rich passive margin from Permian to Early Jurassic times. Subsequently, inversion of this margin initiated in the Middle to Late Jurassic. Cretaceous and Cenozoic deformation only slightly altered the Late Jurassic deformation pattern of the central NCA, such that the early history of inversion has been only mildly overprinted. Initial orogenic deformation in the central NCA (Late Jurassic) was controlled by the location, size and orientation of Triassic salt structures, by the thickness of supra-salt stratigraphy, and possibly by the influence of sub-salt basement faults. Structures of this age are salt overthrusts, plug-fed thrusts, and trains of anticlines and synclines. Middle to Upper Jurassic synorogenic sediments make it possible to date deformation in detail and map out the propagation direction of deformation to be N to NW-directed.

Despite widespread shortening during the Late Jurassic, salt structures were not completely welded, and abundant salt remained into the Early Cretaceous. The Early Cretaceous saw a second phase of deformation led to the development low-angle thrusts with displacement of many kilometers, and the further squeezing of salt structures, with the renewed development of salt allochthons.

Extensional collapse of salt structures ensued during the Late Cretaceous to Paleogene, concentrating above the remaining pods of salt. Despite the exhaustion of salt in the system, structures that originated as salt structures in the Triassic continued to play a critical role in the deformation also into the Neogene.

Grain size reduction induced switch in deformation mechanisms in a salt glacier (Kuh-e-Namak, Dashti, Iran)

Prokop ZÁVADA[1,2]*, Julia SCHMITZ[3] , Janos URAI[†], Karel SCHULMANN[2,4]

[1]*Insitute of Geophysics,Czech Academy of Sciences, Prague, Czech Republic*
[2]*Centre for Lithospheric Research, Czech Geological Survey, Prague, Czech Republic*
[3]*Tectonics and Geodynamics Group, EMR, RWTH Aachen University, Germany*
[4]*EOST, Institute de Physique du Globe, Université de Strasbourg, France*
**Lead presenter, [†]Deceased*

The Kuh-e-Namak (Dashti) salt diapir in Iran represents a well exposed salt structure that consists of a dome and two salt glaciers that were spreading to the north and south from the dome. The dome and adjacent glaciers display a variety of intra-salt folding patterns that indicate recumbent folding of vertical flow layering entering the dome from the diapiric stem and combined downslope viscous spreading and thrusting of salt in both glaciers. We studied a series of microstructures from both the dome and adjacent glaciers using thin-sections of gamma-irradiated salt specimens, electron backscatter diffraction and quantitative analysis of digitized microstructures.

The sequence of samples indicates a transition from dislocation creep dominated recrystallization to fluid-assisted solution precipitation creep and grain-boundary sliding. This is associated with progressive decrease of halite porphyroclasts on behalf of recrystallized matrix of halite grains. Salt in the dome locally contains abundant pores at grain boundaries of large porphyroclasts. Porphyroclasts in domal salt show the highest misorientation values at the grain boundaries and are consumed by almost misorientation-free, rectangular grains. Development of shape preferred orientation (SPO) in glacier salt is inferred from the alignment of the long axis of the elongated halite grains visible in the fabric and rose diagrams of the samples. The grain sizes in domal and glacier salt range between 180 and 500 μm and aspect ratios in average around 2 and up to 4 in the glacier salt. Subgrain piezometry indicates differential stresses of 1.9 to 6.1 MPa, likely reflecting the stress conditions in the cold diapiric stem, because the shear stresses estimated for the glacier are much lower. Estimation for strain rates based on the combination of dislocation creep and solution precipitation creep are in the order of magnitude of 10-10 to 10-09. SPO is interpreted to support the hypothesis that solution-precipitation creep is the dominant recrystallization in glacier salt. Since solution-precipitation creep dominates in salt glaciers at low deviatoric stress, the fine-grained salt deforms much faster than predicted by dislocation creep, allowing the salt glaciers to flow.

Structural characteristic of a bedded rock salt deposit in the Łeba Elevation. Implications for underground storage facility planning

Michał SŁOTWIŃSKI[1]*, Marta ADAMUSZEK[1], Łukasz NOWACKI[2]

[1]*Computational Geology Laboratory, Polish Geological Institute - National Research Institute, Wrocław, Poland*
[2] *Polish Geological Institute - National Research Institute, Warsaw, Poland*
**Lead presenter e-mail: michal.slotwinski@pgi.gov.pl*

Issues of energy security and energy transition cause increased interest in energy storage. One of the most effective methods for energy storage is underground storage of gaseous media, such as natural gas, compressed air, or hydrogen, particularly within caverns leached in rock salt formations. The viability of utilizing a specific rock salt deposit for such caverns depends on many geological factors, including the deposit type (bed, dome, or other), depth, thickness, and internal structure. Given the potential variation of some of the parameters over short distances, it is critical to carefully explore the external and internal structure of deposits.

In this study, we use an example of bedded rock salt Zechstein deposits situated in the Łeba Elevation, which are considered as a prospective area for underground hydrogen storage in Poland. Through a combination of well and seismic data, we obtained a new map showing the top and base of the rock salt as well as its thickness. As compared to the previous work, we significantly improve the resolution and accuracy of information. Within such constrained vertical range of the deposit, we interpreted the internal structure, i.e. localisation of non-salt interlayers and zones of decreased purity of rock salt. Furthermore, we have examined the rock salt grain size variation within the selected boreholes, highlighting their significant impact on the mechanical behaviour of rock salt and the stability of the potential salt caverns.

A comprehensive analysis of various geological factors enabled us to establish constraints on the optimal placement of storage facilities. A key geological factor determining these constraints was the strong variation of thickness, resulting from the system elevations and depressions of the sulphate layer underlying the salt layer – the so-called anhydrite ridges. Secondary constraining factors were related to the internal structure of the salt bed, namely occurrences of thick sulphate (anhydrite and polyhalite) interlayers and the significant admixtures of dispersed clay material in the salt. While the grain size data is too dispersed to serve as a useful constraining tool, it underscored a strong variability crucial for cavern design planning. The provided example clearly shows the importance of geological exploration and interpretation in minimizing risk in the process of developing underground cavern storage facilities.

Session VI

Chair: Artur Sobczyk

Friday 10:15 – 12:00, 26th April

Post-Variscan tectonics in Germany: The role of inherited structures (and can we even tell?)

Jonas KLEY[1]*

[1]*Geoscience Center, University of Göttingen, Germany*
**Lead presenter*

Germany, except for its northernmost part, was affected by the Variscan orogeny until about 300 Ma, immediately followed by the Rotliegend basin-and-range type rift established across both the orogen and its northern foreland. From Zechstein to mid-Triassic time, a superimposed intracontinental basin subsided continuously, accompanied by intermittent low-magnitude extensional tectonics. Especially in northern Germany, extension intensified in Late Triassic through Early Cretaceous time, followed by a Late Cretaceous event of shortening and basin inversion across the country. Renewed rifting in Cenozoic time led to the triradiate arrangement of the Upper and Lower Rhine grabens (URG and LRG) and Eger rift (ER). Apart from the amply documented Late Cretaceous reactivation, these multiple tectonic events have always invited hypotheses explaining specific faults or fault sets as reactivated structures from an earlier phase. However, only some of these are well documented. The largely covered and incompletely known Rotliegend rift comprised a network of SW- and NW-trending basins. many of them probably fault-bounded. The SW-trending basins demonstrably follow the Variscan structural grain which is uniformly SW-NE except for easternmost Germany. NW-striking Variscan transverse structures and/or parallel Rotliegend faults may in part have controlled the predominant NW strike of most Mesozoic structures, as shown in 3D seismic data and by instances where just a few faults of NW-striking sets in Variscan basement have been mapped as continuing into the Mesozoic cover. In other cases, such as the prominent northern Harz fault, reactivation is only inferred with no stratigraphic or structural evidence. Prominent N- to NNE-striking transfer zones which link the main Mesozoic structures apparently have no precursors in the Variscan basement. A long, linear swath of NNE-striking faults extending from the Upper Rhine graben to northern Germany has been interpreted early as an old fault zone running from the Mediterranean to the Oslo rift. In detail, a Rotliegend fault origin is interpreted along the Rhine graben and in northern Germany. The central segment is a poorly understood, very wide and gentle, east-side-up flexure forming the eastern border of a major Buntsandstein depocenter and the Jurassic-Cretaceous Lower Saxony basin, yet with no large basement faults. The Cenozoic rifts generally follow this structural trend (URG), the NW direction (LRG) and the Variscan structural grain (ER), but also crosscut basement structures. Reactivation of inherited structures should not be used as a standard template for interpretation but needs to be demonstrated and understood for each individual case.

Thick- versus thin-skinned thrusting within the NW Qaidam Basin, Tibet, China – insight from high-resolution 3D seismic data

Piotr KRZYWIEC[1]*, Fanwei MENG[2], Adam BARANOWSKI[1], Wenhang LIU[1], Stanisław MAZUR[3]

[1]*Institute of Geological Sciences, Polish Academy of Sciences, Warsaw, Poland*
[2]*School of Resources and Earth Sciences, China University of Mining and Technology, Xuzhou, China*
[3]*Institute of Geological Sciences, Polish Academy of Sciences, Kraków Research Centre, Poland*
**Lead presenter e-mail: piotr.krzywiec@twarda.pan.pl*

Cenozoic closure of the Tethys Ocean in central Asia was associated with formation of an extensive zone of tectonic compressional deformations reaching the N margin of the Tibetan Plateau and beyond. One of the northernmost zones of youngest compressional deformations is known from the NW part of the Qaidam Basin, located within the Tibetan Plateau in W China. Previous structural models for this zone, either based solely on surface field data and rather conceptual, or based on 2D seismic data with limited depth imaging, have suggested the presence of a rather simple thrust fault system rooted within the pre-Cenozoic (Meso-Paleozoic) basement and associated folds developed within the Paleogene-Neogene shallow water to terrestrial sedimentary succession of the Qaidam Basin. High-quality 3D seismic data acquired above the Jandingshan, Heiliangzi i Janbei anticlines in the NW Qaidam Basin proved that a much more complex model should be used to explain the structure and evolution of this compressional belt. The new model, supported by a balanced cross-section constructed using seismic data, consists of two main components: (1) thin-skinned thrusts detached within the Eocene evaporites, and (2) thick-skinned thrusts and backthrusts developed with the deeper Meso-Paleozoic basement. Shallow growth strata precisely imaged by seismic data indicate very recent, Pliocene – Quaternary thrusting, uplift, and localized erosion. The proposed structural model also provides new clues about the origin of present-day salinity of numerous lakes located in the Qaidam Basin. At least partly this salinity might be related to erosion and redeposition of Eocene evaporites that were transported to the surface along recently active thin-skinned thrusts detached within evaporitic horizon.

Seismic data used in this study was kindly provided by China National Petroleum Corporation (PetroChina) which is acknowledged with many thanks. IHS Markit is thanked for providing academic license of the Kingdom seismic interpretation software. This study was supported by statutory research funds of Institute of Geological Sciences, Polish Academy of Sciences.

Mesozoic structural evolution of the Bükk, Darnó and Recsk areas (NE Hungary)

Szilvia KÖVÉR[1,2], János HAAS[2], Ottilia SZIVES[3], Péter OZSVÁRT[4], Ágnes GÖRÖG[5], Éva ORAVECZ[1], Benjamin SCHERMAN[1], László FODOR2[1,*]

[1]*Institute of Geography and Earth Sciences, Eötvös University, Budapest, Hungary*
[2]*HUN-REN Institute of Earth Physics and Space Science, Sopron, Hungary*
[3]*Supervisory Authority for Regulatory Affairs, Budapest, Hungary*
[4]*HUN-REN MTM-ELTE Paleontological Research Group, Budapest, Hungary*
[5]*Hantken Foundation, Budapest, Hungary*
**Lead presenter*

The relationship between the Dinarides-related (Bükk, Darnó, Recsk) and Austroalpine units (ALCAPA) was investigated in space and time in Northern Hungary. 3 areas were regarded: the westernmost Bükk Mts., the Darnó Hill within the Cretaceous(?) to Miocene Darnó Fault Zone, and the westernmost Recsk area, where the Mesozoic basement is located under Paleogene sediments and the Recsk Andesite Complex. Regarding T-J stratigraphy and structural evolution, the following results are found:

- Late Triassic stratigraphy is different, pelagic limestones/platform carbonates on the E, vs. cherty dolomite on the W.
- Early Jurassic sediments are missing on the E, while the succession is continuous (pelagic limestone) on the W. This western part (Recsk) shows significant similarities towards the successions of the coeval Slovenian Basin.
- Mid-Jurassic, probably Bajocian to Bathonian or Callovian normal faults bounded half-grabens in all areas, which was evidenced by extensional structures in outcrops and thickness changes + talus breccias in boreholes.
- While the depositional environment during the J_{2-3} in most of the 3 areas was slope to basin, the presence of the Dinaridic carbonate platform or its imminent slope is verified in the south-westernmost borehole Rm-109.
- The Late Jurassic Darnó mélange is similar to other Neotethyan mélanges; it has a nappe position over the J_{2-3} sedimentary infill of the half-grabens.
- No clear evidence of ophiolitic mélange is present W of the Darnó FZ. Here, the encountered breccia or conglomerate levels were derived from the same basin and can be interpreted as fault-related talus breccia or collapse of the deep marine slope.
- No transport direction is known from the Darnó Hill, but in the surrounding SE facing overturned folds may indicate top-to-ESE emplacement, similarly to the SW Bükk Mts. The original vergency of the folds could be southerly.
- South-verging nappe emplacement and thrusting later distorted by the sinistral shear of the Paleo-Darnó Shear Zone. The sinistral shear zone could be coeval with dextral shearing in the Eastern Bükk dated around 80 Ma. The north-verging thrusting of the Bükk Nappe System over the Uppony Paleozoic along the Nekézseny Thrust is late Cretaceous (~70 Ma).
- We correlate this thrusting with a major deformation during which several north Hungarian units were emplaced on top of units which could be part of the Mesozoic ALCAPA block.

The research was supported by National Research Found 134873 of László Fodor.

Reconstructing the tectonic movements of Adria in the Mesozoic based on quality controlled apparent polar wander path using the GPlates software package

Máté VELKI[1,2]*, Emő MÁRTON[2], Szilvia KÖVÉR[3,4], László FODOR[3,4]

[1]*Eötvös University, Institute of Geography and Earth Sciences, Department of Geophysics and Space Sciences, Budapest, Hungary*
[2]*SARA, Department of Geophysical Research, Paleomagnetic Laboratory, Budapest, Hungary*
[3]*HUN-REN Institute of Earth Physics and Space Sciences, Sopron, Hungary*
[4]*Eötvös University, Institute of Geography and Earth Sciences, Department of Geology, Budapest,Hungary*
**Lead presenter e-mail: velki.mate@gmail.com*

Apparent polar wander paths (APWPs) calculated from paleomagnetic data can provide quantitative information about paleolatitudes and paleo-orientations. A recently submitted work provided a Mesozoic APWP for northern "extended" Adria, based on the integrated paleomagnetic data set of stable and imbricated Adria, as well as the Transdanubian Range. The APWP was defined with different, widely used methods, namely with running mean averaging and spherical spline fitting, resulting in closely correlating trends.

In this study the paleo-positions of Adria between 200 and 70 Ma were represented by the so defined Adriatic APWP in the GPlates software package with the embedded paleomagnetic tools. Contemporaneous relative positions of Adria with respect to Europe, Africa and Iberia were reconstructed by using global models for the latter three, published in 2012 and more recently, in 2021, both using the same paleomagnetic data. These models used different APWP generation methods, and the derivated APWPs are somewhat different. However, the comparison to either of them to the newly compiled APWP for Adria suggests that this latter must have moved independently from Africa in the following steps:

• by a large clockwise rotation followed by a counter-clockwise rotation of an equally large angle between 180–150 Ma and 150–120 Ma, respectively.

• and probably by drifting away from Africa northward between 150 and 115 Ma than back to a more southerly position, close to Africa by 100 Ma.

Reconstruction models of the Mediterranean area are usually based on geological and structural observations and occasionally used selected paleomagnetic data only as a control. The reconstruction of the present study primarily relies on paleomagnetic data, and the reconstruction was tested against geological and tectonic observations.

The research was supported by the project K128625 and K134873 of the NKFIH (National Research, Development and Innovation Office of Hungary).

Tectonic and sedimentary mélanges in the Pieniny Klippen Belt

Jan GOLONKA[1]*, Anna WAŚKOWSKA[1], Kamil CICHOSTĘPSKI[1], Jerzy DEC[1], Monika ŁÓJ[1], Grzegorz BANIA[1], Włodzimierz Jerzy MOŚCICKI[1], Sławomir PORZUCEK[1], Józef CHOWANIEC[2]

[1]Faculty of Geology, Geophysics and Environmental Protection, AGH University of Krakow, Poland
[2]Polish Geothermal Society, Krakow, Poland
**Lead presenter e-mail: jgolonka@agh.edu.pl*

Both tectonic and sedimentary processes (undersea mass movements) contributed to the formation of mélanges in the Pieniny Klippen Belt (PKB). PKB is located in Austria, Slovakia, Poland, Ukraine, and Romania, constituting the 600 kilometers long suture zone between Central and Outer Carpathians. The name Klippen Belt comes from the presence of "Klippen" in this structure, i.e. elements contrasting with the surroundings. The harder and more resistant to erosion Klippen are located among less resistant clastic formations, i.e. sandstones, mudstones and marls. These Klippen are made of limestones and radiolarites that were deposited in the ridge or slope parts of the PKB basins, while the flysch complexes containing sandstones mudstones and marls were deposited in the deeper parts of these basins. . Some of the Klippen are olistoliths, i.e. homogeneous or complex rock blocks of various sizes that were moved by gravity to the deeper zones of flysch basins. Other Klippen entered the flysch formations as a result of tectonic deformations that took place during orogenic movements. Collisions and mutual shifting of lithospheric plates resulted in the formation of the structure of the PKB, which takes the form of the so-called flower structure, limited on both sides by deep faults. After uplift, the PKB was subject to erosion processes, which led to the removal of less durable complexes and the removal of shallower limestone blocks, which today form Klippen clearly visible in the landscape.

Geophysical studies, i.e. seismic, gravimetric and geoelectric, allow obtaining an image of the geological structure of areas where outcrops do not provide sufficient. Seismic methods are based on the analysis of the seismic waves in the Earth's interior. Gravimetric tests record anomalies that reflect the distribution of the bulk density of rock masses, and geoelectric tests use the diversity of rocks in terms of electrical resistance. The results of geophysical research carried out using all three methods on the profiles crossing the Spiskie Pieniny Mountains. There is a very good correlation of geophysical studies with the results of geological mapping.

The mélange characteristics of the PKB is a result of the Cretaceous–Miocene folding, moving and uplifting processes that created a mixture of strike-slip-bounded tectonic blocks, thrust units, as well as toe-thrusts and olistostromes. Both tectonic and sedimentary events contributed to the creation of this mélange.

The research was financed by the National Science Center, grant NCN -2019/35/B/ST10/00241.

Late Cretaceous - early Palaeogene inversion-related tectonic structures in the Sudetes and their northern foothills – short overview and new data

Andrzej GŁUSZYŃSKI[1]*, Paweł ALEKSANDROWSKI[2]

[1]Polish Geological Institute - National Research Institute, Warsaw, Poland
[2]Polish Geological Institute - National Research Institute, Lower Silesia Branch, Wrocław, Poland
**Lead presenter e-mail: aglu@pgi.gov.pl*

The Variscan basement in the Sudetes and their foreland is partly overlain by post-orogenic Permo-Mesozoic sedimentary cover, containing a wide spectrum of contractional tectonic structures, both brittle and ductile, in the past referred to as young Saxonian or Laramide in this area. The largest in size are two regional-scale synclinoria: the North Sudetic and the Intra-Sudetic ones, extended in NW-SE direction. We show a number of examples of tectonic structures scattered throughout the area and coming from quarries, underground mines and natural outcrops, as well as taken from the literature. Presented are also results of our interpretation of newly reprocessed legacy reflection seismic profiles from both the Sudetic synclinoria. The tectonic structures produced in the post-Variscan cover of the Sudetes and the adjacent areas include gentle to moderate folds of buckling and fault-related origin, as well as high-angle reverse faults, some of them showing a strike-slip component. Present are also low-angle thrusts, probably rooted in (older fractures in) the crystalline basement. The structures described as grabens by previous authors, are often bounded by reverse faults (‘reverse grabens’) and reveal strongly synclinal pattern of their sedimentary fill. The top of crystalline basement in the North Sudetic Synclinorium below the cover is synformally down-warped with a wavelength of up to 30 km, whereas on the elevated areas, where the basement top is exposed at the surface, it seems to be, similarly, up-warped (i.e. tectonically buckled). The reviewed compressional structures show, as a rule, NW-SE trending strikes or axes that fit the regionally-known orientation of the Late Cretaceous – Early Palaeogene tectonic shortening direction of NE-SW to NNE-SSW in this part of Europe. The same applies to the regional joint pattern, typically comprising an orthogonal system of steep joints of NW-SE and NE-SW strikes. Some of the reviewed faults with strike-slip component of motion may have been also affected by a later, Late Cenozoic, tectonism. As the low- or medium-angle thrust faults identified from the seismics in the Permo-Mesozoic strata are often rooted in the top levels of the Variscan basement, particularly in the Intra_Sudetic Synclinorium, therefore some elements of the thick-skinned style of shortening can be expected in the deep crystalline basement. It is, therefore, likely that also outside the areas covered with Permo-Mesozoic sedimentary sequences, some (even major) faults interpreted in the Sudetes from surficial geological maps and outcrop relationships in the crystalline basement as vertical or high-angle structures, may have at depth a geometry of low-angle thrusts. This may have important practical implications for e.g. geothermal prospecting in the Sudetes, where the deep groundwaters in the crystalline basement circulate, almost exclusively, along structural discontinuities, such as fault zones and fracture corridors.

Session VII

Chair: Marcin Dąbrowski

Ftriday 13:30 – 15:00, 26th April

Are the Carpathians recently tectonically active?: new challenges and opportunities for the study of present-day tectonic stress and strain

Marek Jarosiński[1]*

[1]*Polish Geological Institute - National Research Institute, Warsaw, Poland*
**Lead presenter e-mail: marek.jarosinski@pgi.gov.pl*

Poland has experienced an episode of shale gas exploration, which extends the scope of geomechanical modelling based on deep borehole data. To show the new opportunities and challenges in the recent stress investigations we present new geomechanical models (GM) for the Polish Outer Carpathians (POC) and the East European Craton (EEC).

In the POC, 3 wells located at the top of the anticlines show a systematic stress rotation from NE-SW to W-E (= trends of the anticlines). For the deepest of these wells, D-1 (5.5 km), a 1D GM was performed, based on the borehole wall failure, hydraulic fracturing tests and continuous profiles of mechanical parameters and pressures. The GM indicated that the upper part of the accretionary wedge, above the Main Thrust Fault (MTF) is in a critical stress state in the strike-slip and thrust faulting tress regimes. Elastic strain decoupling at the MTF indicates its reactivation, leading to thin-skinned compression in its hanging wall, resulting in the S_H rotation due to buckling of the pre-existing anticline. In the footwall of the MTF, further S_H rotation towards N-S was observed and the strike-slip and normal faulting stress regimes were determined, implying that the Carpathian basement decollement is recently inactive. Comparison of the new results with previous stress analysis reveals the complex but consistent stress pattern for the eastern segment of the POC. The NE-SW S_H is consistent with a regional stress direction for the nappes, that could be generated by the ALCAPA push causing thin-skinned compression and folding in the upper part of the accretionary wedge. The lower part of the wedge is inactive, except in the vicinity of the Pieniny Klippen Belt suture, where earthquakes occur. Within the POC, contraction in both principal directions rules out the concept of an ongoing extensional collapse, postulated by some authors.

1D GMs for four wells from the Early Palaeozoic shale sequences of the Baltic Basin indicate strong stress stratification with normal, strike-slip, and reverse faulting stress regimes correlating with the litho-stratigraphical units. In all wells, the gravitational load component of the horizontal stresses dominates over the tectonic component generated by horizontal strains. Despite the large distance between the boreholes (up to 100 km) similar present-day elastic strains are modelled across the Baltic Basin.

The new opportunities arise from the integration of the borehole GMs with the present-day strain rate measured by the permanent GNSS stations, with the seismological data and the rheological models. For the Pomeranian region, a good fit between the directions of S_H and geodetically derived contraction is shown. The measured geodetic strain rates for individual tectonic units are inversely proportional to the integrated strength of the lithosphere. The strike-slip stress regime for the crystalline basement of the EEC was inferred from geodetic strain rates and seismicity. To trigger the Sambian earquakes, 4 Ma of elastic strain accumulation was required to reach the current strain rate. We found that the elastic strain in the crystalline basement is more than an order of magnitude higher than in its shale cover. This could be explained by a higher rate of viscous relaxation in the shale than in the basement. Among the many possibilities offered by GM, a major challenge is the implementation in them viscous relaxation of sedimentary complexes.

Deciphering Meso-Cenozoic exhumation history of the NE Bohemian Massif using low temperature multi-thermochronometry

Artur SOBCZYK[1]*

[1]*Institute of Geological Sciences, University of Wrocław, Poland*
**Lead presenter: artur.sobczyk@uwr.edu.p*

Low-temperature thermochronology, is a technique dedicated to analysing the thermal history of rocks, being typically applied for the temperature range of ~ 40-240°C. Regional analyses of apatite (AHe) and zircon (ZHe) dating using the (U-Th)/He and apatite fission-track (AFT) methods in the Sudetes (NE Bohemian Massif) highlight a pronounced prevalence of Late Cretaceous-Paleogene cooling ages (~45-90 Ma). A comprehensive regional analysis of the AFT dating results distribution suggest existence of two distinct areas of post-Variscan increased bedrock exhumation within the NE Bohemian Massif. To the NW it was represented by the Karkonosze-Izera Massif (KIM) with AFT cooling ages ca. 90 Ma, whereas to the SE by the easternmost Orlica-Śnieżnik Dome (OSD) area (AFT cooling ages ~ 84 Ma). Late Cretaceous build-up of these increased exhumation zones resulted in formation of NE-SW-oriented zone, characterized by delayed Neogene cooling onset. This zone of younger cooling ages extended from the Fore-Sudetic Block, traversing the Sowie Mountains Massif, and reaching the western perimeter of the Intra-Sudetic Basin. Spatial distribution of AFT cooling ages is positively correlated with the inferred 150 km topographic wavelength of the Sudetes. Observed prevalence of Late Cretaceous-Neogene cooling events signifies intensive tectonic exhumation of the Sudetic Block, coupled with basin inversion during the Early Cenozoic. Over the past 60-70 million years, erosion in the Sudetes region has amounted to approximately 3-3.5 km, with an average crustal exhumation estimated at 0.04 km per million years since the Late Cretaceous. Notably, zircon helium dating (ZHe) analyses also reveal Cretaceous and younger cooling ages indicating to erosion of approximately 5-6 km. These observations suggest deep burial of the Sudetes region during the Late Cretaceous marine transgression, challenging previous paleogeography models. The youngest recorded cooling episodes of NE Bohemian Massif correspond to the Eocene (~39-40 Ma), coinciding closely with basaltic volcanism documented by K-Ar and Ar-Ar dating methods. Thermochronological dating reveals that the youngest, Neogene phase of tectonic activity in the NE Bohemian Massif region is not captured in thermochronological records, indicating that Late Cenozoic uplift of individual tectonic blocks in the NE Bohemian Massif area was limited to less than 1.5 km.

Uncommon stress path from the coal seam to a fold hinge zone as an effect of a neotectonic deformation pattern

Maciej J. MENDECKI[1]*, Jacek SZCZYGIEŁ[1], Grzegorz LIZUREK[2], Lesław TEPER[1]

[1]*Institute of Earth Sciences, University of Silesia, Sosnowiec, Poland*
[2]*Institute of Geophysics, Polish Academy of Sciences, Warsaw, Poland*
**Lead presenter*

Usually, mining seismicity is induced by direct operations conducted underground. The causes of such seismicity are mainly excavations, cavings and rockburst prevention blasts. Focal mechanisms of the induced seismic events follow surrounding cracks, directions of longwall advance, and/or gob edges located over or beneath the excavating coal panel. Often, the calculated mechanisms (full seismic tensor moment solutions) show that the dominating component in the source is an isotropic part, which is related to explosion or implosion forces acting there. However, the location of a coal seam can be associated with geological structures disturbing local stress distribution. For such settings, the strain energy is accumulated on weaknesses related to these geological structures: faults, fractures, and folds. The cumulated stress is not enough to produce a seismic event. Still, stress transfer from the excavating field can exceed the local stress value over the endurance limit and trigger a tremor. The mechanisms of the triggered seismic events are often represented by a double couple component, similar to natural events, and reflect the geometrical parameters of discontinuities. Taking into account mentioned above, we analysed mining tremor mechanisms and principal stress directions to compare characteristics of seismic events and stress regimes with tectonic settings in the Bytom Syncline, located in the Upper Silesian Coal Basin, Poland.

The results of seismic moment tensor inversion calculated for 41 events with magnitudes >M2.0 were used to trace changes in types of mechanism (normal, strike-slip, reverse) with the progress of mining from Panel 3, coal seam 503, the Bobrek Mine. The data was sourced from the IS-EPOS Platform, an open data infrastructure for the study of anthropogenic hazards linked to georesource exploitation. The foci were located below the seam and followed a longwall excavation. The computed mechanisms and distribution of spatial-temporal events enabled three clusters representing three different stages of stress regimes to be distinguished. The stress path from the coal seam to its hinge via the syncline limb was deciphered. The calculated principal stress axes indicated the main stress directions present in the studied area, enabling a local model of the derivative pattern of neotectonic deformation to be described. The regime changed from horizontal extension in the syncline limb (first cluster) to transpression (second cluster) to dominating compression in the hinge (third cluster), resulting in reverse fault production. Finally, the results revealed the causes of seismicity in the studied area and showed that the studied events had been mostly triggered.

Hidden Faults: Post-Miocene tectonics of the Northern Calcareous Alps inferred from caves deformation

Jacek SZCZYGIEŁ[1,2]*, Ivo BAROŇ[3], Rostislav MELICHAR[4], Lukas PLAN[5], Ivanka MITROVIĆ-WOODELL[2], Eva KAMINSKY[6], Denis SCHOLZ[7], Bernhard GRASEMANN[2]

[1]*Institute of Earth Sciences, University of Silesia, Sosnowiec, Poland*
[2]*Department of Geology, University of Vienna, Austria*
[3]*Institute of Rock Structure and Mechanics, Czech Academy of Sciences, Czech Republic*
[4]*Department of Geological Sciences, Faculty of Science, Masaryk University, Czech Republic*
[5] *Karst and Cave Group, Natural History Museum, Austria*
[6]*Institute for Soil Physics and Rural Water Management, University of Life Sciences BOKU, Austria*
[7]*Institute for Geosciences, Johannes Gutenberg University Mainz, Germany*
**Lead presenter e-mail: jacekl.szczygiel@us.edu.pl*

The Northern Calcareous Alps (NCA) are intersected by strike-slip faults, which facilitate the mountain range's N-S shortening and E-W stretching. However, pinpointing the timing of fault activation has been challenging due to the need for absolute dating methods for Neogene deposits. Consequently, there exists a gap in our understanding of the tectonic evolution post-Miocene, exacerbated by the destruction of geomorphic signals caused by glaciation. Fortunately, karst caves can serve as indicators of geomorphic displacement, offering insights into timing through 230Th/U dating of broken speleothems. We identified 172 reactivated faults in 28 caves adjacent to major faults, with some dated using the 230Th/U method. Using inversion methods, we computed paleostress.

We observed extensional relay along the Königsee-Lammertal-Traunsee Fault in Göll and Hagengebirge, while in Tennegebirge, we noted dextral shear along the Lammertal fault. In Dachstein, the orientation of faults and their reverse sense indicated N-S shortening. Moving further east, NNE compression related to the Salzach-Ennstal-Mariazell-Puchberg fault (in Totes Gebirge and Hochschwab), as well as the Mur-Mürz Fault, resulted in sinistral shearing along them. The extension along the margins of the Vienna Basin aligns with the pull-apart basin opening mode along the Vienna Basin Transfer Fault. These changes in compression trends between major fault segments are consistent with the broader trend in the Eastern Alps. In the western segment of the NCA, north of the Tauren Window, alignment in the convergence axis indicates dominant N-S shortening. Further east, the influence of the extruded main wedge becomes stronger, leading to compression towards the NE.

Our findings suggest that the NCA has experienced N to NE-trended compression since the Middle Pleistocene, as indicated by 230Th/U dating and possibly since the Pliocene, as inferred from the maximum cave age. Thus, we confirm the prevalence of post-Miocene lateral extrusion over gravitational collapse based on the geological record.

Unearthing the Past: Challenges and Perspectives in Archaeoseismological Exploration Across Southern Poland

Krzysztof GAIDZIK[1]*, Miklós KÁZMÉR[2]

[1]*Institute of Earth Sciences, Unversity of Silesia in Katowice, Sosnowiec, Poland*
[2]*Eötvös University, Budapest, Hungary*
**Lead presenter e-mail: krzysztof.gaidzik@us.edu.pl*

The completeness of seismic catalogs is consistently questionable, given the time limitations of instrumental data and the often sparse and incomplete nature of historical records. Consequently, seismic hazard modeling faces considerable challenges, especially in intraplate regions characterized by low strain rates and corresponding low to moderate seismic activity. The extended recurrence periods typical of such areas render the short observational span of instrumental seismology (approximately 120 years) insufficient for characterizing the seismicity of low-strain regions. This prolonged recurrence also leads to significant gaps in historical records that may underestimate the seismic potential of these regions. On the other hand, worldwide examples prove the occurrence of large earthquakes in seemingly stable continental regions. In addressing these limitations, archaeoseismology may play a pivotal role in bridging historical earthquake record gaps, thereby enhancing seismic hazard assessments. This is particularly true for regions opulent in archeological sites and/or medieval structures (especially churches).

In that respect, Poland presents numerous challenges but also perspectives in archaeoseismological exploration. Due to low seismicity levels, many parts of the country lack instrumental earthquake records, resulting in poor seismic recognition. Historically, some areas, notably the Sudetic Foreland, Teisseyre-Tornquist Zone, and Precambrian Platform, have experienced isolated earthquakes with intensities of 6-7. However, these events are singular and have not recurred. The Western Carpathians, particularly the Pieniny Klippen Belt and Orawa-Nowy Targ Basin, exhibit more seismic activity, with continuous tectonic monitoring in the latter since August 2008 confirming ongoing activity. Many regions in Poland, e.g., Lower Silesia, Holy Cross Mts., Lesser Poland (Małopolska), etc., show a long history of human occupation with abundant medieval to XX-century buildings presenting the rich history of damage/repair/renovation suitable for archaeoseismological studies, however time-limited to 12-13th century AD in most of the cases.

Pilot studies conducted in Lower Silesia, Holy Cross Mts., and other regions of Poland confirm the potential of these sites for archaoseoseismological studies. Nevertheless, they also pose significant challenges, particularly in terms of accurately dating events and identifying the origin of seismic activity. This project is in progress, and further studies are needed complemented by modeling, geophysical surveys, and dating.

Session VIII

Chair: Rafał Sikora

Friday 15:15 – 15:45, 26th April

Depleted highly-mobile landslides and other slope deformations associated to active tectonic ruptures in the Outer Western Carpathians, Czech Republic

Ivo BAROŇ[1]*, Jia-Jyun DONG[2], Rostislav MELICHAR[3], Martin ŠUŤJAK[3], Filip HARTVICH[1], Jan KLIMEŠ[1], Chia-Han TSENG[4], Yi-Chin CHEN[5], Tùng NGUYỄN[2], Che-Ming YANG[6], Václav DUŠEK[3], Lenka KOCIÁNOVÁ[3], Jan ČERNÝ[3], František BÁRTA[3], Régis BRAUCHER[7], Piotr MOSKA[8], Tomasz GOSLAR[9], Li-Wei KUO[2], Cheng-Han LIN[10]

[1]Institute of Rock Structure and Mechanics, Czech Academy of Sciences, Prague, Czech Republic
[2]Department of Earth Sciences, National Central University, Taoyuan, Taiwan
[3]Department of Geological Sciences, Masaryk University, Brno, Czech Republic
[4]Chinese Cultural University, Taipei, Taiwan
[5]National Changhua University of Education, Changhua, Taiwan; [6]National United University, Miaoli, Taiwan
[7]CNRS CEREGE LN2C, Aix en Provence, France; [8]Silesian University of Technology, Gliwice, Poland
[9]Poznan Radiocarbon Laboratory, Poland; [10]National Taiwan University, Taipei, Taiwan
**Lead presenter*

Co-seismic landslides are dangerous secondary effects of earthquakes, but any comprehensive method to distinguish them from the rainfall-triggered ones is still missing. Based on our experience gained in Taiwan and other regions, the seismic triggers lead to intense and rapid rock-mass disintegration and high mobility, and therefore we assume that they might be differentiated from their rainfall-triggered counterparts by a number of morphological and structural characteristics. To test this hypothesis, we have examined present-day landslides in a very active setting with well-known and intensive rainfall and EQ triggers in Taiwan. We used a unique combination of novel and well-established geological, morphometric, statistical, and numerical methods, and compared those ones with the slides in a tectonically similar region of the Outer Western Carpathians in the Czech Republic, where both types of triggers were possible, but less intensive and historical information did not allow to distinguish them.

While the 1999 Chi-Chi EQ and 2022 Taitung EQ coseismic and 2009 Morakot Typhoon-related landslides were investigated in detail in Taiwan, the area of the Outer Western Carpathians was inspected using the high-resolution LiDAR digital terrain models, where hundreds of depleted highly mobile paleolandslides have been identified. Selected landslide and fault cases were then studied by means of structural mapping, geophysical ERT surveying and radiometric dating. Very specific structures of underdip overturned topples at sandstone beds originally dipping downslope have been identified at different scales in the Javorníky Mts. and Vsetínské Hills near the investigated active Holocene faults. Distinct fault activity phases revealed by paleoseismologic methods have been then compared to depleted-landslide ages, revealing possible prehistoric seismotectonic events throughout the entire Holocene and last glacial. Host rock samples were then analysed using standard geomechanical tests, while dynamic behaviour of studied rock types was analysed using the state-of-the-art rotary shear.

instruments. These analyses are crucial for the creation of landslide numerical models and understanding the rock behaviour under the dynamic loading. The research is still under progress and offers an outstanding opportunity to integrate the expertise from Czechia and Taiwan.

These activities have been supported by the Grant Agency of the Czech Republic (GC22-24206J), the Taiwanese National Technological and Science Council (MOST/NTSC 111-2923-M-008-006-MY3) and by the project “RENS - Rock Environment and Natural Resources” of the Technology Agency of the Czech Republic (SS02030023).

Application of magnetic susceptibility anisotropy in landslide accumulations

Václav DUŠEK[1]*, Rostislav MELICHAR[1], Jan ČERNÝ[1], Martin ŠUŤJAK[1], František BÁRTA[1], Ivo BARONŇ[2], Yi-Chin CHEN[3], Jia-Jyun DONG[4], Filip HARTVICH[2], Jir-Ching HU[5], Jan KLIMEŠ[2], Lenka KOCIÁNOVÁ[1], Tùng NGUYỄN[4], Matt ROWBERRY[2], Chia-Han TSENG[6]

[1]*Department of Geological Sciences, Faculty of Science, Masaryk University, Brno, Czech Republic*
[2]*Institute of Rock Structure and Mechanics, Czech Academy of Sciences, Prague, Czech Republic*
[3]*National Changhua University of Education, Taiwan*
[4]*Graduate Institute of Applied Geology, National Central University, Taiwan*
[5]*Department of Geosciences, National Taiwan University, Taiwan*
[6]*Institute of Earth Sciences, Academia Sinica, Taiwan*
**Lead presenter e-mail: 484219@mail.muni.cz*

The Anisotropy of Magnetic Susceptibility (AMS) refers to the preferred orientation of magnetic minerals in rocks and soils. This orientation was induced in the past by a certain process, the character of which can be analyzed using a 3D kappa bridge machine, which measures AMS. To analyze the preferred orientation in landslides, over 700 soil samples have been collected from three recent landslides in Taiwan (including locations Tsaoling, Yiufengershan, and Yuli) and 2 paleolandslides in the Czech Republic (Javorníky Mountains and Pálava region). Results of AMS analysis comprises of two main components: (1) magnetic lineation, which is the line parallel to the direction of maximum stretching of magnetic minerals. In landslides, this component indicates the sense of movement. (2) Second component is magnetic foliation, which is the plane in which the direction of maximum and intermediate stretching lies. These two magnetic characteristics allow us to interpret the position of studied sediments within the landslide mass. In the source area and in the middle part, the magnetic lineation is parallel to the direction of sliding and the magnetic foliation is subhorizontal. The situation is different in the lower part of landslides, where the magnetic lineation is subhorizontal and perpendicular to the direction of movement, and the magnetic foliation is subvertical indicating a displacement of the material sideways. Furthermore, at the frontal part of the Tsaoling landslide, where the mass collided with the bedrock on the opposite hill, the magnetic foliation was steep, almost subvertical, and the magnetic lineation was horizontal. In the material further from the bedrock, simple shear deformation was interpreted with the magnetic foliation rotating around the magnetic lineation. The method was also successful in identifying 2 landslide masses lying on each other in several locations. The method allowed us to determine relative age of such two events as well as interpreting the sense of movement. Based on the preliminary AMS findings, it was proven that AMS is a suitable tool for landslide mass analysis.

The research was supported by the grant project "Coseismic Landslides in Mountain Ranges of Active and Stabilized Accretionary Wedges" funded by the Grant Agency of the Czech Republic (GC22-24206J) and the Taiwanese Ministry of Science and Technology (NTSC 111-2923-M-008-006-MY3).

Formation of under-dip toppling in the Outer Western Carpathian Flysch Belt and its possible paleo seismologic implications

Thanh-Tùng NGUYỄN[1]*, Ivo BAROŇ[2], Jia-Jyun DONG[1], Rostislav MELICHAR[3], Filip HARTVICH[2], Jan KLIMEŠ[2], Jan ČERNÝ[3], Martin ŠUŤJAK[3], Lenka KOCIÁNOVÁ[3], Václav DUŠEK[3], Matt ROWBERRY[2], Régis BRAUCHER[4], Tomasz GOSLAR[5], Chia-Han TSENG[6], Yi-Chin CHEN[7], Cheng-Han LIN[8]

[1]*Graduate Institute of Applied Geology, National Central University, Taoyuan, Taiwan*
[2]*Institute of Rock Structure and Mechanics, Czech Academy of Sciences, Prague, Czech Republic*
[3]*Department of Geological Sciences, Faculty of Science, Masaryk University, Brno, Czech Republic*
[4]*CNRS CEREGE, Aix en Provence Cedex, France*
[5]*Poznan Radiocarbon Laboratory*, *Faculty of Geographical and Geological Sciences, Adam Mickiewicz University, Poland*
[6]*Department of Geology, Chinese Culture University, Taipei City, Taiwan*
[7]*Department of Geography, National Changhua University of Education of Taiwan, Changhua City, Taiwan*
[8]*Department of Civil Engineering, National Taiwan University, Taipei, Taiwan*
**Lead Presenter e-mail: nttung0201tv@gmail.com*

This study examines under-dip toppling in the Outer Western Carpathians, part of the Alpine-Himalayan orogenic belt, focusing on its accretionary wedge composed of Mesozoic and Cenozoic flysch formations. These geological layers, characterized by sandstone and conglomerate beds interbedded with claystone, have been deformed through thrusting processes, creating a landscape susceptible to slope failures. Our research focuses specifically on the phenomenon of under-dip toppling, where sandstone layers steeply dipping downslope bend and overturn along fracture lines. Utilizing high-resolution LiDAR data, we analyze the spatial distribution, geometry, and tectonic settings of toppling events, with a focus on occurrences in SSE-dipping fold limbs within the Javorníky Mountains. The study also addresses the complex geomechanical behavior of these toppling processes, incorporating recent field evidence using structural fault analyses, electrical resistivity tomography (ERT), and 10Be isotopic dating. It reveals ongoing multiphase strike-slip movements at the surface, which might play a pivotal role in initiating toppling mechanisms. A significant advancement of our research is evaluating the geometry of persistent near-surface sandstone formations and conducting pseudo-static analyses to estimate the seismic responses of slopes. Preliminary findings suggest these overturning events may have originated from substantial ancient seismic activities. The application of numerical modeling through the Universal Distinct Element Code (UDEC) involves simulating slope responses to hypothetical seismic acceleration scenarios based on the available waveform data. This approach not only allows us to estimate the possible impact of paleo-seismic events on slope stability but also enhances our knowledge of the region's paleo-seismic history and under-dip toppling dynamics.

The research was funded by the grant project GC22-24206J: "Coseismic Landslides in Mountain Ranges of Active and Stabilized Accretionary Wedges," supported by the Czech Science Foundation and the Taiwanese Ministry of Science and Technology (NTSC 111-2923-M-008-006-MY3).

Structural and paleoseismic conditions of rockfalls and cave collapse in the Khutul Usny valley (Arts Bogd Massif, CAOB, Mongolia)

Rafał SIKORA[1]*, Antoni WÓJCIK[1], Mirosław MASOJĆ[2], Grzegorz MICHALEC[2], Byamba GUNCHINSUREN[3], Marcin SZMIT[4], Józef SZYKULSKI[2]

[1]*Geohazards Center, Polish Geological Institute - National Research Institute, Krakow, Poland*
[2]*Institute of Archaelogy, Wrocław University, Poland*
[3]*Institute of Archaelogy, Mongolian Academy of Science, Mongolia*
[4]*Gdańsk Archaeological Museum, Poland*
**Lead presenter e-mail: rafal.sikora@pgi.gov.pl*

The Arts Bogd massif is located in the eastern part of the Gobi-Altay seismogenic zone, one of the most seismically active areas in the Mongolian part of the Central Asian Orogenic Belt (Ankhtsetseg et al., 2020). There are active regional E-W oriented transpressional or sinistral strike-slip faults (including the Bogd Fault). High-amplitude seismic events (e.g. M=8.1 – Bogd earthquake, 1957) have a major impact on the landform and the occurrence of mass movements in the region. During the Quaternary period many spectacular landform were created as a results of tectonic activity of the basement (Cunningham et al., 2021).

The basement of the south-eastern part of the Arts Bogd massif is composed by andesite-basalts of the Lower Cretaceous Malnai Formation (Togtokh, 1985). There are E-W and NE-SW oriented faults, and the massif is limited from the east by the NNW-SSE thrust fault (with top-to-the East sense of movement). These directions are reflected in the assumptions of the Khutul Usny valley (along the NE-SW trending fault) and Khutul Usny cave (along the NW-SE trending structures with slickensides documented normal-slip displacement). Our research has shown that the front part of the cave collapsed in the past, and there are rock blocks on the slope and in the valley floor documenting the rockfalls. Cave collapse is recorded in the sedimentological and geochemical profile of cave deposits. The layer of debris and the sharp increase of organic matter in the sediments above it correlate with this event. C^{14} dating of fauna bones indicates that the event probably occurred no earlier than 25930 +/-250 BP, and after this time, the deeper part of the cave was "opened" to external environment factors. Valuable lithic artefacts from the Palaeolithic period were discovered in the cave sediments (Masojć et al. 2024). For this reason, it can be assumed that earthquakes could have significantly influenced the functioning of early hunter-gatherer societies.

The analysis of tectonic structures revealed progressive, brittle deformation of rocks within the slope. There are represented by tension cracks, downslope-oriented sliding fractures and Riedel-Skempton shear zones. Very likely that if an earthquake of significant amplitude occurs, there may be a rockfall within the slope and fill part of the valley below.

The research was supported by the National Science Centre, Poland, Project “OPUS17”. No: 2019/33/B/HS3/01113 „Around Tsakhiurtyn Hondi. Research on the Stone Age of the borderland area between Altai and the Gobi desert in Mongolia” and partly by the Polish Geological Institute-NRI founds.

Record of superimposed late- and post-Variscan regional-scale tectonic events at the NE margin of the Bohemian Massif: structural evolution of the Kamionki Graben (SW Poland, Sudetes)

Aleksander KOWALSKI[1]*, Grzegorz PACANOWSKI[2]

[1]*Polish Geological Institute - National Research Institute, Lower Silesia Branch, Wrocław, Poland*
[2]*Polish Geological Institute - National Research Institute, Warsaw, Poland*
**Lead presenter e-mail: aleksander.kowalski@pgi.gov.pl*

Recent results of detailed geological mapping and structural analysis complemented by Electrical Resistivity Tomography (ERT) and 2D Seismic P-wave Refraction Tomography (SRT-P) are used to propose a new structural model for the polyphase evolution of the Kamionki Graben (NE Bohemian Massif). This intriguing tectonic feature is composed of syn- to late-orogenic Mississipian ("Culm") strata, which in geological map view represent an outlier surrounded entirely by the metamorphic rocks of the Góry Sowie Massif.

The Kamionki Carboniferous succession was folded (and, locally, also probably thrusted over the gneissic basement) into the WNW-ESE to W-E- and, less common, NW-SE- oriented folds during the late Mississipian (Namurian) epoch. Transpression generated by the strike-slip (dextral?) displacements may have played an active role in the folding process. The graben development only slightly postdated the folding of the Carboniferous succession and we correlate it with a significant regional uplift and erosion, which was related to the late-orogenic gravitational collapse of the newly formed Variscan orogen. Hence, the main boundary faults of the graben may have been genetically linked with the late Carboniferous–early Permian extensional (transtensional?) episode at the NE Bohemian Massif. The structure of the graben was later reshaped during the Late Cretaceous – early Palaeogene trans-regional tectonic shortening event, which likely led to the reactivation of the main boundary faults of the graben as well large-scale, gentle folding of the Carboniferous strata, visible only in map-view, especially in the northern parts of the graben. We did not observe any apparent evidence of fault dragging of the sedimentary strata, typical of other "synclinal" graben structures observed in the Sudetic region. It can be explained by a relatively rigid behaviour of the uplifted Góry Sowie Block during the Late Cretaceous – early Palaeogene tectonic shortening. The later, Neogene (?), NE-SW-oriented extensional regime resulted in the formation of normal faults and it was responsible for the distinct compartmentalization of the graben.

Our study provides the first description of the internal structure, fault pattern and kinematic evolution of the Kamionki Graben. Strong lithological contrasts between the sedimentary fill of the graben and its crystalline shoulders and floor makes the seismic and resistivity geophysical methods a valuable tool for investigation of its internal structure.

Poster presentations

Poster session I

Thursday 17:00 – 19:00, 25th April

Stratigraphic Evolution of the Salt Stocked-Basin: The Influence of Diapirism and Compressional Tectonics on the Sedimentary Record of the Paskhand anticline (Zagros Fold-and-Thrust Belt, Southern Iran)

Sadegh ADINEH[1,2,3]*, Prokop ZÁVADA[2], Jiři BRUTHANS[2], Soraya HEUSS-AßBICHLER[3], Mohammad ZARE[4], Anke M. FRIEDRICH[3]

[1]*Institute of Geophysics ASCR, Prague, Czech Republic*
[2]*Faculty of Science, Charles University in Prague, Czech Republic*
[3]*Department of Earth and Environmental Sciences, Ludwig-Maximilians-Universität München, Munich, Germany*
[4]*Department of Earth Sciences, Shiraz University, Shiraz, Iran*
**Lead presenter*

The Zagros Fold and Thrust Belt (ZFTB), characterized by its numerous salt diapirism and active tectonic deformation, presents an exceptional natural laboratory for examining the sedimentological and structural impacts of diapiric movement within compressional regimes. Our study focused on a representative salt stocked-basin, where we meticulously documented the halokinetic sequences and associated sedimentary facies adjacent to the salt diapirs.

This research delves into the stratigraphic evolution within the ZFTB in Southern Iran, focusing on the intricate interaction between salt diapirism and compressional tectonics. Utilizing the classical concept of halokinetic sequences, our study sheds light on the reactivation of a specific diapir situated at the core of an anticline. The investigation reveals the deposition of eight distinct sedimentary packages around the Paskhand salt diapir throughout the Oligocene-Miocene period, influenced by the diapir's progressive ascent coupled with the anticline's elevation. The sedimentary record showcases a rhythmic alternation of gypsum, fossiliferous carbonate, and siliciclastic materials, followed by lagoon to slope environment fossiliferous limestone in a reef setting. The culmination of these processes is marked by the thin-skinned tectonics of the uppermost halokinetic sequences being thrust towards the Paskhand salt diapir.

Our findings underscore the pivotal role of compressional forces in the reactivation of salt diapirs, significantly impacting sediment distribution and depositional environments. The detailed mapping and analysis of halokinetic sequences around the diapir highlight the early stages of diapiric rise and subsequent sedimentological responses. This study provides invaluable insights into the stratigraphic sequences' irregular deposition patterns around diapirs in compressional settings, underscoring the dynamic interplay between salt tectonics and sedimentation within the ZFTB.

Through a meticulous examination of the sedimentary records and structural deformations, this research contributes to a deeper understanding of the mechanisms driving stratigraphic evolution in salt stocked-basins. Our findings offer a novel perspective on the interaction between diapirism and compressional tectonics, enhancing our knowledge of sedimentary basin development in regions characterized by active tectonism and salt diapirism. This study not only advances the scientific understanding of the ZFTB's geological framework but also provides a foundation for further exploration and analysis in similar geological settings worldwide.

Record of high-pressure low-temperature metamorphism in garnet-bearing mica schists from AMINV K-1 borehole in Kobierzyce (Lower Silesia, SW Poland)

Kamil BULCEWICZ[1,2]*, Rafał SIKORA[2], Jacek SZCZEPAŃSKI[1], Piotr LENIK[3], Grzegorz ZIELIŃSKI[4]

[1]Institute of Geological Sciences, University of Wrocław, Wrocław, Poland
[2]Geohazards Center, Polish Geological Institute - National National Institute, Krakow, Poland
[3]Polish Geological Institute - National National Institute, Carpathian Branch, Krakow, Poland
[4]Polish Geological Institute - National National Institute, Warsaw, Poland
**Lead presenter e-mail: kamil.bulcewicz@uwr.edu.pl*

The AMINV K-1 borehole has been located approx. 20 km SW of Wrocław. The crystalline rocks has been observed at depth interval of 100.00 - 434.80 m. The obtained material provides a unique insight into the geology of the Variscan basement in the area where the surface exposures are scarce. The borehole profile includes metasedimentary rocks, such as quartz schists, chlorite-schists and garnet-bearing mica schists. In this study, garnet-bearing mica schists have been studied for their metamorphic record.

Our preliminary results on garnet-bearing mica schists from AMINV K-1 borehole indicate that the inspected samples may preserve a record of high-pressure, low-temperature (HP-LP) metamorphism preceding the phase of regional metamorphism. Key observations supporting the occurrence of the HP-LT metamorphic event are as follows: 1) inclusions of e.g. chloritoid, kyanite and rutile in garnet; 2) zoning of garnet, with Mn-rich core, marking its growth during progressive metamorphism; 3) diverse composition of white mica, including phengite. Results of classical geothermobarometry (Si-in-phengite, Ti-in-white mica) show, that phengite have crystallized at the conditions corresponding to 480 - 560oC and ca. 15 - 17 kbar, whereas muscovite crystallized at the conditions <560oC and <10 kbar.

Additionally, EMPA U-Pb monazite dating was carried out on 45 point analyses of 18 monazite grains. Their average age of crystallization was determined at 339±12 Ma.

The studied HP-LT mica schists resemble those of Kamieniec Metamorphic Belt in terms of their metamorphic record. However, their geographical position may indicate that they form an eastern fragment of the Middle Odra Metamorphic Unit, where HP-LT metamorphism has not yet been documented. This question is of great importance for the tectonic interpretation of the structure of the NE margin of the Bohemian Massif and will be addressed in further research.

High-pressure metamorphism of the Micachist Zone in the Kutná hora crystalline complex

Pavlína HASALOVÁ[1]*, Radmila NAHODILOVÁ[1], Martin RACEK[2], Pavla ŠTÍPSKÁ[1]

[1]*Czech Geological Survey, Czech Republic*
[2]*Institute of Petrology and Structural Geology, Faculty of Science, Charles University, Czech Republic*
**Lead presenter*

The Kutná Hora Crystalline Complex (KHCC) is situated between the internal Variscan Moldanubian zone and the low-grade Upper Proterozoic Bohemicum zone in Bohemian Massif. KHCC consists of three major units: the uppermost and the most metamorphosed Gföhl-related unit consisting of migmatites with bodies of HP/HT rocks as granulites, eclogites and garnet peridotites. The underlying MP/MT Kouřim nappe that comprises sequence of migmatites and orthogneiss. And finally, the lowermost Micaschist zone is composed of a sequence of metapelites. It is further subdivided into the Outer Micaschist Zone, with abundant intercalated amphibolite bodies, and the Inner Micaschist Zone with relics of eclogites and peridotites. We aim to understand the P-T-t path of these micaschists, their relation to the surrounding HP rocks (granulites and migmatites) and develop a model for their exhumation.

Micaschist reveal stable mineral assemblage of Grt+Ky+Mu+Bt+St+Plg+Kfs+Qtz. Garnet porphyroblasts in matrix contains inclusions of staurolite and are compositionally zoned with an increase in almandine and pyrope and decrease in spessartine from core to rim (alm0,55 → 0,68, prp0,07 → 0,16, sps0,21 → 0,02). White mica in matrix is either aligned in the foliation or dispersed throughout the matrix. It is phengite (Si = 3.1 - 3.3 p.f.u.; Ti = 0.01- 0.04 p.f.u; Xfe = 0.4 – 0.66) Large phengite flakes are zoned with higher Si in cores (Si = 3.2-3.3 p.fu.), whilst the lowest Si values are at white mica rim (Si = 3.07-3.1 p.f.u.). Staurolitеis common in the matrix as well as in garnet. Staurolite in the matrix has a constant XFe = 0.76–0.79 and Zn = 0.13-0.18 p.f.u. In contrast staurolite inclusions in garnet show much lower Zn content (0.01-0.06 p.f.u.) and larger range of XFe (0.76–0.9). Staurolite shows no compositional zoning and is stable together with kyanite. This suggest that staurolite must remain stable even at such HP conditions. This might be due very high Zn concentration (up to 0.2 pfu), that can stabilize staurolite up to these PT conditions. Based on the preserved HP assemblage we suggest that the micaschist shared the HP conditions with the granulites/migmatites. Moreover, the surrounding migmatites were recently attributed to the Saxothuringian crust, that was subducted during Devonian and the felsic material was then relaminated at the base of the upper plate and exhumed. If the studied micaschist shared already the prograde path with the granulites/migmatites or if they were attached to the granulites later in the lower crust remains matter of debate.

Oxygen isotopic record in Late Cambrian zircons from metamorphic rocks of the Sudetes

Mirosław JASTRZĘBSKI[1]*, Ewa KRZEMIŃSKA[3], Andrzej ŻELAŹNIEWICZ[1], Jiří SLÁMA[2], Marek ŚLIWIŃSKI[1]

[1]*Institute of Geological Sciences, Polish Academy of Sciences, Wrocław, Poland*
[2]*Polish Geological Institute - National Research Institute, Warsaw, Poland*
[3]*Czech Academy of Sciences, Institute of Geology, Prague, Czech Republic*
**Lead presenter e-mail: mjast@twarda.pan.pl*

In the Sudetes, a record of Early Palaeozoic magmatism along the northern margin of Gondwana are 515-480 Ma metagranites and metavolcano-sedimentary successions. To constrain possible sources of the parental magmas for plutonic and volcanic protoliths, zircons from these rocks were subjected to U-Pb dating by LA-ICPMS (CAS, Prague) and to $\delta^{18}O$ isotope analyses by SHRIMP (PGI-Warsaw). For O isotope studies, zircons were retrieved from orthogneisses of the Orlica-Śnieżnik Dome (OSD), Doboszowice Complex and Góry Sowie Massif (GSM), metabasites of the GSM, mica schists of the Stronie Formation in the OSD, and bimodal metavolcanic rocks of the Staré Město Belt.

The c. 495 Ma zircons from the Śnieżnik metagranite revealed relatively low $\delta^{18}Ozrn$ values ranging from 4.38 to 7.57, including those characteristic for mantle signature. Mica schists of the adjacent Stronie Formation revealed c. 10-15 % share of late Cambrian euhedral zircon grains, interpreted as pyroclastic admixture of felsic volcanic component to mainly pelitic sediment. Two zircon samples from those mica schists yielded very similar $\delta^{18}O$ values of 6.17–9.49‰ (average at 7.45‰), and 6.48–7.91‰ (average at 7.29‰, respectively). They indicate that the c. 495 Ma synsedimentary effusive volcanism originated from melting of the lower continental crust. The zircons from metavolcanic rocks of the Stare Město Belt with $\delta^{18}O$ values of 4.3–6.1‰ suggest rather uniform mantle origin of their melts. In contrast to the zircons from felsic metavolcanites with more complex oxygen isotopic range of 2.2–10.5‰ indicating assimilation of some crustal components (higher than mantle $\delta^{18}O$ values) but also exchange with hydrothermally-altered rocks or zircons (lower than mantle $\delta^{18}O$ values).

Two samples of the Doboszowice gneisses have comparable $\delta^{18}O$ values in range 4.58–9.37 and 5.07–9.65‰, respectively, mostly higher than those of the primitive mantle. Late Cambrian zircons from the GSM augen gneisses have $\delta^{18}O$ values in a range of 8.14–11.29‰, the highest among the studied samples, and higher those typical of I-type granitic melt (<8‰). Those gneisses do not have $\delta^{18}Ozrn$ mantle signature and sources of their igneous protolith had substantial amounts of supracrustal material. Nevertheless, the zircon grains from the accompanying, c. 500 Ma metabasite veins have values in a range of 4.92-8.10‰, thus significantly lower than in the host gneisses, with 1/3 grains crystallized from the mantle melt. Our new results show that the c. 495 Ma magmatism in the Sudetes originated from mildly evolved crustal magmas with local pulses of melts from the mantle.

The NCN grants Nos. 2014/15/B/ST10/03938, 2018/29/B/ST10/01120.

Formation of the Tsogt crustal dome in the Mongol-Altai domain during Permian orogeny

Petr JEŘÁBEK[1]*, Ondrej LEXA[1]

[1]*Institute of Petrology and Structural Geology, Charles University, Czech Republic*
**Lead presenter e-mail: jerabek.petr@natur.cuni.cz*

Central Asian Orogenic Belt (CAOB) is the largest world accretionary system consisting of a complex mosaic of crustal blocks of both continental and oceanic origin. It is proposed that the late Paleozoic to early Mesozoic tectonic evolution of the Mongolian tract of the CAOB refletcs progressive convergence between Siberia and North China. Important part of the CAOB evolution is recorded in the Mongol-Altai, represented by the former Ordovician accretionary wedge reworked in a suprasubduction environment from Devonian to Permian during several phases of compression and extension linked to the subducting slab advance and retreat. These events resulted into exposure of several high grade metamorphic core complexes/domes among which the Tsogt dome represents an outstanding example.

The Tsogt complex can be divided into two principal structural-metamorphic domains, the lower grade suprastructure to the NE and the higher grade infrastructure to the SW, separated by a major detachment shear zone. The internal parts of the infrastructure are occupied by felsic gneiss, migmatite, and granite (infrastructure core) which are mantled by amphibolite and high-grade metasediments (infrastructure mantle).

The suprastructure metasediments show low-grade metamorphic foliation S1 affected by two generations of upright folds. The F2 folds are characterized by large to outcrop scale open folds with subhorizontal N-S trending axes and steep originally west-dipping axial planes S2. The orientations of S2 were largely modified by later open folds F4. The Infrastructure, shows migmatitic S1-2 locally completely transposed by a dominant subhorizontal foliation S3, which was subsequently folded by upright F4 folds. In the inner parts of the Infrastructure, Infrastructure core, S3 reaches garnet-sillimanite grade. Garnet also occurs in the earlier migmatite foliation in the Infrastructure mantle. The boundary between the suprastructure and infrastructure is marked by a major detachment zone where the high grade S3 is overprinted at lower metamorphic conditions during exhumation. The U-Pb zircon ages indicate Carboniferous and Permian metamorphism and Ar-Ar ages document late Permian cooling.

Petrological diversity of ultra-high-pressure rocks around the Saidenbach dam (Erzgebirge)

Martin KESEBERG[1]*

[1]*Institut für Geologie Bernhard-von-Cotta-Straße TU Bergakademie Freiberg, Germany*
**Lead presenter*

The Saidenbach reservoir in the Erzgebirge is well known for Variscan ultra-high-pressure (UHP) metamorphic rocks including diamond-bearing felsic rocks and coesite-bearing eclogites. Conditions up to 7 GPa and 1400 °C have been proposed as peak metamorphic conditions for the felsic rocks, but only about 3 GPa and 900 °C for the eclogites. These differences demonstrate the poorly understood relation between the UHP felsic rocks and nearby, as well as regional eclogites. This is further emphasized by the occurrence of the UHP rocks as lenses within high-grade gneisses, in which no evidence for UHP metamorphism has been found yet. Using a combination of optical microscopy, XRF, micro-XRF, and microprobe data, we have systematically studied different rock types from the area around the Saidenbach reservoir including UHP felsic rocks, eclogites, and the adjacent gneisses.

Felsic UHP rocks have been reported in two different variants. The more prominent, coarse-grained type was first described about 25 years ago and has since been the subject of several studies, while another, more fine-grained type has only been recognized recently. Our data is not fully consistent with the currently invoked evidence for a magmatic origin, such as a generally “magmatic texture” or a particular kind of garnet zoning. Although mostly similar to previously described diamond-bearing rocks, our samples show a much larger textural variety, including intensely foliated and banded samples. Garnets in the matrix are characterized by intense reequilibration. Only garnet inclusions in kyanite preserve an earlier metamorphic stage, as shown by their systematically different chemistry. Based on our phase equilibrium calculations, their composition is consistent with formation within the stability field of diamond in excess of 3 GPa. Furthermore, we found new lenses of these diamond-bearing rocks, demonstrating that they occur in a greater area than previously thought.

Eclogites in the area show varying degrees of symplectization that correlate with differences in bulk chemical composition. Despite these differences, all investigated eclogites contain coesite or polycrystalline quartz inclusions that are likely polymorphs after coesite, as well as analogous trends in garnet composition. This argues for a shared metamorphic history, similar to previously proposed pressure-temperatures paths. Most of the host rocks are biotite-bearing high-grade gneisses that show significant migmatization. We find hints at an earlier UHP history, such as monazite exsolutions from apatite, but no conclusive evidence yet.

Pressure-, temperature- and water-dependent melt productivity in felsic rocks – new parametrization and its application in models of porous melt flow

Petra MAIEROVÁ[1], Pavlína HASALOVÁ[1], Pavla ŠTÍPSKÁ[1], Karel SCHULMANN[1,2], Ondřej SOUČEK[3]

[1]*Center for Lithospheric Research, Czech Geological Survey, Prague, Czech Republic*
[2]*Institut Terre et Environnement de Strasbourg, Université de Strasbourg, France*
[3]*Mathematical Institute, Faculty of Mathematics and Physics, Charles University, Prague, Czech Republic*
**Lead presenter*

Melting of the continental crust and transport of the melt through it are key processes that drive its chemical differentiation. Recent numerical models suggest that on time scales of millions of years, flow through microscopic pores may be an important type of melt transport. However, these models assume a very simplified description of melting and cannot be applied to simulate real tectonic settings. To further develop the models, we present a new parametrization of the melt productivity (equilibrium melt fraction at given conditions) that depends on pressure, temperature and water content (in hydrous minerals and free water), and that can be tuned for different chemical rock compositions. It is based on experimentally and theoretically determined positions of wet solidus, liquidus, and muscovite breakdown reaction.

By comparison with natural examples, we demonstrate that our parametrization predicts similar melt fractions as complex thermodynamics-based computations. We incorporate this parametrization in one-dimensional models of porous melt flow through a rock column. With these models, we simulate the thermo-mechanical evolution of felsic continental crust during orogeny mimicking two natural examples – the middle crust in the Variscan Bohemian Massif and the exhumed lower crust in the Tibetan-Himalayan system. In the first case, models predict melt fractions in the middle crust in the 5-10 % range, in agreement with geologic interpretations. In the second case, where more elevated temperature conditions are assumed, the models predict low melt fractions (5-10 %) in the lower crust and higher melt fractions (>20%) in the middle crust, in agreement with geophysical data. In both cases, these values are obtained only if we assume efficient porous flow, which provides a mechanism for compositional differentiation of the crust – formation of a depleted restitic lower crust and enriched fertile upper-middle crust.

Does the emplacement of the East Sudetic pluton result from combined Permian hot spot and far-field extensional dynamics?

Karel SCHULMANN[1,2]*, Anne-Sophie TABAUD[2], Alexandra GUY[1], Stanislaw MAZUR[4], František HROUDA[3,5], Kryštof VERNER[1], Jitka MÍKOVÁ[5], Petr MIXA[1], Vratislav PECINA[1]

[1]*Czech Geological Survey, Prague, Czech Republic*
[2]*Universite de Strasbourg, CNRS, Strasbourg, France*
[3]*Institute of Geological Sciences, Polish Academy of Sciences, Krakow Research Centre, Poland*
[4]*Agico Inc., Brno, Czech Republic*
[5]*Institute of Petrology and Structural Geology, Charles University, Prague, Czech Republic*
**Lead presenter*

In this work we examine and revise magmatic tectonic study of an East Sudetic pluton introduced by Hans Cloos hundred years ago and became a world example of structural analysis of igneous rocks. Combined structural geology, geochronology, anisotropy of magnetic susceptibility (AMS) and gravity studies provided a new geodynamic framework for late Carboniferous crustal anatexis followed by the emplacement of a giant Permian pluton in the East Sudetes. The analysis of gravity maps and gravity modeling allowed defining a 120 km long NNE-SSW trending gravity low, which coincides with the scattered outcrops of Permian granites along the eastern border of the Brunia continental block. This domain constitutes an East Sudetic pluton which intruded the Silesian orogenic wedge. The southern part of the pluton dated at 298 Ma (the Šumperk granodiorite) shows magnetic and macroscopic magmatic to sub-solidus fabrics coherent with a syntectonic granodiorite sheet emplacement along the large scale NNE–SSW sinistral detachment. The central part of the intrusion (the Žulová pluton) shows polyphase deformed partially molten rocks dated at ca 316 Ma, that were intruded by a 6 km thick plutonic complex at ca 290 Ma. The AMS fabrics of the latter intrusion indicate an emplacement governed by the dextral activity of the NW–SE Intra-Sudetic fault system. The northern part of the pluton dated at 312 – 309 Ma (the Strzelin massif and Lipniky intrusion) shows emplacement history governed by NNE-SSW detachment and sub-solidus shearing. The structural history of the pluton is compared to Permian NW–SE dextral and NNE–SSW sinistral crustal scale faults and associated pull-apart sedimentary basins at the scale of the Bohemian Massif. This correlation shows that both emplacement of plutonic rocks and formation of deep sedimentary basins were governed by the same crustal scale extensional framework. The Pennsylvanian crustal melting and Permian intrusion in the Sudetes are discussed in terms of post-orogenic crustal melting and lithospheric thinning affecting the whole NE part of the Bohemian Massif. The structure, age and tectonic features are compared to other major Variscan magmatic provinces at the time. It is proposed that the Sudetic magmatism can be related to a giant northern European volcanic province of the same age. We further discuss a relative contribution of Permian hot spot activity and far field extensional stress on channelized and pervasive magma flow along the periphery of the eastern termination of the Variscan system in Europe.

Pervasive melt migration in large crustal-scale shear zones in southern Madagascar

Alice WANTZ[1]*, Pavlína HASALOVÁ[2], Karel SCHULMANN[1,2], Jean-Emmanuel MARTELAT[3], Pavla ŠTÍPSKÁ[2], Prokop ZÁVADA[2], Alfred SOLOFOMAMPIELY ANDRIAMAMONJY[4] and Heninjara Narimihamina RARIVOARISON[5]

[1]*Institut Terre et Environment de Strasbourg, Université de Strasbourg, France*
[2]*Czech Geological Survey, Prague, Czech Republic*
[3]*Département Sciences de la Terre, Laboratoire de Géologie de LYON, France*
[4]*Mention Sciences de la Terre et de l'Environnement, Université d'Antananarivo, Madagascar*
[5]*Department of Applied Geosciences, German University of Technology in Oman*
**Lead presenter*

In southern Madagascar two main tectono-metamorphic events, corresponding to the East African Orogeny (ca. 630–610 Ma) and the Kuunga Orogeny (ca. 580–515 Ma) were recognized. An early structures include recumbent folds and sub-horizontal foliation S1 that were transposed during a regional east–west shortening resulting into north–south-oriented upright folds, with horizontal axes and new vertical axial planar foliations S2. This second deformation event is coeval with the development of a network of vertical ductile shear zones such as the Ejeda SZ, Ampanihy SZ, Beraketa SZ, Ihosy SZ, Zazafotsy SZ and Tranomaro SZ. These megascale 15–25 km-wide intracrustal near-vertical N-S or NW-SE trending ductile shear zones crosscut the entire high-grade metamorphic basement of southern Madagascar and separate lower-strain domains where complex fold interference patterns are visible. These high-strain zones developed between 580 and 530 Ma with a slight diachronism from the west to east and south to north and are coeval with melting and UHT/HT granulite facies conditions. The granulite facies metamorphism is widespread throughout the whole basement in all lithologies, in the southern part reaching peak conditions of 900–1000°C at 6–10 kbar and slightly lower temperature conditions (≤800°C) to the west, north, and in the Ikalamavony fold-thrust belt to the north–northeast. Importantly, the shear zones reveal large fluid/melt transfer from the depth that caused extensive fluid/melt rock interaction in the shear zone that resulted in localized charnockitisation of the granulites. The melt/fluid flux here was structurally controlled and seems to be penetrative throughout the basement rocks. This offers a unique opportunity to study fluid-assisted pervasive melt migration controlled by localized deformation across the whole crust. In this context, our objective is to understand microscale mechanisms driving the pervasive melt migration and define criteria to recognize it. Additionally, we use U-Pb monazite and zircon chronology to define the timescale of such pervasive melt migration in the crustal shear zones.

Challenges in the numerical fold shape analysis process

Weronika WIESŁAWSKA[1]*, Marta ADAMUSZEK[2]

[1]Institute of Geological Sciences, University of Wroclaw, Poland
[2]Computational Geology Laboratory, Polish Geological Institute - National Research Institute,Wrocław, Poland
**Lead presenter e-mail: weronikawieslawska@gmail.com*

Accurate analysis of the natural fold shape structures is commonly a challenging issue. The analysis generally requires identification of hinges and inflection points essential for determining key fold elements such as amplitude, wavelength, arclength and thickness. While numerical analysis enhances accuracy of the analysis in minimizing the user bias, it faces a number of problems, mainly related to presence of irregularities on the fold interface. The irregularities can represent natural roughness in shape or can result from imprecise digitization, both of which can significantly impact calculating fold curvature, which is a crucial parameter for identification hinges and inflection points. Consequently, numerical analysis can be highly sensitive to the irregularities, making it difficult to accurately interpret the fold shape.

In our study, we concentrate on understanding the digitization process and its associated errors it introduces into the analysis. Employing spline functions in the analysis, we fit the points acquired during digitization and determine their curvature. In the first approach, we analyze the result of the digitization of the cosine function. Focusing on a distinct set of points precisely located on the curve, we explore the role of number of points and their spatial distribution (evenly and unevenly). Moreover, we examine the role of imprecise location of the digitized point (measured as a distance of the point to the cosine curve) to imitate user-operator errors. In all cases, we calculate the misfit between the analytical solution and the numerically determined curvature, utilizing different measures: 1) maximum error, 2) mean error, 3) vector norm, and 4) distance between the observed and expected location of the hinge and inflection points.

In the next step, we employ a package from Fold Geometry Toolbox (FGT), which allows for digitization and the automatic curvature calculation. We describe the digitization error of the cosine curve carried out by over 20 structural geologists and demonstrate the diversity in interpretation of fold shapes. Based on this analysis, we proved a set of recommendations and guidelines of how to digitize the folds in the most accurate way. Finally, we show the results of fold shape analysis of excellent natural fold examples from the salt mines. The analyzed data show great diversity of fold shapes that can develop in multilayer packages.

The work was supported by the National Science Centre, Poland, under research project “Numerical and field studies of anisotropic rocks under large strain: applying micro-POLAR mechanIcS in structural geology (POLARIS)”, no UMO-2020/39/I/ST10/00818.

Magma flow patterns during emplacement of the durbachite Třebíč pluton

Prokop ZÁVADA[1,2]*, Jack PERCIVAL, Pavlína HASALOVÁ[2], Ondrej LEXA[3], Karel SCHULMANN[2,4]

[1]*Insitute of Geophysics,Czech Academy of Sciences, Prague*
[2]*Centre for Lithospheric Research, Czech Geological Survey, Prague,Czech Republic*
[3]*Institute of Petrology and Structural Geology, Charles University,Czech Republic*
[4]*EOST, Institute de Physique du Globe, Université de Strasbourg, France*
**Lead presenter*

The Třebíč pluton represents the largest ultrapotassic durbachite magmatic body in the Variscan orogeny of the Bohemian massif. The durbachite rocks of the Moldanubian Zone, conspicuously associated with lower crustal granulites, are interpreted as a mixture of lower lithospheric partial melts and anatectic crustal melts emplaced in middle crustal levels in the terminal stages of the Variscan orogeny (335-340Ma). The Třebíč pluton has a triangular shape in the map-view and is surrounded by the Varied Group of the Drosendorf Assembladge (paragneisses and migmatized gneisses) on the west and the Gföhl Assembladge (dominantly anatectic orthogneissess and migmatites) that consists of the lower crustal and upper mantle rocks. The emplacement of the Třebíč durbachite and its internal magmatic fabric is attributed to the succession of compressional/transpressional deformation producing the S1 vertical fabrics in the metamorphic host rocks, followed by exhumation of the lower crustal orogenic domain and middle crustal spreading producing the penetrative flat deformation fabrics S2.

In our contribution, we address the mode of magmatic flow inside the durbachite Třebíč body and the magmatic fabric transposition in the framework of their host rock deformation evolution. We evaluate the magmatic fabrics by means of anisotropy of magnetic susceptibility together with fabric analysis using oriented thin-sections. We recognize three types of fabrics: 1) clustered pattern of principal magnetic directions, vertical magnetic lineations and east-west trending vertical magnetic foliations (central part of the pluton), 2) clustered principal directions of the AMS ellipsoid with shallowly plunging magnetic lineations and steeply dipping magnetic foliations (dipping to the south in the central part of the pluton and to the southwest in the northern margin of the pluton), and 3) flat-lying magnetic foliations and north-south trending and shallowly plunging magnetic lineations in the eastern part of the pluton and the southerly oriented apophysis of the pluton.

The goal of our study is to constrain the flow evolution of the magma and first map the domains, where original vertical magmatic flow is transformed to lateral magmatic flow. This transition is associated with magmatic fabric transpositions, manifested for example by folding of the dense crystal mush. This is recorded in the durbachite magma microstructure and also the magnetic shape and anisotropy diagrams and clustering patterns of the principal directions of the AMS. These magmatic flow fabric patterns and magma transpositions reflect vertical magma flow and then spreading in the middle crustal levels conforming to the folding and shearing of the host rocks in the terminal stages on the eastern margin of the Variscan orogeny in the Bohemian Massif.

Sheath fold structures from the Altaussee salt mine

Marta ADAMUSZEK[1]*, Marcin OLKOWICZ[1], Marcin DABROWSKI[1], Mariusz FIAŁKIEWICZ[1], Bartłomiej GROCHMAL[1], Thomas LEITNER[3], Oscar FERNANDEZ[2]

[1]Computational Geology Laboratory, Polish Geological Institute - National Research Institute,, Wrocław, Poland
[2]Department of Geology, University of Vienna, Austria
[3]Salinen AG, Altaussee, Austria
**Lead presenter e-mail: marta.adamuszek@pgi.gov.pl*

The Altaussee salt mine located within the Northern Calcareous Alps (Austria) exposes a Permian to Triassic evaporitic succession. The entire succession has been extensively deformed from Middle Triassic to Neogene, which led to the formation of a complex tectonic melange. The salt-bearing strata within the mine are characterized by the abundance of brecciated fragments of anhydrite, polyhalite, sandstone and limestone. The fragment sizes reach up to several meters in diameter. The halite content in these deposits is estimated to be between 30% and 65%.

In the mine, the most spectacular structures are the folds that developed around or in the close vicinity to the brecciated clasts. The clasts appear as either isolated clasts or as group of clasts forming clusters. The visibility of these structures is significantly enhanced by the alternating thin red and greyish layers occurring in the halite-rich matrix, allowing for detailed observation of their complex morphology.

Our study focuses on well-exposed structures in the salt cavern ceiling, which covers approximately 4000 square meters. Utilizing a tailored photogrammetric approach, image post processing techniques and using lidar data as reference, we generated detailed orthophoto map of 1000 square meters of cavern ceiling with resolution of 1 mm/pixel. In the cavern, numerous closed contour patterns were documented, indicative of potential sheath fold development. The shape of the closed contours rarely has a regular elliptic shape. More commonly the contours are characterized with complex pattern including shapes curved around the neighboring clasts, folded eye shapes, or tie-shapes that resulted from the eye-shapes squeezed between two neighboring clasts.

We propose that the sheath folds could have formed due to flow perturbation around rigid or deformable inclusions during simple shear deformation. Using 3D numerical modelling, we show the structures that can develop around deformable viscous inclusions under far-field simple shear. Additionally, we examined the sinking processes and subsequent deformation stages that may influence or alter the morphology of these sheath-like structures.

The work was supported by the National Science Centre, Poland, under research project “Numerical and field studies of anisotropic rocks under large strain: applying micro-POLAR mechanIcS in structural geology (POLARIS)”, no UMO-2020/39/I/ST10/00818.

Famous tectonic phenomena in E of Bohemia (Czech Republic)

Jan JURÁČEK[1]*

[1]*Museum of Eastern Bohemia in Hradec Králové, Czech Republic*
**Lead presenter e-mail: j.juracek@muzeumhk.cz*

The aim of this contribution is to point out on varied tectonic phenomena related to the Variscan (post-) orogenic events and the post-Variscan tectonics in the area of E Bohemia (the Czech Republic) or the (Pre-) Sudetes respectively. This area is mostly formed by the Crystalline Complex units esp. in the Krkonoše Mts. and the Orlické hory Mts. The foothill is in a dominance of the Carboniferous-Permian volcanic-sedimentary complex and the deposits of the Bohemian Cretaceous Basin including the Police Basin and the Upper Nysa Kłodzka Graben. Triassic, Tertiary and Quaternary sedimentary and volcanic rocks built up small areas.

The metamorphites of the Crystalline Complex units (e. g. the Nové Město Unit) and its Carboniferous to Permian cover are affected by folding and faulting (manifested by slickensides, striation and mineral growth). Folded metagreywacke and quartz veins from the vicinity of Dobruška, N-S strike-slip fault near Hoštejn, famously dipping strata near Vrchlabí, folded chlorite-sericite phyllites with a double lineation system near Mlázovice and phenomenal slickensides in basaltic andesites from Rožmitál quarry near Broumov were selected. An evidence of the post-Variscan extension by normal faults is from the most prominent locality of Triassic sandstones is the Krákorka quarry at the town Červený Kostelec. Cretaceous rocks esp. sandstones, siltstones and claystones were disturbed by as synsedimentary tectonics (e.g. folding at the village Vrbatův Kostelec, normal fault near the village Březina) as polyphase post-Cretaceous fault rejuvenation of the crystalline basement. Steeply dipped bedding planes were located e.g. in the zone of the Hronov-Poříč Fault at the village Velké Svatoňovice or in the area of the Kyšperk Fault close to the town Lanškroun. Other rupture is sinistral reverse fault with striated hydrothermal calcite veins superimposed on the plume structure at the town Ústí nad Orlicí. Normal fault in the Jílovice Fault zone is prooved by excellent striated hydrothermal calcite veins with roof growth stages. The Zvičina Fault as sinistral strike-slip in the Cenomanians sandstones is located at the town Dvůr Králové. Normal fault in the Badenian marine deposits is in the surroundings of the town Lanškroun whereas small volcano the Malá Horka Hill was abrupted by E–W strike-slip fault close to the town Lázně Bělohrad. Extension event prooved by rotation landslides and normal faults due to angle shear took place in old sandstone quarries in the surroundings of the town Hořice.

Acknowledgement*:* The contribution was sponsored in the frame of internal research projects in the Museum of Eastern Bohemia in Hradec Králové (CZ).

Anisotropy of magnetic susceptibility: how to connect with microstructure?

Matěj MACHEK[1], Vladimír KUSBACH[1]*, Zuzana ROXEROVÁ[1]

[1]*Institute of Geophysics, Czech Academy of Sciences, Prague, Czech Republic*
**Lead presenter e-mail: kusbach@ig.cas.cz*

Valuable insights into the forces that shaped the rock can be gained through studying it's fabric and microstructure. For instance, studying the fabric of a shear zone can reveal the direction and intensity of past tectonic forces, informing earthquake hazard assessments. Examining the fabric of sedimentary rocks can unveil details about ancient currents and depositional environments.

The evaluation of rock structure using anisotropy of magnetic properties is a widely used approach in structural geology. Magnetic fabric serves as a fine recorder of rock deformation and flow dynamics. However, geological processes frequently result in distinctive individual subfabrics, making the interpretation of the anisotropy of magnetic susceptibility (AMS) quite challenging. To effectively interpret AMS within complex rock systems, numerical modeling of magnetic fabric based on rock microstructure appears to be the most promising way. Advances in microstructure 3D imaging facilitate the exploration of different approaches to model the anisotropy of magnetic susceptibility.

Analogous shear zone experiments using plaster of Paris have illustrated key factors for interpretation of magnetic fabric in deformation zones, in particular the localization and partitioning of deformation. X-Ray micro-tomography data obtained across analog shear zones serve as the basis for testing various modeling approaches of AMS, using the preferred orientation of distinct phases such as magnetite, pores, and anhydrite. The comparison of modeled results with measured AMS provides insights into the potential of microstructure-based modeling for interpreting magnetic fabric and inversely evaluating unknown rock textures. Similarities between the plaster deformation mechanisms and crystal mushes were also described, indicating a self-organized slip of crystals. Anhydrite crystal relics exhibit three preferred orientations, including a possibly rotated primary fabric and two conjugated microshear planes of aligned crystals developed during shearing.

This observation suggests that AMS modeling, when employed for interpreting rock-structure forming processes, need not be confined solely to the shape or crystallographic preferred orientation of magnetic carriers, especially when they are present in very low amounts and are difficult to identify.

Mechanical models of the ductile deformation of layered rocks

Marcin DĄBROWSKI[1]*

[1]*Computational Geology Laboratory, Polish Geological Institute - National Research Institute, Wrocław, Poland*
**Lead presenter e-mail: marcin.dabrowski@pgi.gov.pl*

Layered and foliated rocks may exhibit viscous anisotropy, which has a major influence on the style of their deformation. Mechanical anisotropy affects the velocity and strain rate fields as well as large strain development of structures. Viscously anisotropy bodies are not only inherently mechanically instable, but they also keep a 'memory' of deformation due to their evolving internal structure.

Willis [1964] derived an analytical solution treating an elliptical inclusion embedded in a homogeneous anisotropic elastic matrix subject to a uniform load in the far field. I adapt this solution to the case of incompressible viscous media and a friction-less, slit-like slipping surface to study the evolution of flanking structures in anisotropic shear zones. The analytical solution is exact for the initial state of homogeneous planar anisotropy, but it also provides useful insights into the early stages of deformation. Moreover, it can be used to approximately study large strain deformation structures that form in a power-law host rock around flow perturbing objects such as slip surfaces and inclusions. Here, both resolved and upscaled numerical simulations are used to examine the impact of host layering on the perturbing flow and structure development around a rotating slip surface in simple shear.

The work was supported by the National Science Centre, Poland, under research project "Numerical and field studies of anisotropic rocks under large strain: applying micro-POLAR mechanIcS in structural geology (POLARIS)", no UMO-2020/39/I/ST10/00818.

Can salt pillows form during inversion of evaporite-filled half-graben? Insights from numerical and analogue modeling

Marta ADAMUSZEK[1]*, Piotr KRZYWIEC[2], Laura FILBÀ[3], Mark G. ROWAN[4], Oriol FERRER[3]

[1]*Computational Geology Laboratory, Polish Geological Institute - National Research Institute, Wrocław, Poland*
[2]*Institute of Geological Sciences, Polish Academy of Sciences, Warsaw, Poland*
[3]*Institut de Recerca UB-Geomodels, Departament de Dinàmica de la Terra i de l'Oceà, Facultat de Ciències de la Terra, Universitat de Barcelona (UB), Barcelona, Spain*
[4]*Rowan Consulting Inc., Boulder, Colorado, USA*
**Lead presenter e-mail: marta.adamuszek@pgi.gov.pl*

The most common mechanism that leads to the formation of salt pillows is lateral migration of salt (evaporites) triggered by thin-skinned extension or contractional folding of supra-salt overburden. A much less frequently considered mechanism is inversion of evaporite-filled half-graben. A fundamental question related to such a setting is whether a thick evaporitic succession will allow for a spatially linked salt pillow to develop within the supra-salt succession or, instead, it might flow laterally away from the inversion zone due to its low viscosity and the weight of the overburden. In order to answer this question, we examined the formation of the Szubin salt pillow structure, located in the central part of the Mid-Polish Anticlinorium, that was formed during Late Cretaceous inversion of the Polish Basin. Data from two boreholes, Szubin IG-1 and Bydgoszcz IG-1, reveal a generally continuous sequence of Zechstein cyclothems with notably different thicknesses. The observation of locally increased evaporite thickness within specific layers of individual cyclothems suggests syn-depositional activity during Permian (Zechstein) evaporite deposition within a half-graben. According to a qualitative model proposed earlier (Krzywiec et al., 2019, Z. Dt. Ges. Geowiss.), inversion of this half-graben filled by syn-tectonic Zechstein evaporites led to buckling of the supra-salt Mesozoic cover and formation of large salt pillow directly above uplifted hanging wall. Combined analogue and numerical modeling was conducted and aimed at testing this model. Our tests incorporated various geometrical, mechanical, erosion, and sedimentation parameters. We found that the geometry of the half-graben, particularly its width and depth, strongly influences the shape and size of resultant salt pillow structures, mainly dictated by the amount of material accumulated within the half-graben. The mechanical parameters of salt also play a significant role, with higher effective viscosity promoting larger and more asymmetric anticline development, while lower viscosity leads to lateral flow and internal deformation of the salt.

A comparison of seismic data with both analogue and numerical models reveals a high degree of correspondence, supporting the plausibility of the Szubin structure development scenario of syn-depositional half-graben activity followed by inversion. Our findings contribute to a better understanding of salt structure formation in this region and shed light on potential tectonic activity during the Permian period.

The work was supported by the National Science Centre, Poland, under research project "Numerical and field studies of anisotropic rocks under large strain: applying micro-POLAR mechanIcS in structural geology (POLARIS)", no UMO-2020/39/I/ST10/00818.

Fault zone detecting using digital terrain model (DEM) analysis and seismic refraction tomography (SRT), Holy Cross Moutains (Poland)

Piotr WILKOŁAZKI[1]*

[1]*Polish Geological Institute - National Reasearch Institute, Warsaw, Poland*
**Lead presenter e-mail: piotr.wilkolazki@pgi.gov.pl*

In countries of temperate climate, such as Poland, the recognition of fault zones directly in the field is difficult due to densely urbanized areas and lush vegetation. Remote sensing methods, including digital terrain model (DEM) analysis, offer initial insights but can be inaccurate and need field verification on geological sites. Therefore application of near surface seismic surveys allows for verification and visualization of various geological settings including fault zones.

This study focuses on the recognition of fault zones in the Łysogóry Unit - northern part of the late Palaeozoic Holy Cross Mountains Fold Belt (HCMFB). The results of DEM based analysis combined with archival cartographic data of the region allowed for the creation of a map featuring both known and newly identified faults in the Łysogóry Unit. Based on that map, shallow seismic refraction tomography with active measurement system of 750-meter-long and 5 meter spacing between geophones was surveyed in two selected areas.

On the first section, which was conducted parallel to the geological layers, four vertical or almost vertical zones with reduced P-wave velocity values are visible. These zones are interpreted as fault zones located approximately 200 meters apart each other. One of them is 50 meters deep and narrow, while the others are 50-70 meters wide and extend to the full depth of the cross-section.

On the second section, conducted perpendicular to the geological layers, a clear contrast is observed between the southern part (composed of Devonian carbonate rocks) and the northern part (composed of Cambrian sandstone rocks) of the section. The boundary between these two parts correlates with the Holy Cross Fault, the major fault of the HCM region. This fault is depicted on the section as a zone inclined towards the south. Additionally, on the velocity section, another almost vertical fault zone is visible in the southern part of the cross-section.

The relationship between rock mass strength and deformation in the Bükk Mts, Hungary

Richard William MCINTOSH[1]*, Seyed Jamal Aldin HOSSEINI[1]

[1]*Department of Mineralogy and Geology, University of Debrecen, Hungary*
**Lead presenter e-mail: mcintosh.richard@science.unideb.hu*

The strength of natural rock masses has been assessed by the authors based on Rock Mass Rating (RMR) of selected outcrops in a study area in the Bükk Mountains, Hungary. The results suggest that RMR values are determined by not rock type or formation as highly similar rocks show greatly differing values. Probably the grade of deformation of the individual rock masses influence fundamentally rock mass strength as deformation results in a great diversity of discontinuities in the exposed rock masses reducing significantly their strength.

Outcrops with the highest RMR values expose more compact, continuous rock masses that are deformed as a continuous unit. Some of the major peaks and ridges are composed of such good quality rock masses. In contrast, low RMR values are found in outcrops exposing strongly deformed rock masses with strong foliation and/or dense fractures and/or folded structures. Lowest RMR values indicate very low strength and extremely poor quality rock masses in the outcrops. Such strongly deformed rock masses generally occur at the junction of primary Mohr joints or along major faults.

The spatial distribution of the RMR values suggests that low values tend to occur along the edges of major or smaller structural blocks while higher values tend to be found with outcrops inside such structural blocks.

Both high and low strength rock masses are reflected in topography in the form in specific morphological features. Low strength rock masses are usually found along major valleys or at the intersection of significant valleys. However, not only surface landforms reflect the strength of rock masses and thus the grade of their deformation but subsurface karst features also indicate rock mass strength. Caves especially likely to occur in zones of high structural deformation and thus low rock mass strength. Cave passages seem to follow primary joint systems or major faults based on the comparative analysis of the orientation of several dozen cave passages and the strike directions of primary joints measured on the surface near the caves.

Tectonometamorphic history of the Erzgebirge – open questions

Martin B. Keseberg[1], Thorsten J. Nagel[1]*

[1]*Institut für Geologie Bernhard-von-Cotta-Straße TU Bergakademie, Freiberg, Germany*
**Lead presenter*

We are in the process of making a tectonometamorphic map of the Erzgebirge for the Saxonian Geological Survey (LfULG). Here, we present the preliminary state of this work. We review published and archived data, collect and investigate new samples and do structural field work. We follow the scheme of previous studies and distinguish four major allochthonous units in the Erzgebirge: Basal Gneis Unit, Gneis-Eclogite Unit, Mica schist-Eclogite Unit, and Phyllite Unit.

In the course of this project we would like to address the following open questions:

1. Where are tectonic boundaries between these units? Which subunits can be distinguished?

2. Do high-pressure/ultrahigh-pressure (HP/UHP) conditions form various clusters? If so, how many clusters exist and what is their extent? Currently, the most common approach is to distinguish two HP and one UHP cluster. However, it is uncertain if the UHP cluster should be subdivided further due to the extreme conditions suggested for rocks around the Saidenbach reservoir. In addition, metamorphic conditions between the two non-UHP clusters seem transitional, but occur in different tectonic units.

3. Are high-pressure rocks solitary occurrences in a matrix with different pressure-temperature evolutions or did the units share a common evolution? If units behaved coherently – how do the high-pressure clusters fit into this picture and where are the associated tectonic boundaries?

4. Does the main foliation in the high-pressure units reflect exhumation from eclogite-facies conditions, exhumation from mid-crustal levels or even something else?

5. What explains the overall distribution of metamorphism in the Erzgebirge? While high-pressure and Barrovian conditions seem to fade out towards higher structural levels in the west, the eastern border of the Erzgebirge towards the Elbe Zone is metamorphically abrupt, represents a major structural jump and shows similarities to an extensional detachment fault.

Fault-related fold structures of the Moravo-Silesian fold and thrust belt

Mariusz FIAŁKIEWICZ[1], Bartłomiej GROCHMAL[1]*, Marcin DĄBROWSKI[1]

[1]Computational Geology Laboratory, Polish Geological Institute - National Research Institute,Wrocław, Poland
**Lead presenter e-mail: bgroc@pgi.gov.pl*

The Moravo-Silesian fold and thrust belt (MSFTB) is located to the east of the Bohemian Massif in the northeastern part of Czech Republic and in south-western Poland. This syn-orogenic structure consist of up to 7.5 km tick sedimentary succession deposited over Brunovistulicum and is interpreted to as a deformed Variscian foreland basin. MSFTB is exposed in the Nizký Jesenik Mountains in the north and in the Drahany Uplands in the south, separated by the Olomouc Depression. Four formations are distinguished within Nizký Jesenik Mountains: Andelska Hora Fm (shales, siltstones and greywackes, lower-middle Visean), Horni Benesov Fm (mostly greywackes, middle Visean), Moravice Fm (shales and siltstones with intercalations of greywackes, upper Visean) and Hradec-Kyjovice Fm (shales, siltstones and greywackes, upper Visean-Namurian A). MSFTB is elongated in the north-south to northeast-southwest direction with thrusts striking mainly northeast-southwest and fold axes trending mainly north-south.

Here, we present structural data gathered during fieldwork within the northern part of the Nizký Jesenik Mountains. We performed aerial and regular imagery surveys to collect photographic documentation, which enabled us to construct detailed 3D models of the selected quarries and outcrops of the MSFTB. Acquired images were processed using photogrammetric software, in which 3D models that provide a high-resolution representation of the complex deformation pattern within a given outcrop or quarry were constructed. The use of photogrammetry allowed us to overcome traditional limitations associated with field-based structural analysis. We have analyzed the obtained models in CloudCompare software to extract quantitative data on the fold geometry and on the orientations of brittle structures such as faults and joints. Through our study, we aim to shed light on the tectonic evolution and deformation mechanisms that have shaped the Moravo-Silesian fold and thrust belt during the Variscan deformation stage.

The work was supported by the National Science Centre, Poland, under research project “Numerical and field studies of anisotropic rocks under large strain: applying micro-POLAR mechanIcS in structural geology (POLARIS)”, no UMO-2020/39/I/ST10/00818.

Leucocratic rocks at the contacts between orthogneisses and metasedimentary rocks in the Lądek-Śnieżnik Metamorphic Unit, Sudetes

Wojciech STAWIKOWSKI[1]*, Mirosław JASTRZĘBSKI[2]

[1]*Institute of Geology, Adam Mickiewicz University, Poznań, Poland*
[2]*Institute of Geological Sciences, Polish Academy of Sciences, Research Centre in Wrocław, Poland*
**Lead presenter e-mail: wojst@amu.edu.pl*

The Lądek-Śnieżnik Metamorphic Unit (LSMU), representing an eastern part of the Orlica-Śnieżnik Dome (Sudetes, NE Bohemian Massif), is a tectonically complex regional unit formed during the Variscan orogeny. It is built mostly of meta-plutonic and meta-(volcano)sedimentary rocks. Both these lithological groups at their mutual contacts record amphibolite-facies conditions. The meta-plutonic group is represented by the orthogneisses with the Cambro-Ordovician protolith age. They reveal different grade and style of deformation resulting in high textural variability (from augen to laminated and even homogenous varieties). On the other hand, the lithologically diversified meta-(volcano)sedimentary suite has Late Neoproterozoic to Cambrian protoliths. The nature of boundaries between the LSMU metagranitoids and supracrustal rocks (primary - intrusive or secondary - tectonic) is still not deciphered.

In two localities with the direct contacts of the orthogneisses with metasediments (represented by paragneisses, schists and quartzites), situated near Międzygórze and Sienna, the small (tens of cm-scale) bodies of fine-grained, leucocratic rocks have been observed. Their occurrence has been treated as a new, additional premise for either intrusive or tectonic character of the co-occurrence of metagranitoids and metasediments in the LSMU. Based on the observations in poorly exposed outcrops, both the type of protolith (para- or ortho-), and the formation mechanism of the leucocratic rocks (metamorphosed aplitoid veins? quartzitic rocks modified due to ductile shearing at the contact with orthogneisses?) were impossible to deduce. Therefore, geochemical studies of major and trace elements, including REEs, have been conducted. Their results document an unequivocal affinity of the leucocratic rocks to the orthogneisses. The patterns of trace element and REE spider diagrams drawn for orthogneisses and leucocratics are very similar in shape (usually, but not always with lower content of elements in case of the leucocratic rocks). In contrast, the metasedimentary rocks from the contact zones give distinctly different patterns. Such results suggest aplitic origin of the leucocratics, and consequently, the intrusive orthogneisses/metasediments boundary. However, strongly mylonitized gneisses from the narrow shear zone located within the metagranitoids show similar trend of the trace element content depletion.

The geochemical characteristic of the studied orthogneisses sampled in the contact zones with the metasediments in the two mentioned localities and at the third contact, close to Kamienica is internally consistent, and concordant with the geochemical data for the inner parts of the orthogneissic domains in the MSLU. They belong to peraluminous granites, and at the geotectonic discrimination diagrams occupy fields of syncollisional and/or volcanic arc granitoids.

Photogrammetry as a tool to improve recognition of fold and fault patterns: field examples from the Northern Calcareous Alps (Austria, Hallstatt region)

Marcin OLKOWICZ[1]*, Bartłomiej GROCHMAL[1], Mariusz FIAŁKIEWICZ[1], Marta ADAMUSZEK[1], Marcin DĄBROWSKI[1]

[1]*Computational Geology Laboratory, Polish Geological Institute - National Research Institute, Wrocław, Poland*
**Lead presenter e-mail: marcin.olkowicz@pgi.gov.pl*

Photogrammetry has become a well-established field method of imaging geological structures. Due to its flexibility, it can be used in a wide range of applications ranging from the micro scale with millimeter-sized objects to the macro scale, where modeled objects reach a size of several hundreds of meters or more. Combined with the easy availability of digital cameras, drones, high performance PC computers and ongoing development of user-friendly software, photogrammetry is more accessible for none specialized users than ever before. In modern state of art photogrammetric workflow, from taking images to construction of the final model, only a low entry level is required, making this technique widely available.

In our study, we show examples of photogrammetric applications in structural analysis, where it is used to document and then to describe and analyze fault and fold structures in outcrops of different scale and for varied geological setting. The presented results are based on data collected during a 10-day field campaign in the Northern Calcareous Alps (Austria, Hallstatt region). We have used photogrammetric technique to document selected outcrops in the form of digital outcrop models, which were next analyzed to recover structural data on the geometry of fault and fold structures. Our works covered a variety of outcrops from large-scale, human-inaccessible walls imaged with a lightweight drone, through classic mesoscale surface outcrops, to those located in underground mine passages. Despite the use of the same photogrammetric processing workflow for all the studied outcrops, the image acquisition during the field works required some modifications to create high-quality models. As a result of our work, we present the basic guidelines and workflows for different style outcrops along with the structural data gathered from those models.

The work was supported by the National Science Centre, Poland, under research project “Numerical and field studies of anisotropic rocks under large strain: applying micro-POLAR mechanIcS in structural geology (POLARIS)”, no UMO-2020/39/I/ST10/00818.

Poster session II

Friday 17:00 – 19:00, 26th April

Quaternary tectonic activity imprinted on the river terrace in Brno

Benjamín FOJTÍK[1], Rostislav MELICHAR[1]*, Ivo BAROŇ[2], Jan ČERNÝ[1], Kurt DECKER[3], Václav DUŠEK[1], Filip HARTVICH[2], Martin ŠUŤJAK[1], Dalibor VŠIANSKÝ[1], Piotr MOSKA[4], Thanh-Tùng NGUYỄN[5]

[1]Department of Geological Sciences,Masaryk University, Brno,Czech Republic
[2]Institute of Rock Structure and Mechanics,Czech Academy of Sciences, Prague,Czech Republic
[3]Department of Geology,University of Vienna, Austria
[4]Silesian University of Technology,Gliwice,Poland
[5]Graduate Institute of Applied Geology, National Central University,Taoyuan,Taiwan
**Lead presenter e-mail: fojtk@mail.muni.cz*

A new outcrop of the Upper Pleistocene river terrace has been exposed in the central part of Brno City. Excavation works for a new department store uncovered complex sedimentary sequences composed of river sandy gravel, grave sand, and silt covered by loess. Relatively fine sand about 2 m thick with silty intercalations forms the lower portion of the outcrop, while dominating coarse gravel layers above a light bordering sequence are on top of it. The loess is positioned within a small tectonic trough of meter-scale dimensions. The whole sequence is discordantly covered by loess-like soil (colluvium) and artificial deposit. As we assumed that this pattern relates to a young fault tectonics, the outcrop was further examined by a complex of methods.

Firstly, the outcrop was divided into a 1×1 m grid for better visualization in the photogrammetric mosaic. Further analyses of the mosaics and structural analyses of the outcrop revealed that the horst-and-graben structures were formed and bordered by several generations of faults. The faults are characterized by both dextral and sinistral components. The left-lateral faults revealed an offset of approximately 270 mm towards the east. The dextral normal fault of 066°/82° offset the strata for about 150 mm roughly toward the ESE direction. Individual strata visually wedge against each other progressively from NW to SE. In addition to young faulting activity, water escape structures were observed. These structures were formed either concurrently with the faulting or later, but not before the faults emerged. Their genesis might be associated with seismic activity. The water escape structures (i.e., sandy veins) and larger faults are enriched with calcite. In these areas, sediment bleaching occurred, highlighting tectonic ruptures. The whole structure forms an anticline with the through near its axis according to the electrical resistance tomography profile.

As the upper layer of loess is following the tectonic disruption of the strata below, it can be suggested that the terrace was “tectonically active” after the deposition of loess. The age of the lower sandy sequence is approximately 21.2 ± 1.3 ka, while the age of the upper gravel is approximately 11.77 ± 0.78 ka according to OSL dating. The sagged loess revealed about the same age of about 11.99 ± 0.67 ka and the whole tectonic deformation is postdated by the not deformed uppermost colluvium of 4.12 ± 0.25 ka. Between the colluvium and the gravel, there are distinct lobes and wedges on top of some faults. Originally, they were interpreted as colluvial fault-scarp wedges, but their relatively old age of 115.3 ± 0.71 ka and 111.4 ± 0.89 ka, respectively, which was dated on very fine quartz grains of 0.15–0.20 mm, indicates rather their transport from the basal sequences of the terrace along the faults in form of sand bowls.

The research was supported by the grant project “Coseismic Landslides in Mountain Ranges of Active and Stabilized Accretionary Wedges” funded by the Grant Agency of the Czech Republic (GC22-24206J) and the Taiwanese Ministry of Science and Technology (NTSC 111-2923-M-008-006-MY3).

Structural analysis and paleostress investigation along Szőc Fault (Bakony Mountains, western Hungary)

Anwar AL HIJOUJ[1]*, Gábor CSILLAG[3], Melinda FIALOWSKI[1], László FODOR[2,1]

[1]*Department of Geology, Institute of Geography and Earth Sciences, Eötvös Loránd University, Budapest, Hungary*
[2]*HUN-REN Institute of Earth Physics and Space Science, Sopron, Hungary*
[3]*Research Centre for Astronomy and Earth Sciences, Institute for Geological and Geochemical Research, Budapest, Hungary*
**Lead presenter*

In the southern Bakony Mts. of the Transdanubian Range (TR), Hungary, the authors conducted field structural measurements, fault-slip analysis, and reambulation-type structural geological mapping. For the Szőc study area, a new structural-geological map was compiled using structural observations, existing maps, and borehole data base. The main structure is the Szőc Fault which is part of the system of NW–SE striking dextral faults of the TR but was not studied earlier in detail. The Szőc Fault is perfectly exposed in a former bauxite mine, where the northern block was composed of Upper Triassic Haupdolomite while the southern block consists of the Middle Eocene Gánt Bauxite and Szőc Limestone Formations.

In the entire area three tectonic phases were separated by the analysis of stress field. The deformation history started with NW–SE compression. It resulted in thrust faults of NE–SW strike. The age of this deformation can be Cretaceous (Albian to Coniacian) based on regional structural evolution. Then a major dextral shearing phase occurred due to a strike-slip or transpressional stress field with NNW–SSE maximum horizontal stress axis. This main dextral shear along the Szőc Fault appears to have occurred in the Middle Miocene, as a final stage in the strike-slip displacement in the TR. The third phase was an extensional deformation with minimum principal stress axis in E–W to SE–NW direction. It resulted in the formation of N–S conjugate normal faults and joints probably in the Late Miocene, these structures cut across the main dextral fault.

The southeastern segment of the Szőc Fault is covered by Late Miocene sediments. However, the NE-trending Litér Thrust of Cretaceous age has not been cut by the extension of the fault. Thus, the Szőc Fault should have a termination near or below the Late Miocene cover. To characterize this termination, the Upper Triassic Hauptdolomite was studied east of Taliándörögd. Here the NW-SE striking strike slip fault marked with N-S maximum principal stress debranches into several faults partly in a local releasing bend or to horsetail terminations with normal faults of SE-NW to N-S directions. Local N-S shortening is also present in form of outcrop-scale thrust faults contributing to strain accommodation. This termination within the core of the Bakony is unique because in most cases Miocene dextral faults died out along reactivated Cretaceous thrusts in the south-east part of the TR.

The research was supported by the National Development and Innovation Office OTKA No. 134873.

Tectonic environment of the Neogene magmatism in the Pieniny Klippen Belt

Jakub BAZARNIK[1]*, Piotr LENIK[1]

[1]*Polish Geological Institute - National Research Institute, Carpathian Branch; Krakow, Poland*
**Lead presenter e-mail: jakub.bazarnik@pgi.gov.pl*

Miocene andesitic rocks intrude both the Pieniny Klippen Belt and Magura nappe in the Polish part of Western Carpathians (Birkenmajer 2003, BulPAS; Birkenmajer & Pécskay 2000, SGeolPol; Nejbert et al. 2012, Lithos). They form small-volume hypabyssal dykes and sills and represent a calc-alkaline magmatic event. The age of andesitic magmatism ranges from 12.8 Ma to 10.8 Ma, mainly resolved using the K-Ar method (e.g. Pécskay et al. 2015, ASGP), however, some data from zircon dating are also present (e.g. Anczkiewicz & Anczkiewicz, 2016 ChemGeol).

The Pieniny Klippen Belt comprises deformed Mesozoic to Neogene sedimentary rocks. It forms a narrow, tectonic structure that separates the Outer and Inner Carpathians. The Magura nappe mainly comprises sandstones and mudstones, and it is the southernmost unit of Outer Carpathian flysch sediments.

Although many specialists (e.g. Nejbert et al. 2012, Lithos, Anczkiewicz & Anczkiewicz, 2016 ChemGeol) have studied the chemical composition of Miocene andesites in the Pieniny area, their tectonic environment is still unclear. It has been proposed that the origin of andesitic magma is from partial melting of the metasomatized lithospheric mantle as well as derivation from an enriched MORB type mantle which underwent modification.

New results from chemical composition analysis of major elements indicate that the chemistry of analyzed rocks varies from basaltic trachyandesites and basaltic andesites, through andesites sensu stricto to dacites (TAS classification, after Le Maitre 2002 Cambridge), and they have the composition of calc-alkaline and (in minority) high-K calc-alkaline series magmas (Peccerillo & Taylor 1976 ContrMinPetr). They also show a visible influence of slab melting (Pearce & Peate 1995 AREP). Studies of trace element ratios indicate that these rocks were formed on the active continental margin (Bailey 1981 ChemGeol) and magma for their formation was influenced by the subduction environment (Pearce & Peate 1995 AREP).

In addition to the interpretation of the chemical composition, further in-depth studies on the analysis of the isotopic composition (including Sr, Sm-Nd, Pb) carried out on a representative population of samples also require further detail.

Acknowledgement: The research is supported by the National Fund for Environmental Protection and Water Management project No. 22.2301.2001.00.1.

Sedimentary traces of Late Pleistocene seismic activity in glacigenic sediments in the Southern Peribalticum area (NE Germany, Lithuania, Latvia)

Szymon BELZYT[1]*, Małgorzata PISARSKA-JAMROŻY[2], GREBAL project team[2]

[1]*Institute of Geological Sciences, University of Wrocław, Wrocław Poland*
[2]*Institute of Geology, Adam Mickiewicz University in Poznań, Poland*
**Lead presenter e-mail: szymon.belzyt@uwr.edu.pl*

Comprehensive sedimentological, geochronological and stratigraphical studies of layers interpreted as seismites, i.e. layers of sediments affected by earthquake shaking, widely used as a secondary, off-fault evidences of palaeoseismic activity, have been conducted in five study sites located within Southern Peribalticum area – Dwasieden (Rügen Island, NE Germany), Weisser Berg (Usedom Island, NE Germany), Slinkis (Dubysa river valley, central Lithuania), Dyburiai (Minija river valley, NW Lithuania) and Baltmuiža (Piejūra Lowland, W Latvia). The studied layers occur within Pleistocene, unconsolidated silty-sandy sedimentary successions representing lacustrine, glacilacustrine and fluvial sedimentary environments.

Seismites are recognized on the base of several criteria, including an occurrence of intralayer liquefaction-induced soft-sediment deformation structures (SSDS), large lateral extent and continuity of deformed layers, and sandwich-like (or pancake-like) distribution of layers, i.e. vertical repetition of deformed layers interbedded with undeformed sediments. The time periods of sediment deposition and the subsequent deformation are estimated for each study site on the base of OSL datings results and stratigraphic context, including the relation to the ice-sheet front position. The study results are supplemented with modelling of the Coulomb Failure Stress changes in time for the particular study areas, with the different input parameters of the subsurface faults, which reactivation might have been responsible for the seismic activity. For the selected study sites, the Schaabe fault, Usedom Fault Zone and Strelasund Fault in Northern Germany, and Telšiai fault zone in Lithuania were preliminarily identified as the fault(s) or fault zones possibly capable for generating earthquakes in Late Pleistocene, with recommendation of further structural, geomorphological or geophysical studies.

According to our interpretation, the distribution and number of seismites indicate that low- to moderate-magnitude earthquakes related to the growth or decay of the ice cover (caused by reactivation of pre-Quaternary faults induced by glacioisostatic rebound or glacial earthquakes / icequakes) were more frequent than hitherto reported. In addition, seismic activity occurred not only during deglaciation, but also during the glaciation of the study area (i.a. in the area of moat – a crustal depression between the forebulge and the advancing ice-sheet front). The interpreted earthquakes were related not only to the Weichselian glaciation (MIS 2-5), but also to Saalian glaciation (MIS 6).

The study is a result of the research projects no. 2015/19/B/ST10/00661 (GREBAL project) and 2019/35/N/ST10/03401 financed by the National Science Center, Poland.

Kinematic modelling of fault-related structures within anisotropic layered rocks of Northern Calcareous Alps (Eastern Alps, Austria)

Mariusz FIAŁKIEWICZ[1]*, Bartłomiej GROCHMAL[1], Marcin OLKOWICZ[1], Marcin DĄBROWSKI[1], Bernhard GRASEMANN[2], Oscar FERNANDEZ[2]

[1]*Computational Geology Laboratory, Polish Geological Institute - National Research Institute, Wrocław, Poland*
[2]*Department of Geology, University of Vienna, Austria*
**Lead presenter e-mail: mfia@pgi.gov.pl*

The presented study is a part of a broader project delving into both field and numerical examinations of tectonic structures development within fold-and-thrust belts. The primary focus is on the evolution of fault-related structures in layered rocks. Existing deformation models predominantly embrace a kinematic approach, where layering is treated as passive, overlooking rheological effects such as mechanical anisotropy, which plays an important role in layered rocks commonly found within fold-and-thrust belts.

In our investigation into the role of mechanical anisotropy, we examined folding and thrusting in the central Northern Calcareous Alps (NCA), encompassing the Permo-Mesozoic sediments of the Upper Austroalpine unit. This fold and thrust belt feature folds formed along overthrusts, including fault-bend folds and fault-propagation folds but also the out-of-sequence overthrusts. The tectonic evolution of NCA is significantly influenced by sedimentary facies, with nappes imbricated during Jurassic and Cretaceous thrusting. Our focal points were the Scythian mixed clastic-carbonate sediments of the Werfen Fm (SW of Hallstatt), located at the base of the fold-and-thrust system, and the Upper Jurassic limestones of the Oberalm Fm, located SE of Bad Ischl that are deformed syndepositionally into thrusts and folds forming the shallowest part of the fold-and-thrust belt during the Jurassic deformation stage.

Fieldwork encompassed gathering orientation measurements of various tectonic structures, and capturing photographic documentation which allowed to produce georeferenced photogrammetric models. Digital outcrop models, in the form of georeferenced textured polygon meshes, were created in order to integrate spatial data with detailed geological mapping results and collect additional data.

The limitations inherent in kinematic modeling to represent real-world strain patterns were confirmed through sequential restoration and kinematic forward modeling in Move software. Notably, hybrid modes of kinematic models provided more acceptable results, underscoring the significant influence of rheological contrasts within the sedimentary pile on the distribution of folding and faulting. Our observations, focusing on meter-scale structures, suggest a level of strain not typically addressed in regional-scale cross-sections, emphasizing the importance of considering strongly anisotropic strain distribution within sedimentary units when performing kinematic modeling of regional-scale structures.

The work was supported by the National Science Centre, Poland, under research project “Numerical and field studies of anisotropic rocks under large strain: applying micro-POLAR mechanIcS in structural geology (POLARIS)”, no UMO-2020/39/I/ST10/00818.

Active tectonics of the Vértes Hills (Hungary) based on precise characterization of earthquakes and geological-geomorphological data

László FODOR[1,2,*], Eszter BÉKÉSI[1], Barbara CZECZE[1], Gábor CSILLAG[3], Dániel KALMÁR[1], Márta KISZELY[1], Bálint SÜLE[1], Anna ŚWIERCZEWSKA[4], Antek TOKARSKI[5]

[1]*HUN-REN Institute of Earth Physics and Space Science, Sopron, Hungary*
[2]*Institute of Geography and Earth Sciences, Eötvös University, Budapest, Hungary*
[3]*HUN-REN Research Centre for Astronomy and Earth Sciences*
[4]*Faculty of Geology, Geophysics and Environmental Protection, AGH University of Krakow, Poland*
[5]*Institute Geological Science, Polish Academy of Sciences, Krakow Research Centre, Poland*
**Lead presenter*

Hungary is marked by a moderate seismicity which represents a hazard for the society and infrastructure. However, location of active faults is difficult to determine because of insufficient knowledge of potential faults and inaccurate location of earthquakes.

New temporary seismic stations were employed in the central part of the Pannonian Basin, in the Vértes Hills (Fig. 1) where historical (e.g., 1810, Mór) and instrumentally recorded earthquakes are frequent. The stations monitored the supposedly active Mór Graben and the aftershocks of the Oroszlány 2011 earthquake (Fig. 2). The earthquakes registered in 2020-2022 near Mór and the aftershocks of 2011 near Oroszlány were analysed, and the hypocentres were determined by modern methodological approach. These data were compared by mapped faults which were classified as „post-rift" having been formed after 11 Ma.

New approaches permitted the separation of natural earthquakes from seismic events induced by quarry blasting. 6 earthquake swarms were detected in the 2020-2022 period and ca. 100 aftershocks is 2011. Small-magnitude earthquakes were recorded. New approaches resulted in a much more accurate hypocentre determination both for earthquakes near Oroszlány (2011) and near Mór (2020-2022). In both cases, steep slip planes could be determined. Earthquakes can now be connected to mapped faults; the Gesztes, Mór, Pusztavám and Eastern Vértes Faults, respectively. Other structural indices for neotectonics involve the presence of fractured pebbles, breccia zones, and thicker Quaternary sediment pile in the hanging wall block. Combined structural and morphological indices are ponded drainage pattern in hanging wall block together with wind gaps in the footwall, diverted drainage and capture of creeks. Indirect signs are strongly deformed Quaternary sediments which could form by earthquake shaking (seismites) but also non-tectonically by deformation of frozen upper layers along slopes. In one case this deformation occurred in late Pleistocene between 75 and 79 ky.

Together with these structural geological and morphological indices, a new map of active faults was constructed. This map can serve as the basis for future earthquake hazard estimations.

The research was supported by National Research Found 134873 of László Fodor.

Thin-skinned vs. thick-skinned shortening of the Transdanubian Range: the switch from Neothetian obduction to the formation of the Eoalpine orogeny

Gábor HÉJA[1]*, Márton PALOTAI[1], Gyula MAROS[1], Tamás BUDAI[2], Zsolt KERCSMÁR[1], Szilvia KÖVÉR[3], Ádám CSICSEK[4], László FODOR[3]

[1]*Supervisory Authority for Regulatory Affairs, Hungary, Budapest, Hungary*
[2]*University of Pécs, Hungary*
[3]*HUN-REN Institute of Earth Physics and Space Science, Sopron, Hungary*
[4]*Eötvös University, Institute of Geography and Earth Sciences, Department of Geology, Budapest, Hungary*
**Lead presenter e-mail: hejagabor@hotmail.com*

The aim of this study is to give an overview on the most important Cretaceous compressional structures of the Transdanubian Range (TR), and to place them into a regional context within the tectonic evolution of the Alpine region. In order to do that, three regional cross-sections were constructed across the southwestern, central, and northeastern parts of the TR, respectively.

The Cretaceous compressional structures of the northeastern Transdanubian Range outline a south-vergent thin-skinned fold-and-thrust belt that resulted in the imbrication of the Triassic – Early Cretaceous sedimentary cover above a shallow detachment within the Triassic succession. These structures are associated with the Early Cretaceous foreland basin of the northeastern Transdanubian Range that developed in the foreland of the Neotethyan obducted ophiolite nappes in a lower plate position.

In contrast, the sections through the central and southwestern Transdanubian Range are dominated by thick-skinned deformation, where both the Permian – Early Cretaceous sedimentary cover and the Variscan basement are affected by folding. These thick-skinned structures are NW-SE oriented in the central TR, and gradually turn into a N-S trend in the southwestern Transdanubian Range Unit. The onset of thick-skinned deformation is early Albian. This deformation is related to the Eoalpine orogeny, in which the Transdanubian Range was in the upper plate position with respect to the Eoalpine intracontinental subduction.

The transition in time and space from thin-skinned to thick-skinned deformation reflects the switch of the Transdanubian Range from lower to upper plate position.

New interpretation of selected tectonic structures - eastern part of the Polish Outer Carpathians

Adam KOZŁOWSKI[1]*, Aleksander GĄSIENICA[1], Arkadiusz DROZD[2], Krzysztof PIENIĄDZ[3]

[1]Polish Geological Institute - National Research Institute, Carpathian Branch, Krakow, Poland
[2]Oil and Gas Institute - National Research Institute, Krakow, Poland
[3]Faculty of Geology, Geophysics and Environmental Protection, AGH University of Krakow, Poland
**Lead presenter e-mail: adam.kozlowski@pgi.gov.pl*

The Carpathian orogen is a part of the mountain range which belongs to geological structures formed during the Alpine orogeny. The traditional and commonly used subdivision of the Polish segment of the Carpathians is based on a distinction between the Inner Carpathians and the Outer Carpathians. The study area is located in the eastern part of the Polish Outer Carpathians, built from formations belonging to the Silesian and Subsilesian units. In this area the Silesian unit (nappe) is divided into two minor parts – the Central Carpathian Depression and Czarnorzeki anticline which is overthrusted on Subsilesian unit.

As part of the implementation of the update of the Detailed Geological Map of Poland in scale 1:50 000 (Jedlicze and Rymanów sheets), INGA INNKARP project, a reinterpretation of the Potok anticline and the Węglówka zone was undertaken. The reinterpretation was based on borehole, cartographic and seismic data.

According to the new interpretation of the Potok anticline in the vicinity of Krosno, the oldest, Istebna Beds may be internally detached together with hanging wall anticlines. It is possible that this occurred as a result of shortening of the foreland of the anticline, which caused overthrust onto southern limb of the Moderówka syncline. Each successive thrust is related to the previous one, forming an imbricate fan structure. In this way, a series of thrusts may have developed on the southern limb of the anticline and consequently uplifted the older formations, from the southern limb towards the surface.

The Subsilesian unit in the vicinity of Mała Krasna is overthrusted by Lower Cretaceous formations of the Silesian unit. Reinterpretation of available borehole data made it possible to delineate several overlying tectonic thrusts forming a duplex. The duplex would have been formed at the stage of overthrusting of the Silesian and Subsilesian units on the Skole unit. With the formation of successive detachments, the angle of inclination of the original overlaps would increase, causing significant stacking within the Subsilesian unit, the equivalent of which at the surface are so-called the first and second Węglówka folds.

The seismic network of the University of Silesia as a part of AdriaArray Project

Maciej J. MENDECKI[1]*, Wojciech CZUBA[2], Piotr ŚRODA[2], Tomasz JANIK[2], Julia REWERS[2], Somayeh ABDOLLAHI[2], Monika BOCIARSKA[2], Szymon MALINOWSKI[3]

[1]*Institute of Earth Sciences, University of Silesia, Sosnowiec, Poland*
[2]*Institute of Geophysics, Polish Academy of Sciences, Warsaw, Poland*
[3]*Institute of Geophysics, University of Warsaw, Poland*
**Lead presenter*

The Institute of Geophysics, Polish Academy of Sciences, together with the University of Silesia in Katowice and the University of Warsaw installed the seismic instrument pool of broadband stations deployed in Southern Poland for the needs of the AdriaArray project. The project aimed to geophysical studies of the Upper Mantle between the Carpathians and the Mediterranean Sea. The University of Silesia arranged 7 seismometer stations from the Opawskie Mountains through the Upper Silesian Coal Basin to the Beskid Mały, Southern Poland. Together with 22 stations of the Institute of Geophysics and the University of Warsaw, the seismological network in Poland consists of 29 sensors. The cooperation of these Polish institutions is represented as the Polish AdriaArray Group. The Silesian sensors are six 151-OBSERVER seismometers and one COLT 60 seismometer. Both types were manufactured by RefTek. They are operating since 2019, providing continues and high quality seismic data.

AdriaArray is a multi-national effort to cover the Adriatic Plate and its active margins in the central Mediterranean by a dense regional array of seismic stations to understand the causes of active tectonics and volcanic fields in the region. Plate-scale observations are complemented by local and LargeN experiments in key areas. The AdriaArray region reaches from the Massive Central in the west to the Carpathians in the east, from the Alps in the north to the Calabrian Arc and mainland Greece in the south.

Polish part of the seismic array will extend to the North of the Carpathian orogen, reaching much older units – Precambrian East European Craton and adjacent Palaeozoic blocks. As a zone of contact of three large geological systems with contrasting age of consolidation (from Proterozoic to Cainozoic), this area is of particular importance for geodynamical studies. Collected data will be analysed using P- and S-wave receiver functions, SKS wave splitting analysis, ambient noise interferometry, measurements of surface wave dispersion curves and modelling based on data from local events, models of three-dimensional distribution of seismic wave velocities and densities will be obtained. Inversion analysis will allow for determining P- and S-wave velocity models of the crust and the upper mantle beneath the Adriatic plate and its surroundings. Analyses of seismicity and multi-scale passive seismic imaging will lay the ground for a physical understanding and modelling of plate deformation and associated geohazards.

Acknowledgement: „The work was supported by the National Science Centre, Poland, under research project „Passive Seismic Studies of the Lithosphere and Asthenosphere of the Southern Poland (Carpathian area)", No. UMO-2019/35/B/ST10/01628".

Finite strain distribution in kinematic models of fault-related folding

Szymon MOL[1,2]*, Marcin DĄBROWSKI[1]

[1]*Computational Geology Laboratory, Polish Geological Institute - National Research Institute, Wrocław, Poland*
[2]*Institute of Geological Sciences, Jagiellonian University, Krakow, Poland*
**Lead presenter e-mail: szymon.mol@student.uj.edu.pl*

Fault-related folds are associated with faulting both in space and in time. The understanding of fault-related folding mechanisms is crucial for example in industrial applications due to the fact that geophysical imaging is usually of poor quality in the vicinity of faults. Thus, the improved models of fault-related folding can lead to better predictions of structural traps. In general, fault-related folds are divided into three genetic groups: detachment folds, fault-bend folds, and fault-propagation folds. Kinematic and mechanical models represent two major approaches to modelling of fault-related folding. Kinematic models only include the description of movement, whereas mechanical models try to incorporate the physical description of deformation (stress and strain fields) and its relationship to physical properties of rocks (such as viscosity, elastic stiffness etc.). The ease of use is the main advantage of kinematic modelling, however, not all kinematic models are simplistic. For example, a kinematic trishear model incorporates a number of parameters that can be tuned to obtain realistic solutions.

The poster presents selected models of fault-related folds with special focus on kinematic models. Displayed models include all three geometrical types of fault-related folding. Besides showing the systematic parametric dependence of various models, diagrams include the spatial distribution of finite strain.

The work was supported by the National Science Centre, Poland, under research project “Numerical and field studies of anisotropic rocks under large strain: applying micro-POLAR mechanIcS in structural geology (POLARIS)”, no UMO-2020/39/I/ST10/00818.

Miocene volcanism in the Slanské Vrchy Mountains, eastern Slovakia

Jörg OSTENDORF[1]*, Robert ANCZKIEWICZ[1], Milan KOHÚT[2]

[1]*Institute of Geological Sciences, Polish Academy of Sciences, Krakow Research Centre, Poland*
[2] *Earth Science Institute, Slovak Academy of Sciences, Bratislava, Slovakia*
**Lead presenter e-mail: j.ostendorf@ingpan.krakow.pl*

The c. 50 km long, N-S trending Slanské Vrchy volcanic chain is located at the western flank of the Miocene Transcarpathian basin system in eastern Slovakia. The volcanics are in general represented by andesites and dacites. More mafic volcanics were not found, except for one basaltic andesite enclave, which, however, has not the most primitive isotopic composition of the studied samples. Robust concordant U–Pb zircon ages are indistinguishable for the andesites (n=5) and dacites (n=3) and range from 12.2 ± 0.2 Ma to 11.8 ± 0.2 Ma, indicating that volcanism postdated collision in the Western Carpathians. Isotopic compositions of the basaltic andesite, andesites, and dacites are overlapping and well correlated ($^{87}Sr/^{86}Sr(12Ma)$ = 0.7071 to 0.7104, $\varepsilon Nd(12Ma)$ = –7.0 to –1.0, and $\varepsilon Hf(12\ Ma)$ = –6.2 to +2.8), which reflect contributions of mantle and crustal components to the volcanic system. A general lack of correlations between fractionation indicators (e.g., SiO2) and isotope ratios as well as overlapping isotopic compositions for the andesites and the dacites preclude simple coupled assimilation fractional crystallization (AFC) processes. Furthermore, the overall scarcity of inherited zircon points to limited assimilation at upper crustal levels. Accordingly, the genesis of Slanské Vrchy volcanics most likely involved processes of mixing, assimilation, storage, and homogenization (MASH) in lower crustal zones where mantle-derived melts interacted with the lower crust. Initial melt generation in the mantle was either triggered by decompression melting or by lower crustal delamination, but details on the nature of the mantle source remain indistinct because initial signatures of primitive mantle melts were obscured by lower crustal hybridization processes. Further modifications of the hybrid magmas ascending from lower crustal zones by fractional crystallization and mixing occurred probably in complex multi-level crustal plumbing systems.

An updated model of the Cenozoic cover of the Fore-Sudetic Block: implications for its neotectonic activity

Michał SŁOTWIŃSKI[1]*, Janusz BADURA[2], Marcin DĄBROWSKI[1]

[1]*Computational Geology Laboratory, Polish Geological Institute - National Research Institute, Wrocław, Poland*
[2]*Polish Geological Institute - National Research Institute, Lower Silesia Branch, Wrocław, Poland (retired researcher)*
**Lead presenter e-mail: michal.slotwinski@pgi.gov.pl*

The Fore-Sudetic Block (FSB) is a tectonic unit located in the northern part of the Bohemian Massif. In contrast to the adjacent Sudetes, where the recent uplift resulted in large-scale exposure of the crystalline basement, the Fore-Sudetic Block is largely buried under a cover of the Cenozoic sediments, with only local outcrops of the basement rocks. The sub-Cenozoic surface is presumed to have been predominantly levelled by erosion prior the deposition of the Cenozoic strata. Thus, most steep irregularities of the crystalline basement of the FSB can be attributed to neotectonic activity. Moreover, the stark contrast between the lithological and physical properties of the cover (mostly clastic, weakly lithified sediments) and the basement (metamorphic and plutonic rocks) facilitates geophysical imaging of their contact.

The FSB has already been subject to several studies focusing on its Cenozoic cover (e.g., Badura and Przybylski, 2000; Badura et al., 2004). However, the recent two decades have brought both new survey data and the development of new digital modelling techniques that can be utilised to verify and refine the old models. Hence, we have constructed an updated model, which builds on about 40% more of both borehole and geoelectric datapoints compared to its predecessors. Additionally, it benefits from modern digital modelling methods, including the discrete approach to modelling of dislocation zones. The obtained structural model provides a robust framework for systematically identifying potential neotectonic dislocation zones within the Cenozoic basement level of the FSB.

The presented model shows appreciable differences upon comparison to the preceding interpretations in several areas, notably in the Ziębice area, along the Fore-Sudetic Marginal Fault and in the southern periphery of Middle Odra Fault Zone. Furthermore, the internal complexities of two prominent grabens, the Roztoka-Mokrzeszów and Paczków grabens, have been identified in much finer detail. The model is a significant step forward towards better understanding of the Cenozoic tectonics in the Sudetic region. Further efforts should focus on constraining the exact timing of the tectonic activity recorded within the Cenozoic cover.

Badura, J., Przybylski, B., 2000. Mapa neotektoniczna Dolnego Śląska (Neotectonic Map of Lower Silesia), Unpublished, in-house report from the archives of Lower Silesian Branch of Polish Geological Institrute.

Badura, J., Przybylski, B., Zuchiewicz, W., 2004. Cainozoic evolution of Lower Silesia, SW Poland: a new interpretation in the light of sub-Cainozoic and sub-Quaternary topography. Acta Geodynamica et Geomaterialia 1.

First insights into the LiDAR-driven structural analysis of the Bystre Slice (Outer Carpathians)

Piotr STRZELECKI[1]*, Radosław SZCZĘCH[1,2], Jakub ANDRZEJAK[1,2*] Marta ESMUND[1,2]

[1]Faculty of Geology, Geophysics and Environmental Protection, AGH University of Krakow, Poland
[2]Students' Scientific Association AZYMUT, AGH University of Krakow, Poland
**Lead presenters e-mail: piotr.strzelecki@agh.edu.pl*

Light Detection and Ranging (LiDAR) has revolutionized geological sciences by providing high-resolution topographic details for accurate surface mapping. Its capacity to penetrate vegetation offers a unique perspective, allowing the recognition of linear geological features with unparalleled precision and enabling the identification and mapping of faults, fractures, and other structural elements that may go undetected by traditional techniques.

The Bystre Slice is a tectonic feature located within the Fore-Dukla Zone, a prominent tectonic zone situated within the Silesian Nappe, separating it from the Dukla Nappe. The Bystre Slice stands out as a unique geological site due to the remarkable presence of metallic mineralization in Cretaceous and Paleogene rocks. The significance of this site lies in the fact that the mineralization is closely associated with faults and linked to hydrothermal processes occurring after a major tectonic shortening within this part of the Outer Carpathians. Hence, the recognition and detailed analysis of the fault network are pivotal as they serve as pathways for hydrothermal fluids responsible for the formation of mineralization.

In general, the primary direction of shortening, as recorded by the folded strata, indicates NE-SW oriented shortening both within the Bystre Slice and its close surroundings. Based on LiDAR data analysis, two additional mutually closely orthogonal trends were identified, showing approximately N-S and E-W oriented shortening. These trends are represented by map-scale thrusts and strike-slip faults, both present within the Bystre Slice and its close surroundings. These faults cut through the structure, with the primary trend indicating their later origin. Additionally, LiDAR reveals how lithostratigraphic units mechanically play a role, with competent units exhibiting brittle faulting, while incompetent lithostratigraphic units are being refolded.

The study indicates that recently identified features might have played a role in fluid migration and mineralization. Additionally, it underscores the significance of utilizing LiDAR data in geological mapping.

Progressive development of an accretionary wedge margin from oblique thrust to strike-slip fault (Mikulov-Falkenstein Fault, Outer Western Carpathians)

Martin ŠUŤJAK[1]*, Rostislav MELICHAR[1], Ivo BAROŇ[2], Yi-Chin CHEN[3], Jan ČERNÝ[1], Jia-Jyun DONG[4], Václav DUŠEK[1], Filip HARTVICH[2], Jan KLIMEŠ[2], Lenka KOCIÁNOVÁ[1], Tùng NGUYỄN[4], Matt ROWBERRY[2], Chia-Han TSENG[5]

[1]Department of Geological Sciences, Masaryk University, Brno, Czech Republic
[2]Institute of Rock Structure and Mechanics, Czech Academy of Sciences, Prague, Czech Republic
[3]Department of Geography, National Changhua University of Education, Changhua, Taiwan
[4]Department of Earth Sciences, National Central University, Taoyuan, Taiwan
[5]Institute of Earth Sciences, Academia Sinica, Taipei, Taiwan.
**Lead presenter e-mail: sutjak@mail.muni.cz*

The Outer Western Carpathians are fractured by several syn-thrust and post-thrust faults. One of them, the Mikulov-Falkenstein Fault, has been studied using a combination of surface and subsurface methods. The former comprised the analysis of a LiDAR digital terrain model with 1 m resolution, interpretation of ortophotos and compass measurements of fault-slip data, while the latter comprised the analysis of ERT profiles and 2D seismic reflection profiles interpreted with the aid of borehole data. Paleostress analysis has also been used to understand the stress history and progressive development of the fault. By combining these methods, it has been possible to define a distinct N-S directed fault zone that intersects or delineates the majority of the Jurassic limestone nappe outcrops around the highlands of Pavlov Hills. This almost continuous fault zone runs for several kilometers on the Czech side of the border and extends further south to Austria. The thrusted Jurassic limestone bodies are cut by the fault zone, which tectonically crushed the limestone. The mapped pattern of the fault zone suggests branching and reattaching with the production of lenticular tectonic slices. Consequently, we interpret the fault as a prominent sinistral shear zone. This is indicated on the surface by block displacement on Svatý kopeček Hill and by the orientation of the accompanying subvertical Riedel shears with identified horizontal lineation. Subsurface kinematic indication derives from the interpretation of a prominent negative flower structure in the deep seismic profiles, just beneath the fault zone. The ERT profiles have revealed that the limestone bodies are tectonically bound by accompanying fault branches. Moreover, paleostress analysis suggest that fault zone activity can be divided into three main stages: (i) NW-SE thrust faults indicate thrusting of the Carpathian accretion wedge over the Bohemian Massif; (ii) NW-SE strike-slip faulting, during which the fault blocks moved along the faults in the direction of propagating wedge; (iii) N-S strike-slip faulting, marking the change in compression direction and transition from thrusting to a strike-slip regime. The main movement along the fault is probably of the late Miocene age and probably continues to the present day.

The research was supported by the grant project GC22-24206J: "Coseismic Landslides in Mountain Ranges of Active and Stabilized Accretionary Wedges,"

Deformation bands in the Red River Fault Zone, Vietnam: preliminary findings

Piotr STRZELECKI[1], Le Duc ANH[2], Anna ŚWIERCZEWSKA[1]*, Antek K. TOKARSKI[3], Nguyen Quoc CUONG[2], Phan Dong PHA[2]

[1]*Faculty of Geology, Geophysics and Environmental Protection, AGH University of Krakow, Poland*
[2]*Vietnam Academy of Science and Technology, Vietnam*
[3]*Institute of Geological Science, Polish Academy of Sciences, Krakow Research Centre, Poland*
**Lead presenter e-mail: anna.swierczewska@agh.edu.pl*

The Red River Fault Zone (RRFZ) is a prominent geological feature spanning across Southeast Asia, with a length exceeding 1,200 kilometers. This complex tectonic boundary separates the South China Block from the Indochina Block, standing as evidence of the dynamic geological processes shaping the region. The RRFZ plays a crucial role in seismic activity, landscape evolution, and societal impact, making it a focal point for geological studies and a critical factor for regional development and disaster resilience. Continued research on the RRFZ is essential for enhancing our understanding of tectonic processes and improving strategies to mitigate earthquake risks in this seismically active area.

The RRFZ is characterized by an intricate network of faults and folds, reflecting ongoing tectonic processes in the region. It primarily functions as a strike-slip fault system with differentiated vertical movements along its faults. During the Miocene evolution of the RRFZ, several sedimentary basins formed along it. The Miocene infill of these basins typically consists of conglomerates intercalated with sandstone layers and mudstones.

For the first time, deformation bands have been documented in Vietnam within two Miocene sedimentary basins developed along the RRFZ, located approximately 200 kilometers apart. Deformation bands were identified in the basins near Lao Cai and Viet Tri cities. At both sites, these bands were recognized within sandstone successions, recording basin extension. However, deformation bands seem to have formed at different tilting of the host rock and under distinct diagenetic and burial conditions. It appears that in the vicinity of Lao Cai city, they experienced a greater impact of burial conditions, while near Viet Tri, they are typically found in very poorly lithified strata and appear to be structures formed at shallower depths.

The goal is to shed light on the on the structural evolution of both the sedimentary basins and the RRFZ. This objective involves defining the scaling relationship between burial conditions and stress fields to achieve a more profound comprehension of the basin formation processes along the RRFZ.

Acknowledgments: the research was supported by project VAST05.01/23-24 and AGH Statutory funds.

Late Pleistocene surface fault rupture in slow-deforming Podhale Basin (Western Carpathians): implications for paleoseismology and geodynamics

Jacek SZCZYGIEŁ[1]*, Jerzy ZASADNI[2], Piotr KŁAPYTA[3], Marta WOSZCZYCKA[1], Krzysztof GAIDZIK[1], Maciej MENDECKI[1], Artur SOBCZYK[4], Christoph GRÜTZNER[5]

[1]*Institute of Earth Sciences, University of Silesia, Sosnowiec, Poland*
[2]*Faculty of Geology, Geophysics and Environmental Protection, AGH University of Krakow, Poland*
[3]*Institute of Geography and Spatial Management, Jagiellonian University, Poland*
[4]*Institute of Geological Sciences, University of Wrocław, Poland*
[5]*Institute of Geological Sciences, Friedrich-Schiller-Universität Jena, Germany*
**Lead presenter*

While earthquakes mainly occur along active tectonic plate boundaries, they are also recorded outside of these zones. Areas with low deformation rates and minor relative displacements, such as continental interiors or mature orogens (e.g., the Western Carpathians), may represent significant, albeit still insufficiently recognized, seismic hazard zones. Secondary effects associated with earthquakes, such as landslides, are documented much more frequently due to the lower magnitude of seismic events required to trigger them. However, due to the multitude of potential causes of secondary deformation, their origin often remains speculative. Therefore, documenting primary effects, such as surface fault ruptures, is crucial for recognizing past seismic activity. Although surface fault ruptures have been reported in intraplate regions, they are generally sporadic occurrences. An analysis of LiDAR DEM data in the SE Podhale area revealed the presence of a morphological scarp near the village of Brzegi, which may represent a geomorphological manifestation of a surface fault rupture in the Podhale Basin. We employed a standard paleoseismology analysis to recognize the observed structure, including geological and geomorphological mapping, high-resolution terrain modeling, ERT and GPR geophysical methods, and trench investigations. However, suitable geological material for geochronological analyses could not be obtained during the study. Therefore, in an attempt to determine the age of the fault, scarp diffusion modeling was conducted. The collected data are not definitive in the identification of the morphological scarp origin. Nonetheless, a comprehensive analysis of all gathered data allows for the hypothesis that assuming a seismic-tectonic origin of the scarp in Brzegi, the associated fault may have generated earthquakes of magnitude ~M6. Furthermore, the documented dextral offset fits into the context of the late Neogene tectonic evolution of the Western Carpathians. Conversely, the degree of scarp erosion and its superposition relative to terrain features suggest that the fault in Brzegi was likely active during the late Pleistocene.

Tectonic Złatne Unit in the Pieniny Klippen Belt

Anna WAŚKOWSKA[1]*, Jan GOLONKA[1], Kamil CICHOSTĘPSKI[1], Jerzy DEC[1], Monika ŁÓJ[1], Grzegorz BANIA[1], Włodzimierz Jerzy MOŚCICKI[1], Sławomir PORZUCEK[1], Józef CHOWANIEC[2]

[1]Faculty of Geology, Geophysics and Environmental Protection, AGH University of Krakow, Poland
[2]Polish Geothermal Society, Krakow, Poland
**Lead presenter*

Wacław Sikora (1971) distinguished the Złatne Succession deposited in the deep part of the Złatne Basin that constituted the southeastern branch of Alpine Tethys. The Złatne Basin occupied the area on the south from the Czorsztyn Ridge which separated the Złatne Basin from Magura Basin. The stratigraphic inventory of the Złatne Basin includes the deep water Jurassic–Lower Cretaceous rocks, followed by the Albian–Neogene flysch sequences. These sequences include sedimentary mélange containing large olistoliths of Triassic–Paleogene rocks, mainly limestones.

Albian flysch sedimentation began the synorogenic stage of basin development which was initiated by the subduction of the oceanic basement of the Alpine Tethys under the Central Carpathian Plate. An accretionary prism was formed, which at the end of the Cretaceous began to collide with the Czorsztyn Ridge. A piggy-back basin was formed after this collision. Turbidite and pelagic sedimentation continued until the Neogene in this basin. During orogenic movements, the formations of the Złatne Basin were transformed into the Złatne tectonic unit, belonging to the structure of the Pieniny Klippen Belt. This unit is best exposed in the Spiš Pieniny Mountains in Poland and in the Haligovce - Vel'ký Lipník area in the Małe Pieniny Mountains in Slovakia. It displays nappe character well visible in the deep seismic profiles. The other geophysical surveys, SRT, gravity and geoelectric revealed the relationship between Złatne and other tectonic units of Pieniny Klippen Belt in the Spiš Pieniny Mountains in Poland. The Pieniny Klippen Belt marks the suture zone between Central Carpathian and North European plates as well as the boundary between Central and Outer Carpathians. The significant reduction of the width of Alpine Tethys basins happened during the tectonic evolution, and now the Pieniny Klippen Belt structure is three to five kilometers wide. Both tectonic and sedimentary processes contributed to the origin of mélanges in the Pieniny Klippen Belt. The tectonic processes resulted in the creation of a complex structure expressed in existence of nappes and secondary thrust units, as well as strike-slip faults of different orientation. The mass transportation sedimentary processes produced toe-thrusts and olistostromes.

This research was financially supported by the Polish National Science Center grant NCN – 2019/35/B/ST10/00241.

Deformation events of the Permian Boda Claystone recorded by tectonic veins (Tisza Mega-unit, Mecsek Mts.)

Ervin HRABOVSZKI[1,2]*, Péter MOLNÁR[3], Félix SCHUBERT[1]

[1]*Department of Mineralogy, Geochemistry and Petrology, University of Szeged, Hungary*
[2]*Department of Mineralogy and Geology, University of Debrecen, Hungary*
[3]*Public Limited Company for Radioactive Waste Management, Hungary*
**Lead presenter e-mail: ervin.hrabovszki@geo.u-szeged.hu*

The Permian Boda Claystone Formation is in the focus of a national research program in Hungary, aiming to select a site for the deep geological disposal of high-level radioactive waste. The distribution and porosity-permeability parameters of the formation make it suitable for isolating such waste; however, fractures and mineral veins can significantly modify its fluid retention capacity. The research aims to determine whether the vein generations previously identified in the BAF–2 borehole of the Boda Claystone can be found in other parts of the claystone body. As part of this large-scale project, in this manuscript, the veins of the BAF–2, and BAF–3, –3A boreholes are compared to reveal their genetic relationships and connection with regional tectonics. In the BAF–2, four vein generations are present, veins with cone-in-core structures (VeinCIC), straight veins (VeinSTR), en-echelon veins (VeinECH), and breccia veins (VeinBR). The main cement minerals are calcite and anhydrite. The combined interpretation of d18OV-SMOW and fluid inclusion microthermometric data of calcite cements suggests basinal brine origin for most parent fluids, but meteoric in the case of VeinBR. Within the BAF–3, –3A boreholes six vein generations can be identified, four of which coincide with those observed in the BAF–2. Further vein generations are characterised by a crack-seal texture of stretched calcite crystals (VeinC-S) and relatively high (>5 cm) thickness (VeinTH) of anhydrite-dolomite filling. In the case of VeinTH, the fluid origin is basinal brine, while the VeinC-S presumably reflects the mixing of brine and meteoric fluids. Due to the unoriented drill cores, the stress fields related to different veins cannot be determined, but the following conclusions can be made. Based on its microstructure, the VeinCIC is related to atectonic, diagenetic processes. The VeinSTR was formed in an extensional regime. Members of the VeinC-S crosscut the VeinSTR generation suggesting their relative age, and their syntectonic texture suggests pure extensional vein formation. The VeinECH group records compressional tectonics. In the case of VeinBR, in-situ rock fragmentation textures suggest hydraulic brecciation as one of the youngest events. Considering all this, establishing a correlation between vein formation and regional tectonics proves to be a challenging task, and the direct link between them has not yet been explored, highlighting the necessity for further investigation.

Acknowledgements: This research was financially supported, and its publication was permitted by the Public Limited Company for Radioactive Waste Management, Hungary. The project is supported by the National Research, Development and Innovation Office (OTKA PD 147180).

Reconstructing Neogene landscape and tectonic history of the NE Bohemian Massif using paleokarst sediment palynology from the Orlica-Śnieżnik Dome marbles

Artur SOBCZYK[1]*, Elżbieta WOROBIEC[2], Marcin OLKOWICZ[3], Jacek SZCZYGIEŁ[4]

[1]*Institute of Geological Sciences, University of Wrocław, Poland*
[2]*Władysław Szafer Institute of Botany, Polish Academy of Sciences, Krakow, Poland*
[3]*Computational Geology Laboratory, Polish Geological Institute - National Research Institute, Wrocław, Poland*
[4]*Institute of Earth Sciences, University of Silesia, Sosnowiec, Poland*
**Lead presenter*

The discovery of newly unearthed paleokarst sediments in the Eastern Sudetes represents a significant advancement in our efforts to piece together the landscape and tectonic history of the NE Bohemian Massif during the Neogene (Sobczyk et al., 2024). Through detailed palynological analysis of seven samples extracted from the karst fissure, we were able to study the distribution of pollen grains, spores of plants as well as non-pollen palynomorphs, such as algal and fungal microremains, within each sediment layer. Our findings unveiled a rich array of pre-Quaternary taxa, including "paleotropical" species, embedded within the deposits. Notably, pollen analysis shed light on the prevailing climatic conditions during the deposition of the Nowy Waliszów karst infill, suggesting a warm temperate and humid climate. The vegetation profile indicated the presence of wetland flora comprising swamp forests, riparian forests, and shrub bogs alongside mesophytic forests. These recorded taxa are emblematic of flat and undulating terrains, preceding the emergence of the current mountainous relief exceeding 1000 meters, as well as the formation of the primary European triple drainage divide in the Śnieżnik Massif. Paleokarst palynology provides compelling evidence for a Mid-Miocene onset (~15 ± 1.5 Ma) of environmental transformations in the Sudetes region, attributed to the accelerated tectonic uplift of the Śnieżnik Massif, propelled by the eastern boundary faults delineating the Upper Nysa Kłodzka Graben and Orlica–Śnieżnik Dome tectonic blocks. The presence of Miocene paleokarst sediments in Nowy Waliszów indicates a relatively modest uplift rate of 0.10 mm/a, which has influenced the landscape evolution in the northwest part of the Śnieżnik Massif from the late Mid-Miocene (Serravallian/Sarmatian) through the Pliocene.

Fault patter and extension during the Miocene syn-rift phase in the central Pannonian Basin (Pilis-Buda Hills); fault geometry analysis and cross section balancing

Melinda FIALOWSKI[1]*, Barbara BEKE[1], László FODOR[2,1]

[1]*Eötvös Loránd University, Department of Physical and Applied Geology, Budapest, Hungary*
[2]*HUN-REN Institute of Earth Physics and Space Science, Sopron, Hungary*
**Lead presenter*

The aim of this study is to describe the fault pattern on a geological map made along an NNE-SSW cross section and balance the NNE-SSW cross section to get a better understanding of the amount of the extension in the study region. Even though former maps already exist of the region, field observations revealed that those maps need major updates. One of the reasons is surly that general understanding of fault patterns developed greatly during the past decades. Thus, the fault pattern presented on the updated geological map differs considerably from former maps.

While comparing stereograms with the geometry of the fault pattern, main deformation phases were separated. Further complications raised however, that a continuous transition of fault and stress axes directions occurred between successive phases thus distinguishing between different deformational events was often difficult. On map view stepovers, relay ramps, curved fault traces, merging and debranching fault segments further complicated the understanding of the fault pattern.

The earliest phase occurred as a NNW–SSE extension that formed ENE-WSW striking faults. These structures formed probably prior to the the syn-rift phase during the latest Oligocene – earliest Miocene. During the early syn-rift phase extensional direction rotated to NNE–SSW and resulted in WNW–ESE striking faults with extensional character after 18.5 Ma. The relationship of the stress field change to vertical-axis rotation events is not yet clear. During the next stage of the syn-rift phase, due to a vertical-axis rotation event, the extension direction changed to a NE–SW. Typical structures are NW–SE striking normal faults and simultaneous N–S striking sinistral and (W)NW–(E)SE striking dextral faults. Probably after the last rotation event another phase was observed, probably started in the late Badenian (~13.8 Ma), when within a W–E to WNW–ESE extension N–S to NNE-SSW striking faults appeared. These were the youngest observed structures in the region. A noticeable complication is that the same extensional direction also occurred during the Cretaceous as well which often cannot be distinguished from a younger extension with similar direction, if being measured in Mesozoic formations. However, tilt test of fractures to horizontal position of Triassic beds can lead to separation of pre-tilt fracture system.

Acknowledgements: The research was supported by the OTKA grant 134873 of the Hungarian National Research, Development and Innovation Office.

Tectonics of the Silesian and Skole Nappes contact in the eastern part of the Węglówka tectonic window

Rafał NASIŁOWSKI[1]*

[1]*Polish Geological Institute - National Research Institute, Warsaw, Poland*
**Lead presenter e-mail: rnas@pgi.gov.pl*

The poster presents the geological structure of the contact between the Silesian and Skolian Nappes in the eastern part of the Węglówka tectonic window, based on the reinterpretation of cartographic material, reservoir data, seismic profiles and the Digital Elevation Model supported by field studies.

The subsurface structure of the regional folds occurring in the study area was analyzed in the Silesian Nappe the dichotomous structure of the Potoka anticline was confirmed, with its box-like geometry with detachment fold features in the shallower parts, while sequence of duplexes in the deeper parts. A model for the formation of the Iskrzynia anticline and the Korczyna anticline as a result of fault propagation was proposed. In addition, the structure of the Turzego Pola anticline was described. It was showed to have formed as a result of the detachment folding, and flat-ramp-flat thrusting style. In the southern wing of this anticline, contractional faults have been interpreted on the seismic profiles. The isolated fragment of the Bonarówka thrust was described, confirming its brachysyncline geometry with a west-dipping axis. It has been suggested that it has a structural similarity with the Brzozowa syncline. In the Sub-Silesian Nappe, three anticlines belonging to the Węglówka tectonic window were described in the Sub-Silesian Nappe, confirming that they were detached and thrusted northward resulting in strongly reduced basal anticlinal wings.

The small-scale tectonic structures such as folds, faults, fractures and slickensides with slip-sense indicators were also documented. The lineaments indicated based on the DEM have been correlated with faults studied in the field. Thus, sets of regional strike-slip faults that are oblique to the axis of regional folds were determined. The research results indicate a model of the formation of the Węglówka and Bonarówka tectonic units in the form of duplexes with thin-skinned folds lying on them.

A pilot network of InSAR reflectors in the Śnieżnik Massive – preliminary assumptions

Mateusz DROŻDŻEWSKI[1]*, Bartłomiej GROCHMAL[1], Marcin OLKOWICZ[1],Zbigniew PERSKI[2], Marcin DĄBROWSKI[1]

[1]*Computational Geology Laboratory, Polish Geological Institute - National Research Institute, Wrocław, Poland*
[2] *Geohazards Center, Polish Geological Institute - National Research Institute, Krakow, Poland*
**Lead presenter e-mail: mateusz.drozdzewski@pgi.gov.pl*

Synthetic Aperture Radar Interferometry (InSAR) is a crucial satellite technique for surface deformation monitoring with sub-centimeter accuracy. One of the dedicated missions for collecting InSAR observations is the Sentinel 1 mission, which consists of two satellites orbiting in the opposite direction, from south to north (ascending) and from north to south (descending). The data time series from Sentinel 1 mission are available trough the European Ground Motion Service (EGMS). The data in the EGMS service are available as 3 types of products: the 'Basic level' that represents the relative displacements in the Line-of-Sight Direction (LoS). The second product named 'Calibrated data' corresponds to the basic measurements referenced to the model derived from Global Navigational Satellite Systems (GNSS) and, thus, the InSAR observations are adjusted to the Earth-Centered Earth-Fixed Reference Frame (ECEF). Finally, the East–West and Up components are resolved in the 'Ortho product' delivered for 100 x100 m spatial grid resolution.

The density of points producing sufficiently strong reflections in the InSAR technique strongly depends on the land cover of the region of interest. In general, the vegetated areas mark a lower density of registered InSAR points than the urban areas that typically exhibit more stable reflectors. In the areas with high vegetation and a correspondingly low resolution of InSAR reflections, the number of reflections could be improved by installing artificial stabilized corner reflectors with known coordinates derived from GNSS measurements.

Within this work, we present the design of a corner reflector network that will be established in the high-vegetated Śnieżnik massive area to provide state-of-the-art continuous monitoring of the poorly recognized present-day geodynamic processes in the Śnieżnik massive area. Taking the approach of long-term monitoring will enable us to capture the motion of the studied tectonic structures with a sub-millimeter accuracy.

Formation of the active Tabas Fold Belt as result of transpression and rotation of the tectonic blocks, Tabas block, Iran

Andrzej KONON[1*], Alireza NADIMI[2], Mateusz MIKOŁAJCZAK[3], Barbara RYBAK-OSTROWSKA[1], Michał WYGLĄDAŁA[1], Soheila BOUZARI[4], Soheyla BEYGI[2]

[1]Faculty of Geology, University of Warsaw, Poland*
[2]Department of Geology, Faculty of Science, University of Isfahan, Isfahan, Iran
[3]Institute of Geological Sciences, Polish Academy of Sciences, Warsaw, Poland
[4]Islamic Azad University, North Tehran Branch, Geology Department, Tehran, Iran
[*] Lead presenter e-mail: andrzej.konon@uw.edu.pl

The formation of the active Tabas fold belt (TFB) was controlled by large-scale dextral transpression along the Nayband fault and the counter-clockwise rotation of the Tabas and Lut blocks. During the late Pliocene(?) – Quaternary, a continuous change of far-field stress from 30° to nearly 10° resulted in the inversion of the Tabas Basin. As a result of the deformation started to form the right-stepping buckle folds composed of Miocene-Pliocene rocks. During the next stage, the counterclockwise rotation of the Lut block caused the Shotori deformation belt to be pushed, which facilitated the development of the en échelon pattern of strike-slip faults. As a result, the sinistral strike-slip faults dissected the Neogene folds and changed their trends. To better understand the structure of the Tabas fold belt, an attempt was made to perform two-dimensional forward modeling based on gravity and magnetic data along a profile perpendicular to the belt and geomechanical modeling based on the BEM technique for the entire belt. The results of the two-dimensional forward modeling compared with cartographic data, field geological observations and depth of distribution of earthquakes allowed for the proposal of a model of the structure of the TBF consisting of an upper thin-skinned fold belt and a lower thick-skinned thrust belt. Geomechanical modeling, which made it possible to consider a change in regional stresses from 30° to nearly 0°, indicates the possibility of southward migration of uplift centres along thrusts that bound the folds. The field observations of the Quaternary growth strata associated with progressive limb rotation during folding, the offset of the alluvial fans and the hills recognized along the major and second-order strike-slip faults that cut the folds as well as the tendency to migration of vertical surface displacements along the thrusts display the recent activity of the Tabas fold belt, confirmed by present-day seismicity and GPS measurements within the Tabas block.

Field trips

DOI: http://dx.doi.org/10.7306/CETEG2024-1

Pre – Conference excursion guide

From Neoproterozoic sedimentation on the Peri-Gondwanan extended shelf to the Variscan collision of terranes. The history preserved in the Kamieniec Ząbkowicki metamorphic belt and the Doboszowice metamorphic complex

Jacek Szczepański[1], Mirosław Jastrzębski[2], Sławomir Ilnicki[3], Robert Anczkiewicz[4]

1. University of Wrocław, Institute of Geological Sciences, jacek.szczepanski@uwr.edu.pl
2. Polish Academy of Sciences, Research Centre in Wroclaw, mjast@interia.pl
3. University of Warsaw, Department of Geochemistry, Mineralogy and Petrology, slawomir.ilnicki@uw.edu.pl
4. Polish Academy of Sciences, Research Centre in Kraków, ndaczki@cyfronet.pl

The field trip is focused on rock successions exposed in the Kamieniec Metamorphic Belt (KMB) and the Doboszowice Metamorphic Complex (DMC) located in the Fore-Sudetic Block at the NE margin of the Bohemian Massif (Fig. 1). Here, the crystalline basement forms small and isolated outcrops, emerging only in places from the overlying Cenozoic cover. This part of the Bohemian Massif is located at the eastern extremity of the Central European Variscides that exposes three major units from west to east: 1) the Teplá-Barrandian Unit consisting of Neoproterozoic basement and its Early Palaeozoic cover that according to some authors is exposed in the Góry Sowie Block (GSB); 2) the Saxothuringian Unit that is exposed both west of the GSB in the Karkonosze-Izera Massif and east of the GSB in the KMB and the DMC; and 3) the Brunovistulian Neoproterozoic basement with Early to Late Palaeozoic cover that is exposed in the East Sudetes represented by the Strzelin Crystalline Massif and the Jeseniky Mts. Generally, metamorphic complexes of the Bohemian Massif have recently been interpreted as the result of a long-lasting Andean-type convergence and collision of the Saxothuringian, Teplá-Barrandian and Brunovistulian Units of the Central European Variscides (e.g. Schulmann et al. 2009; Mazur et al., 2010; Chopin et al., 2012).

The aim of the pre-conference field trip is to present the latest data and interpretations on the provenance of the detrital material, its maximum depositional age and the tectonic setting of deposition, as well as the structural and metamorphic evolution of the KMC and DMC within the framework of the Central European Variscides.

The KMB forms c. 25 km long and 5 km wide longitudinal belt between the Góry Sowie Massif and the Niemcza Shear Zone in the west and the Strzelin Crystalline Massif (including the Lipowe Hills) in the east (Fig. 1). A volcano-sedimentary succession exposed in the KMB is dominated by mica schists (stops 1 and 2) intercalated with scarce paragneisses, marbles, quartz-graphite schists, eclogites (stop 2) and felsic metavolcanics (stop 1, Fig. 2). The latter are interpreted as tuffs or lava flows (Dziedzicowa, 1966) or sills (Szczepański et al., 2023). On the contrary, the DMC is a c. 6 km long exposure of crystalline basement located south-east of the KMB and directly west of the Niedźwiedź Amphibolite Massif (NAM, Fig. 1). The DMC may be divided into western and eastern parts (Fig. 2). The western part exposes the Doboszowice orthogneiss with Cambro-Ordovician protolith age (stop 3). The eastern part is mainly composed of the migmatic Chałupki paragneiss

(stop 4) interleaved with scarce mica schists and metabasalts of unknown age.

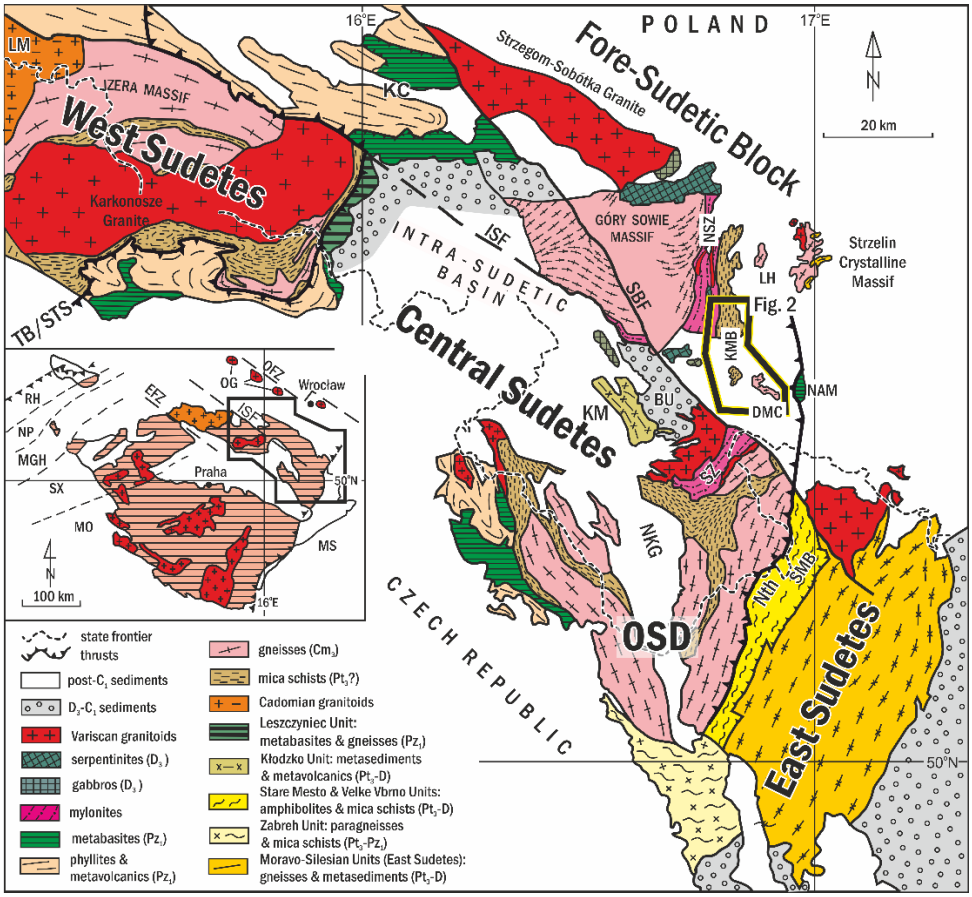

Fig. 1. Geological sketch map of the Sudetes after Mazur et al. (2006). Abbreviations: BU — Bardo Unit; KC – Kaczawa Complex; KM — Kłodzko massif; KMB – Kamieniec Metamorphic Belt; DMC – Doboszowice Metamorphic Complex; LM — Lusatian massif; NKG – Nysa Kłodzka Graben, NAM — Niedźwiedź Massif; NSZ – Niemcza Shear Zone; LH – Lipowe Hills Massif; OSD — Orlica-Śnieżnik Dome; SMB—Staré Město Belt. Sutures and faults: ISF — Intra-Sudetic fault; Nth – Nyznerov thrust; SBF — Sudetic boundary fault; TB/STS — Teplá-Barrandian/Saxothuringian suture. Abbreviations in inset: EFZ – Elbe Fault Zone, MGH — Mid-German Crystalline High; MO — Moldanubian zone; MS — Moravo-Silesian zone; NP — Northern Phyllite zone; OG – Odra granitoids, OFZ – Odra Fault Zone, RH — Rhenohercynian zone; SX — Saxothuringian zone. Age assignments: Pt — Proterozoic; Pz — Palaeozoic; Cm — Cambrian; Or — Ordovician; D — Devonian; C — Carboniferous; 1 — Early; 2 — Middle.

Age and provenance of rock successions

The protolith age of the volcano-sedimentary successions exposed in the KMB and DMC is poorly known. The available data suggest that the maximum depositional age (MDA) of the KMB and the adjacent Lipowe Hills mica schists is in the range of c. 560-570 Ma (Neoproterozoic, Oberc-Dziedzic et al., 2018; Jastrzębski et al., 2020), while the Chałupki paragneiss from the DMC has a late Cambrian MDA (Jastrzębski et al., 2023). However, Szczepański et al. (2023) argue that the mica schist from the KMB displays the MDA at 529 Ma (early Cambrian), whereas the paragneiss from the DMC displays the MDA at 456 Ma (Upper Ordovician).

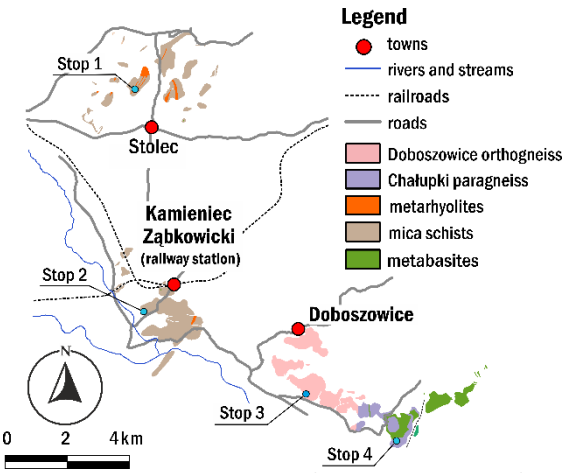

Fig. 2. Geological sketch map of the southern part of the Kamieniec Metamorphic Belt and the Doboszowice Metamorphic Complex.

Consequently, the published zircon age spectra suggest that the studied volcano-sedimentary successions exposed in the eastern part of the Fore-Sudetic Block may represent two different rock sequences in terms of MDA. In addition, a sedimentary succession of the KMB was injected by several rhyolitic sills. Interpretation of the metarhyolites as sills is supported by their very consistent chemical composition and textural features, with no evidence of e.g. degassing. The zircons from the KMB metarhyolites are dominated by an age peak of 510 Ma that is interpreted as the time of magmatic emplacement. Rare Neoproterozoic and Archaean inheritance points to the involvement of an older crustal component in magma genesis.

Based on the trace element composition, the metasedimentary successions from the KMB and DMC are interpreted to be derived from a felsic source and their chemical composition was not significantly affected by alteration during transport (Fig. 3).

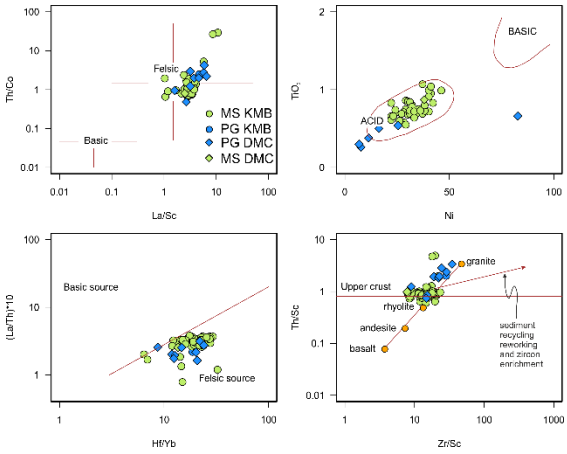

Fig. 3. Diagrams illustrating lithology of the source area after (a) Cullers (2002), (b) Floyd, Winchester & Park (1989), (c) Hladil et al. (2003), and (d) the influence of sediment recycling and zircon enrichment on chemical composition of the investigated quartzites after McLennan et al. (1993). MS – mica schists, PG – paragneisses.

Furthermore, the chemical composition of the mica schists and paragneisses from the KMB and DMC is typical of sediments derived from erosion of suprasubduction complexes (Fig. 4).

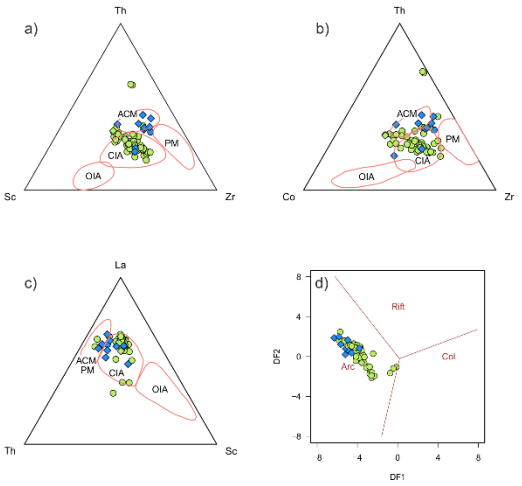

Fig. 4. a-c) Discrimination diagrams showing tectonic setting of deposition of the protolith to the mica schists and paragneisses of the Kamieniec Metamorphic Belt and the Doboszowice Metamorphic Complex. After Bhatia & Crook (1986). Abbreviations: PM – passive margin, CIA – continental island arc, ACM – Active continental margin, OIA - oceanic island arc. d) discriminant-function multi-dimensional diagram after Verma & Armstrong-Altrin (2013). Abbreviations: Arc – arc related setting, Rift – continental rift setting, Col – collisional setting. Samples fall in the field typical of arc-related sediments. Symbols as in Fig. 3.

Available detrital zircon ages from Cambro-Ordovician sedimentary successions covering the Saxothuringian and Teplá-Barrandian Units exposed in the Sudetes clearly indicate that all these Neoproterozoic crustal fragments were derived from the same cratonic areas and Cadomian arc-related basement (Fig. 5) located at the northern periphery of Gondwana, close to the West African Craton or Trans-Saharan Belt (Fig. 6; corresponding references are given on Fig. 6).

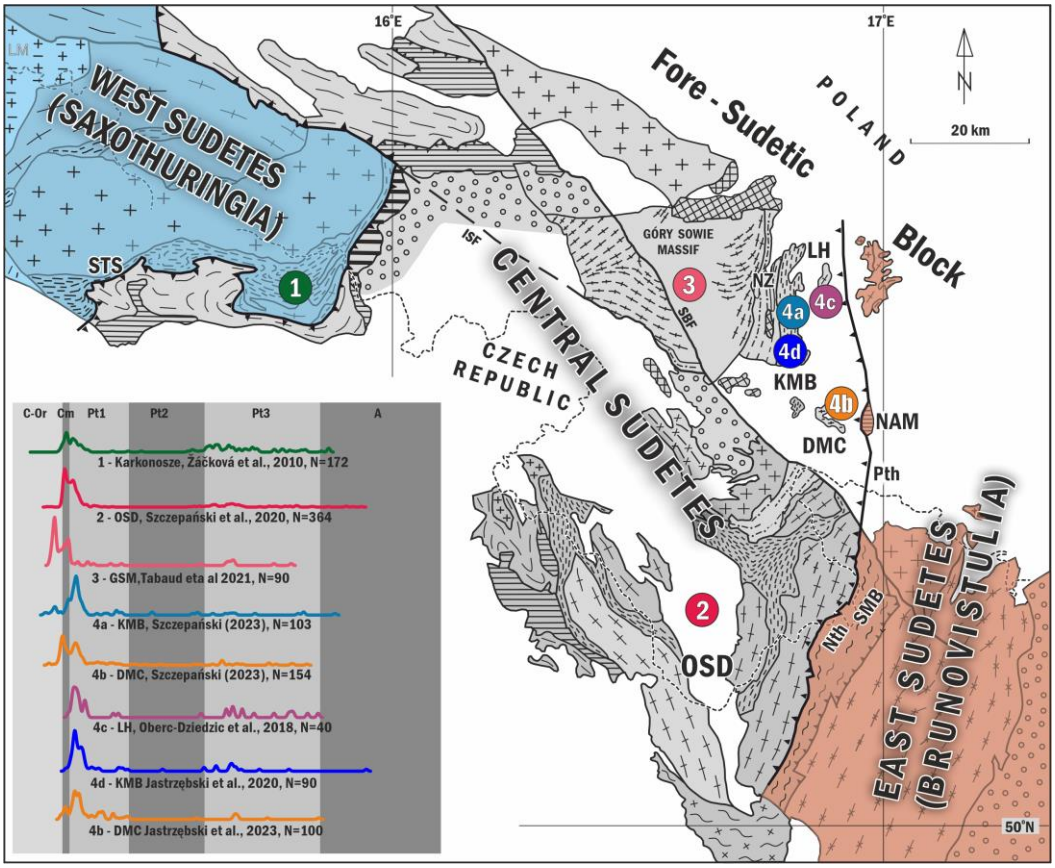

Fig. 5. Comparison of zircon age spectra obtained for various crustal domains from the Sudetes shown on the geological sketch map of the Sudetes after Mazur et al. (2006). Kernel density plots for detrital zircons from: 1. Karkonosze (Žáčková et al., 2010), 2. Orlica-Śnieżnik Dome ; 3. Góry Sowie Massif (Szczepański et al., 2020; Tabaud et al., 2021)**; 4a. Kamieniec Metamorphic Belt (Szczepański et al., 2023), 4b – Doboszowice Crystalline Massif (Szczepański et al., 2023; Jastrzębski et al., 2023), 4c – Lipowe Hills (Oberc-Dziedzic et al., 2018); 4d – Kamieniec Metamorphic Belt (Jastrzębski et al., 2020); 5. Brunovistulia (Friedl et al., 2004; Mazur et al., 2010), 6. Staré Město Belt (Śliwiński et al., 2022). Abbreviations: STS – Saxothuringian suture, OSD – Orlica-Śnieżnik Dome, DMC – Doboszowice Crystalline Massif, KMB – Kamieniec Metamorphic Belt, NZ – Niemcza Zone, LH – Lipowe Hills, NAM – Niedźwiedź amphibolite Massif, Pth – Paczków thrust, Nth – Nyznerov thrust, SMB – Staré Město Belt. Abbreviations in inset: C-Or – Carboniferous-Ordovician, Cm – Cambrian, Pt1 – Neoproterozoic, Pt2 – Mesoproterozoic, Pt2 – Paleoproterozoic, A – Archean. Abreviations: Ph – Phanerozoic, Pt1 – Neoproterozoic, Pt2 – Mesoproterozoic, Pt2 – Paleoproterozoic, A – Archean.**

Consequently, we support suggestions that during the Cambro-Ordovician time Cadomian crustal fragments now exposed in the western and central parts of the Fore-Sudetic Block were dispersed along the northern periphery of Gondwana, most probably forming an extended shelf that developed on a passive continental margin (Fig. 6; e.g. Drost et al., 2011; Žák and Sláma 2018; Collett et al., 2021; Tabaud et al., 2021; Collett et al., 2022).

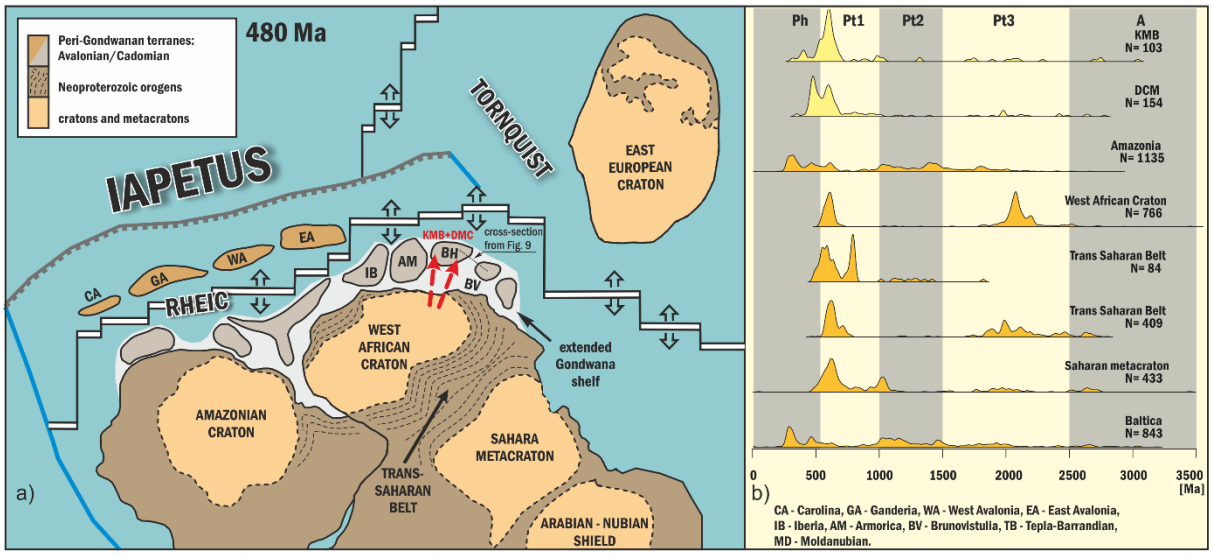

Fig. 6. a) Tentative simplified reconstruction of Western Gondwana extended passive margin during the Early Ordovician, modified after (Domeier, 2016) and (Torsvik, 2017). Abbreviations: CA – Carolina, GA – Ganderia, WA – West Avalonia, EA – East Avalonia, IB – Iberia, AM – Armorica, BV – Brunovistulia, BH – Saxothuringia, Tepla-Barrandian and – Moldanubia, KMB – Kamieniec Metamorphic Belt, DMC – Doboszowice Metamorphic Complex. Red arrows indicate the main directon of sedimentary transport. Types of lithospheric boundaries: black-white – spreading ridge, grey – subduction, blue – transform. b) Kernel density plots for detrital zircons from: Kamieniec Metamorphic Belt (Szczepański et al., 2023), Doboszowice Metamorphic Complex (Szczepański et al., 2023), Amazonian Craton (Gaucher et al., 2008; Geraldes et al., 2014; Pankhurst et al., 2016, West African Craton (Abati et al., 2010), Trans-Saharan Belt – Tuareg Shield (Henry et al., 2009), Trans-Saharan Belt (Peucat et al., 2003; Abdallah et al., 2007; Bendaoud et al., 2008; Bosch et al., 2016), Saharan Metacraton (Meinhold et al., 2011) and Baltica (Valverde-Vaquero et al., 2000; Kristoffersen et al., 2014; Kuznetsov et al., 2014). Kernel density plots were designed via the R software environment (R Core Team, 2012).

Age of tectonothermal events

The volcano-sedimentary successions comprised in the KMB and DMC suffered a Variscan metamorphism and deformation. According to several authors, it was related to continental collision between Gondwana-derived crustal domains represented by the Teplá-Barrandian, Saxothuringian and Brunovistulian domains (e.g. Schulmann et al., 2009; Chopin et al., 2012; Jastrzębski et al., 2020; Szczepański et al., 2022; Szczepański & Goleń, 2022).

Time constraints on the age of metamorphism and the related deformation in this part of the Fore-Sudetic Block have been supplied by ^{40}Ar-^{39}Ar geochronology on hornblende, yielding two distinct ages of 331.9±1.7 Ma and 376 Ma for hornblende-bearing rocks from the Niemcza Shear Zone (NSZ in Fig. 1) and the KMB, respectively (Steltenpohl et al., 1993). The volcano-sedimentary succession of the Kamieniec Metamorphic Belt was also intruded by syn- to post-tectonic granodiorites dated at 330–340 Ma by U-Pb and Pb-Pb methods on zircons (Oliver et al., 1993; Kröner and Hegner, 1998). Furthermore, ages in the range of 380 and 330 Ma were obtained using U-Pb and Pb-Pb method on zircons from syntectonic diorites and monzodiorites from the adjacent Niemcza Shear Zone (Pietranik et al. 2013; Pietranik and Majka 2017). The age of the tectonothermal event recorded in the KMB has recently been estimated at c. 330 Ma (Jastrzębski et al., 2020) and in the DMC at c. 346–341 Ma based on ICP–MS U–Th–Pb dating of monazite (Jastrzębski et al., 2023). Variscan age of tectonothermal event is confirmed by the youngest single zircon grains documented in the

metasediment samples from the KMB and DMC showing ages of c. 330-320 Ma that are interpreted as reflecting lead loss owing to the Variscan thermal overprint (Szczepański et al., 2023). This is in agreement with Lu–Hf and Sm–Nd garnet dating of the Chałupki paragneiss, which shows that these rocks were metamorphosed between c. 347 Ma and c. 337 Ma (Szczepański et al., 2022). Consequently, the time frame for Variscan tectono-thermal activity in this area covers the time span from c. 380 Ma to c. 330 Ma.

Deformation and metamorphism

Three main ductile deformation events: D1 to D3, were documented in the KMB and DMC. Generally, rocks of the DMC preserve relics of older deformation events (D1 and D2), whereas the mica schists of the KMB usually contain structures of all the documented deformation events (D1 to D3).

D1 structures

The oldest, D1, structures comprise the S1 foliation which is mostly sub-vertical in the KMB and sub-horizontal in the paragneisses of the DCM (Fig. 7). It was documented as either mesoscopic, penetrative planar structures observed in the field (Fig. 8a, c and f), relic structures preserved in microlithons between younger cleavage planes or as inclusion trails conserved within inner parts of garnet porphyroblasts (Fig. 8b and e). The S1 planes observed in the field and preserved in rocks of the KMB display no signs of clear metamorphic differentiation. Particular layers show variable thickness and are oriented parallel to lithologic boundaries (Fig. 8a), suggesting that the S1 may be parallel to bedding. In the KMB the S1 schistosity generally dips at high angles towards SE or NW (Fig. 7a). However, in places in the KMB and in the DMC the S1 foliation shows a nearly horizontal orientation or dips at shallow angles towards the NW or SE in the normal limbs of younger F2 folds (Fig. 7a and e). The original orientation of the S1 foliation is unknown because it is scattered along a great circle due to the F2 folding (Fig. 7a, e and f). In strongly deformed portions of the mica schists of the KMB, the only relics of the S1 foliation are inclusion trails conserved mostly in garnet porphyroblasts (Fig. 8b and e). These inclusion trails are rectilinear or, occasionally, folded (Fig. 8b and e) and comprise mainly rutile, quartz, white mica and chloritoid. The S1 planes preserved in the Chałupki paragneiss are marked by migmatitic laminae that contains the L1 mineral lineation oriented E-W (Fig. 7e). In rock sections parallel to this lineation and perpendicular to the S1 planes a set of kinematic indicators including sigma type feldspar porphyroclasts was documented. All these kinematic indicators point to top-to-E sense of non-coaxial shear during the D1 event (Fig. 8c).

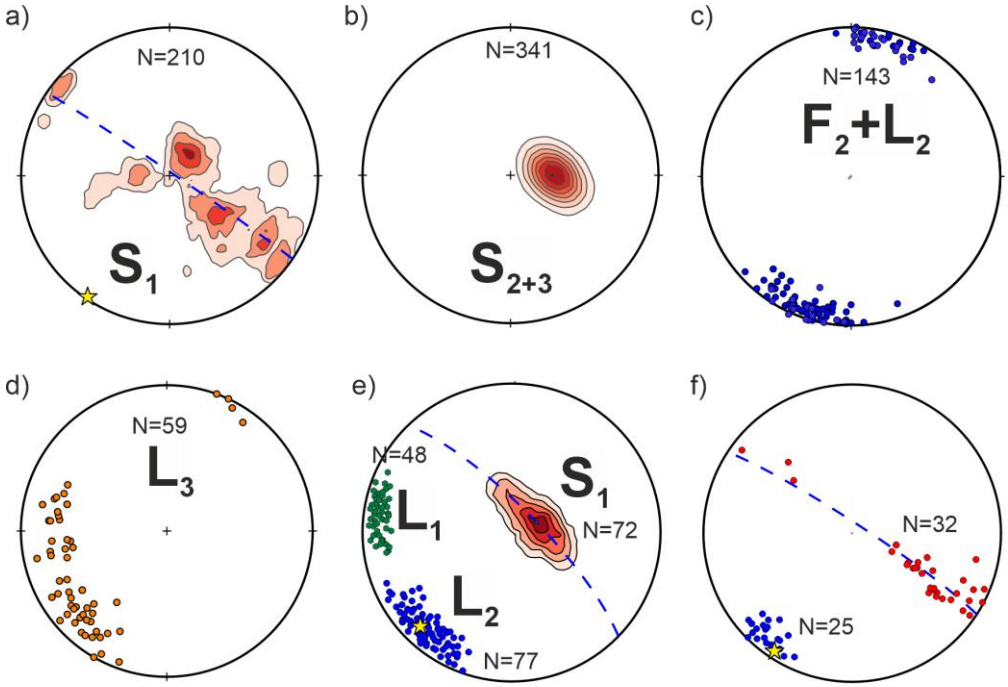

Fig. 7. Equal-area lower hemisphere projections showing: (a) scatter of mostly steep S1 foliation in the KMB, yellow star - axis of great-circle girdle of foliation, blue dashed line - great-circle girdle of foliation, (b) orientation of S2+3 planes in the KMB, (c) orientation of F2 folds and L2 lineation in the KMB, (d) orientation of L3 mineral lineation in the KMB, (e) contour lines - scatter of mostly subhorizontal S1 foliation in the Chałupki paragneiss of the DMC, yellow star - axis of great-circle girdle of foliation, blue dashed line - great-circle girdle of foliation, green points are for L1 mineral lineation, blue points are for L2 mineral lineation, (f) red points are for S1 foliation in the Doboszowice orthogneiss of the DMC, yellow star - axis of great-circle girdle of S1 foliation, blue dashed line - great-circle girdle of foliation, blue points are for L2 mineral lineation.

D2 structures

The D2 structures are represented by the F2 folds, the subhorizontal S2 axial planar cleavage and the L2 lineation. The scale of the F2 folds grades from open, several meter- through centimetre- to millimetre-scale asymmetric structures with their axes trending NNE-SSW (Fig. 7c). In many outcrops, rootless isoclinal folds have been documented in NE-SW oriented cross-sections, which we interpret as sections through the F2 folds that are slightly oblique to their axes. Therefore, the commonly observed elongated quartz lenses may represent hinges or limbs of the F2 folds. The subhorizontal S2 cleavage developed parallel to the axial planes of the F2 folds (Fig. 8d). The newly formed S2 planes dip towards the WSW to W at moderate to shallow angles (Fig. 7b). The S2 planes represent a cleavage in those places where the F2 folds are of considerable size and mica schists are intercalated with abundant quartzofeldspathic schists. Elsewhere, the S2 planes define mostly a penetrative foliation. Garnet grains, usually reaching 5–8 mm and, sporadically, even 30 mm in diameter, are often characterized by the occurrence of rectilinear or folded inclusion trails (Fig. 8b and e). The F2 folding resulted in the scatter of the S1 foliation along a great circle with a subhorizontal axis extending in the NNE-SSW direction (Fig. 7a, e and f). Lineation developed parallel to the F2 axes is preserved on the S1 and S2 planes, striking generally NNE-SSW to NE-SW (Fig. 7c, e and f). In places, the mineral lineation L2m is defined by parallel alignment of white mica flakes, and, locally, an intersection lineation L2i formed by intersection of the S1 and S2 planes. On the

contrary no signs of the L1 lineation was documented in rocks of the KMB.

D3 structures

The D3 deformation resulted in reactivation of the older S2 planes and led to the formation of the composite S2+3 planar structures that vary in their frequency of occurrence. The S2+3 foliation dips at moderate to shallow angles towards the W (Fig. 7b). Locally, a NE-SW to nearly E-W trending L3 mineral lineation on the S2+3 planes is preserved, being defined by parallel alignment of mica flakes (Fig. 7d). The orientation of the L3 mineral lineation changes from NE-SW, where the S2+3 planes are non-penetrative, to nearly E-W, where the S2+3 foliation becomes penetrative. The rock sections perpendicular to the S2+3 planes and parallel to the L3 mineral lineation reveal such kinematic indicators as S-C structures, sigma type porphyroblasts, extensional crenulation cleavage and sigmoidal inclusion trails. All these indicators document a top-to-SW or top-to-W sense of non-coaxial shear related to the D3 deformation (Fig. 8g and h). The domains with preserved asymmetric D3 fabric are sometimes filled with granitic material forming ~10–25 cm long lenses aligned parallel to the main S2+3 foliation. Sigmoidal inclusion trails conserved in garnet grains, plagioclase and andalusite porphyroblasts suggest synkinematic growth of these minerals during the D3 event (Fig. 8h). Furthermore, staurolite grains aligned mostly parallel to the main S2+3 foliation indicate syn-D3 growth.

Mineral assemblages stable during deformation

In the KMB the deformation events D1 to D3 are characterized by two different sets of stable mineral assemblages M1 and M2. The M1 assemblage coexisted during the D1 and the beginning of the D2 deformation events, whereas the assemblage M2 was stable at least during the terminal phase of the D2 event and the entire D3 deformation. The proposed assignment of mineral assemblages to particular deformation events is mainly based on garnet porphyroblasts displaying diverse inclusion sets with strikingly different geometry, which implies that two generations of garnets are preserved. The first garnet generation (Grt1) contains mostly chloritoid and rutile inclusions that are sporadically accompanied by chlorite and pseudomorphs after lawsonite. These inclusion sets in some porphyroblasts are developed as rectilinear, while in others as folded inclusion trails (Fig. 8b and e). The second garnet generation (Grt2) displays mostly sigmoidal ilmenite inclusions (Fig. 8h) accompanied by staurolite, plagioclase and biotite. In some samples both types of complex garnet porphyroblasts occur (Grt1 and Grt2, Fig. 8b). In such porphyroblasts inclusion trails display strikingly different orientation and composition of Ti-rich mineral phases (rutile in Grt1 and ilmenite in Grt2). Consequently, ilmenite in Grt2 points to garnet growth at P–T conditions related to exhumation (Cao et al. 2021; Szczepański et al. 2021). Importantly, the ilmenite inclusions preserved in Grt2 extend into the rock matrix. As suggested by the geometry of the observed inclusion trails, grading from rectilinear to slightly folded, the Grt1 must have started to grow during the D1 and likely continued through to the initial phases of the D2 event. The Grt2 crystallized synkinematically with respect to the D3 non-coaxial shearing. Importantly, the KMB mica schists are characterized by the occurrence of two groups of white mica that differ significantly in Si content. The Ms1 mica displays phengitic composition with up to 3.40 Si apfu, while the Ms2 white mica shows muscovite composition with up to 3.20 Si apfu.

The calculated P–T conditions for the early stage of metamorphism and related deformation (M_1 and D_1) in the KMB are at c. 485±25°C and 18±1.8 kbar. Subsequently, the D_3-M_2 events underwent at P–T conditions ranging from 520±26°C and 6±0.6 kbar through 555±28°C and 7 kbar±0.7 to ~590±30°C and 3–4±0.4 kbar.

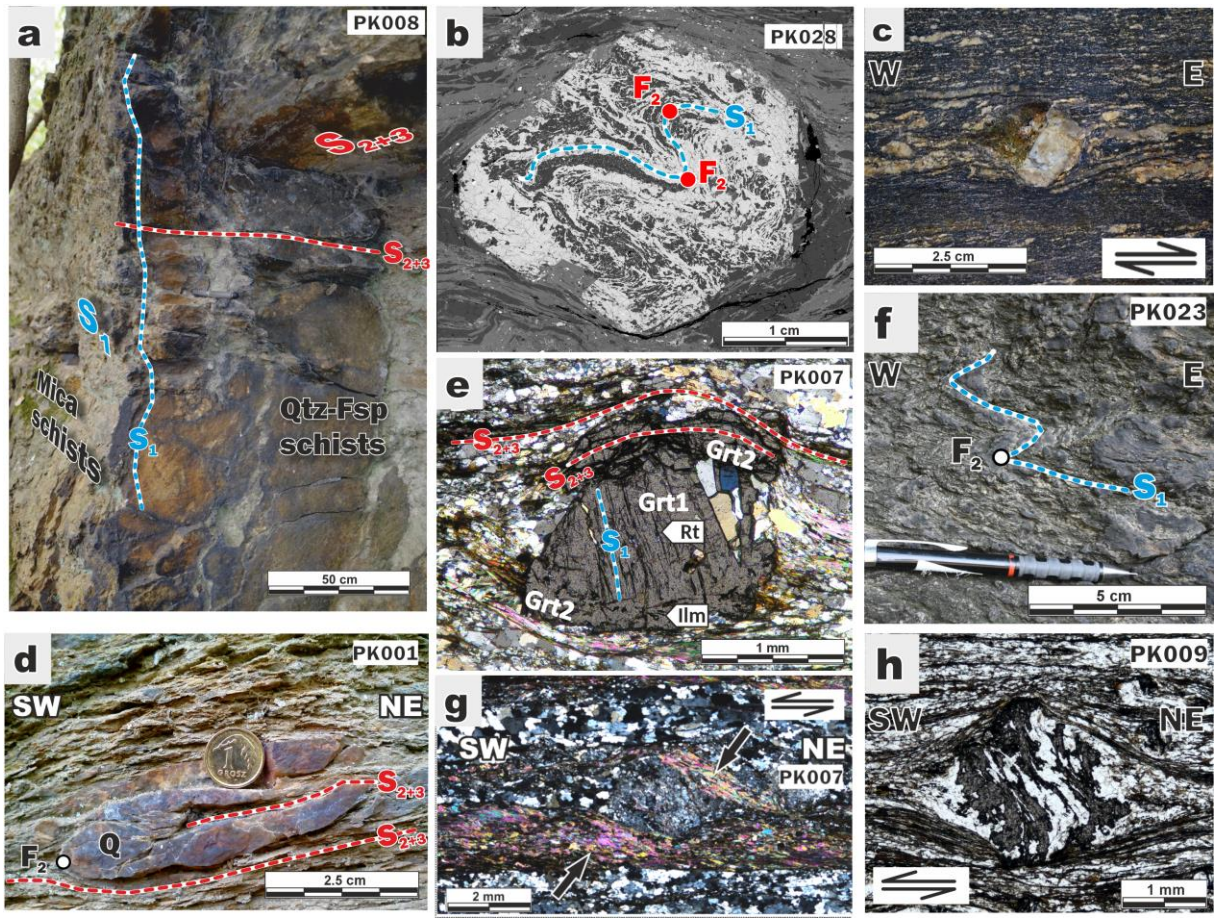

Fig. 8. (a) Field photographs documenting steep older S1 fabric (blue dashed line) oriented parallel to the lithological boundary and in places overprinted by non-penetrative shallow S2+3 planes (red dashed line), KMB mica schist, (b) photomicrograph showing S_1 planes refolded into F_2 folds preserved in garnet porphyroblast in the KMB mica schist, (c) sigma-type feldspar porphyroclast in the Chalupki paragneiss documenting top-to-E kinematics of D_1 event, (d) F_2 isoclinal fold in the KMB mica schist, (e) complex garnet porphyroblast; preserved in its inner part inclusion trails define S_1 planes (early garnet generation – Grt1), and S_2 planes conserved in its rim part continue into the matrix of the rock (late garnet generation – Grt2), the KMB mica schist, (f) cm-scale F_2 folds in mica schists from the KMB, (g) asymmetric pressure shadows filled with quartz and deformation mats (arrows) filled with white mica developed around plagioclase porphyroblast documenting top-to-SW kinematics of D_3 event, (h) sigmoidal inclusion trails preserved in Grt2 documenting top-to-SW kinematics of the D_3 event.

The paragneiss from the DMC is characterized by two mineral assemblages that originated during prograde metamorphism and resulted from two distinct metamorphic events M1 and M2. The younger and well-preserved HT–MP paragenesis M2 overgrowing the older and poorly preserved HP–LT mineral assemblage M1. The M1 paragenesis comprises scarcely preserved phengitic white mica with Si contents reaching up to 3.38 apfu and forming cores of white mica grains and relics of rutile grains preserved in abundant ilmenite crystals. Both equilibrium modelling and

conventional geothermobarometry are inconclusive but suggest pressures of ca. 12–18 kbar at temperatures of c. 500–570°C for the M1 event. In contrast, the younger and well-preserved the M2 paragenesis contains abundant K-white mica with low Si content (< 3.15 apfu) accompanied by garnet, plagioclase, staurolite, kyanite and ilmenite. The HT–MP nature of the M2 event is supported by P–T modelling of garnet growth, indicating a progression of P and T during garnet growth and a maximum pressure and temperature of its formation of c. 660°C at 9 kbar.

Towards a new tectonometamorphic model

Recently, Szczepański and Goleń (2022) proposed a new tectonometamorphic model of the evolution of the eastern part of the Fore-Sudetic Block during the Variscan orogeny. They interpreted the M1 and D1 events as a result of subduction of the protolith of mica- and quartzofeldspatic schists of the KMB to depth of ~65–70 km in relation to the collision between the Saxothuringian and Brunovistulian terranes. This was followed by exhumation to mid-crustal level (of ~20–25 km) during the D2 event. Subsequently, the D3-M2 events show evidence of non-coaxial flow of possibly overthickened, hot and mechanically unstable orogenic crust at mid-crustal level. We postulate that the granitoid magmatism occurring at this stage of the KMB evolution may have been responsible for mechanical weakening of an overthickened nappe pile, thus facilitating reactivation of the already existing foliation and enabling the second stage of exhumation (D3 event).

According to Mazur and Józefiak (1999), the KMB, together with the adjacent DMC, comprises three refolded tectonic units interpreted as fragments of crystalline nappes with different metamorphic records. The base of the refolded nappe pile is defined by the Paczków thrust, which separates it from the underlying metabasites of the Niedźwiedź Massif (Pth in Fig. 1, Mazur and Józefiak 1999). It is believed that the Paczków thrust represents a northern continuation of the Nýznerov thrust, separating the metamorphic complexes of the Central and East Sudetes (Fig. 1; Skacel, 1989).

According to Mazur and Józefiak (1999), the nappe stacking (D1) and folding (D2) of the whole nappe pile was related to east-west directed shortening that had resulted from a collision between crustal domains that are now interpreted to correspond to the Brunovistulian (East Sudetes) and Saxothuringian (Central Sudetes) terranes (e.g. Mazur et al., 2015). During the terminal stage of the evolution of the KMB, the overthickened and mechanically unstable nappe pile was affected by a SW-directed gravitational collapse, producing low-angle normal-slip shear zones (D3). The data presented by Szczepański et al. (2022) and Szczepański and Goleń (2022) on the described tectonometamorphic events are, to some degree, in agreement with the tectonic model proposed by Mazur and Józefiak (1999) for the evolution of the KMB. According to this model, the volcano-sedimentary succession of the Kamieniec Metamorphic Belt was affected by east-vergent folds formed in response to the Variscan collision between the Saxothuringian and Brunovistulian terranes. Data presented by Szczepański and Goleń (2022) reinforces this model and shows that the regional-scale folding can be interpreted as coeval with the first stage of the exhumation of the entire KMB to a mid-crustal level (D2 event). The important difference between models proposed by Szczepański and Goleń (2022) and Mazur and Józefiak (1999) is the discovery of HP–LT metamorphic record, which allow to identify that folding of the KMB succession was related to exhumation within the collision zone from depths corresponding to ~18 kbar.

It is interesting to note the difference in temperature of the M2 metamorphic event recorded in rock complexes of the DMC and KMB. The difference is c. 70–80°C and is, therefore, beyond the error of the methods used to reconstruct the P–T conditions of metamorphism in both units. This is consistent with the observed migmatization in the DMC and its absence in the KMB, although, the rock successions of the DMC are located only 3 km SE of the KMB. Furthermore, temperatures of metamorphism increase towards the E in the direction of the NAM, which is located directly east of the DMC, where they reach max. 790°C (Puziewicz and Koepke 2001; Awdankiewicz 2008). This implies a very steep geothermal gradient during the M2 metamorphism, precluding heating by large-scale processes such as thickening, shearing and thermal relaxation. It seems that the most plausible explanation for the higher temperatures of the M2 event in the DMC is related to local heat source caused by a nearby and relatively small granitoid intrusion. Such an intrusion can be exemplified by the Staré Město granitoid. Although, the above mentioned granitoid to the NE of the Sudetic Boundary Fault and are not exposed on the surface, it is highly probable that they continue within the border zone between Brunovistulia and Saxothuringia towards the NAM. This view is supported by similar metamorphic records preserved both in the rocks of the NAM and the Staré Město Belt, manifested by incipient melting preserved in the rocks of both units which occurred at c. 770–790°C and 12–13 kbar (Parry et al. 1997; Puziewicz and Koepke 2001; Awdankiewicz 2008; Jastrzębski 2012). Furthermore, the episodes associated with granitoid emplacement ranging in age from 344 to 336 correlate well with the time of garnet formation in the DMC and KMB mica schists reported in the next section (Parry et al. 1997; Štípska et al. 2004; Jastrzębski 2012; Skrzypek et al. 2014).

Chronology and dynamics of Variscan collision between Saxothuringia and Brunovistulia recorded by metamorphic successions of the DMC and KMB

The available data allow to propose a time-frame for the events related to the Variscan collision of Saxothuringia and Brunovistulia, now exposed in the eastern part of the Fore-Sudetic Block. This includes the burial of volcano-sedimentary successions of the KMB and DMC within the subduction zone followed by their exhumation in front of the rigid Brunovistulian crustal domain. Exhumation of the KMB and DMC rock successions was associated with folding, which is best documented in mica schists exposed in the KMB (Szczepański et al. 2022; Szczepański and Goleń 2022). The described scenario is similar to that proposed for the Orlica-Śnieżnik dome, located in the Central Sudetes, i.e. to the south of the KMB and DMC, and described by Chopin et al. (2012) and Mazur et al. (2012). The model invoking eastward subduction is supported by the occurrence of Devonian metamorphosed suprasubduction basic and intermediate volcanics, documented in the Brunovistulian basement and dated at c. 371 Ma (Janoušek et al. 2014), and Devonian quartzites of the Jegłowa Beds with supra-subduction characteristics, outcropping in the Strzelin Massif (Szczepański 2007).

The latter massif is interpreted as a part of the crystalline basement of the Brunovistulian terrane exposed on the Fore-Sudetic Block (Oberc-Dziedzic et al. 2003). Consequently, the described metamorphosed Devonian metavolcanics and quartz-rich sediments with suprasubduction characteristics resulted from the oceanic subduction stage preceding the collision between Saxothuringia and Brunovistulia. The time of closure of the

oceanic domain between Saxothuringia and Brunovistulia, resulting in continental collision, is most likely recorded by the core of garnet grains from mica schist sample collected in the KMB, dated at 344.6±1.1 Ma by the Lu–Hf method. These garnet grains bear a well-preserved record of HP–LT metamorphism (Szczepański et al., 2022). Furthermore, garnets form this sample contain thin rims produced during the MP–MT event (Szczepański et al., 2022). Therefore, we interpret the obtained Lu–Hf age of garnet from this sample as approximately the age of the HP–LT event. Consequently, the transition from oceanic subduction stage to continental collision took c. 27 Ma and occurred between c. 371 and c. 344 Ma. Interestingly, the same age within error of 345.5±5.0 Ma was also obtained for the garnet core from paragneiss sample from the DMC. However, according to mineral equilibria modelling this garnet started to grow at pressure of 4 kbar, which is considerably lower compared to this recorded by the garnet core from mica schists sample collected in the KMB. A similar within error Lu–Hf age of 346.9±3.6 Ma was also obtained for the whole garnet from paragneiss sample from DCM. This suggests that the exhumation from depth corresponding to 18 kbar to shallow crustal level equivalent to 4 kbar was most probably a relatively fast process. On the other hand, the thermal peak of the M2 metamorphism suffered by the rocks of the DMC is most probably recorded by the Sm–Nd garnet rim dating from paragneiss sample delivering an age of 337.3±6.6 Ma. Therefore, the growth of garnet in sample MD01-18 corresponding to the M2 episode took place in the time interval between 345.5 Ma and 337.3 Ma giving c. 8.2 Ma. This time interval fits quite well with the time of granitoid intrusions penetrating the Staré Město Belt and possibly also the NAM.

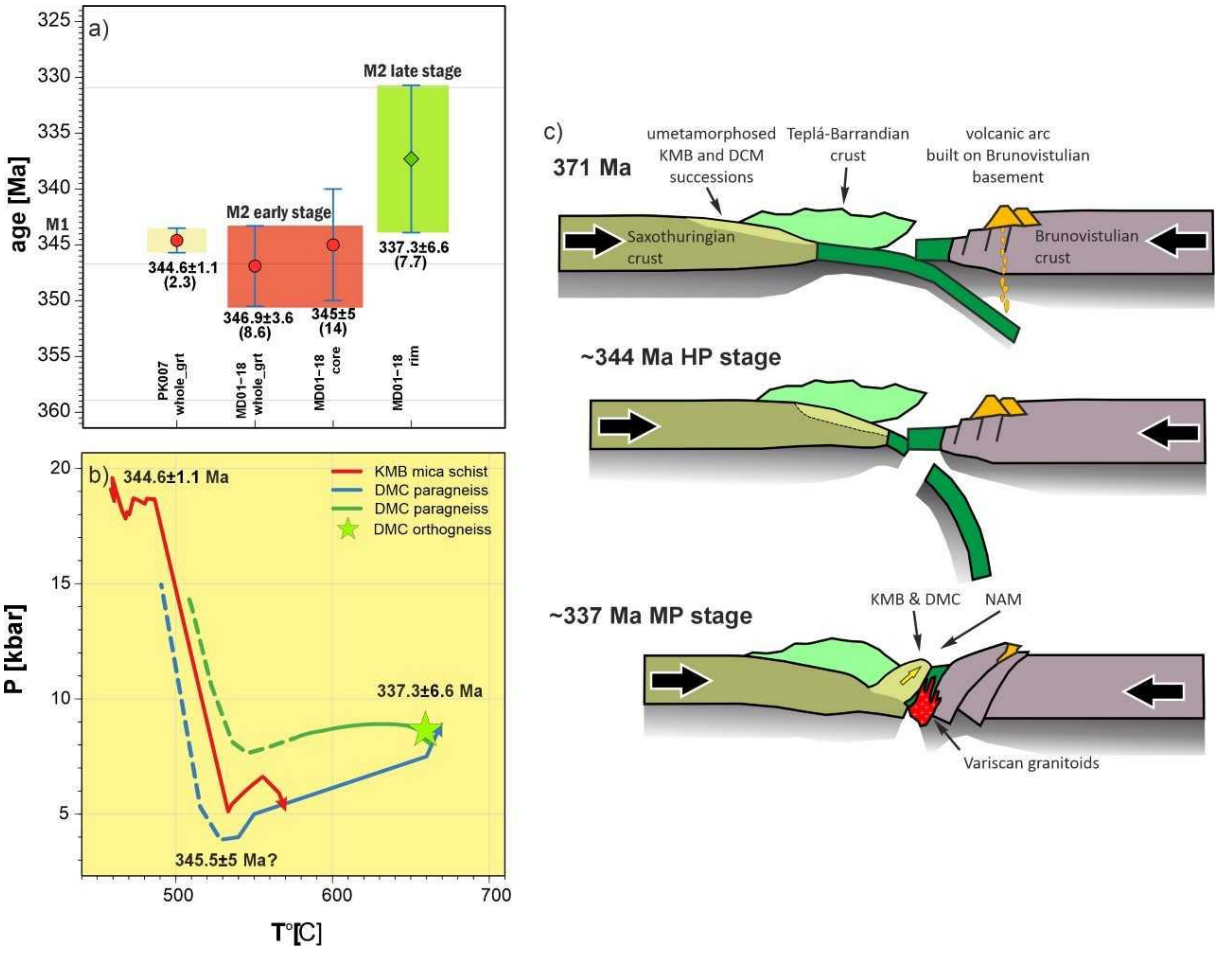

Fig. 9. (a) summary of garnet dating using Lu–Hf (red circles) and Sm–Nd (green diamonds) methods; whole grt is for whole garnet dating, core and rim is for core and rim dating, respectively; error bars are shown with blue lines; (b) Summary of inferred P–T paths calculated for the investigated samples. The solid lines mark the part of the P–T path reconstructed based on garnet composition, while dashed lines mark the P–T path portions reconstructed based on other minerals (mainly white mica composition); green star is for thermal peak of the M2 metamorphism responsible for garnet growth in sample MD09-02; dates are based on Lu–Hf and Sm–Nd garnet dating presented in Fig. 9a. (c) Tectonic model (not to scale) showing a possible mechanism of burial and exhumation of the DMC and KMB successions.

Stop 1 – Stolec

GPS coordinates: 50.5971817N, 16.8741775E
Position and lithology: volcanosedimentary succession of the Kamieniec Metamorphic Belt
Described problems: provenance,
maximum depositional age,
early Palaeozoic volcanism,
Variscan tectonometamorphic record_ _ _ _ _ _ _ _ _ _

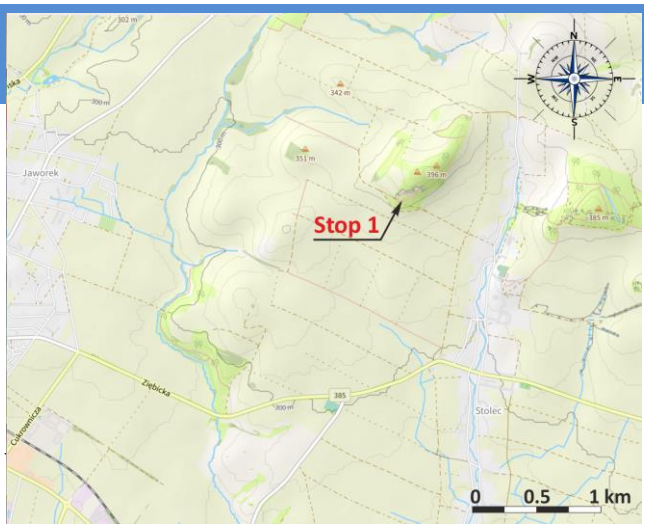

Provenance and maximum depositional age

Mica schists with several centimetres to a few decimetres of felsic metavolcanites are exposed in the visited abandoned quarry in Stolec. For provenance studies, zircon age spectra of mica schists from the Kamieniec Ząbkowicki Metamorphic Belt were obtained by U-Pb LA-ICP-MS dating. The youngest detrital age population of grains indicates the maximum depositional age of these rocks at c. 529 Ma, suggesting that the sedimentary protolith of the Kamieniec Ząbkowicki metapelites were probably deposited in an Early Palaeozoic sedimentary basin (Szczepański et al., 2023; Jastrzębski et al., 2020). Zircon dating revealed a predominance of Neoproterozoic grains, representing 45 to 68% of the zircon analyses in the studied samples . The detrital zircon ages, clustered between 1.1--0.53 Ga and 2.2-1.8 Ga, with only a few Mesoproterozoic zircon ages (Fig. 5), indicate a West African and/or Trans-Saharan provenance for the studied volcanic-sedimentary rocks. (Jastrzębski et al., 2020, Szczepański et al., 2023).

Early Palaeozoic volcanism

Felsic volcanics interspersed among mica schists exposed in the KMB succession are quartzo-feldspathic, fine-grained rocks with the dominant mineral assemblage Qz + Kfs + Ms + Bt + Opq. A very fine-grained matrix (Kfs + Qz ± Ms) contains dispersed K-feldspar porphyroblasts of <2mm in diameter. In terms of chemical composition (Fig. 10a) these rocks correspond to rhyolites of subalkaline, strongly peraluminous affinity (A/CNK, A/NK: 1.1–2.3, CIPW normative corundum up to 7.6%). The rocks show enrichment in LREE ([La/Sm]CN 2.8–5.5, [La/Yb]CN = 3.8–13.6), strong Eu negative anomaly ([Eu/Eu*]CN = 0.11–0.36) but weak fractionation of MREE over HREE ([Gd/Yb]CN 1.0–1.5). Compared to the upper continental crust (Fig. 10c), they are depleted in HFSE (e.g., Nb, Zr, Ti) and in compatible elements (V, Co). The inconsistent behaviour of LILE vs. SiO_2 implies some element mobility during metamorphic events. Variations in major and trace elements suggest fractionation of plagioclase, biotite, apatite, ilmenite, and cordierite with some zircon and perhaps monazite. Alternatively, these chemical features may, at least in part, mirror the melt source, as the upper and/or middle crust displays depletion in high-field-strength elements (Taylor and McLennan, 1985). The continental crust-related origin of metarhyolites

protolith is also supported by the peraluminous, corundum-normative composition of the rocks and low Nb/Th (0.2-0.7), Zr/Nb (8-23) ratios. Moreover, a high LREE/HFSE ratio and Th concentration together with weak fractionation of MREE over HREE imply the generation of magma in a subduction-related environment. Based on petrogenetic diagrams (not shown here) we interpret that immature, quartz-feldspathic-rich sediments (greywackes or psammites originally deposited in arc environments, e.g., active continental margin) gave rise to felsic melts (Fig. 10b) which next were emplaced in a post-collisional to post-orogenic (transitional) setting. The process of anatexis was itself induced by heat input from the upwelling asthenosphere and it followed syn-collisional crustal thickening of a limited degree. Consequently, the progression of the tectonic setting from post-collisional toward anorogenic, presumably extensional regime could have taken place. The time of magmatic emplacement is estimated at late Cambrian by the dominant age 512.4 ± 4.1 Ma of metarhyolite zircons. Their rare Neoproterozoic and Archaean inherited ages (c. 560, 630 and 2588 Ma) indicate, albeit minor, involvement of an older crustal (detrital) component recycled in the magma source.

We correlate the origin of the metarhyolite protolith with other late Cambrian, S-type, peraluminous (meta-)granites from the Saxothuringian domain in the West Sudetes and those from the Moldanubian and Teplá-Barrandian domains but not the Brunovistulian domain. They mark the end of the Cadomian orogeny (arc- Gondwana continent collision) and the onset of Cambro-Ordovician rifting correlated with intrusions into transitional crust at the Gondwanan peripheries (Szczepański et al., 2023).

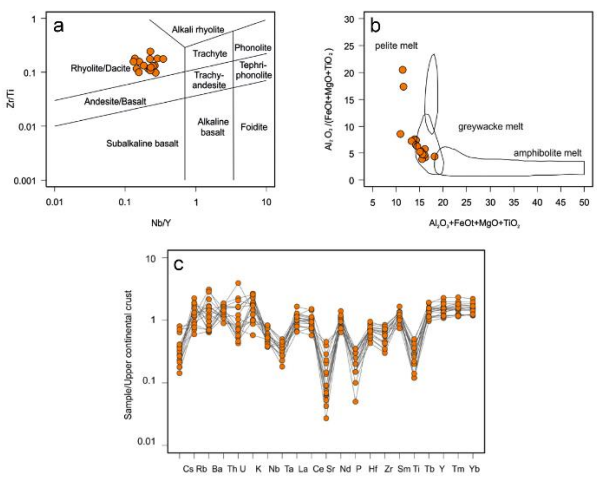

Fig. 10. Geochemical features of the meta-rhyolites of the Kamieniec Metamorphic Belt (Szczepański et al., 2023). a. Classification diagram of (Winchester and Floyd, 1977). b. diagram of (Jung et al., 2009) with fields from granitic melts generated experimentally from metapelites, greywackes and amphibolites. c. Incompatible trace elements abundances normalized to upper continental crust (Taylor and McLennan, 1985).

Variscan tectonometamorphic record

The outcrop is dominated by the S1 foliation that is deformed by the metre-scale F2 folds. Their axes are generally subhorizontal and oriented NW-SE. As a result the S1 foliation in different parts of the outcrop shows orientation varying from subvertical to subhorizontal (Fig. 11). Locally, on the steep limbs of the F2 folds the S2 subhorizontal cleavage may be observed.

The metamorphic record documented in this area was reconstructed based on sample PK007 collected c. 2 km SE of this outcrop. The mica schist sample PK007 (Fig. 12) displays millimetre-sized garnet porphyroblasts in a schistose matrix mainly consisting of quartz, K-white mica, biotite and chlorite. Accessory minerals are paragonite, margarite, rutile, ilmenite, zircon, and apatite. In the rock matrix, millimetre-thick and strongly elongated quartz-lenses alternate with laminae composed of muscovite, rare biotite, and chlorite. However, refolded quartz lenses and white mica

plates oblique to the penetrative foliation are preserved throughout the sample, giving rise to two sets of foliations (S1 and S2, Fig. 12). Similar two foliations are also occasionally preserved in garnet porhyroblasts (Fig. 8e).

Subhedral garnet porphyroblasts range from 0.2 up to 2 mm in size, and they often contain polymineralic inclusions comprising chloritoid, K-white mica and paragonite as well as margarite, clinozoisite, and quartz (Fig. 13). We interpret the latter type of polymineralic inclusions potentially as pseudomorphs after lawsonite that could have been produced according to the following mineral reaction (Chatterjee, 1976; Gomez-Pugnaire, Visona, & Franz, 1985):

$$5Lws = 2Czo + Mrg + 2Qz + 8H_2O.$$

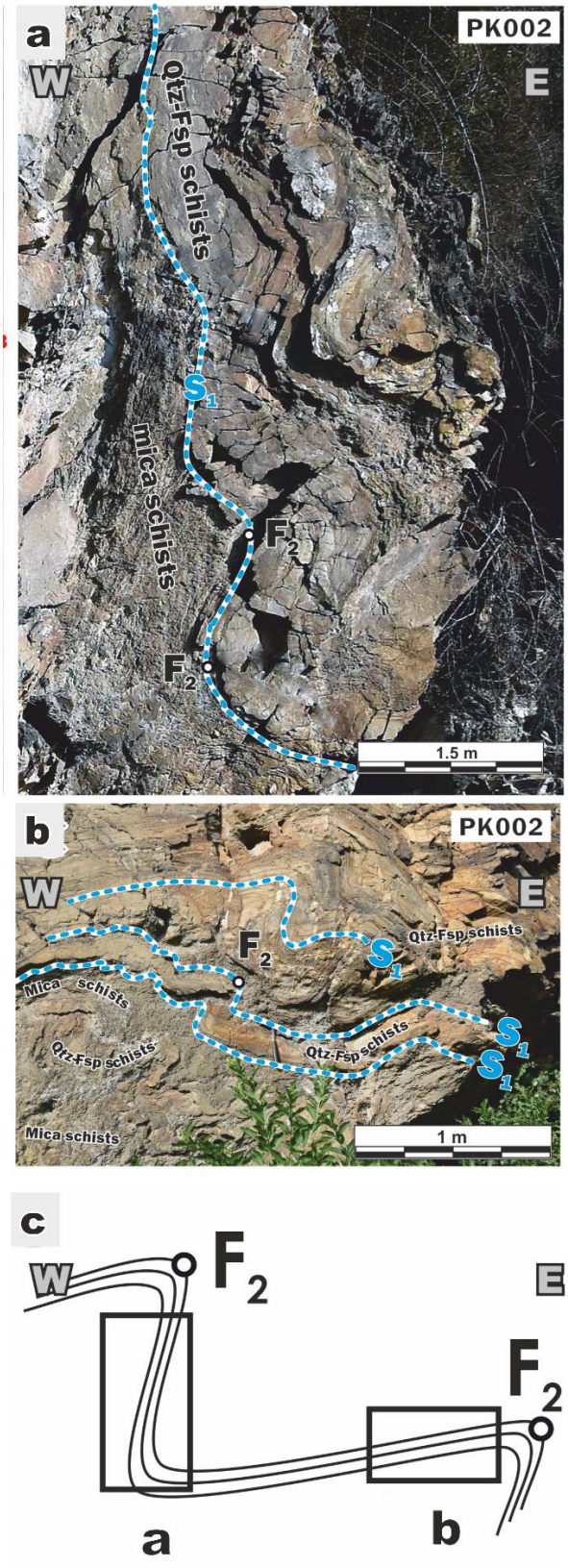

Fig. 11. (a) and (b) Field photographs documenting variably inclined older S1 fabric (blue dashed line) oriented parallel to the lithological boundaries. (c) Cartoon showing position of photographs with respect to F2 fold visible in outcrop near Stolec.

Garnet grains in the PK007 sample typically exhibit complex chemical zonation (Figs. 14), with bell-shaped spessartine profile in their core (X_{sps} decreasing from ~ 23 to 10%), sharp spessartine increase in the inner rim (X_{sps} ~ 15), followed by its decrease towards the outer rim (X_{sps} ~ 9). The variation in spessartine content is coupled with a gradual core-to-rim increase of almandine content (X_{alm} from ca. 57 to 72). Grossular concentration displays relatively low value in the inner core (X_{grs} ~ 12.5 to 17.5), which increases outwards in the most part of the outer core and rim (X_{grs} ~ 18 to 20). However, the grossular concentration decreases rapidly at the interface between outer core and inner rim, as well as in outer rim (X_{grs} ~ 14 and 10, respectively, Fig. 14 and 15). We interpret the described chemical zonation as formed in response to two distinct stages of garnet growth. We use Grt1 to denote the garnet forming the internal parts of garnet grains, and Grt2 for garnet rims. Interestingly, Grt1 entraps rutile inclusions, while Grt2 contains mostly ilmenite inclusions, indicating that both garnet types were equilibrated under different P-T conditions. This conclusion is also confirmed by the occurrence of polimineral clinozoisite, margarite and quartz inclusions within Grt1, which we have interpreted as presumed pseudomorphs after lawsonite (Fig. 13). Furthermore, chloritoid inclusions in Grt1 form blasts with grain size of up to 100 microns (Fig. 13), showing quite uniform chemical composition characterized by X(cld) [=Fe/(Mg+Fe)] ranging from 0.79 to 0.88. Additionally, rare chlorite inclusions were documented in both Grt1 and Grt2.

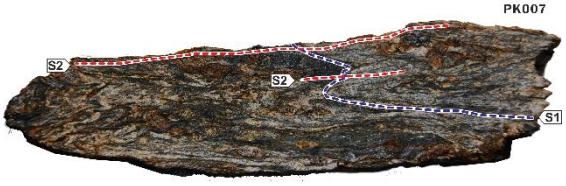

Fig. 12. Photograph showing two sets of foliations preserved in sample PK007. The older planar structure S1 is refolded.

K-white mica may be grouped into highly-abundant low Si grains for which Si content ranges from 3.0 to 3.20 apfu and a less frequent set displaying phengitic composition with Si content ranging from 3.25 to 3.45 apfu (Fig. 15). The phengitic white micas were documented in rock matrix, mostly in the microlithons, but also in the cleavage domains, and as inclusions in the core parts of garnet grains (Grt1). Low Si K-white mica grains occur abundantly in the matrix of the investigated sample, often within the cleavage domains, and they are also preserved as inclusions in the Grt2.

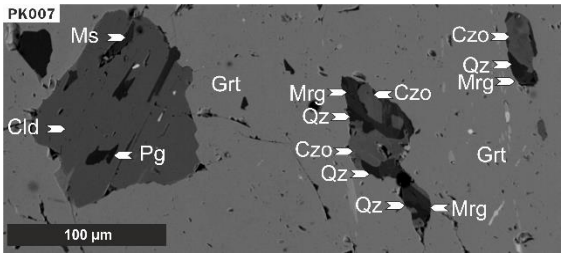

Fig. 13. Backscattered electron image showing the textures of polymineralic inclusions in garnets from sample PK007. Polymineralic inclusions consisting of Ctd + Ms + Pg and Mrg + Qz + Czo.

Plagioclase occurs in the matrix, generally forming small grains reaching up to 0.03 mm in diameter as well as porphyroblasts with diameter of up to 0.5 mm. Small matrix grains display an oligoclase composition, with maximum 22 mol% of An, and porphyroblasts show albitic cores, with developed oligoclase rims, which are well developed in the pressure shadows. Therefore, we suggest that plagioclase probably forms two generations represented by an older Pl1 with an albitic composition and a younger Pl2 with an oligoclase composition.

Small biotite flakes were documented as inclusions in Grt2 as well matrix grains in the inspected PK007 mica schist sample. Biotite is characterized by X_{Mg} varying from 0.29 to 0.52.

Based on textural observations, we distinguish three mineral assemblages in mica schist sample PK007: the M1 assemblage represented by Grt1 and Cld + Ph + Pg + [Lws] + Chl +Rt + Qz predominantly forming inclusions in Grt1. Mineral phases reported in square brackets represent presumed pseudomorphs. Phengitic white mica, chlorite and rutile are also present in the matrix of the inspected sample. The M2 assemblage represented by Grt2 and Ms + Bt + Pl1+ Chl +Ilm + Qz is observed in the Grt2 grains as well as in the matrix and the M3 assemblage comprising Ms + Bt + Pl2+ Chl +Ilm + Qz is observed exclusively in the matrix of the inspected sample.

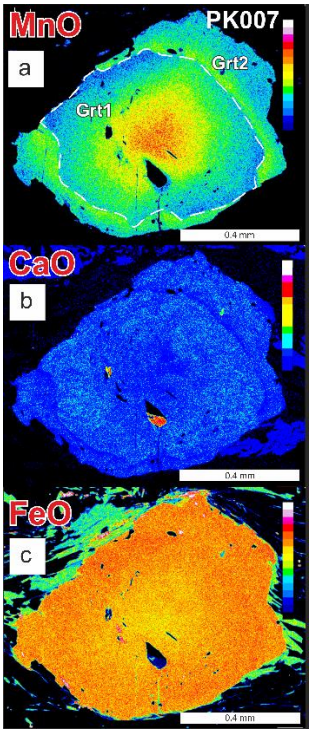

Fig. 14. X-Ray maps illustrating chemical zoning of garnet porphyroblasts from PK007 mica schist. a. Mn, b. Ca and c. Fe.

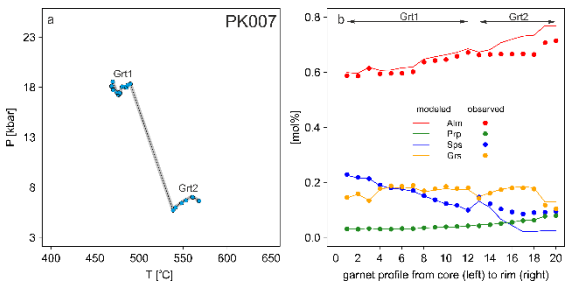

Fig. 15. Results of thermodynamic modelling for sample PK007: (a) reconstructed P-T path, (b) modeled vs measured chemical profiles in garnet. A core to rim sector of the profile was analysed.

To describe the P-T history of the PK007 sample we separately modelled the P-T history of the core (Grt1) and rim (Grt2) parts using the approach proposed by Moynihan & Pattison (2013). The obtained P-T paths and a comparison of observed and modelled garnet chemical profiles are presented in Fig. 14.

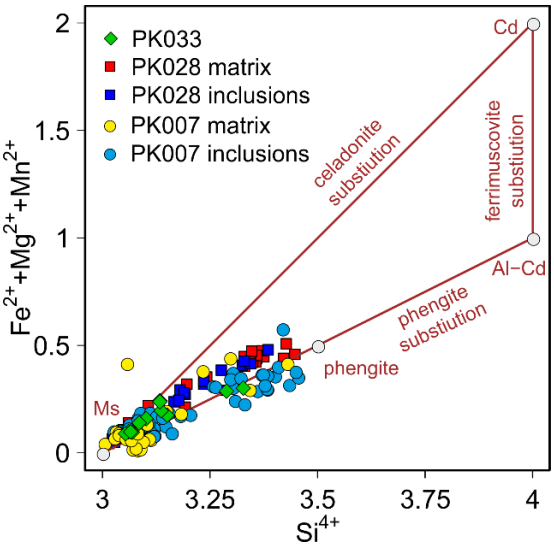

Fig. 16. Compositional variations of white micas in the investigated mica schists from the Kamieniec Metamorphic Belt.

The generally prograde P-T path for Grt1 is rather irregular. It starts at ca. 468°C and 18.1 kbar and ends at 490°C and 18.3 kbar (Fig. 15a). According to thermodynamic modelling, the core part of garnet grain (Grt1) in this sample was equilibrated within the stability field of Grt + Ph + Pg + Cld + Lws + Chl +Rt + Qz, which is consistent with the observed set of inclusions and presumed Lws pseudomorphs preserved in garnet grains (Fig. 13).

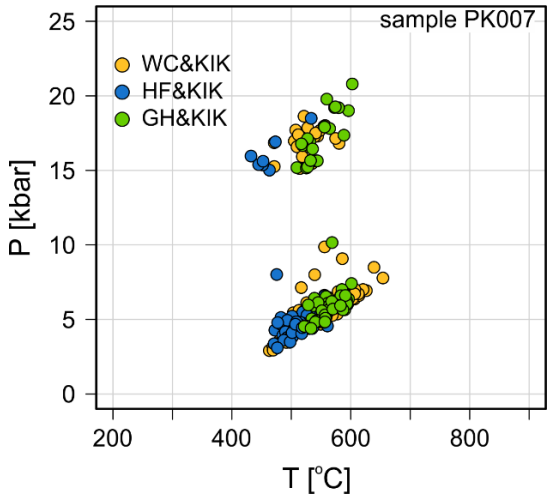

Fig. 17. Results of geothermobarometric calculations for sample PK007. KIK - Si in phengite geobarometer (Kamzolkin et al., 2016). WC - Ti in white mica geothermometer (Wu and Chen, 2015). Garnet-muscovite geothermometer in calibration of HF - Hynes & Forest (1988) and GH - Green & Hellmann (1982).

Results of thermodynamic modelling clearly indicated that during the HP stage lawsonite should be present in a relatively small amount, only slightly exceeding 2 vol%. Furthermore, X_{Mg} of chloritoid should fall in the range of 0.1 – 0.14, which agrees well with the observed composition of this mineral.

The effective bulk rock composition calculated at the end of Grt1 growth was used as an input for reconstructing of P-T conditions during Grt2 growth. The reconstructed prograde P-T path is located in low pressure region of the analysed P-T space at ca. 538-568°C and 5.7-7.1 kbar (Fig. 15a). As a result, the core of Grt2 was equilibrated in the stability field of Grt + Pl + Bt + Ms + Chl + Ilm which is compatible with commonly preserved ilmenite inclusions in Grt2, as well as plagioclase observed in the matrix of the sample. Pressure and temperature differences during the transition between Grt1 and Grt2 yields 13 kbar and ca. 50°C (Fig. 15a). According to our thermodynamic modelling, the simplest explanation for strongly limited garnet growth at the transition between Grt1 and Grt2 is that reconstructed P-T path is nearly parallel to garnet vol% isopleths. A fast decompression rate may be an additional factor suppressing garnet growth at this stage. Unfortunately, this is only a speculation as the grains of both garnet types are too small to be separately dated to test this hypothesis.

The P-T path reconstructed based on the Grt2 composition ends in the stability field of Pl2 + Grt + Bt + Ms + Chl + Ilm. However, the reconstructed PT path may constitute an incomplete record of garnet growth. A careful inspection of the chemical profiles shows a slight spessartine increase in the outer rim (Fig. 15a), and garnet grains from this sample show very irregular shapes (Fig. 14). Both observations are indicative of garnet-consuming resorption, which could be responsible for the partial dissolution of garnet grains.

According to thermodynamic modelling, the core and rim parts of garnet grains in the sample PK007 were formed in contrastingly different P-T conditions. This is confirmed by the diverse inclusion sets preserved in various parts of these garnets, including white mica. The K-white mica in sample PK007 display variable chemical composition, varying from phengite to muscovite with low Si content and paragonite (Fig. 16). To estimate the P-T conditions of white mica formation in all the analysed sample, we have applied Si in phengite geobarometer (Kamzolkin et al., 2016) coupled with Ti in white mica geothermometer (Wu and Chen, 2015). The advantage of these tools is that they are based on the composition of the same mineral. However, the Ti in white mica geothermometer was calibrated for a low-pressure mineral assemblage comprising ilmenite and sillimanite, and the latter mineral is not present in the inspected samples. Therefore, we have supplemented these calculations by applying garnet-muscovite geothermometer in two calibrations formulated for metapelites

metamorphosed at high pressures Green & Hellmann, 1982; Hynes & Forest, 1988). The results of geothermobarometric calculations are presented in Fig. 17.

The two chemical groups of white micas observed in sample PK007 occupy different textural position. The grains with the lowest Si content were mostly documented in the cleavage zones as well as in Grt2, i.e., in the rim parts of the garnet grains. Conversely, phengitic white mica grains were mostly documented in the microlithons as well as in Grt1. We suggest that the observed bimodal distribution of Si content in white micas may at least partly be a record of decompression. Given that the inferred P-T paths trend nearly perpendicular to white mica Si isopleths, the record preserved in white mica is more complete than that preserved in the chemical zoning of garnet grains.

Stop 2 – Kamieniec Ząbkowicki

GPS coordinates: 50.5276617N, 16.8795256E
Position and lithology: mica schists and eclogite of the Kamieniec Metamorphic Belt
Described problems: Variscan tectonometamorphic record

– – – – – – – – – – – – – –

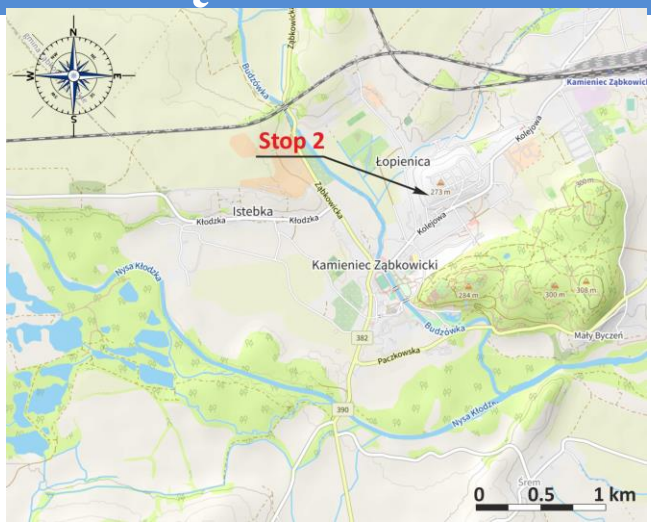

In the outcrop, small eclogite bodies (lenses, pods) are embedded in the prevailing metapelites (mica schists), however, the former ones are found in the form of loose boulders or blocks. The study of metamorphic record preserved in the outcrop was based predominantly on eclogites, nevertheless, a sample of mica schist was also collected for comparative purposes.

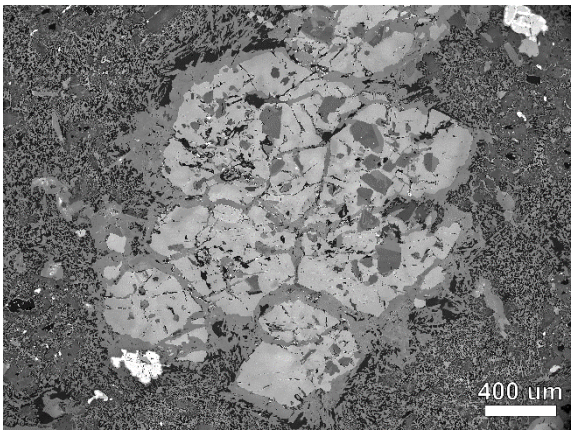

Fig. 18. Back-scattered electrons image of garnet cluster in eclogite from the KMB.

Petrographic outline and mineral chemical composition

Eclogites

Eclogites show random texture and are composed of garnet porphyroblasts set in the fine-grained matrix of clinopyroxene, plagioclase, amphibole, epidote, white mica and quartz. Accessory phases include rutile, ilmenite, apatite, calcite and zircon.

Garnet forms euhedral to subhedral porphyroblasts (up to 1.5 mm in diameter) aggregated in clusters of several crystals (Fig. 18). Porphyroblasts contain numerous, randomly distributed inclusions of clinopyroxene (omphacite), white mica (phengite), amphibole, biotite, apatite, rutile and quartz. Some of the inclusions form rectangular, poly-mineral

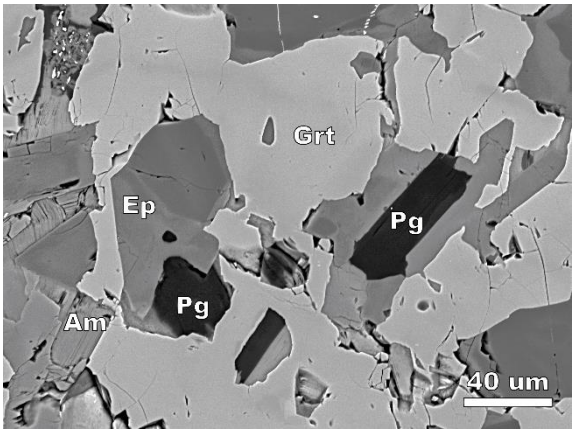

aggregates (Ep + Am + Pg ± Qz ± Pl ± Ky; Fig. 19). We interpret them as pseudomorphs after lawsonite (cf. Orozbaev et al., 2015, Tsujimori and Ernst, 2014, Zeng et al., 2019). Garnet shows continuous, prograde chemical zoning (Fig. 20) of spessartine (bell-shaped distribution from ca. 0.30 to 0.01 rimwards), almandine (from 0.38 up to 0.66 rimwards) and pyrope (ca. 0.01 in the core to <0.26 at the rim). Grossular does not display substantial changes in distribution across the crystals.

Fig. 19. Back-scattered electrons image of poly-mineral inclusions in garnet in eclogite from the KMB interpreted as pseudomorphs after lawsonite.

Matrix is dominated by omphacite variously replaced by fine-grained Cpx + Pl symplectites (Fig. 21a). The same textures are observed in the omphacite inclusions found in garnet porphyroblasts. All omphacite relics have similar composition and their XJd reaches in maximum 0.46–0.49. Clinopyroxene that replaces omphacite is less Na-rich and corresponds to diopside or augite. In turn, symplectitic clinopyroxene is partly overgrown by amphibole, which ranges from pargasite to Mg-hornblende to actinolite. This composition is in contrast to the amphiboles present as garnet inclusions or directly overgrowing garnet porphyroblasts (ferro-sadanagaite or ferro-pargasite).

White mica occurs in two types. The first one is

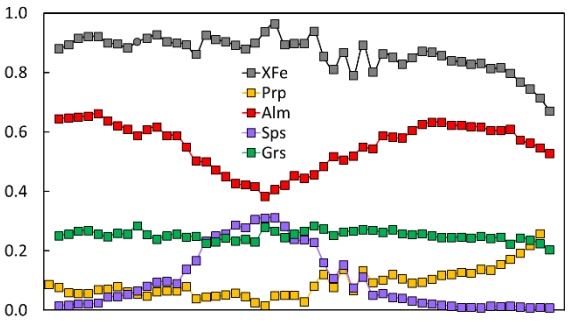

present in the matrix or as inclusions in garnet and has the composition of phengite with Si^{4+} up to 3.49 apfu and X_{Na} <0.11 (X_{Na} = Na/(Na + K + Ca)). It is partly or completely pseudomorphed by Bt + Pl symplectites (Fig. 21b). The second type of white mica corresponds to paragonite (Si c. 3.00 apfu, X_{Na} >0.80). Its presence is confined to mineral aggregates in pseudomorphs after lawsonite.

Fig. 20. Chemical variation of the representative garnet porphyroblast from the KMB eclogite.

Epidote belongs to the clinozoisite subgroup (Armbruster et al., 2006) and shows a chemical zoning with cores richer in Al than the rims. At places, crystals in the matrix have higher concentrations of REE in their cores. Plagioclase composition depends on its textural position. In Cpx + Pl symplectites it is albite, whilst in post-phengite symplectites and pseudomorphs after lawsonite the anorthite content is higher (oligoclase–andesine). Rutile forms tiny blasts in garnet and omphacite relics, however, in the matrix it occurs as elongated aggregates (up to 3 mm long). The mineral is often partly overgrown by ilmenite and titanite. Apatite was documented both as inclusions in garnet and in the matrix. Its composition is characterized by a varied concentration of F and a very low of Cl.

The textural position of the minerals and the observed breakdown structures led us to recognition of two mineral assemblages: 1) a prograde-baric peak assemblage Grt (rim) + Omp + Ph + Amp + Rt + Lws + Qz + Ap, and 2) a retrograde assemblage Cpx + Pl + Bt + Pg + Ep + Amp + Ilm-Ttn + Qz ± Ky identified in pseudomorphs after phases of the first assemblage (garnet, omphacite, phengite, lawsonite). It appears that only garnet cores preserved the composition pertinent to the incipient stages of metamorphic progression.

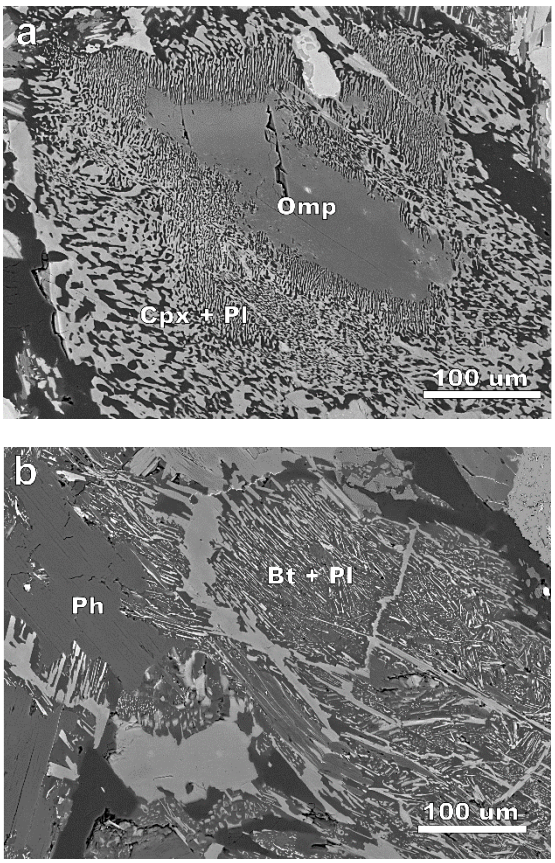

Fig. 21. Symplectites in the eclogite of the KMB: a. clinopyroxene and plagioclase after omphacite, b. biotite and plagioclase after phengites.

Mica schists

The mica schist sample comprises garnet porphyroblasts embedded in a coarse-grained, strongly laminated matrix (the S1 planes refolded by younger F2 folds) composed of quartz, K-white mica with minor biotite, andalusite, plagioclase, staurolite and chlorite. Accessory minerals are rutile, ilmenite, margarite, paragonite, chloritoid, epidote, zircon and apatite.

Subhedral porphyroblasts of garnet (4–8 mm in size) contain inclusions of chloritoid, K-white mica, paragonite, margarite, chlorite, staurolite, biotite, plagioclase, clinozoisite, rutile and quartz (Figs. 22). Parallel alignment of rutile needles marks the S1 planes in porphyroblast (Figs. 23b). Garnet blasts show prograde chemical zonation (Fig. 23a), with a bell-shaped spessartine profile (X_{sps} from ca. 0.09 in the core to nearly 0 rimwards) and a gradual core-to-rim increase of almandine (X_{alm} from ca. 0.70 to 0.80). Grossular concentration is stable in the inner core (X_{grs} 0.18–0.21) but decreases sharply outward (X_{grs} 0.08–0.10). Pyrope content gradually increases rimwards (X_{prp} from ca. 0.04 to 0.14).

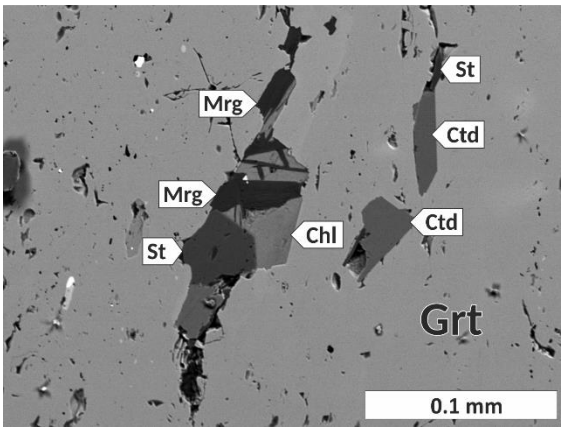

Fig. 22. Back-scattered electrons image of poly-mineral inclusions in garnet in mica schist from the KMB.

Two types of K-white mica are present: 1) blasts with high Si content (up to 3.44 apfu) which are aligned parallel to the S1 foliation, 2) blasts with low Si content (ca. 3.10 apfu; Fig. 24) mostly documented within the axial planes of the F2 folds.

Plagioclase grains in the matrix have albite composition, while the inclusions in garnet are richer in anorthite content (oligoclase). Biotite and rare chlorite blasts present in the rock matrix are richer in Mg than their inclusions in garnet. Staurolite found in the matrix shows homogeneous

chemical composition (X_{Mg} = 0.13–0.17), but inclusions in garnet are varied compositionally (X_{Mg} = 0.04–0.15).

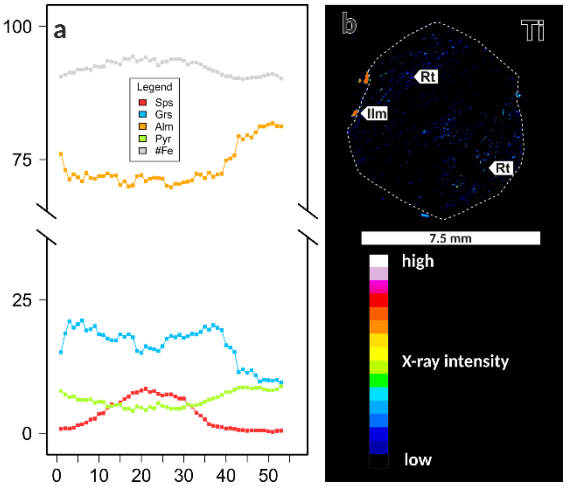

Fig. 23. a. Chemical variation of the representative garnet porphyroblast from the KMB mica schist. b. X-Ray map of Ti illustrating rectilinear inclusion trails of rutile preserved in garnet porphyroblast from PK023 mica schist

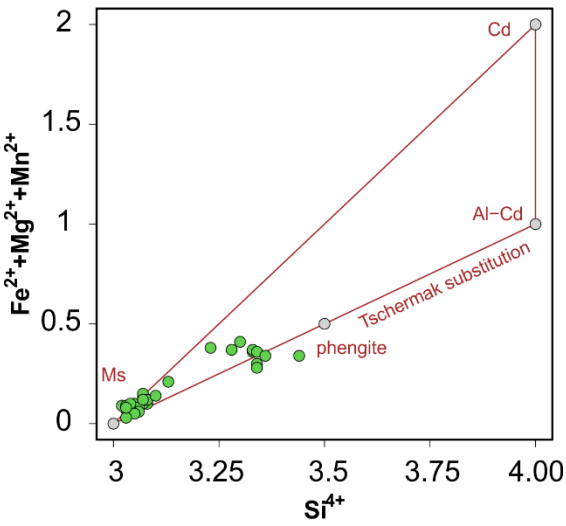

Fig. 24. Compositional variations of white micas in the investigated mica schists from the Kamieniec Metamorphic Belt.

Finally, we distinguish two mineral assemblages in the investigated mica schist: 1) M1 assemblage mostly occurring as inclusions in garnet porphyroblasts (Grt + Cld + Ph + Pg + Chl +Rt + Qz), 2) M2 assemblage observed as inclusions in garnet and in the matrix (Ms + Bt + Mrg + Pl + St + Ilm + And + Qz).

Metamorphic record

Eclogites

The P-T path reconstructed for eclogites is shown in Fig. 24. The prograde segment up to baric peak is based on thermodynamic modelling of phase equilibria, while the second part of the loop is derived from conventional geothermobarometry. The first stage was estimated by intersection of isopleths for relic Mn-rich core of garnet and yielded 470°C and 12–13 kbar. The following stage of metamorphism was reconstructed with reference to the composition of Grt (rim) + Ph + Omp and taking into account the chemical fractionation of the rock by the progressive growth of garnet. The compositional isopleths for the minerals of the metamorphic peak assemblage indicate pressure from 24 to 27 kbar in a narrow temperature range of 550–570°C. The model shows that lawsonite joined the mineral assemblage during the prograde portion of the P-T loop. It also predicts that the abundance of lawsonite was <5 vol.% at the baric peak conditions. Thus the lawsonite-out boundary sets the low-P limit of the inferred P-T conditions with the implication that lawsonite must have disappeared with the onset of retrogression. These inferences are compatible with our textural observations and interpretation of poly-mineral inclusions in garnet (Fig. 24).

The estimation of HP conditions by means of conventional geothermobarometry confirmed these results. A selection of calibrations for Grt + Cpx (Omp) in quartz-bearing and kyanite-free mineral assemblage yielded pressures of ca. 24 kbar at ca. 550°C. We also used Raman elastic barometer for apatite inclusions in garnet (AiG) aiming at independent estimation of pressure conditions. The calculated composition-corrected entrapment pressures of apatite inclusions combined with the Zr-in-Rt geothermometer (Kohn, 2020) for rutile

inclusions point to pressures of ca. 23 kbar and validate the above results.

Fig. 24. The P–T path reconstructed for the studied eclogites (ECL) and the sample of the mica schists (MS) from the KMB.

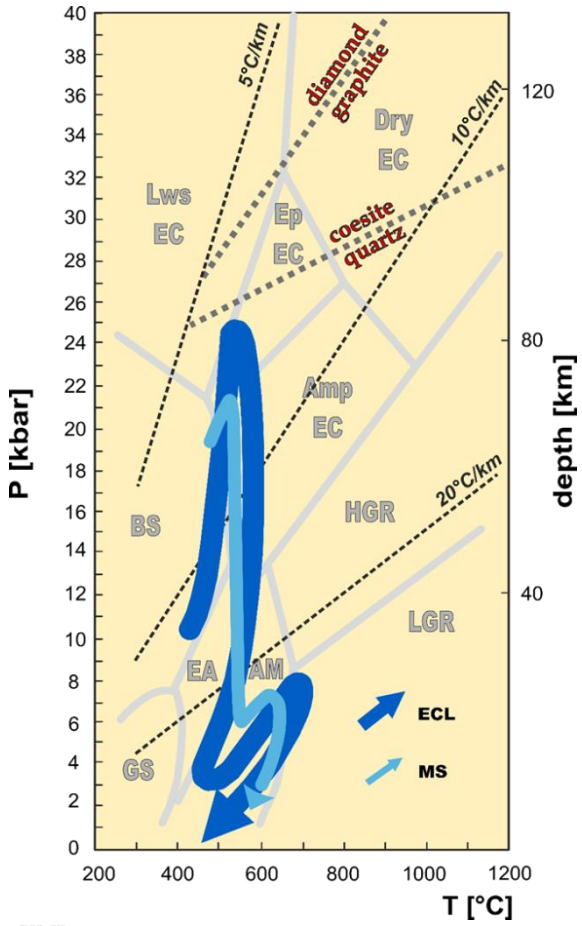

The subsequent stages of metamorphism seen in the outcrop are predominantly documented by compositional changes in amphibole ± plagioclase. They show second progression of metamorphic conditions starting at <3.5 kbar and <550°C up to-medium pressures (ca.7 kbar) reaching a thermal peak of 650-690°C. The final exhumation stage must have ended the P–T trajectory at shallow crustal levels.

Mica schists

The reconstruction of P-T path for the mica schist sample was based on garnet composition (Fig. 24). The calculation show that growth of garnet started at c. 480°C and 19.5 kbar and continued up to c. 520°C and c. 21 kbar. The model predicts the Si content in white mica of ca. 3.40 apfu, which corresponds directly with our mineral-chemical observations. The calculations suggest that lawsonite (<2 vol.%) was present at the onset of garnet crystallization but subsequently it reacted out. This is consistent with the lack of lawsonite in the mica schist studied.

Moreover, calculations imply that phases post-dating garnet growth (Pl + low-Si Ms + St + Ilm) are related to a pressure drop to ca. 5–8 kbar (Fig. 24). The composition of the model-predicted white mica (Si ca. 3.05 apfu) and staurolite (X_{Mg}: 0.12–0.14) is in good agreement with the respective minerals present in the matrix. The topology of the staurolite model isopleths suggests a P–T increase from ca. 530°C and 6 kbar to ca. 640°C and 6–7 kbar. In turn, the presence of andalusite points to a subsequent drop in pressure to <4 kbar at ca. 600°C.

The contrastingly different P-T conditions experienced by the mica schist sample during metamorphic evolution suggested by thermodynamic modelling, were consistently confirmed by conventional geothermobarometry based on white mica and garnet mineral composition. The applied combination of calibrations of geothermobarometers devised for Grt + Ph + Ms metapelites indicate that phengitic white micas crystallized predominantly at ca. 13-20 kbar, while the low-Si white mica flakes equilibrated at pressures of c. 3-10 kbar (Fig. 24).

Summary

Nearly identical metamorphic evolution and the shape of P–T path were obtained for eclogites and mica schists collected from the same outcrop. The metamorphic evolution was multistage and defines a clockwise P–T trajectory that comprises a prograde segment up to the baric peak (HP-LT episode, cold subduction), then a retrogression path followed by a LP-HT episode (thermal peak) and

terminates with a final exhumation to shallow crustal levels.

Stop 3 – Doboszowice

GPS coordinates: 50.5002281N, 16.9589100E
Position and lithology: orthogneiss
of the Doboszowice Metamorphic Complex
Described problems: early Palaeozoic
magmatism,
Variscan metamorphic record

Early Palaeozoic magmatism

In the abandoned quarry at Pomianów Górny the Doboszowice orthogneiss is exposed. It is two-mica, medium-grained L-tectonite, composed of quartz, plagioclase, K-feldspar, muscovite, biotite and accessory garnet. The magmatic protolith of the Doboszowice orthogneiss was formed during the Cambro-Ordovician tectono-magmatic event, similar to other orthogneisses of the West and Central Sudetic part of the Bohemian Massif. The published isotopic zircon data from the Doboszowice orthogneisses show U-Pb ages of 488 ± 6 Ma (Concordia age, U-Pb SHRIMP, Mazur et al., 2010), 494 ± 5 Ma (Concordia age, U-Pb LA-ICPMS, Jastrzębski et al., 2023) and 500 ± 16 Ma (upper intercept age, U-Pb LA-ICPMS, Jastrzębski et al., 2023) (Fig. 25). Inherited age populations are very abundant and cluster at c. 540 Ma, 560–550 Ma, 605–585 Ma (most prominent), and 1.9 Ga (Jastrzębski et al., 2023), which generally concurs with the main features of detrital zircon age spectra of Early Paleozoic metasedimentary rocks visited during this excursion. The Doboszowice orthogneiss contains inserts of metasedimentary rocks of unknown protolith age (Jastrzębski et al., 2023, Fig. 25a). These orthogneisses are geochemically Si-rich (73-78 wt% of SiO_2), calc-alkaline and peraluminous with A/CNK ranging from 1.05 to 1.35, which suggest that they originated from melting of a sedimentary rock (Buriánková et al., 1999). At the geotectonic discrimination diagrams, the Doboszowice orthogneisses occupy a field of volcanic arc granite, close to the boundaries with ocean-ridge granites and within-plate granites (Mazur et al., 2010). Oxygen isotopic composition in c. 500-495 Ma old zircons indicate δ18O values that are generally higher than those of the primitive mantle (Fig. 25b and c), which confirms a Si-rich composition of the parent magma. This observation and abundance of the inherited zircons imply a predominant contribution from a Neoproterozoic continental crust in magma formation.

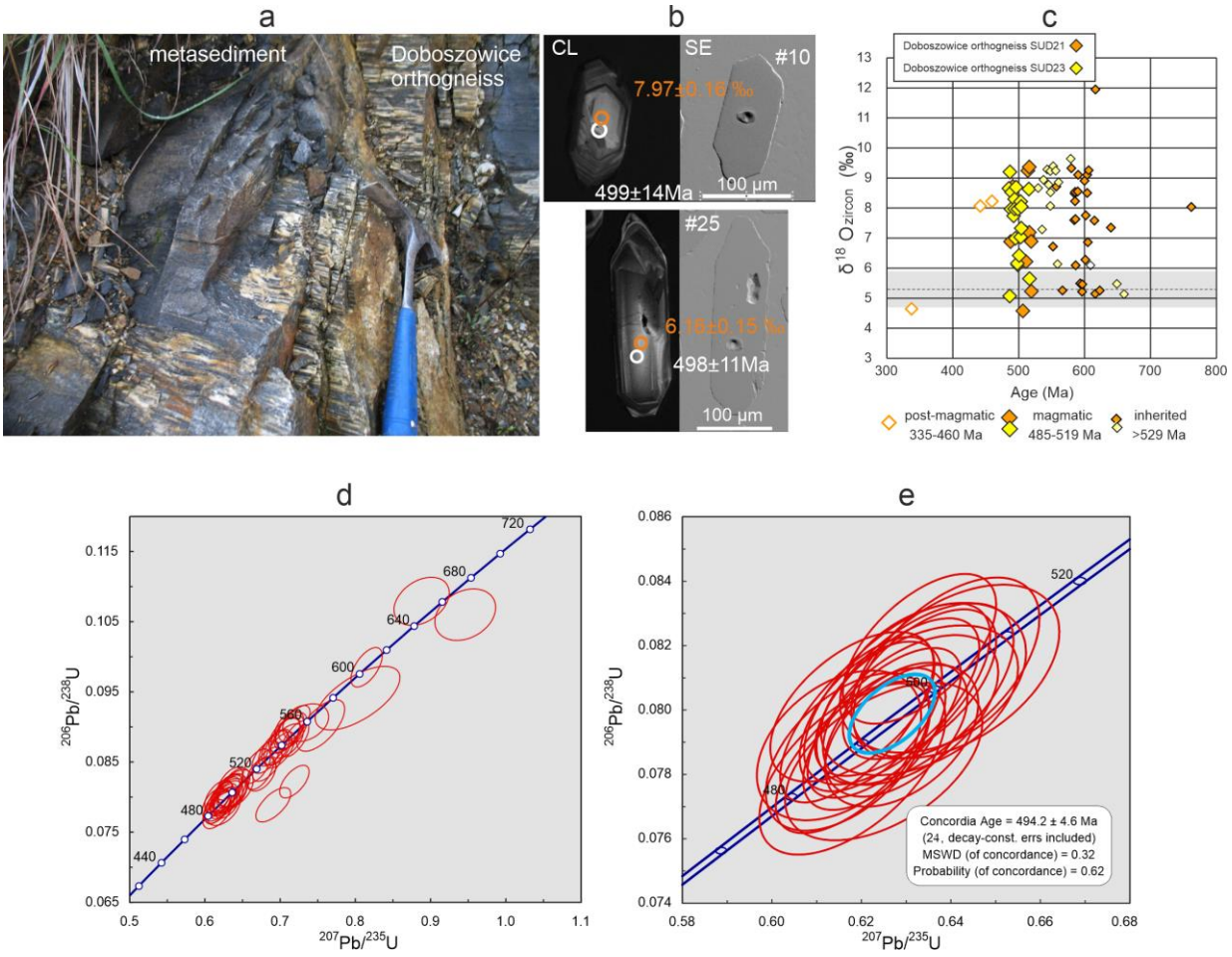

Fig 25. a) The Doboszowice orthogneisses contacting with metasedimentary rocks (Doboszowice quarry). b) U-Pb and O isotopic data in representative 500 Ma zircon grains. Spot labels of U-Pb dates (white) and O isotope data (orange). c) Results of δ18O isotopic analysis in zircon. Mantle-equilibrated value for δ18O in zircon (5.3 ± 0.6‰, 2σ, Valley, 2003) is indicated by grey color. d). Concordia U-Pb plot for the sample SUD23 collected in the visited quarry. e) Concordia U-Pb plot in the early Palaeozoic range for the same sample.

Variscan metamorphic record

The outcrop is composed of the orthogneiss consisting of quartz, K-feldspar, plagioclase, white and dark micas, and rare garnet grains. Accessory minerals are zircon, apatite and ilmenite.

The rock consists of partly recrystallized K-feldspar porphyroclasts (up to 1.5 cm in size, X_{Or} 94–99) and quartz laminae (0.5–1 mm thick) alternating with lenses composed of completely recrystallized plagioclase and thin biotite–muscovite layers. Plagioclase shows relatively stable composition (X_{Ab} 0.88–0.91). Small garnet grains (0.1–0.3 mm in size) display generally flat core chemical profile and are rich in almandine (Fig. 26, X_{slm} 63–70, X_{prp} 1–3, X_{grs} 18–30, X_{sps} 2–10; Table).

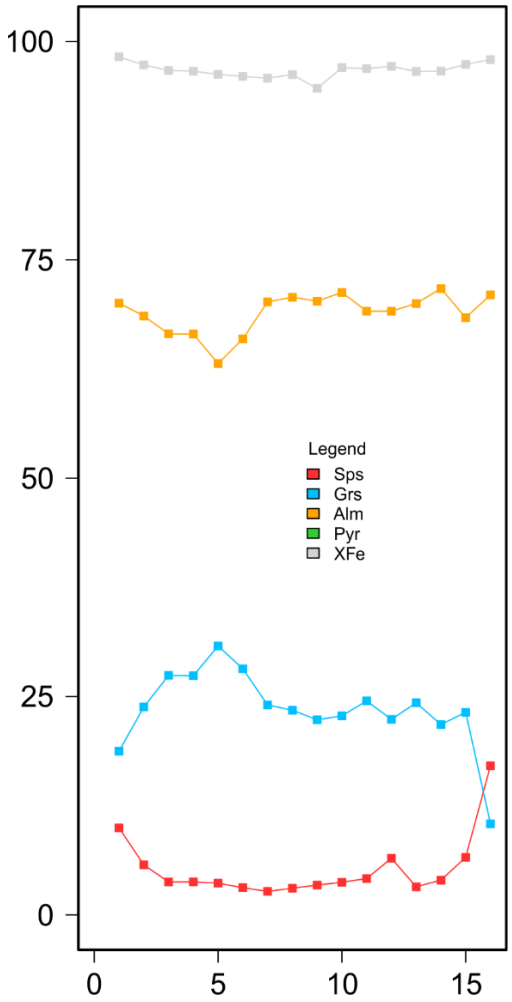

Fig. 26. Chemical zoning of representative garnet grain from sample MD09-02.

On the other hand, compared to the core, the chemical composition of the rim is characterised by a marked increase in spessartine, coupled with a decrease in grossular content and variations in almandine content. In terms of chemical composition white mica can be divided into two groups differing by Si content (Fig. 27). Abundant group Ms1 displays phengitic composition and is characterized by Si content ranging from 3.22 to 3.37 apfu and usually forms core parts of white mica grains (Fig. 27). The group Ms2 shows considerably lower Si content falling in the range of 3.11 to 3.15 apfu and forms mostly rim parts of white mica flakes. Biotite has X_{Mg} = 12–20% and Ti = 0.05–0.29 apfu. Apatite is a common accessory mineral, while ilmenite occurs extremely rare.

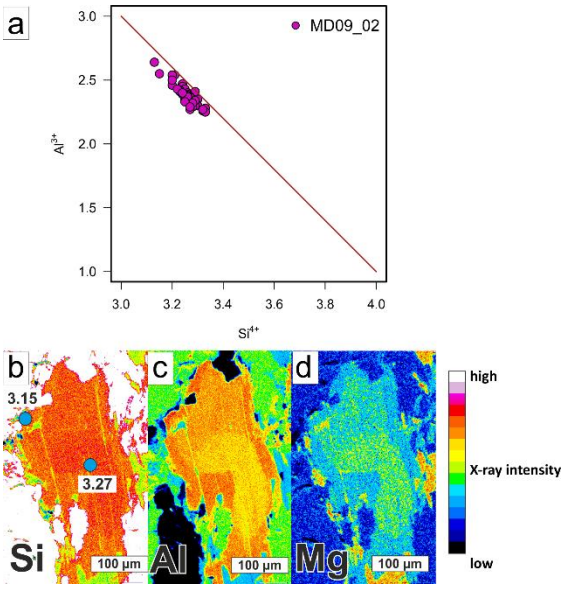

Fig. 27. X-Ray maps illustrating chemical zoning of white mica from sample MD09-02. a. Si, b. Al and c. Mg.

Based on textural observations we distinguish two mineral assemblages in the MD09-02 orthogneiss sample. The M1 assemblage is represented by white mica Ms1, with relatively high Si content corresponding to a possible high–P history of the rock. The M2 assemblage comprises Grt + Ms2 + Bt + Pl+ Kfs + Ilm + Qz.

Orthogneiss sample MD09-02 contains small garnet grains with strongly diffusionally modified profiles, which prevent calculation of a P–T path based on garnet composition. However, the calculated pseudosection coupled with isopleths corresponding to the composition of the garnet core allows estimation of maximum temperature and pressure of diffusional equilibration of garnet (Fig. 28a).

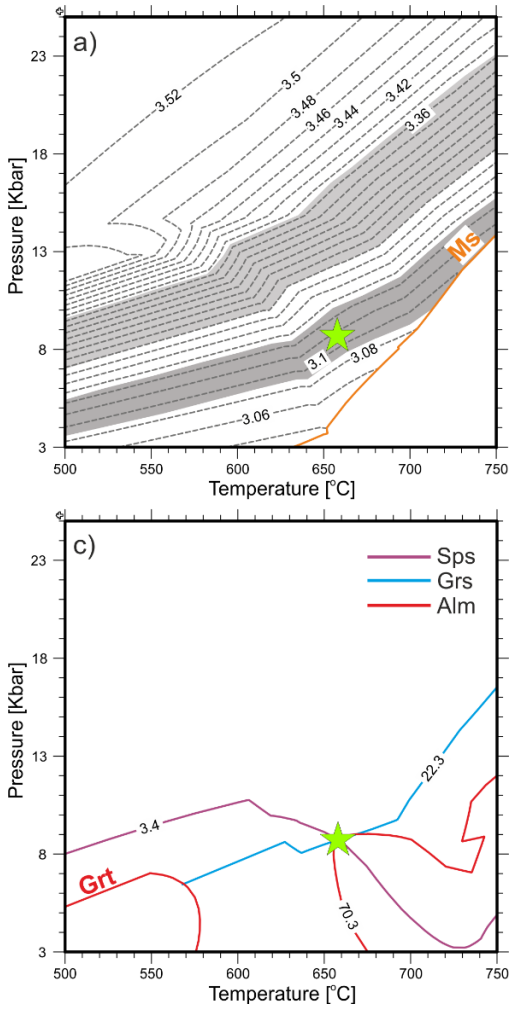

Fig. 28. Phase diagram modelling results for sample MD09-02 using the core composition of Grt and bulk rock composition; a. compositional isopleths of Si in K- white mica. Ms-out reaction is additionally shown. The composition of observed white mica flakes is indicated by grey areas. b Isopleths shown for almandine (red), grossular (blue), and spessartine (purple). Green star at the intersection of isopleths marks P–T conditions of garnet requilibration during HT metamorphism at the thermal peak of the M2 metamorphism. Green star is also shown on diagrams a and b.

Isopleths calculated for the garnet core indicate that it was stable at c. 9 kbar and 660°C (Fig. 28b).

The results of the conventional geothermobarometry show that the two compositional K-white mica groups i.e. with high and low Si content identified in the orthogneiss sample equilibrated at contrastingly different PT conditions (Fig. 29). White mica Ms1 with high Si contents shows pressures of its formation in the range of c. 16 to 22 kbar at ~590 to 720°C. On the other hand, low Si white mica Ms2 is characterized by pressures of its formation ranging from ~6 to 11 kbar at ~500 to 700°C. Consequently, textural relationship between the two compositional white mica groups support our suggestion that the observed distribution of Si content in white micas may represent a record of the MP–HT event overprinting the earlier HP metamorphic episode. The only important discrepancy that becomes apparent when comparing the results of white mica geothermobarometry with thermodynamic calculations is that the P–T conditions for white mica Ms1 from orthogneiss generally indicate high temperatures of its formation. This is the function of high Ti contents of the inspected white mica grains. However, it appears that temperature calculations for white mica Ms1 should be taken with caution, as the M1 mineral assemblage lacks ilmenite and Al_2SiO_5 phase, which are prerequisite for the application of this tool.

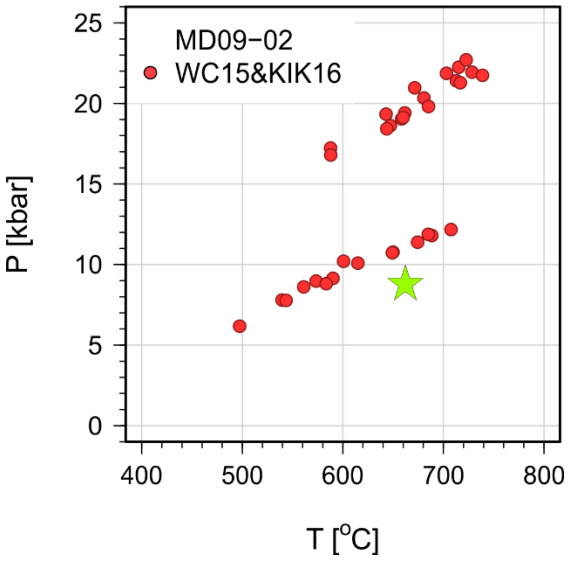

Fig. 29. Results of geothermobarometric calculations for sample MD09-02. KIK16 – Si in phengite geobarometer (Kamzolkin et al., 2016). WC15 - Ti in white mica geothermometer (Wu & Chen, 2015).

Stop 4 – Chałupki

GPS coordinates: 50.4864144N, 17.0045381E
Position and lithology: paragneiss
of the Doboszowice Metamorphic Complex
Described problems: provenance,
maximum depositional age,
Variscan tectonometamorphic record

Provenance and maximum depositional age

The Chałupki paragneisses are migmatitic, medium- to coarse-grained foliated rocks, composed of quartz, plagioclase, muscovite, biotite and garnet. In the visited part of the abandoned quarry, the paragneisses are intercalated with garnitiferous mica schists.

Detailed petrography of both rock types is described in the section devoted to Variscan tectonometamorphic record. The LA-ICP-MS zircon dating for the Chałupki paragneiss showed predominance of Neoproterozoic zircons, similar to the mica schists exposed in the Kamieniec Metamorphic Belt (Jastrzębski et al., 2023, Szczepański et al., 2023) (Fig. 5). The source area(s) for the sedimentary basin consisted of Cryogenian to Ediacaran crystalline rocks, with some Palaeoproterozoic component, but lacking Mesoproterozoic zircons. The provenance studies on the migmatitic Chałupki paragneiss thus indicate that the deposition of their sedimentary protolith took place in the western and/or northern African periphery of Gondwana (Jastrzębski et al., 2023, Szczepański et al., 2023). However, in contrast to the Kamieniec Ząbkowicki mica schists, the Chałupki paragneisses contain an additional Early Ordovician age cluster which makes up c. 10% of the zircon population. This, 510–488 Ma age cluster is formed by the most euhehral zircon crystals that might either come from erosion of the adjacent Cambro-Ordovician orthogneisses (Szczepański et al., 2023) or represent synsedimentary volcanogenic/pyroclastic admixture accompanying the sediment deposition (Jastrzębski et al., 2023). According to these interpretations, the youngest zircon age peak in the Chałupki paragneisses represents either the maximum depositional age, or the depositional age.

Variscan tectonometamorphic record

The outcrop is dominated by generally subhorizontal the S1 foliation that is locally deformed by centimetre-scale the F2 folds. Their axes are generally subhorizontal and oriented NNW-SSE. On the S1 foliation there are preserved two mineral lineations. The L1 lineation is marked by parallel alignment of white mica flakes, while the S2 lineation is marked by elongated feldspar patches.

Two samples – the mica schist MD01-18 and the paragneiss MD01-02 were investigated to decipher P-T history of the volcano-sedimentary succession exposed in the eastern part of the DCM.

Petrography and mineral chemistry of the mica schists from the Doboszowice Metamorphic Complex

The mica schist sample MD01-18 contains garnet porphyroblasts in a schistose matrix comprising quartz, K-white mica, biotite, margarite, staurolite and kyanite. Accessory minerals are rutile, ilmenite, zircon, apatite and tourmaline.

Subhedral garnet porphyroblasts range from 1 to 9 mm in size and they often contain inclusions of quartz, K-white mica, staurolite, tourmaline, ilmenite, and sporadically rutile. Garnet grains in the MD01-18 sample typically exhibit prograde growth chemical zonation (Fig. 30a),

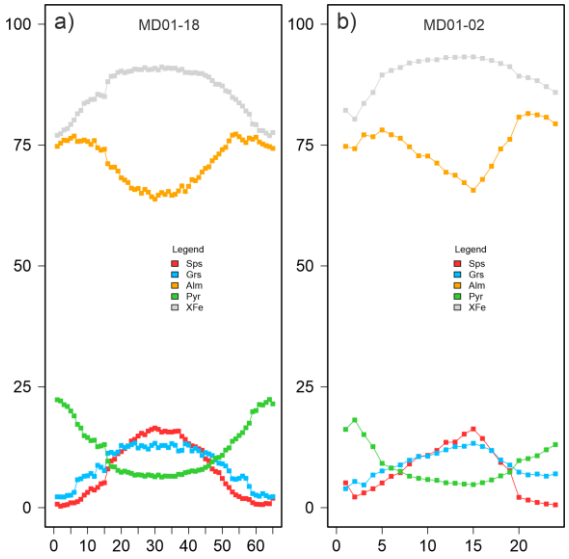

Fig. 30. Chemical zoning of representative garnet grains from: a) mica schist sample MD01-18 and b) paragneiss sample MD01-02. XFe = Fe/(Fe + Mg).

with bell-shaped spessartine profile (X_{sps} decreasing from ~ 16 to nearly 0) coupled with a gradual core-to-rim increase of almandine (X_{alm} increasing from ~ 66 to 76) and pyrope (X_{prp} increasing from ~ 6 to 22) content. Grossular concentration displays relatively stable value in the core (X_{grs} ~ 11 to 13), and decreases outwards (X_{grs} ~ 2). A small increase in X_{sps} content associated with decrease of X_{alm} and X_{prp} is observed in the outermost rim, which is characteristic of a resorption process operating during late metamorphism (e.g. Anderson and Buckley 1973). In terms of Ti-bearing phases garnet grains in this sample entrap mostly ilmenite inclusions with preserved relics of rutile in their cores (Fig. 31a). However, sporadically rutile needles are observed in the rim parts of garnet grains (Fig. 31b). Furthermore, larger ilmenite grains present in the rock matrix also contain rutile inclusions.

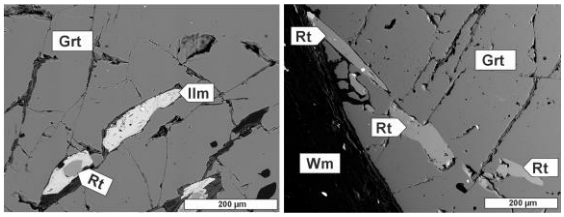

Fig. 31. Backscattered electron images of Ti-bearing phases preserved (a) as inclusions of ilmenite overgrowing rutile in a garnet from the sample MD01-18 and (b) as rutile inclusions in the resorbed rim portion of a garnet from sample MD010-18.

White mica may be grouped into four chemical varieties represented by: (i) scarcely preserved K-white mica flakes Ms1, that were documented both in the core parts of larger K-white mica plates or as isolated grains mostly preserved within quartz layers, with Si content falling in the range between 3.18 and 3.38 Si apfu (Figs. 32a and d), (ii) highly-abundant, reaching up to 3 mm in length, K-white mica grains Ms2 with Si content ranging from 3.08 to 3.15 apfu forming rims of Ms1 grains or isolated larger flakes (Figs. 32a, b and d), (iii) fine-grained aggregates of K-white mica flakes Ms3 with Si content ranging from 3.0 to 3.05 apfu forming isolated clusters and rims developed around Ms2 white mica flakes, staurolite or kyanite (Figs. 32b, c and d) and (iiii) margarite grains Mrg with X_{Mrg} ranging from 65 to 90 ml% forming fine-grained aggregates surrounding kyanite crystals and often associated with Ms3 white mica (Fig. 32c and d).

Documented margarite aggregate is characterized by paragonite content reaching up to 19 mol%. Ti content varies from 0 (for Mrg) to 0.06 for the K-white micas Ms1 to Ms3.

Plagioclase occurs sporadically forming small grains reaching up to 0.03 mm in diameter or larger porphyroblasts up to 1 mm in diameter. Documented grains reveal a diverse chemical composition and are represented by: (i) oligoclase ranging from 9.5 to 11.2 mol% of X_{An} and (ii) albite with maximum 1.7 mol% of X_{An}. Small staurolite crystals, up to 0.2 mm in size, occur as inclusions in white mica Ms2 and as inclusions in garnet grains. It is characterized by XMg between 6 and 19. Kyanite blasts range from 0.25 mm to 0.5 mm and occur mostly as inclusions within K-white mica Ms2. Some kyanite blasts are surrounded by fine-grained aggregate composed of margarite and K-white mica Ms3 (Fig. 32c). Small biotite flakes documented in the rock matrix are characterized by XMg varying from 31 to 43.

Based on textural observations, we distinguish three mineral assemblages in the mica schist sample MD01-18. The M1 assemblage is represented by relics of phengitic white mica Ms1 scarcely preserved in the matrix and rutile that is preserved within core parts of larger ilmenite grains. This mineral assemblage may be indicative of relatively high–P history of the inspected sample. The M2 assemblage is represented by Grt and Ms2 + Pl + St + Ky + Bt + Ilm + Rt. The M3 mineral assemblage is represented by Ms3 + Mrg.

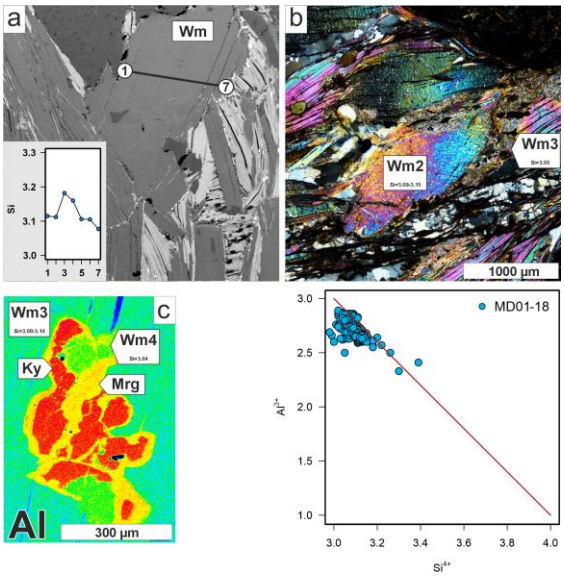

Fig. 32. (a) Backscattered electron image showing white mica Ms1 overgrown by white mica Ms2. Inset shows Si content along profile 1-7. (b) large white mica Ms2 overgrown by fine-grained white mica Ms3. (c) X - Ray map of Al distribution showing kyanite replaced by mixture of margarite (Mrg) and low-Si K white mica (Wm3) from sample MD01-18. (d) Compositional variation of white micas in the MD01-18 mica schist sample from the DMC.

Petrography and mineral chemistry of the Chałupki paragneiss

The sample MD01-02 is a coarse-grained, garnet-bearing paragneiss composed of garnet, quartz, plagioclase, white mica, biotite, chlorite, and accessory ilmenite, rutile, apatite, xenotime and zircon. Garnet grains are anhedral and reach a maximum of 4 mm in diameter. They display clear chemical zonation with bell-shaped spessartine profile (X_{sps} decreasing from ~ 16 to 2) coupled with a gradual core-to-rim increase of almandine (X_{alm} increasing from ~ 66 to 78) and pyrope (X_{prp} increasing from ~ 4 to 18) content. Grossular is gradually decreasing from core to rim (X_{grs} ~ 13 to 4) (Fig. 30b). Occasionally, there is observed a small increase in X_{sps} associated with X_{prp} and X_{alm} decrease in the outermost rim, suggesting that chemical composition of some garnet rims were locally modified by resorption (Fig. 30b, e.g. Anderson and Buckley 1973). Garnet grains in this sample contain mostly ilmenite inclusions.

However, sporadically rutile needles are observed in the resorbed rim parts of garnet grains or within late cracks. Interestingly, Ti-bearing phases form mostly separate grains. However, in places where rutile and ilmenite are in contact their textural relationships may indicate simultaneous growth.

White mica flakes are 0.5–3.0 mm long and are characterized by variable Si content. Those flakes with Si varying from 3.15 to 3.22 apfu correspond to white micas Ms1 (forming core parts of the analysed plates). Those flakes with Si content below 3.15 apfu (forming rims of the analysed plates) correspond to Ms2 K-white mica observed in the MD01-18 sample (Fig. 33). Rare biotite grains are 0.3 mm long and display XMg in the range of 32–47, and Ti ranging from 0.01–0.14. Plagioclase occurs exclusively in the matrix as blasts reaching up to 3 mm, and its composition varies from albite to oligoclase (X_{An} 7 to 16). Chlorite mostly fills late cracks within garnet grains and sporadically occurs as isolated grains in the rock matrix.

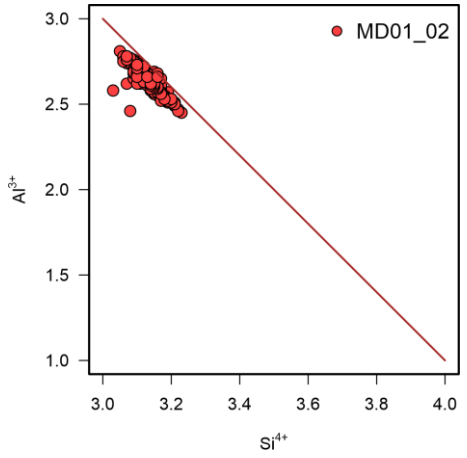

Fig. 33. Compositional variation of white mica in the MD01-02 paragneiss sample from the DMC.

Based on textural observations, we distinguish two mineral assemblages in the paragneiss sample MD01-02 that are represented by the M1 assemblage comprising rare Ms1 grains and the M2 assemblage composed of Grt and Ms2 + Pl + Bt + Rt + Ilm.

P-T history of the Chałupki paragneiss and the mica schist inlier

Sample MD01-18

The reconstructed P–T path for garnet from sample MD01-18 is shown in Fig. 34. Our calculations indicate that garnet growth started at 525°C and 4.0 kbar and ceased at 660°C and 8.0 kbar within the stability field of garnet, plagioclase, K-white mica, biotite, kyanite and ilmenite, at the lower stability limit of the melt and very close to the lower stability limit of rutile (Fig. 34). Furthermore, the reconstructed P–T path intersects the staurolite stability field. The described set of mineral stability fields intersected by the reconstructed P–T path is generally consistent with the M2 mineral assemblage documented in the inspected sample. The only lacking mineral included in the M2 assemblage is rutile. However, it is preserved in the resorbed rim portion of garnet grains or in the rock matrix. Consequently, the presence of rutile clearly indicates that both P and T must have slightly increased (c. 0.5 kbar and 10-20°C) after garnet growth ceased. This appears to be consistent with the modelled final step of garnet growth, which shows a slight increase in P and T (Fig. 32).

Furthermore, the inspected mica schist also contains a few white mica plates with relatively high Si contents, ranging from 3.18 to 3.38 apfu (Fig. 30), implying pressures of metamorphism of c. 12 to 25 kbar in the analysed temperature range of 500–750°C based on compositional isopleths (Fig. 32). Provided that phengitic white micas mostly form core parts of Ms2 white mica plates, they appear to be a record of a P–T history preceding garnet growth. This history was most likely characterised by temperatures at least below

c. 640^{o}C as the inspected mica schist show no evidence of melt formation. Otherwise, according to thermodynamic calculations, a large part of the metamorphic history of the investigated sample would have taken place in the melt stability field. Consequently, the maximum pressures of the M1 event would be between 12 to 25 kbar in the temperature range of 500 to max. 640^{o}C.

The inspected sample also contains margarite, which was most likely formed on the retrograde path after garnet formation. Considering the textural position of margarite, it was most probably formed as a partial pseudomorph after kyanite as a result of external CaO supply following the simplified mineral reaction:

$$Als + H_2O + CaO = Mrg$$

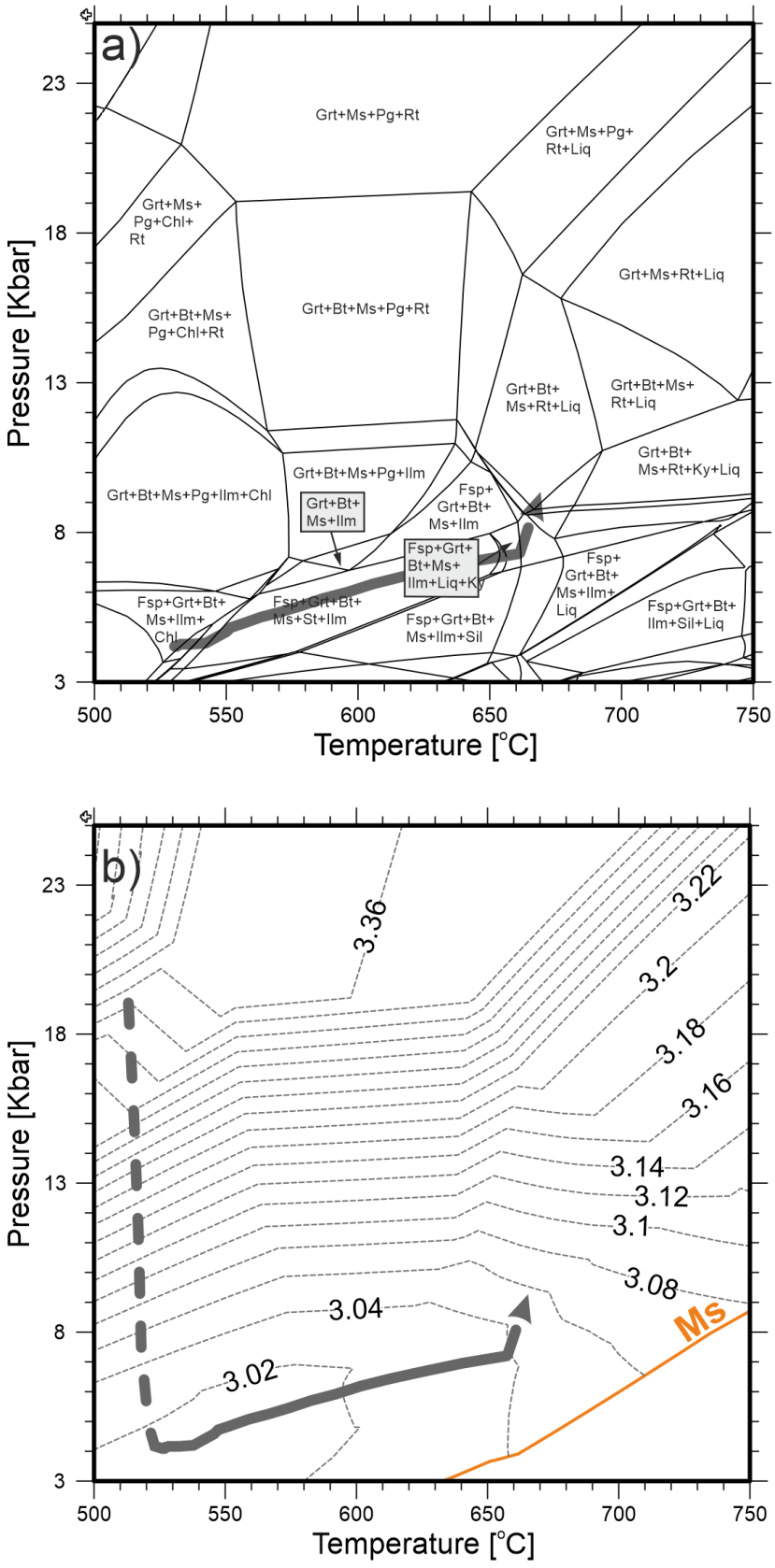

Fig. 34. Phase diagram modelling results for sample MD01-18 using the core composition of Grt and bulk rock composition; a. isochemical phase diagram, b. Compositional isopleths of Si in K- white mica. The stability field of white mica is additionally shown. Grey arrow on diagrams b and d is for the modelled P–T path.

It appears that the decomposition of Ca-bearing phases such as garnet or plagioclase may have served as a source of CaO for margarite formation according to the following simplified reactions (Baltatzis and Katagas, 1981):

$$Als + H_2O + Grs = Mrg + Qtz$$

$$Als + H_2O + An = Mrg + Qtz$$

The decomposition of anorthite and kyanite occurs in the P–T range of c. 538 to 575 and 5 to 7 kbar (Spear, 1993). Furthermore, margarite and quartz are low pressure products of the above reaction, consistent with our suggestion that margarite was produced on a retrograde path.

Sample MD01-02

The reconstructed P–T path for garnet composition of mica schist sample MD01-02 is shown in Fig. 35. Garnet growth modelling indicates that the garnet started to crystallize at 588^{o}C and 8.3 kbar, and ceased at 662^{o}C and 8.1 kbar within the stability field of garnet, plagioclase, biotite, K-white mica, ilmenite and melt (Fig. 35). Furthermore, garnet must have formed concurrently with low-Si white mica (c. 3.06 apfu, Fig. 35b). These minerals represent in fact the M2 mineral assemblage observed in the examined sample. Furthermore, the sample displays signs of incipient melting in agreement with thermodynamic calculations. On the other hand, this mica schist also contains several white mica plates with relatively high Si content, reaching up to 3.22 apfu (Fig. 33) and suggesting pressures of c. 11 to 18 kbar in the analysed temperature range based on compositional isopleths. However, considering that these high-Si white mica form core parts of the analysed flakes, we suggest that their formation preceded garnet crystallization. Considering the traces of only incipient melting observed in this sample, it seems that this part of the metamorphic history underwent in the temperatures lower than c. 570^{o}C and pressures not exceeding c. 15 kbar. Higher temperatures and, consequently, higher pressures, according to the predictions of thermodynamic calculations, would result in an unexpectedly high volume of generated melt of even 25 vol%.

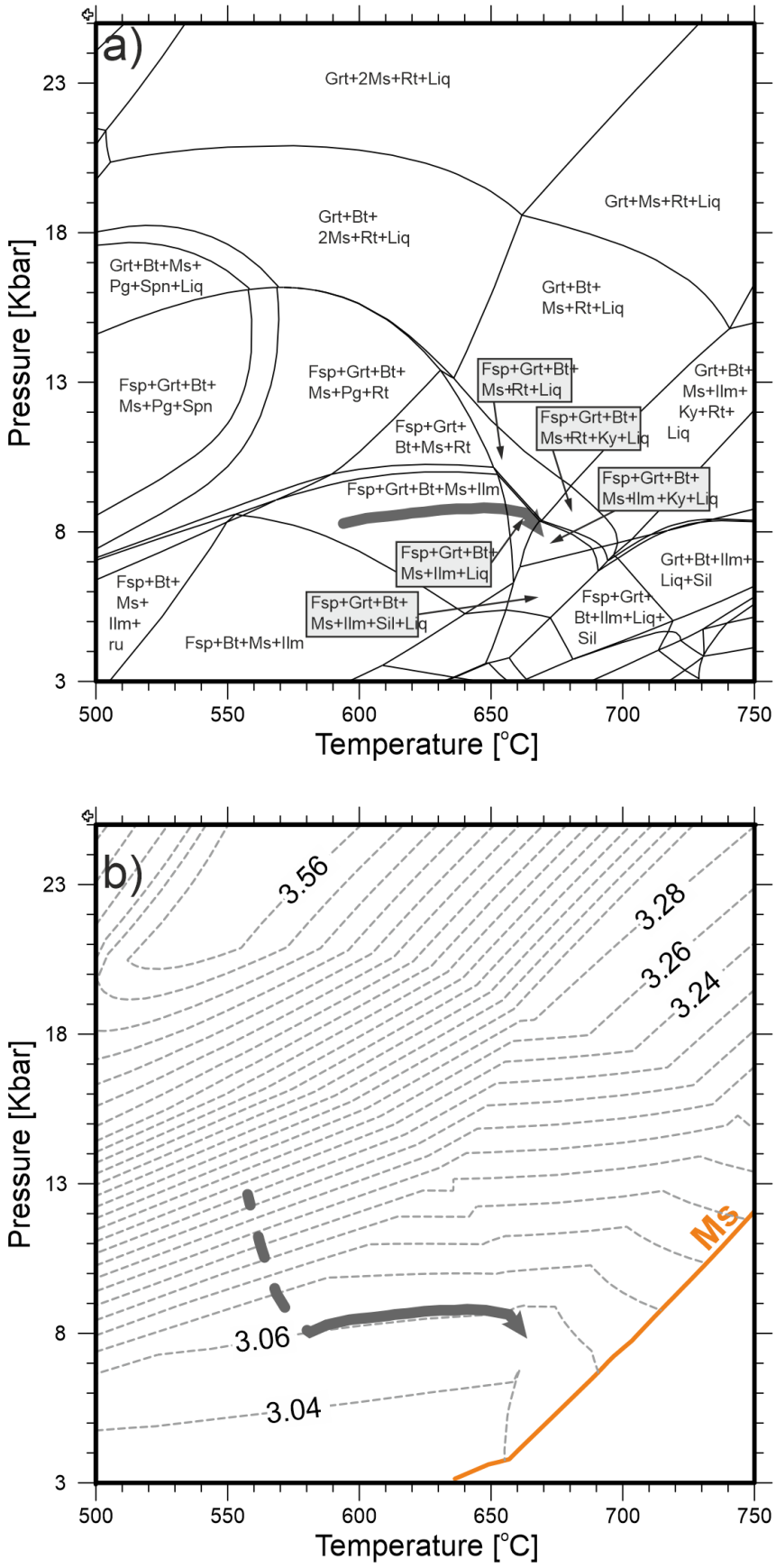

Fig. 35. Phase diagram modelling results for sample MD01-02 using the core composition of Grt and bulk rock composition; a. isochemical phase diagram, b. Compositional isopleths of Si in K- white mica. The stability field of white mica is additionally shown. Grey arrow on diagrams b and d is for the modelled P–T path.

Age of metamorphic events

Sample MD01-18 contained relatively large, up to 9 mm garnet crystals suitable for separate core and rim dating. Garnet cores, despite showing some scatter, define a decent quality, 345.3 ± 5.0 Ma Lu-Hf isochron (MSWD = 14) whereas garnet rims define only a rough age of 356± 40 Ma. The low precision of the latter age is associated with very low $^{176}Lu/^{177}Hf$ ratios (0.09-0.11) observed in garnet rims that are only slightly higher from the whole rock $^{176}Lu/^{177}Hf$ = 0.05. Additionally, we included all obtained data from core and rim into age calculations, which together with the whole rock define 346.9±3.6 Ma age (MSWD = 8.6). Similar to Lu-Hf analyses, Sm-Nd dating of garnet cores revealed excess scatter among the analysed fractions, which together with the whole rock define a poor quality age of 348 ± 17 Ma (MSWD = 55). Garnet rims together with the whole rock define 337.3 ± 6.6 Ma age (MSWD = 7.7).

Acknowledgements

We are grateful for the financial support provided by NCN research grants 2015/17/B/ST10/02212 (for JS, SI and RA) and 2018/29/B/ST10/01120 (for MJ). We would also like to thank Małgorzata Nowak for carefully reviewing the final version of the text.

References

Abati, J., Aghzer, A.M., Gerdes, A., Ennih, N., 2010. Detrital zircon ages of Neoproterozoic sequences of the Moroccan Anti-Atlas belt. Precambrian Research 181, 115–128. https://doi.org/10.1016/j.precamres.2010.05.018

Abdallah, N., Liégeois, J.-P., De Waele, B., Fezaa, N., Ouabadi, A., 2007. The Temaguessine Fe-cordierite orbicular granite (Central Hoggar, Algeria): U–Pb SHRIMP age, petrology, origin and geodynamical consequences for the late Pan-African magmatism of the Tuareg shield. Journal of African Earth Sciences 49, 153–178. https://doi.org/10.1016/j.jafrearsci.2007.08.005

Anderson, D.E., Buckley, G.R., 1973. Zoning in garnets?Diffusion models. Contr. Mineral. and Petrol. 40, 87–104. https://doi.org/10.1007/BF00378168

Armbruster, T., Bonazzi, P., Akasaka, M., Bermanec, V., Chopin, C., Gieré, R., Heuss-Assbichler, S., Liebscher, A., Menchetti, S., Pan, Y., Pasero, M., 2006. Recommended nomenclature of epidote-group minerals. European Journal of Mineralogy 18, 551–567. https://doi.org/10.1127/0935-1221/2006/0018-0551

Awdankiewicz, H., 2008. The petrology and geochemistryof the metabasites of the Niedzwiedz Massifin the Fore-Sudetic Block. Prace Państwowego Instytutu Geologicznego 189, 5–56.

Baltatzis, E., Katagas, C., 1981. Margarite pseudomorphs after kyanite in Glen Esk, Scotland. American Mineralogist 66, 213–216.

Bendaoud, A., Ouzegane, K., Godard, G., Liégeois, J.-P., Kienast, J.-R., Bruguier, O., Drareni, A., 2008. Geochronology and metamorphic P - T - X evolution of the Eburnean granulite-facies metapelites of Tidjenouine (Central Hoggar, Algeria): witness of the LATEA metacratonic evolution. Geological Society, London, Special Publications 297, 111–146. https://doi.org/10.1144/SP297.6

Bhatia, M.R., Crook, K.A.W., 1986. Trace element characteristics of graywackes and tectonic setting discrimination of sedimentary basins. Contributions to Mineralogy and Petrology 92, 181–193.

Bosch, D., Bruguier, O., Caby, R., Buscail, F., Hammor, D., 2016. Orogenic development of the Adrar des Iforas (Tuareg Shield, NE Mali): New geochemical and geochronological data and geodynamic implications. Journal of Geodynamics 96, 104–130. https://doi.org/10.1016/j.jog.2015.09.002

Buriánková, K., Hanžl, P., Mazur, S., Melichar, R., Leichmann, J., 1999. Geochemistry of the Doboszowice Orthogneisses and its Correlation with Rocks of the Silesicum and Moravicum. Geolines 8, 11.

Cao, W., Massonne, H.-J., Liang, X., 2021. Partial melting due to breakdown of phengite and amphibole in retrogressed eclogite of deep Precambrian crust: An example from the Algonquin terrane, western Grenville Province, Canada. Precambrian Research 352, 105965. https://doi.org/10.1016/j.precamres.2020.105965

Chatterjee, 1976. Margarite stability and compatibility relations in the system CaO-Al2O3-SiO2-H2O as a pressure-temperature indicator. American Mineralogist 61, 699–709.

Chopin, F., Schulmann, K., Skrzypek, E., Lehmann, J., Dujardin, J.R., Martelat, J.E., Lexa, O., Corsini, M., Edel, J.B., Štípská, P., Pitra, P., 2012. Crustal influx, indentation, ductile thinning and gravity redistribution in a continental wedge: Building a Moldanubian mantled gneiss dome with underthrust Saxothuringian material (European Variscan belt). Tectonics 31. https://doi.org/10.1029/2011TC002951

Collett, S., Schulmann, K., Deiller, P., Štípská, P., Peřestý, V., Ulrich, M., Jiang, Y., de Hoÿm de Marien, L., Míková, J., 2022. Reconstruction of the mid-Devonian HP-HT metamorphic event in the Bohemian Massif (European Variscan belt). Geoscience Frontiers 13, 101374. https://doi.org/10.1016/j.gsf.2022.101374

Collett, S., Štípská, P., Schulmann, K., Míková, J., Kröner, A., 2021. Tectonic significance of the Variscan suture between Brunovistulia and the Bohemian Massif. Journal of the Geological Society 178, jgs2020-176. https://doi.org/10.1144/jgs2020-176

Cullers, R.L., 2002. Implications of elemental concentrations for provenance, redox conditions, and metamorphic studies of shales and limestones near Pueblo, CO, USA. Chemical Geology 191, 305–327. https://doi.org/10.1016/S0009-2541(02)00133-X

Domeier, M., 2016. A plate tectonic scenario for the Iapetus and Rheic oceans. Gondwana Research 36, 275–295. https://doi.org/10.1016/j.gr.2015.08.003

Drost, K., Gerdes, A., Jeffries, T., Linnemann, U., Storey, C., 2011. Provenance of Neoproterozoic and early Paleozoic siliciclastic rocks of the Teplá-Barrandian unit (Bohemian Massif): Evidence from U–Pb detrital zircon ages. Gondwana Research 19, 213–231. https://doi.org/10.1016/j.gr.2010.05.003

Dziedzicowa, H., 1966. Seria łupków krystalicznych na wschód od strefy Niemczy w świetle nowych badań. The schists series east of the Niemcza Zone in the light of new investigations, (in Polish, English summary). Z geologii Ziem Zachod-nich 101–118.

Floyd, P.A., Winchester, J.A., Park, R.G., 1989. Geochemistry and tectonic setting of Lewisian clastic metasediments of the early Proterozoic Loch Maree Group of Gairloch, NW Scotland. Precambrian Res 45, 203–214.

Friedl, G., Finger, F., Paquette, J.-L., von Quadt, A., McNaughton, N.J., Fletcher, I.R., 2004. Pre-Variscan geological events in the Austrian part of the Bohemian Massif deduced from U-Pb zircon ages. International Journal of Earth Sciences 93, 802–823.

Gaucher, C., Finney, S., Poire, D., Valencia, V., Grove, M., Blanco, G., Pamoukaghlian, K., Peral, L., 2008. Detrital zircon ages of Neoproterozoic sedimentary successions in Uruguay and Argentina: Insights into the geological evolution of the Río de la Plata Craton. Precambrian Research 167, 150–170. https://doi.org/10.1016/j.precamres.2008.07.006

Geraldes, M.C., Nogueira, C., Vargas-Mattos, G., Matos, R., Teixeira, W., Valencia, V., Ruiz, J., 2014. U–Pb detrital zircon ages from the Aguapeí Group (Brazil): Implications for the geological evolution of the SW border of the Amazonian Craton. Precambrian Research 244, 306–316. https://doi.org/10.1016/j.precamres.2014.02.001

Gomez-Pugnaire, M.T., Visona, D., Franz, G., 1985. Kyanite, margarite and paragonite in pseudomorphs in amphibolitized eclogites from the Betic Cordilleras, Spain. Chemical Geology 50, 129–141. https://doi.org/10.1016/0009-2541(85)90116-0

Green, T., Hellmann, P., 1982. Fe-Mg partitioning between coexisting garnet and phengite at high pressure, and comments on a garnetphengite geothermometer. Lithos 15, 253–266.

Henry, B., Liégeois, J.P., Nouar, O., Derder, M.E.M., Bayou, B., Bruguier, O., Ouabadi, A., Belhai, D., Amenna, M., Hemmi, A., Ayache, M.,

2009. Repeated granitoid intrusions during the Neoproterozoic along the western boundary of the Saharan metacraton, Eastern Hoggar, Tuareg shield, Algeria: An AMS and U–Pb zircon age study. Tectonophysics 474, 417–434. https://doi.org/10.1016/j.tecto.2009.04.022

Hladil, J., Patocka, F., Kachlik, V., Melichar, R., Hubacik, M., 2003. Metamorphosed carbonates of Krkonose Mountains and Paleozoic evolution of Sudetic terranes (NE Bohemia, Czech Republic). GEOLOGICA CARPATHICA 54, 281–297.

Hynes, A., Forest, R.C., 1988. Empirical garnet-muscovite geothermometry in low-grade metapelites, Selwyn Range (Canadian Rockies). J Metamorph Geol 6, 297–309. https://doi.org/10.1111/j.1525-1314.1988.tb00422.x

Janoušek, V., Aichler, J., Hanžl, P., Gerdes, A., Erban, V., Žáček, V., Pecina, V., Pudilová, M., Hrdličková, K., Mixa, P., Žáčková, E., 2014. Constraining genesis and geotectonic setting of metavolcanic complexes: a multidisciplinary study of the Devonian Vrbno Group (Hrubý Jeseník Mts., Czech Republic). Int J Earth Sci (Geol Rundsch) 103, 455–483. https://doi.org/10.1007/s00531-013-0975-4

Jastrzębski, M., 2012. New insights into the polyphase evolution of the Variscan suture zone: evidence from the Staré Město Belt, NE Bohemian Massif. Geol. Mag. 149, 945–963. https://doi.org/10.1017/S0016756812000040

Jastrzębski, M., Budzyń, B., Stawikowski, W., 2017. Cambro-Ordovician vs Devono-Carboniferous geodynamic evolution of the Bohemian Massif: evidence from *P–T–t* studies in the Orlica–Śnieżnik Dome, SW Poland. Geological Magazine 156, 447–470. https://doi.org/10.1017/S0016756817000887

Jastrzębski, M., Machowiak, K., Krzemińska, E., Lang Farmer, G., Larionov, A.N., Murtezi, M., Majka, J., Sergeev, S., Ripley, E.M., Whitehouse, M., 2018. Geochronology, petrogenesis and geodynamic significance of the Visean igneous rocks in the Central Sudetes, northeastern Bohemian Massif. Lithos 316–317, 385–405. https://doi.org/10.1016/j.lithos.2018.07.034

Jastrzębski, M., Żelaźniewicz, A., Budzyń, B., Sláma, J., Konečny, P., 2020a. Age constraints on the Pre-Variscan and Variscan thermal events in the Kamieniec Ząbkowicki Metamorphic belt (the Fore-Sudetic Block, SW Poland). ASGP 90, 27–49. https://doi.org/10.14241/asgp.2020.05

Jastrzębski, M., Żelaźniewicz, A., Budzyń, B., Sláma, J., Konečny, P., 2020b. Age constraints on the Pre-Variscan and Variscan thermal events in the Kamieniec Ząbkowicki Metamorphic belt (the Fore-Sudetic Block, SW Poland). ASGP 90, 27–49. https://doi.org/10.14241/asgp.2020.05

Jastrzębski, M., Żelaźniewicz, A., Murtezi, M., Larionov, A.N., Sergeev, S., 2015. The Moldanubian Thrust Zone — A terrane boundary in the Central European Variscides refined based on lithostratigraphy and U–Pb zircon geochronology. Lithos 220–223, 116–132. https://doi.org/10.1016/j.lithos.2015.01.023

Jastrzębski, M., Żelaźniewicz, A., Stawikowski, W., Budzyń, B., Krzemińska, E., Machowiak, K., Madej, S., Białek, D., Sláma, J., Czupyt, Z., Jaźwa, A., 2023. The eastern part of the Saxothuringian Terrane characterized by zircon and monazite data from the Doboszowice Metamorphic Complex in the Sudetes (SW Poland). ASGP. https://doi.org/10.14241/asgp.2023.11

Jung, S., Masberg, P., Mihm, D., Hoernes, S., 2009. Partial melting of diverse crustal sources - Constraints from Sr-Nd-O isotope compositions of quartz diorite-granodiorite-leucogranite associations (Kaoko Belt, Namibia). Lithos 111, 236–251. https://doi.org/10.1016/j.lithos.2008.10.010

Kamzolkin, V.A., Ivanov, S.D., Konilov, A.N., 2016. Empirical phengite geobarometer: Background, calibration, and application. Geol. Ore Deposits 58, 613–622. https://doi.org/10.1134/S1075701516080092

Kohn, M.J., 2020. A refined zirconium-in-rutile thermometer. American Mineralogist 105, 963–971. https://doi.org/10.2138/AM-2020-7091/MACHINEREADABLECITATION/RIS

Kristoffersen, M., Andersen, T., Andresen, A., 2014. U–Pb age and Lu–Hf signatures of detrital zircon from Palaeozoic sandstones in the Oslo Rift, Norway. Geological Magazine 151, 816–829. https://doi.org/10.1017/S0016756813000885

Krogh, E.J., Raheim, A., 1978. Temperature and pressure dependence of Fe-Mg partitioning between garnet and phengite, with particular reference to eclogites. Contr. Mineral. and Petrol. 66, 75–80. https://doi.org/10.1007/BF00376087

Kröner, A., Hegner, E., 1998. Geochemistry, single zircon ages and Sm-Nd systematics of granitoid rocks from the Gory Sowie (Owl Mts), Polish west Sudetes: evidence for early Palaeozoic arc-related plutonism. J Geol Soc London 155, 711–724.

Kuznetsov, N.B., Meert, J.G., Romanyuk, T.V., 2014. Ages of detrital zircons (U/Pb, LA-ICP-MS) from the Latest Neoproterozoic–Middle Cambrian(?) Asha Group and Early Devonian Takaty Formation, the Southwestern Urals: A test of an Australia-Baltica connection within Rodinia. Precambrian Research 244, 288–305. https://doi.org/10.1016/j.precamres.2013.09.011

Mazur, S., Aleksandrowski, P., Kryza, R., Oberc-Dziedzic, T., 2006. The Variscan Orogen in Poland. GEOLOGICAL QUARTERLY 50, 89–118.

Mazur, S., Józefiak, D., 1999. Structural record of Variscan thrusting and subsequent extensional collapse in the mica schists from vicinities of Kamieniec Ząbkowicki, Sudetic foreland, SW Poland. Annales Societatis Geologorum Poloniae 69, 1–26.

Mazur, S., Kröner, A., Szczepański, J., Turniak, K., Hanžl, P., Melichar, R., Rodionov, N.V., Paderin, I., Sergeev, S.A., 2010. Single zircon U/Pb ages and geochemistry of granitoid gneisses from SW Poland: evidence for an Avalonian affinity of the Brunian microcontinent. Geol Mag 147, 508–526.

Mazur, S., Szczepański, J., Turniak, K., McNaughton, N.J., 2012. Location of the Rheic suture in the eastern Bohemian Massif: evidence from detrital zircon data. Terra Nova 24, 199–206. https://doi.org/10.1111/j.1365-3121.2011.01053.x

Mazur, S., Turniak, K., Szczepański, J., McNaughton, N.J., 2015. Vestiges of Saxothuringian crust in the Central Sudetes, Bohemian Massif: Zircon evidence of a recycled subducted slab provenance. Gondwana Research 27, 825–839. https://doi.org/10.1016/j.gr.2013.11.005

McLennan, S.M., Hemming, S., McDaniel, D.K., Hanson, G.N., 1993. Geochemical approaches to sedimentation, provenance, and tectonics. Special Paper - Geological Society of America 284, 21–40.

Meinhold, G., Morton, A.C., Fanning, C.M., Frei, D., Howard, J.P., Phillips, R.J., Strogen, D., Whitham, A.G., 2011. Evidence from detrital zircons for recycling of Mesoproterozoic and Neoproterozoic crust recorded in Paleozoic and Mesozoic sandstones of southern Libya. Earth and Planetary Science Letters 312, 164–175. https://doi.org/10.1016/j.epsl.2011.09.056

Moynihan, D.P., Pattison, D.R.M., 2013. An automated method for the calculation of *P-T* paths from garnet zoning, with application to metapelitic schist from the Kootenay Arc, British Columbia, Canada. Journal of Metamorphic Geology 31, 525–548. https://doi.org/10.1111/jmg.12032

Oberc-Dziedzic, T., Klimas, K., Kryza, R., Fanning, C., 2003. SHRIMP U-Pb zircon geochronology of the Strzelin gneiss, SW Poland: Evidence for a neoproterozoic thermal event in the Fore-Sudetic Block, Central European Variscides. INTERNATIONAL JOURNAL OF EARTH SCIENCES 92, 701–711.

Oberc-Dziedzic, T., Kryza, R., Madej, S., Pin, C., 2018. The Saxothuringian Terrane affinity of the metamorphic Stachów Complex (Strzelin Massif, Fore-Sudetic Block, Poland) inferred from zircon ages. Geological Quarterly 62. https://doi.org/10.7306/gq.1405

Oliver, G., Corfu, F., Krogh, T., 1993. U-Pb ages from SW Poland - evidence for a Caledonian suture zone between Baltica and Gondwana. J Geol Soc London 150, 355–369.

Orozbaev, R., Hirajima, T., Bakirov, Apas, Takasu, A., Maki, K., Yoshida, K., Sakiev, K., Bakirov, Azamat, Hirata, T., Tagiri, M., Togonbaeva, A., 2015. Trace element characteristics of clinozoisite pseudomorphs after lawsonite in talc-garnet-chloritoid schists from the Makbal UHP Complex, northern Kyrgyz Tian-Shan. Lithos 226, 98–115. https://doi.org/10.1016/j.lithos.2014.10.008

Pankhurst, R.J., Hervé, F., Fanning, C.M., Calderón, M., Niemeyer, H., Griem-Klee, S., Soto, F., 2016. The pre-Mesozoic rocks of northern Chile: U–Pb ages, and Hf and O isotopes. Earth-Science Reviews 152, 88–105. https://doi.org/10.1016/j.earscirev.2015.11.009

Parry, M., Štípská, P., Schulmann, K., Hrouda, F., Ježek, J., Kröner, A., 1997. Tonalite sill emplacement at an oblique plate boundary: northeastern margin of the Bohemian Massif. Tectonophysics 280, 61–81.

Peucat, J.J., Drareni, A., Latouche, L., Deloule, E., Vidal, P., 2003. U–Pb zircon (TIMS and SIMS) and Sm–Nd whole-rock geochronology of the Gour Oumelalen granulitic basement, Hoggar massif, Tuareg shield, Algeria. Journal of African Earth Sciences 37, 229–239. https://doi.org/10.1016/j.jafrearsci.2003.03.001

Pietranik, A., Majka, J., 2017. The Wilkow syenite – the unique remnant of the 380-360 Ma magmatic event at the Gondwana north-eastern margin. Mineralogia - Special Papers 47, 37.

Pietranik, A., Storey, C., Kierczak, J., 2013. The Niemcza diorites and moznodiorites (Sudetes, SW Poland): a record of changing geotectonic setting at ca. 340 Ma. Geological Quarterly 57. https://doi.org/10.7306/gq.1084

Puziewicz, J., Koepke, J., 2001. Partial melting of garnet-hornblende granofels and the crystallisation of igneous epidote in the Niedźwiedź Amphibolite Massif (Fore-Sudetic Block, SW Poland). Neues Jahrbuch für Mineralogie, Monatshefte 12, 529–547.

R Core Team, 2012. R: A language and environment for statistical computing. R Foundation for Statistical Computing.

Schulmann, K., Konopásek, J., Janousek, V., Lexa, O., Lardeaux, J.-M., Edel, J.-B., Stípská, P., Ulrich, S., 2009. An Andean type Palaeozoic convergence in the Bohemian Massif. Comptes Rendus Geosciences 341, 266–286.

Skacel, J., 1989. Crossing of the Lugian boundary fault with Nyznerov dislocation belt between Vapenna and Javornik in Silesia. Acta Universitatis Palackianae Olomucensis 95, 31–45.

Skrzypek, E., Lehmann, J., Szczepański, J., Anczkiewicz, R., Štípská, P., Schulmann, K., Kröner, A., Bia\lek, D., 2014. Time-scale of deformation and intertectonic phases revealed by P–T–D–t relationships in the orogenic middle crust of the Orlica-Śnieżnik Dome, Polish/Czech Central Sudetes. Journal of Metamorphic Geology 32, 981–1003.

Śliwiński, M., Jastrzębski, M., Sláma, J., 2022. Detrital zircon analysis of metasedimentary rocks of the Staré Mìsto Belt, Sudetes: implications for the provenance and evolution of the eastern margin of the Saxothuringian terrane, NE Bohemian Massif. Geological Quarterly 66, 1–21.

Spear, F.S., 1993. Metamorphic Phase Equilibria and Pressure-Temperature-Time Paths. Mineralogical Society of America 779.

Steltenpohl, M.G., Cymerman, Z., Krogh, E.J., Kunk, M.J., 1993. Exhumation of eclogitized continental basement during Variscan lithospheric delamination and gravitational collapse, Sudety Mountains, Poland. Geology 21, 1111–1114.

Štípska, P., Schulmann, K., Kröner, A., 2004. Vertical extrusion and middle crustal spreading of omphacite granulite: a model of syn-convergent exhumation (Bohemian Massif, Czech Republic). Journal of Metamorphic Geology 22, 179–198.

Szczepański, J., 2007. A vestige of an Early Devonian active continental margin in the East Sudetes (SW Poland) - evidence from geochemistry of the Jegłowa Beds, Strzelin Massif. Geological Quarterly 51, 271–284.

Szczepański, J, Anczkiewicz, R., Marciniak, D., 2022. P-T conditions and chronology of the Variscan collision in the easternmost part of the Saxothuringian crust. Mineralogia – Special Papers 50, 88.

Szczepański, J., Goleń, M., 2022. Tracing exhumation record in high-pressure micaschists: A new tectonometamorphic model of the evolution of the eastern part of the Fore Sudetic Block, Kamieniec Metamorphic Belt, NE Bohemian Massif, SW Poland. Geochemistry 82, 125859. https://doi.org/10.1016/j.chemer.2021.125859

Szczepański, J., Kaszuba, G., Anczkiewicz, R., Ilnicki, S., 2023a. Provenance of the early Palaeozoic volcano-sedimentary successions from eastern part of the Central Sudetes: implications for the tectonic evolution of the NE Bohemian Massif. Geol. Mag. 160, 1498–1534. https://doi.org/10.1017/S0016756823000523

Szczepański, J., Kaszuba, G., Anczkiewicz, R., Ilnicki, S., 2023b. Provenance of the early Palaeozoic volcano-sedimentary successions from eastern part of the Central Sudetes: implications for

the tectonic evolution of the NE Bohemian Massif. Geological Magazine 1–37. https://doi.org/10.1017/S0016756823000523

Szczepański, J., Turniak, K., Anczkiewicz, R., Gleichner, P., 2020. Dating of detrital zircons and tracing the provenance of quartzites from the Bystrzyckie Mts: implications for the tectonic setting of the Early Palaeozoic sedimentary basin developed on the Gondwana margin. Int J Earth Sci (Geol Rundsch). https://doi.org/10.1007/s00531-020-01888-8

Szczepański, Jacek, Zhong, X., Dąbrowski, M., Wang, H., Goleń, M., 2022a. Combined phase diagram modelling and quartz-in-garnet barometry of *HP* metapelites from the Kamieniec Metamorphic Belt (NE Bohemian Massif). Journal Metamorphic Geology 40, 3–37. https://doi.org/10.1111/jmg.12608

Szczepański, Jacek, Zhong, X., Dąbrowski, M., Wang, H., Goleń, M., 2022b. Combined phase diagram modelling and quartz-in-garnet barometry of *HP* metapelites from the Kamieniec Metamorphic Belt (NE Bohemian Massif). Journal of Metamorphic Geology jmg.12608. https://doi.org/10.1111/jmg.12608

Tabaud, A.S., Štípská, P., Mazur, S., Schulmann, K., Míková, J., Wong, J., Sun, M., 2021. Evolution of a Cambro-Ordovician active margin in northern Gondwana: Geochemical and zircon geochronological evidence from the Góry Sowie metasedimentary rocks, Poland. Gondwana Research 90, 1–26. https://doi.org/10.1016/j.gr.2020.10.011

Taylor, S.R., McLennan, S.M., 1985. The Continental Crust: Its Composition and Evolution; An Examination of the Geochemical Record Preserved in Sedimentary Rocks. Blackwell Science Publications, Oxford.

Torsvik, T.H., 2017. Earth history and palaeogeography: Trond H. Torsvik, University of Oslo, and L. Robin M. Cocks, The Natural History Museum, London.

Tsujimori, T., Ernst, W.G., 2014. Lawsonite blueschists and lawsonite eclogites as proxies for palaeo-subduction zone processes: a review. Journal of Metamorphic Geology 32, 437–454. https://doi.org/10.1111/JMG.12057Valley, J.W., 2003. Oxygen Isotopes in Zircon. Reviews in Mineralogy and Geochemistry 53, 343–385. https://doi.org/10.2113/0530343

Valverde-Vaquero, P., Dörr, W., Belka, Z., Franke, W., Wiszniewska, J., Schastok, J., 2000. U–Pb single-grain dating of detrital zircon in the Cambrian of central Poland: implications for Gondwana versus Baltica provenance studies. Earth and Planetary Science Letters 184, 225–240. https://doi.org/10.1016/S0012-821X(00)00312-5

Verma, S.P., Armstrong-Altrin, J.S., 2013. New multi-dimensional diagrams for tectonic discrimination of siliciclastic sediments and their application to Precambrian basins. Chemical Geology 355, 117–133. https://doi.org/10.1016/j.chemgeo.2013.07.014

Winchester, J.A., Floyd, P.A., 1977. Geochemical discrimination of different magma series and their differentiation products using immobile elements. Chemical Geology 20, 325–343. https://doi.org/10.1016/0009-2541(77)90057-2

Wu, C.-M., Chen, H.-X., 2015. Calibration of a Ti-in-muscovite geothermometer for ilmenite- and Al2SiO5-bearing metapelites. Lithos 212–215, 122–127. https://doi.org/10.1016/j.lithos.2014.11.008

Žáčková, E., Konopásek, J., Košler, J., Jeřábek, P., 2010. Detrital zircon populations in quartzites of the Krkonoše–Jizera Massif: implications for pre-collisional history of the Saxothuringian Domain in the Bohemian Massif. Geological Magazine 149, 443–458. https://doi.org/10.1017/S0016756811000744

Žák, J., Sláma, J., 2018. How far did the Cadomian ‘terranes’ travel from Gondwana during early Palaeozoic? A critical reappraisal based on detrital zircon geochronology. International Geology Review 60, 319–338. https://doi.org/10.1080/00206814.2017.1334599

Zeng, L., Zhang, L., Yue, J., Li, X., 2019. Ultrahigh-pressure and high-P lawsonite eclogites in Muzhaerte, Chinese western Tianshan. Journal of Metamorphic Geology 37, 717–743. https://doi.org/10.1111/JMG.12482

DOI: http://dx.doi.org/10.7306/CETEG2024-2

Post – Conference excursion guide

Late- to post-Variscan structural evolution of tectonic grabens on top of the Góry Sowie Massif

Aleksander Kowalski[1]

[1]Polish Geological Institute-National Research Institute, aleksander.kowalski@pgi.gov.pl

The area situated at the NE margin of the Bohemian Massif (BM), located between the Middle Odra Fault in the NE and the Upper Elbe Fault Zone in the SW (Fig. 1), and traditionally referred to as the Sudetes (e.g. Aleksandrowski et al., 1999; Don and Żelaźniewicz, 1990; Kryza et al., 2004; Mazur et al., 2006), exposes a mosaic of fault-bounded, multiply deformed, Variscan crystalline basement units covered by unmetamorphosed rocks of lower Carboniferous (Mississipian) to Upper Cretaceous age. In the Sudetes these sedimentary-volcanic successions are preserved within large-scale synclinorial structures as well as smaller, but still kilometre-scale grabens (Don and Żelaźniewicz, 1990; Głuszyński and Aleksandrowski, 2022; Solecki, 1994). These features are usually downthrown or downfolded into the Variscan crystalline basement. Apart from the two main synclinorial structures located in the Sudetes – the Intra-Sudetic and the North-Sudetic synclinoria (Augustyniak and Grocholski, 1968; Dziedzic and Teisseyre, 1990; Nemec et al., 1982; Solecki, 1994), the late Paleozoic sedimentary successions occur locally on top of the crystalline Variscan basement. Remnants of once much more widespread Carboniferous sedimentary succession are preserved on top of the Góry Sowie Massif (GSM) – a high- to medium-grade metamorphic unit, situated in the Central Sudetes (Cymerman, 1998; Grocholski, 1967; Żelaźniewicz, 1987). The GSM is a triangular-shaped, fault-bounded unit (Fig. 1) composed of migmatitic paragneissess, with subordinate orthogneiss, metabasite and felsic granulite bodies (Grocholski, 1967; Gunia, 1999; Jastrzębski et al., 2021; Tabaud et al., 2021; Żelaźniewicz, 1990, 1987). The paragneisses of the GSM originated probably from flysch-like graywackes as well as pelitic sediments of middle to early Cambrian age (Gunia, 1999; Tabaud et al., 2021; Żelaźniewicz, 1987), whilst magmatic protolith of orthogneiss is dated at the late Cambrian to Early Ordovician (Kröner and Hegner 1998; Kryza and Fanning 2007). The rock protolith of gneisses was metamorphosed under amphibolite facies conditions at c. 380-370 Ma (Van Breemen et al., 1988), whereas felsic granulite and peridotite bodies had undergone earlier (at c. 400 Ma; Brueckner et al., 1996; O'Brien et al., 1997), ultra high pressure–high temperature (UHP–HT) granulite facies metamorphism.

Metamorphic processes had ceased in the Late Devonian (Cymerman, 1998; Jastrzębski et al., 2021; Żelaźniewicz, 1987) and were followed by rapid exhumation of the massif at the end of the Devonian (Bröcker et al., 1998; Żelaźniewicz, 1987).

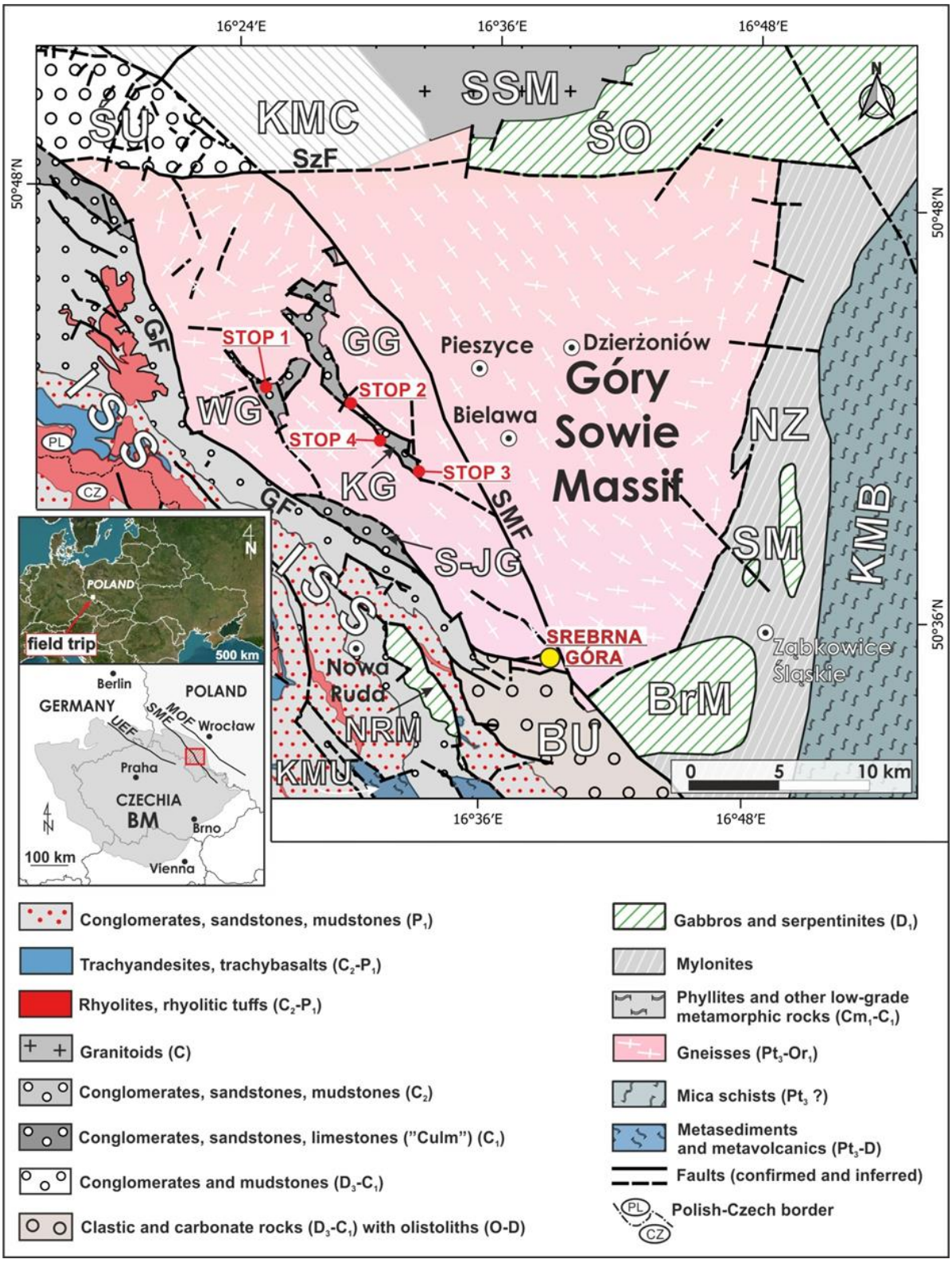

Fig. 1. Tectonic sketch map of the Góry Sowie Massif and surrounding tectonic units (compiled after Sawicki, 1995 and based on author's own data), together with their location in the Bohemian Massif and Central Europe (inset). Abbreviations: BrM – Braszowice Ophiolite Massif, BU – Bardo Unit, GG – Glinno Graben, ISS – Intra-Sudetic Synclinorium, KG – Kamionki Graben, KMB — Kamieniec Metamorphic Belt, KMC – Kaczawa Metamorphic Complex, KMU – Kłodzko Metamorphic Unit, NRM – Nowa Ruda Ophiolite Massif, NZ – Niemcza Shear Zone, S-JG – Sokolec-Jugów Graben, SM – Szklary Ophiolite Massif, SSM – Strzegom-Sobótka Granitoid Massif, ŚO – Ślęża Ophiolite Massif, ŚU – Świebodzice Unit, WG – Walim Graben. Faults: GF – Głuszyca Fault, SMF – Sudetic Marginal Fault, SzF – Szczawienko Fault.

The Góry Sowie Massif is currently interpreted as an allochtonous terrane assigned jointly to the Teplá-Barrandian/Bohemian microplate, located close to the northern peripheries of Gondwana during Cambrian–Ordovician (Catalán et al., 2021; Franke and Żelaźniewicz, 2023; Jastrzębski et al., 2021; Tabaud et al., 2021).

The metamorphic unit of the GSM is dissected by NW-SE and NE-SW striking fault zones (Fig. 1; Grocholski 1967; Żelaźniewicz 1987; Cymerman 2004). The most prominent of these is the NW-SE-trending Sudetic Marginal Fault which separates the elevated, southwestern part of the massif (Sowie Mts Block), from its northeastern, downthrown part situated on the Fore-Sudetic Block. To the NW the GSM borders - across the Szczawienko Fault - with the Świebodzice Unit (in the older literature also called the Świebodzice Depression or Świebodzice Synclinorium; Teisseyre 1956; Nemec et al. 1980; Porębski 1981; Porębski 1990) which contains up to 4 km thick succession of strongly deformed and folded, coarse clastic and minor carbonate syn- to late orogenic Upper Devonian (?)–lower Carboniferous sediments. The late orogenic clastic Carboniferous deposits of the Intra-Sudetic Synclinorium as well as the syn- to late orogenic, Devonian(?)–lower Carboniferous sedimentary rocks of the Bardo Unit occur to the west and south of the Góry Sowie Massif, respectively. These units are also bordered by and separated from the GSM by regional-size fault zones (Fig. 1).

Remnants of the Mississipian sedimentary succession resting on top of the GSM are known only from the uplifted Sowie Mts Block located to the southwest of the Sudetic Marginal Fault (Fig. 1). This succession, historically referred to as the "*Culm of the Sowie Mountains*" (Łapot, 1988, 1986; Oberc, 1972; Żakowa and Żak, 1962), is preserved within a number of small, mainly NW-SE trending, fault-bounded grabens and half-grabens. These tectonic units include: the Walim, Glinno, Kamionki and Sokolec-Jugów grabens. Although the remnants of the GSM's sedimentary cover preserved within these grabens have been addressed in several, mainly paleontological and petrographic studies (Łapot, 1986, 1988; Muszer, 2014; Muszer et al., 2016a; Żakowa, 1960, 1966a; Żakowa and Żak, 1962), their structural characteristics have received little attention. The main goal of the post-conference field trip is to discuss the structural evolution of these intriguing tectonic features, which probably represent erosional relics of an originally broader late-Variscan basin system. The field trip stops are located within the Walim (WG; Stop 1), Glinno (GG; Stop 2) and Kamionki grabens (KG; Stops 3,4; Fig. 1).

The Carboniferous sedimentary succession of the Sowie Mountains – lithology and stratigraphy

The Carboniferous strata preserved within the tectonic grabens of the GSM include middle Viséan(?) to Namurian(?) continental and marine deposits (Fig. 2) (Muszer et al., 2016a, 2016b; Żakowa, 1960, 1966a; Żakowa and Żak, 1962). These deposits can be considered as stratigraphic equivalents of the adjacent tectonic units, i.e. the Intra-Sudetic Synclinorium (Dziedzic and Teisseyre, 1990; Mastalerz, 1995; Teisseyre, 1975); the Świebodzice Depression (Nemec et al., 1980; Porębski, 1990, 1981) and the Bardo Structure (Haydukiewicz, 1990; Wajsprych, 1978), and occur within isolated, narrow tectonic grabens or half-grabens (Oberc, 1972).

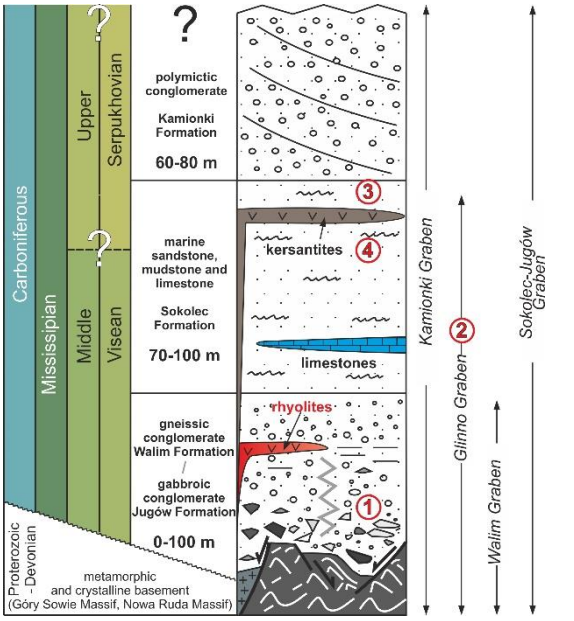

Fig. 2. Simplified scheme showing stratigraphy, lithology, extent and thickness of the sedimentary succession in the tectonic grabens developed on top of the Góry Sowie Massif.

The Carboniferous sedimentary succession of the GSM attains 300 metres in thickness and has been subdivided lithologically into three informal lithostratigraphic members (Łapot, 1986; Żakowa, 1966a; Żakowa and Żak, 1962). The succession begins with poorly sorted, ”gneissic” and “gabbroic” conglomerates and sedimentary breccias (Fig. 3) that overlie the GSM metamorphic basement. The name Walim Formation is proposed here for these deposits which are exposed locally over the GSM. The conglomerates are interpreted by the present author as deposits of alluvial fans developed along tectonically active, high-relief margins of a wider intramontane (?) basin. The conglomerates pass upward (and possibly laterally) into marine sandstones and mudstones, up to 100 m thick. Based on findings of macrofauna, these deposits were primarily dated at the late Viséan (Żakowa, 1960; Żakowa and Żak, 1962) whereas Muszer et al. (2016) suggest that they may represent Namurian(?). The marine sandstones and mudstones were previously informally assigned to the Sokolec Beds (Żakowa, 1966b) and currently are referred here to as the Sokolec Formation. The uppermost member of the Carboniferous succession in the GSM consists of a ca. 80 m-thick, Namurian(?) polymictic conglomerate, well exposed in the central and northern sectors of the Kamionki Graben (Żakowa and Żak 1962) and within the Sokolec-Jugów Graben (not described here). The conglomerate, assigned by the present author to the Kamionki Formation, is interpreted as deposit of fan deltas which entered the early Carboniferous basin from the north and north-west.

Fig. 3. Poorly sorted conglomerates of the Walim Formation composed of gneissic and migmatite pebbles and boulders; outcrop near the “Dino” market in Walim (GPS coordinates: 50° 42' 15.64" N, 16° 26' 20.96" E).

Walim Graben

The Walim Graben (WG) constitutes a distinct, irregularly-shaped, fault-bounded tectonic feature, ca. 3 km long and up to 1,3 km wide, which trends from NNW to SSE, mainly along the Walimka stream valley (Fig. 4). The basement and shoulders of the graben are built of Góry Sowie metamorphic rocks, mainly gneisses (biotite gneisses, migmatites and migmatite gneisses; Grocholski, 1965). The boundary fault zones of the graben, referred to as the Western- and Eastern Walim Faults (the WWF and EWF, respectively; Fig. 4), separate the sedimentary fill of the graben from its crystalline-rock shoulders.

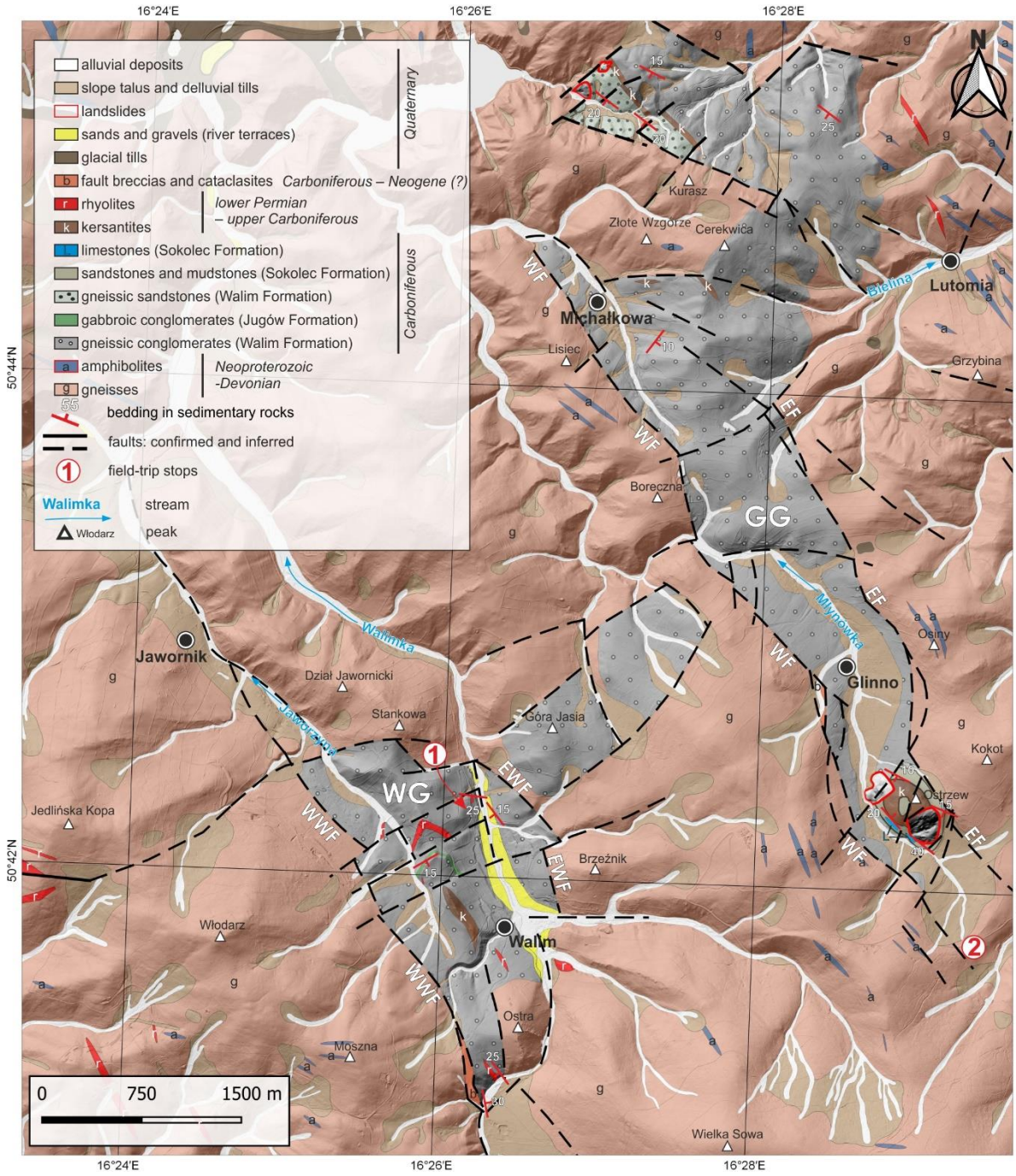

Fig. 4. Geological map of the Walim and Glinno Grabens (for location see Figure 1) showing location of field trip stops. Basement geology simplified from Grocholski (1962); geology of sedimentary rocks based on author's own maps. Extent of Quaternary deposits drawn by Joanna Brytan (PGI-NRI). Abbreviations: GG – Glinno Graben, EF – Eastern Glinno Fault, EWF – Eastern Walim Fault, WWF – Western Walim Fault, WF – Western Glinno Fault, WG – Walim Graben.

The vertical and (possible) horizontal displacement components associated with certain faults cannot be unambiguously determined due to a lack of borehole data. The southernmost part of the WG is a narrow, NNW-SSE trending, fault-bounded block filled with gneissic conglomerates of the Walim Formation and separated to the west from the gneissic basement horst by a cataclasite zone, up to 600 m long and ca. 80 m wide (Fig. 4). In the southernmost part of the graben occurs a narrow dyke of (upper Carboniferous(?)) rhyolitoid, oriented parallel to the graben's margins. The central sector of the graben also exposes gneissic conglomerates and is cut by transverse, WSW-ENE trending faults which do not display significant throws. The gneissic conglomerates dip at 15–25° towards the S and SW (Fig. 4) and interfinger with gabbroic conglomerates of the Jugów Formation (Fig. 4). The entire sedimentary succession of the WG is cut by upper Carboniferous(?) rhyolite and kersantite dykes and sills. Toward the NNW the Walim Graben narrows to a width of ca. 800 m. In the northernmost segment of the graben, its boundary faults probably converge and are buried under the Quaternary alluvial deposits of the Jaworzyna stream valley.

To the northeast of the Walim, the Eastern Walim Fault separates the main graben from an unnamed, smaller NE-SW half-graben structure covered by a thin carpet of gneissic conglomerates.

Glinno Graben

The Glinno Graben (GG) is another example of a tectonic graben with asymmetric, irregular structure, c. 7.5 km long and up to 1.5 km wide (Fig. 4). It extends from the head of the Bojanicka Woda stream in the north, through the vicinity of the village of Michałkowa, to the head of the Młynówka stream south of Glinno (Fig. 5).

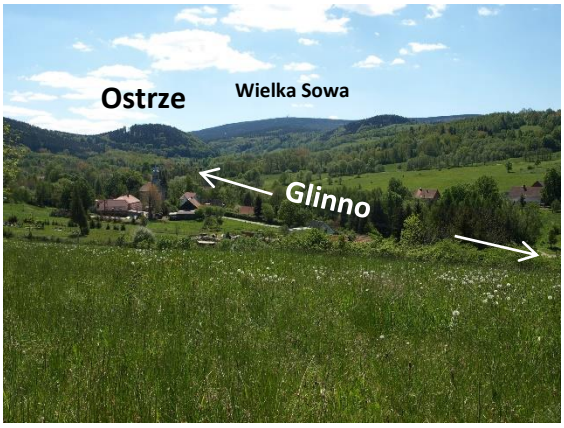

Fig. 5. Morphological depression related to the Glinno Graben. View from the north. Ostrzew hill (713 m a.s.l.) rises ca. 150 m above the flat bottom of the graben interior filled with gneissic conglomerates of the Walim Formation. The hill is built of sandstones and mudstones of the Sokolec Fromation intruded by kersantite sill (cf. Fig. 4). Wielka Sowa (1015 m a.s.l.) – the highest top of the Góry Sowie Mountains built of gneisses of the GSM is in the background.

The GG consists of at least three distinct, tectonic subunits. In the the northernmost part of the graben, a WNW-ESE trending half-graben structure exposes gneissic conglomerates and sandstones of the Walim Formation. The strata are poorly exposed, dip gently at 15 to 20° to the SW (Fig. 4) and are cut by narrow, WNW-ESE-trending lamprophyre dykes. To the east of the Bojanicka Woda stream head, the half-graben described is bounded by a NNE-SSW-oriented, fault-bounded gneissic block covered by gneissic conglomerates that rest directly on the metamorphic basement of the Góry Sowie Massif. To the S and SW, the block merges with the main body of the GG, bounded by nearly-parallel, NW-SE-trending faults, here named as the Western and Eastern Glinno faults (WF and EF, respectively) and exposes only gneissic conglomerates. The mappable faults have a total trace length of ca. 6.5 km (WF) and 4 km (EF), respectively. The southernmost part of the GG contains a morphological elevation built of

sandstones and mudstones (Sokolec Formation), which together form a distinct, residual outlier (Ostrzew hill; 551 m a.s.l.), elevatad ca. 150 m above the flat bottom of the graben interior (see description of Stop 3). Ostrzew hill is well visible from the Stop 2 of our field trip. The southern boundary of the Glinno Graben is defined by the NE-SW trending unnamed fault which is covered in the stream head of Młynówka by delluvial sediments. The main boundary faults of the GG continue to the SE into the Western and Eastern Kamionki Faults, respectively (Fig. 1).

Kamionki Graben

On the map, the Kamionki Graben (KG) constitutes a narrow, triangular-shaped, fault-bounded tectonic feature, ca. 4 km long and up to 500 m wide, which trend SE to NW to the west from the Kamionka stream valley. The graben structure coincides with the morphological depression in the Góry Sowie Mountains (Fig. 6).

The graben is formed on crystalline basement of Góry Sowie (partly migmatic paragneisses with minor serpentinite and amphibolite bodies; Gawroński, 1961; Grocholski, 1967; Fig. 7). The boundary fault zones of the graben, referred to here as the Western- and Eastern Kamionki and Pniaki faults (the WF, EF and PF respectively; Fig. 7), separate the sedimentary fill of the graben from its crystalline-rock shoulders. All these fault zones are manifested by distinct rectilinear escarpments and arrays of water springs and peat bogs. The fault zones extend laterally into the metamorphic basement of the GSM (Fig. 7).

The vertical and possibly horizontal displacement components related to particular faults cannot be unambiguously determined from the mapping data. The position of the basal Carboniferous unconformity, intersected by hydrogeological boreholes at 110 and 143 m below the surface, does not allow for an unequivocal determination of the vertical displacement component of the graben's floor on the boundary faults (Fig. 7).

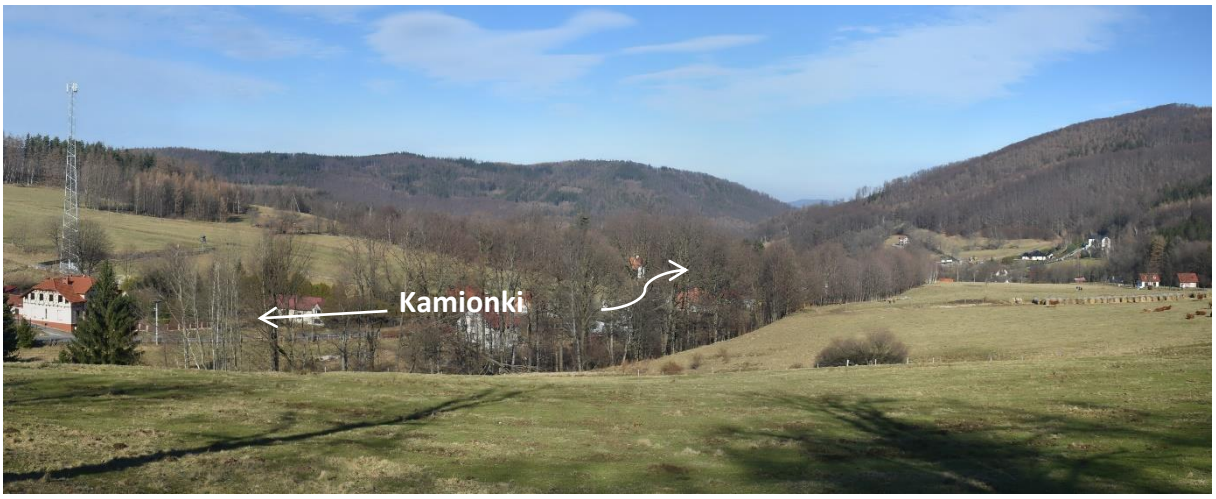

Fig. 6. Morphological depression related to the Kamionki Graben. View from the south. Kamionki village and the valley of the Kamionka stream are visible. Several outcrops of Carboniferous strata are located along the stream (Stop 3).

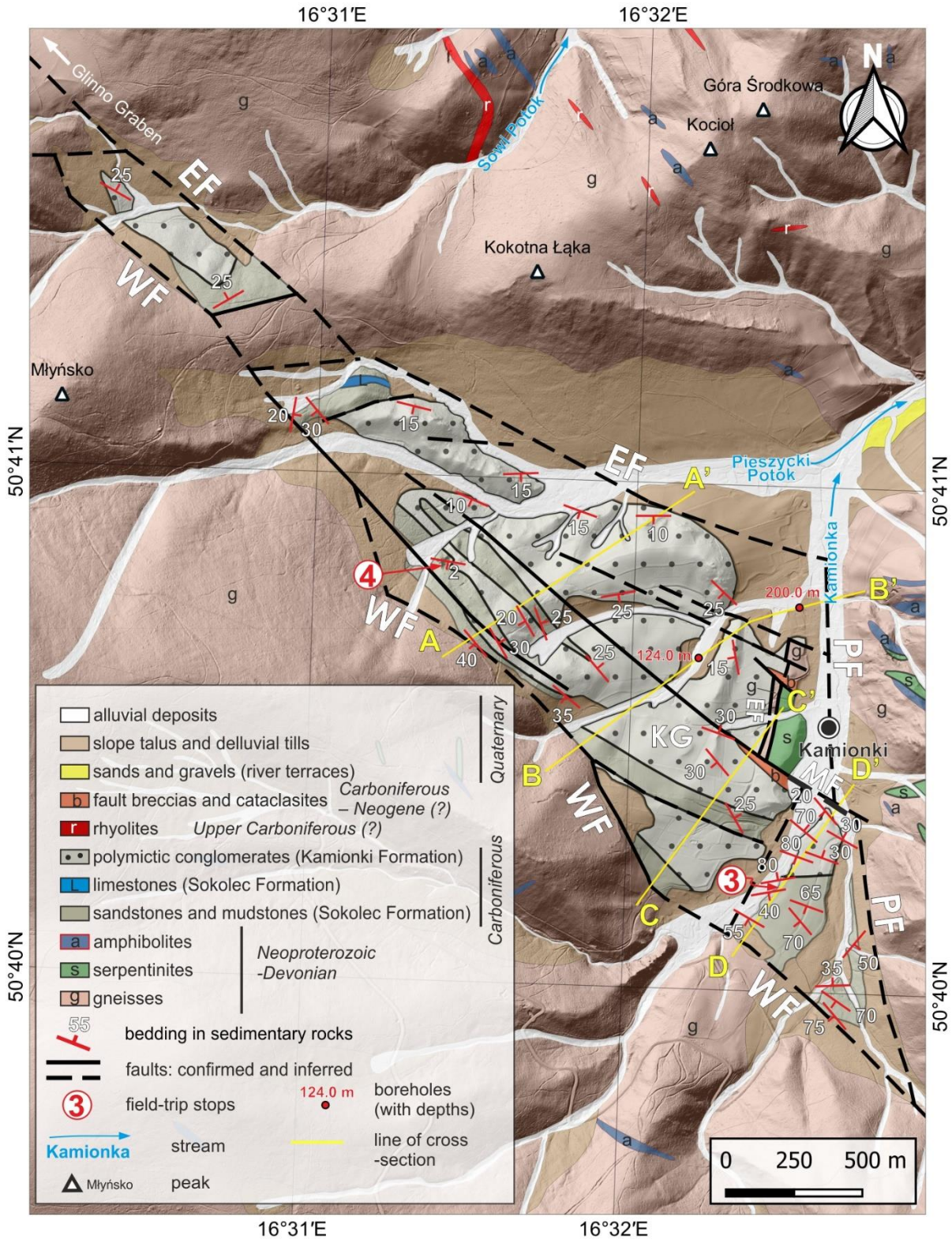

Fig. 7. Geological map of the Kamionki Graben (for location see Figure 1). Locations of geological cross-sections presented in Figure 8 (AA', BB', CC' and DD'). Cross-section C-C' was performed among others based on interpreted, SRT-P and ERT geophysical profiles (Kowalski and Pacanowski, 2024). Note the location of field trip stops referred to in the text and of two boreholes. Basement geology simplified from Gawroński (1961), geology of sedimentary rocks based on author's own geological mapping. Abbreviations: KG – Kamionki Graben, EF – Eastern Kamionki Fault, PF – Pniaki Fault, WF – Western Kamionki Fault.

The geological map and cross sections of the Kamionki Graben (Figs. 7 and 8) show the WNW-ESE trending faults which divide the graben's fill into several blocks. The north-westernmost part of the KG represents a single narrow NW-SE trending block (the Młyńsko Graben of Oberc, 1972) filled with Carboniferous sandstones and conglomerates and separated from the main graben body by a basement horst occuring between the WSW-ENE striking boundary faults of the graben. The northern part of the graben is characterised by the occurrence of Namurian(?) polymict conglomerates exposed along the Eastern Kamionki Fault and dipping at 15–25° towards the S and SW (Fig. 7). The structure of this part of the KG is well constrained due to exposure of the conglomerates as small-scale tors. Towards the east, the strike of the bedding within the conglomarates changes from E-W to nearly N-S. In this portion of the graben, the Pniaki Fault is oriented approximately N-S and buried under the Kamionka stream valley alluvial deposits (Fig. 7). The western part of the graben exposes NW-SE trending mappable folds with sandstones exposing anticline hinges (Figs 7,8).

In general, the limbs of these nearly symmetric folds dip moderately ca. 25–40° towards the NE and SW with their axes plunging gently to the NW and SE. The map-scale folds, oriented parallel to the structural trend of the graben, are cut by faults trending parallel or sub-parallel to the fold axes. The lowermost fill member of the KG, the gneissic conglomerate of the Walim Formation, is nowhere exposed at the surface in the KG and has not been intersected by hydrogeological boreholes made in the central part of the graben. However, the gneissic conglomerates most probably occur at the bottom of the downfaulted, northernmost part of the graben (Fig. 8, A–A' cross section). On the other hand, these conglomerates are well exposed within the Glinno Graben, located ca. 2 km towards the NW of the KG (Figs 1, 4; Żakowa 1960; Oberc 1972). The middle segment of the KG is dismembered by the NW-SE trending Middle Kamionki Fault (MF). The fault shows up to 50 m of throw gradually decreasing towards the NW, and it divides the overall graben structure into two smaller domains, the southern of almost nearly rhomboidal shape and the northern triangular one. Geological mapping revealed the existence of distinct cataclasite zones up to 50 m wide, aligned along the southern and northern sectors of the fault zone (Figs 7,8), between sedimentary rocks and their metamorphic basement. These zones consist of fault gouges and breccias composed of angular fragments of gneiss. To the NE of the Middle Kamionki Fault, the graben is cut by two, relatively minor, NW-SE trending discontinuities (Figs. 7, 8). Towards the SE the KG narrows to ca. 50 m in width and exposes Viséan sandstones, which are folded and probably thrusted over the crystalline basement (cross-section DD', Fig. 8). At the southernmost end of the graben, the Western Kamionki and the Pniaki faults converge to form a single, NNW-SSE striking fault.

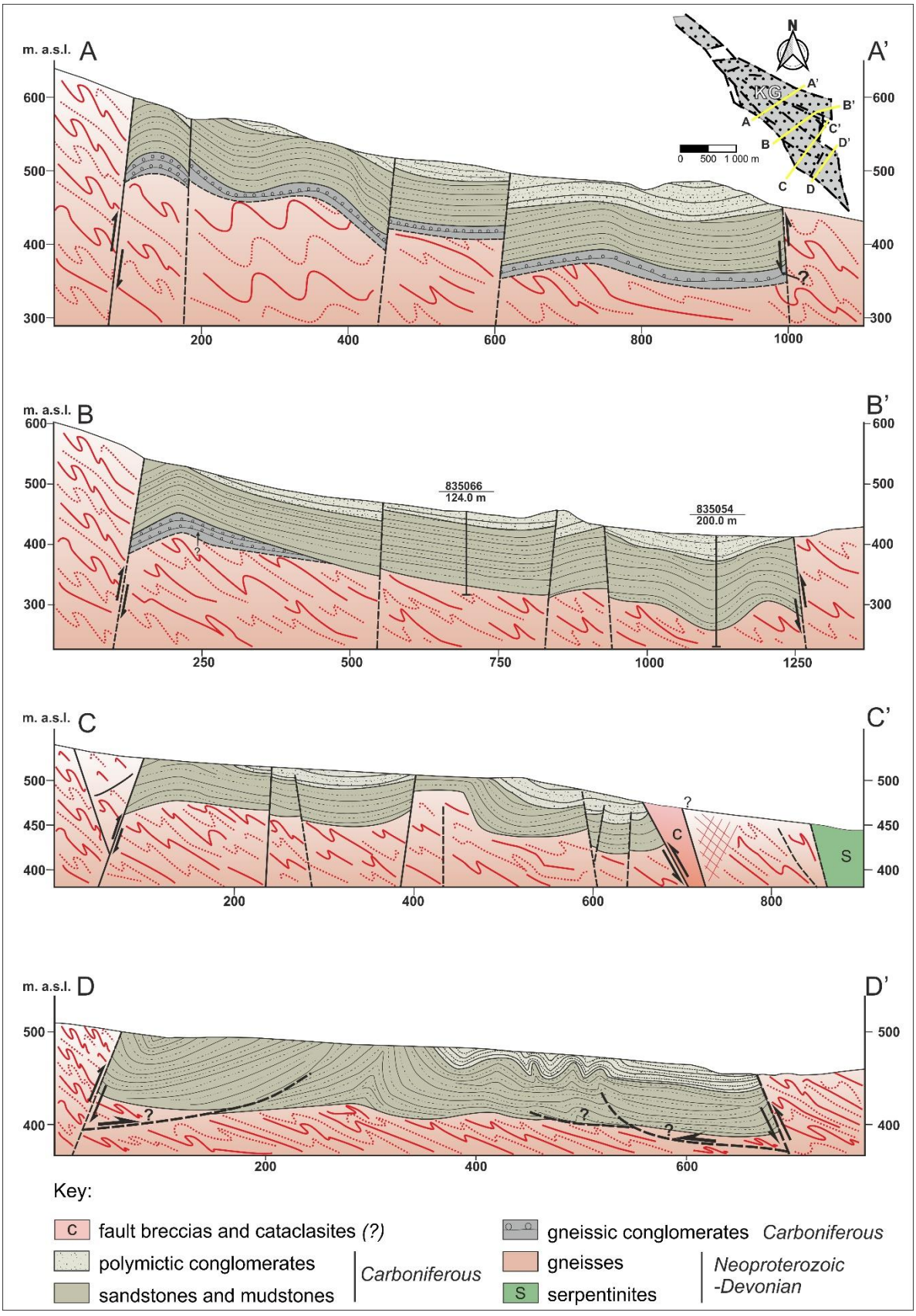

Fig. 8. Geological sections across the Kamionki Graben based on mapping field traverses, borehole data and geophysical profiles (C-C' cross-section based on: Kowalski and Pacanowski, 2024). See inset map in the upper right corner and Figure 7 for location of each of the cross-section.

Structural evolution of tectonic grabens on top of the Góry Sowie Massif – an example of the Kamionki Graben

Due to the very limited number of outcrops, sparse fault-slip data and the lack of a clear Meso-Cenozoic geological record in the uplifted area of the Góry Sowie Block, a precise reconstruction of its structural evolution faces considerable difficulties. Nevertheless, the evolution of tectonic grabens developed on top of the GSM can be roughly reconstructed, using the criteria of the superposition and relationships between the ductile and brittle tectonic deformation structures preserved in the sedimentary and metamorphic rocks of the KG area. Palaeostress data from adjacent geological units exposing younger, slightly deformed lower Permian to Upper Cretaceous strata, may also be useful in this task. Based on the results of geological mapping, structural analysis and geophysical survey (Kowalski, Pacanowski, 2024), the interpretation proposed here assumes a relatively complex, polyphase (at least four-stage) development of the Kamionki Graben area, began in the Carboniferous and lasted until the late Cenozoic.

The Carboniferous succession of the Góry Sowie Massif was folded (and, locally, also probably thrusted over the gneissic basement) into the WNW-ESE to W-E and, less frequently, NW-SE oriented folds at the end of the Mississipian (Namurian (?)) epoch. The fold axes (Figs 9, 10) are nearly perpendicular to the direction of the interpreted NNE-SSW to N-S horizontal compression at the NE forelands of the Bohemian Massif during the end-Variscan orogeny (Mazur et al., 2020). Meso-scale folds affecting the Carboniferous strata of the KG will be presented at Stop 3 of this field trip. The fold structures of similar geometry are widespread in the Carboniferous strata deposited in the system of late-orogenic, collision-related, foreland- and intra-montane basins that developed at the NE and E margins of the Bohemian Massif (e.g. Hartley and Otava 2001; Bábek et al. 2004; Narkiewicz 2007; Mazur et al. 2010; Narkiewicz 2020). The meso-scale folds attributed to this regional shortening event are the most common structures in the southernmost portion of the Kamionki Graben between its boundary faults. The average shortening (P) axis orientation obtained from dextral faults (referred to as the I fault population; Fig. 9) in the Kamionki Graben reflects similar, overall NNE-SSW to NE-SW compression direction (Fig. 9). Therefore, it cannot not be excluded that the transpression generated by the strike-slip dextral (?) displacements may have played an active role in the folding process.

The formation of the Kamionki Graben included displacements along NNW-SSE to NW-SE striking high-angle faults (Fig. 10). They have occurred over a long period between the Namurian (Late Mississipian) and Neogene, starting someone between the late Carboniferous and early Permian. The development of the graben must have occurred only slightly after the folding of the Carboniferous succession and is correlated by the author with a significant, late Carboniferous–early Permian regional uplift and erosion, associated with the gravitational collapse of the newly formed Variscan orogen (e.g. Mazur et al. 2006). Various parts of the GSM were then progressively exhumed and supplied gneissic detritus to the surrounding sedimentary basins, e.g. the Intra-Sudetic (Mastalerz, 1996), the Świebodzice (Nemec et al., 1980; Porębski, 1981) and the Bardo (Wajsprych, 1978) basins.

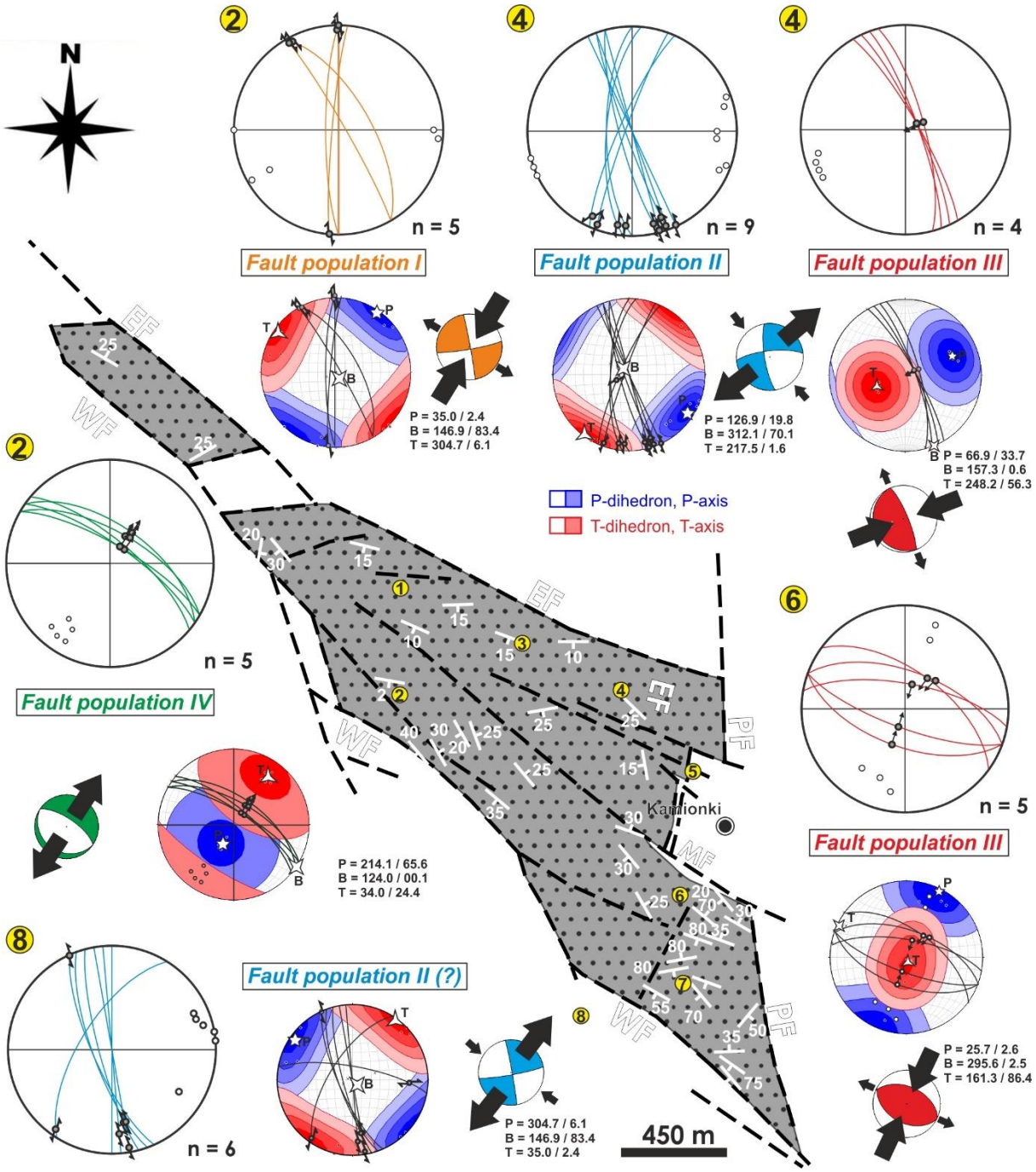

Fig. 9. Kinematic data collected on minor faults and interpretation of the principal axes of finite strain ellipsoids calculated using PBT method – moment tensor analysis for the four homogenous fault systems (populations) I–IV distinguished in the Kamionki Graben. The collected fault planes orientations are presented on the great circle diagrams with marked poles. Striae on fault planes are presented as dots with arrows indicating the sense of displacement of the hanging wall block. The inset "beachball plots" obtained from moment tensor analysis show shortening (P) and extension (T) quadrants.

On the other hand, Aramowicz et al. (2006), postulated, on the basis of apatite fission-track dating (AFT), that the shoulders of the Kamionki Graben, together with the entire Góry Sowie Block, were probably partly covered by Carboniferous and Permian sediments during the late Carboniferous and Permian times. These results suggest a significant episode of burial under a thick cover of Paleozoic clastic sediments.

Based on the above, the author interprets the NNW-SSE to NNE-SSW striking, strike-slip (mainly sinistral) faults of the population II (Fig. 9) as the result of NE-SW to WNW-ESE regional extension (transtension) in the late-Carboniferous–early Permian times (Fig. 10). These faults must have been reactivated during the latest, successive tectonic events affecting the Carboniferous succession preserved on top of the Góry Sowie Massif (Fig. 10). Sinistral movement along the nearby Intra-Sudetic (Głuszyca) Fault, striking parallel to the Kamionki Graben, between the late Carboniferous and early Permian has been postulated by Aleksandrowski et al. (1997). The inferred, late Carboniferous–early Permian extensional stage correlates (was coincidental?) with the widespread subsidence event associated with the initial stages of development of the Polish Basin (Krzywiec et al., 2022). The formation of kersantite and rhyolite dykes with a predominant NW-SE to NNW-SSE orientation, which are exposed in the Góry Sowie Massif area (Awdankiewicz, 2007; Grocholski, 1967), as well as the emplacement of volcanic and sub-volcanic bodies in the adjacent Intra-Sudetic Basin (Awdankiewicz, 2022, 1999), appear to be genetically linked to this evolutionary stage.

The Late Cretaceous–Paleogene uplift of the Góry Sowie Massif along the Sudetic Marginal- and Głuszyca faults to the NE and SW, respectively, must have resulted in a subsequent erosion of the mountainous part of the massif (Fig. 10). The uplift was due to the Late Cretaceous–Palaeogene, regional, NE-SW-oriented tectonic compression and the concomitant inversion, which affected the western and central European Alpine foreland (Głuszyński and Aleksandrowski, 2022; Kley and Voigt, 2008; Mazur et al., 2005; Rosenbaum et al., 2002; Voigt et al., 2021). An average orientation of shortening (P) axis calculated from fault population III (Fig. 9) corresponds to the regionally reported paleostress and regional-tectonic data documenting this Late Cretaceous–early Cenozoic deformation of the NE fringe of the Bohemian Massif (Coubal et al., 2015; Głuszyński and Aleksandrowski, 2022; Kowalski, 2021; Novakova, 2015; Pešková et al., 2010; Sobczyk and Szczygieł, 2021). Relatively uniform, NE-SW to ENE-WSW oriented compressional stress regime is interpreted as a result of far-field effects of the Europe-Iberia-Africa plate convergence at ca. 86–70 Ma (Kley and Voigt, 2008; Rosenbaum et al., 2002). A broad range of similarly oriented, inversion structures (both brittle and ductile) related to this deformation event is commonly observed throughout Central Europe in the foreland of the Alpine-Carpathian deformation front (Głuszyński and Aleksandrowski, 2022; Kley and Voigt, 2008; Kozdrój and Cymerman, 2003; Krzywiec et al., 2022, 2018; Mazur et al., 2005; Voigt et al., 2021). These structures include low- to high-angle reverse and normal faults, thrusts delimiting basement highs, inverted basins and grabens, as well as marginal troughs (Voigt et al., 2021). The total amount of denudation of the Góry Sowie massif, linked with this tectonic event is estimated at 4–8 km (Aramowicz et al., 2006) and

at least 4 km for the adjacent Intra-Sudetic Basin (Botor et al., 2019). Based on the apatite fission track (AFT) data and thermal modelling results, Danišik et al. (2012) argued that the reverse faults and low-angle thrusts were active in the Sudetic region between 85-70 Ma.

Normal faults of the population IV (Figs 9, 10), oriented nearly parallel to the graben's elongation are likely associated with the most recent stage of the brittle deformation linked to the NE-SW-oriented extensional regime. These faults are parallel to the strike lines of the NW-SE oriented faults that displace sedimentary rocks within the KG. This stress orientation can be correlated with the youngest brittle deformations revealed by fault-slip data and recorded in the vicinity of the Sudetic Marginal Fault (Krzyszkowski and Olejnik, 1998; Krzyszkowski and Pijet, 1993; Migoń et al., 2023; Różycka et al., 2021). A sub-recent neotectonic transformation of the pre-existing faults cannot be excluded in the study area. Neotectonic, extensional fault reactivation may have influenced the formation of the present-day valley network, especially of the Kamionka river valley. The rectilinear course of this valley may be explained by the fault activity.

Another important issue is origin of the systematic joints in the studied sedimentary rocks. The WNW-ESE to NW-SE and NE-SW trending joint sets, similar to those from the grabens on top of the GSM, were also observed within the Permo-Mesozoic rocks exposed in the nearby Intra-Sudetic and North-Sudetic synclinoria (Jerzykiewicz, 1968; Solecki, 1994). Although these latter joint sets are interpreted as Late Cretaceous–early Palaeogene in age (Głuszyński and Aleksandrowski, 2022; Jerzykiewicz, 1968; Solecki, 2011), it cannot be excluded that in the study area the initiation and development of the joint pattern was linked with stress field that had occurred during the waning stages of the Variscan orogeny. Such late Variscan joints were eventually rotated during successive phases of brittle and ductile deformations. Due to limited number of outcrops in the Kamionki Graben area this issue requires systematic research in the future, also in the areas of adjacent tectonic units composed mainly of strongly folded Carboniferous sedimentary strata (i.e. the Świebodzice Depression and the Bardo Structure; cf. Oberc 1972; Wajsprych, 1978; Porębski 1990).

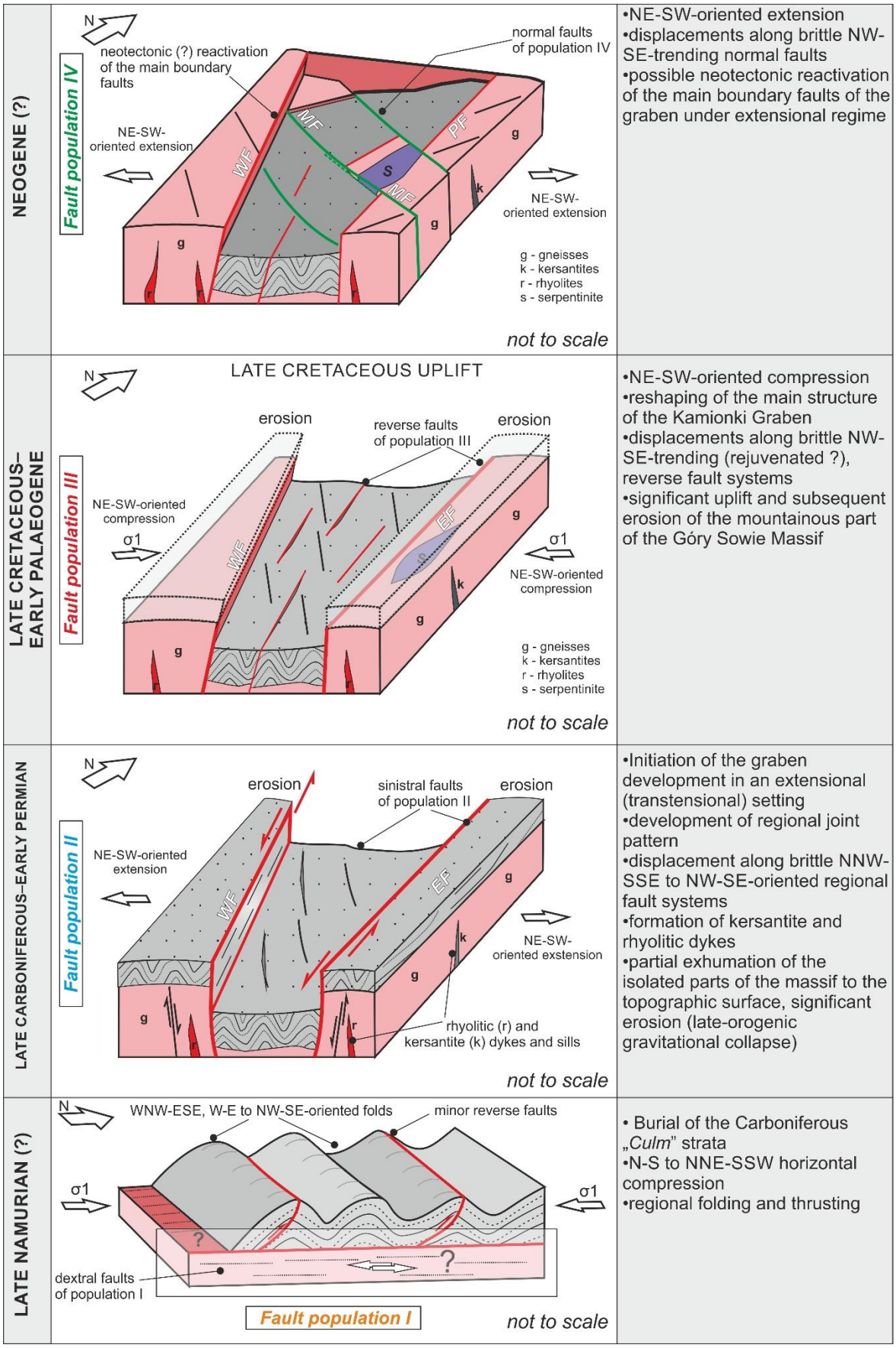

Fig. 10. Schematic model showing evolution of the Kamionki Graben. For further explanations see the text.

References

Aleksandrowski, P., Kryza, R., Mazur, S., Pin, C., Zalasiewicz, J.A., 1999. The Polish Sudetes: Caledonian or Variscan? Transactions of the Royal Society of Edinburgh: Earth Sciences 90, 127–146. https://doi.org/10.1017/S0263593300007197

Aleksandrowski, P., Kryza, R., Mazur, S., Żaba, J., 1997. Kinematic data on major Variscan strike-slip faults and shear zones in the Polish Sudetes, northeast Bohemian Massif. Geological Magazine 133, 727–739.

Aramowicz, A., Anczkiewicz, A., Mazur, S., 2006. Fission-track dating of apatite from the Góry Sowie Massif, Polish Sudetes, NE Bohemian Massif: Implications of post-Variscan denudation and uplift. Neues Jahrbuch für Mineralogie - Abhandlungen 182, 221–229. https://doi.org/10.1127/0077-7757/2006/0046

Augustyniak, K., Grocholski, A., 1968. Geological structure and outline of the development of the Intra-Sudetic depression. Biuletyn Instytutu Geologicznego XVII, 87–111.

Awdankiewicz, M., 2022. Polyphase Permo-Carboniferous magmatism adjacent to the Intra-Sudetic Fault: constraints from U–Pb SHRIMP zircon study of felsic subvolcanic intrusions in the Intra-Sudetic Basin, SW Poland. International Journal of Earth Sciences 111, 2199–2224. https://doi.org/10.1007/s00531-022-02232-y

Awdankiewicz, M., 2007. Late Palaeozoic lamprophyres and associated mafic subvolcanic rocks of the Sudetes (SW Poland): petrology, geochemistry and petrogenesis. Geologia Sudetica 39, 11–97.

Awdankiewicz, M., 1999. Volcanism in a late Variscan intramontane trough: Carboniferous and Permian volcanic centres of the Intra-Sudetic Basin, SW Poland. Geologia Sudetica 32, 13–47.

Bábek, O., Mikuláš, R., Zapletal, J., Lehotskỳ, T., 2004. Combined tectonic-sediment supply-driven cycles in a Lower Carboniferous deep-marine foreland basin, Moravice Formation, Czech Republic. International Journal of Earth Sciences 93, 241–261.

Botor, D., Anczkiewicz, A.A., Mazur, S., Siwecki, T., 2019. Post-Variscan thermal history of the Intra-Sudetic Basin (Sudetes, Bohemian Massif) based on apatite fission track analysis. International Journal of Earth Sciences 108, 2561–2576. https://doi.org/10.1007/s00531-019-01777-9

Bröcker, M., Żelaźniewicz, A., Enders, M., 1998. Rb–Sr and U–Pb geochronology of migmatitic gneisses from the Góry Sowie (West Sudetes, Poland): the importance of Mid–Late Devonian metamorphism. Journal of the Geological Society 155, 1025–1036. https://doi.org/10.1144/gsjgs.155.6.1025

Brueckner, H., Blusztajn, J., Bakun-Czubarow, N., 1996. Trace element and Sm–Nd 'age'zoning in garnets from peridotites of the Caledonian and Variscan Mountains and tectonic implications. Journal of Metamorphic Geology 14, 61–73. https://doi.org/10.1111/j.1525-1314.1996.00061.x

Catalán, J.R.M., Schulmann, K., Ghienne, J.-F., 2021. The Mid-Variscan Allochthon: Keys from correlation, partial retrodeformation and plate-tectonic reconstruction to unlock the geometry of a non-cylindrical belt. Earth-Science Reviews 220, 103700. https://doi.org/10.1016/j.earscirev.2021.103700

Coubal, M., Málek, J., Adamovič, J., Štěpančíková, P., 2015. Late Cretaceous and Cenozoic dynamics of the Bohemian Massif inferred from the paleostress history of the Lusatian Fault Belt. Journal of Geodynamics 87, 26–49. https://doi.org/10.1016/j.jog.2015.02.006

Cymerman, Z., 2004. Tectonic map of the Sudetes and the Fore-Sudetic Block.

Cymerman, Z., 1998. The Góry Sowie Terrane: a key to understanding the Palaeozoic evolution of the Sudetes area and beyond. Geological Quarterly 42, 379–400.

Danisik, M., Štěpančíková, P., Evans, N., 2012. Constraining long-term denudation and faulting history in intraplate regions by multisystem thermochronology: An example of the Sudetic Marginal Fault (Bohemian Massif, central Europe). Tectonics 31, 2003. https://doi.org/10.1029/2011TC003012

Don, J., Żelaźniewicz, A., 1990. The Sudetes - boundaries, subdivision and tectonic position. Neues Jahrbuch für Geologie und Paläontologie 179, 121–127.

Dziedzic, K., Teisseyre, A.K., 1990. The Hercynian molasse and younger deposits in the Intra-Sudetic Depression, SW Poland. Neues Jahrbuch für Geologie und Paläontologie 179, 285–305.

Franke, W., Żelaźniewicz, A., 2023. Variscan evolution of the Bohemian Massif (Central Europe): Fiction, facts and problems. Gondwana Research 124, 351–377. https://doi.org/10.1016/j.gr.2023.06.012

Gawroński, O., 1961. Szczegółowa Mapa Geologiczna Sudetów. Arkusz Pieszyce.

Głuszyński, A., Aleksandrowski, P., 2022. Late Cretaceous–Early Palaeogene inversion-related tectonic structures at the NE margin of the Bohemian Massif (SW Poland and northern Czechia). Solid Earth Discussions 1–39.

Grocholski, W., 1967. Structure of the Sowie Mts. (in Polish with English summary). Geologia Sudetica 3, 181–249.

Grocholski, W., 1965. Objaśnienia do Szczegółowej Mapy Geologicznej Sudetów. Arkusz Walim 1:25 000 (in Polish). Wydawnictwa Geologiczne Warszawa.

Grocholski, W., 1962. Szczegółowa Mapa Geologiczna Sudetów Arkusz Walim 1:25 000 (in Polish). Wydawnictwa Geologiczne Warszawa.

Gunia, T., 1999. Microfossils from the high-grade metamorphic rocks in the Góry Sowie Mts. (Sudetes area) and their stratigraphical importance. Geological Quarterly 43, 519–536.

Hartley, A.J., Otava, J., 2001. Sediment provenance and dispersal in a deep marine foreland basin: the Lower Carboniferous Culm Basin, Czech Republic. Journal of the Geological Society 158, 137–150.

Haydukiewicz, J., 1990. Stratigraphy of Paleozoic rocks of the Góry Bardzkie and some remarks on their sedimentation (Poland). Neues Jahrbuch für Geologie und Paläontologie 179, 275–284.

Jastrzębski, M., Budzyń, B., Żelaźniewicz, A., Konečnỳ, P., Sláma, J., Kozub-Budzyń, G.A., Skrzypek, E., Jaźwa, A., 2021. Eo-Variscan metamorphism in the Bohemian Massif: Thermodynamic modelling and monazite geochronology of gneisses and granulites of the Góry Sowie Massif, SW Poland. Journal of Metamorphic Geology 39, 751–779. https://doi.org/DOI: 10.1111/jmg.12589

Jerzykiewicz, T., 1968. Remarks on the origin and orientation of joints in the Upper Cretaceous rocks of the Intrasudetic Basin. Geologia Sudetica 4, 465–478.

Kley, J., Voigt, T., 2008. Late Cretaceous intraplate thrusting in central Europe: Effect of Africa-Iberia-Europe convergence, not Alpine collision. Geology 36, 839–842. https://doi.org/doi: 10.1130/G24930A.1

Kowalski, A., 2021. Multistage structural evolution of the end-Cretaceous–Cenozoic Wleń Graben (the Sudetes, NE Bohemian Massif) – a contribution to the post-Variscan tectonic history of SW Poland. Annales Societatis Geologorum Poloniae 37–66. https://doi.org/doi: https://doi.org/10.14241/asgp.2020.21

Kowalski, A., Pacanowski, G., 2024. Record of superimposed late- and post-Variscan regional-scale tectonic events at the NE margin of the Bohemian Massif: structural evolution of the Kamionki Graben (SW Poland, Sudetes). In: 20th CETEG Meeting, Srebrna Góra, 24-27.04.2024.

Kozdrój, W., Cymerman, Z., 2003. Alpine tectonic inversion–principal mechanism of the Variscan basement uplift and exhumation in the Sudety Mts. Geolines 16, 59–60.

Kröner, A., Hegner, E., 1998. Geochemistry, single zircon ages and Sm–Nd systematics of granitoid rocks from the Góry Sowie (Owl Mts), Polish West Sudetes: evidence for early arc-related plutonism. Journal of the Geological Society 155, 711–724. https://doi.org/doi.org/10.1144/gsjgs.155.4.0711

Kryza, R., Fanning, C.M., 2007. Devonian deep-crustal metamorphism and exhumation in the Variscan Orogen: evidence from

SHRIMP zircon ages from the HT-HP granulites and migmatites of the Góry Sowie (Polish Sudetes). Geodinamica Acta 20, 159–175. https://doi.org/doi.org/10.3166/ga.20.159-175

Kryza, R., Mazur, S., Oberc-Dziedzic, T., 2004. The Sudetic geological mosaic: Insights into the root of the Variscan orogen. Przegląd Geologiczny 52, 761–773.

Krzyszkowski, D., Olejnik, W., 1998. The Quaternary evolution of landscape and neotectonics of the Sowie Mts range, Sudeten, Southwestern Poland. Geologia Sudetica 31, 221–239.

Krzyszkowski, D., Pijet, E., 1993. Morphological effects of Pleistocene fault activity in the Sowie Mts., southwestern Poland. Zeitschrift für Geomorphologie, N. F., Suppl.-Bd.,94, 243-259. 94, 243–259.

Krzywiec, P., Kufrasa, M., Poprawa, P., Mazur, S., Koperska, M., Ślemp, P., 2022. Together but separate: decoupled Variscan (late Carboniferous) and Alpine (Late Cretaceous–Paleogene) inversion tectonics in NW Poland. Solid Earth 13, 639–658. https://doi.org/10.5194/se-13-639-2022

Krzywiec, P., Stachowska, A., Stypa, A., 2018. The only way is up–on Mesozoic uplifts and basin inversion events in SE Poland. Geological Society, London, Special Publications 469, 33–57. https://doi.org/10.1144/SP469.14

Łapot, W., 1988. Petrography of the Sowie Mts. Kulm. Bulletin of the Polish Academy of Sciences. Earth Sciences 36, 183–195.

Łapot, W., 1986. Petrography of Carboniferous rocks from the Sowie Mts (Sudetes) (in Polish with English summary). Geologia Sudetica 21, 1–144.

Mastalerz, K., 1996. Fluvial sedimentation of the coal-bearing Žacleř Formation (Westphalian) in the Wałbrzych Basin, SW Poland (in Polish with English summary). Prace Geologiczno-Mineralogiczne, Z badań karbonu i permu w Sudetach LII, 21–85.

Mastalerz, K., 1995. Deposits of high-density turbidity currents on fan-delta slopes: an example from the upper Visean Szczawno formation, Intrasudetic Basin, Poland. Sedimentary Geology 98, 121–146. https://doi.org/10.1016/0037-0738(95)00030-C

Mazur, S., Aleksandrowski, P., Kryza, R., Oberc-Dziedzic, T., 2006. The Variscan Orogen in Poland. Geological Quarterly 50, 89–118.

Mazur, S., Aleksandrowski, P., Turniak, K., Krzemiński, L., Mastalerz, K., Górecka-Nowak, A., Kurowski, L., Krzywiec, P., Żelaźniewicz, A., Fanning, M., 2010. Uplift and late orogenic deformation of the Central European Variscan belt as revealed by sediment provenance and structural record in the Carboniferous foreland basin of western Poland. International Journal of Earth Sciences 99, 47–64.

Mazur, S., Paweł, A., Gągała, Ł., Krzywiec, P., Żaba, J., Gaidzik, K., Sikora, R., 2020. Late Palaeozoic strike-slip tectonics versus oroclinal bending at the SW outskirts of Baltica: case of the Variscan belt's eastern end in Poland. International Journal of Earth Sciences 109. https://doi.org/10.1007/s00531-019-01814-7

Mazur, S., Scheck-Wenderoth, M., Krzywiec, P., 2005. Different modes of the Late Cretaceous–Early Tertiary inversion in the North German and Polish basins. International Journal of Earth Sciences 94, 782–798. https://doi.org/10.1007/s00531-005-0016-z

Migoń, P., Latocha-Wites, A., Jancewicz, K., 2023. Geomorphology of the Sowie Mountains (Sudetes, SW Poland) – landform patterns and anthropogenic impact 96, 103–129. https://doi.org/10.7163/GPol.0248

Muszer, J., 2014. A new species of Lambdarina (Rhynchonellida, Brachiopoda) from the Viséan of central Sudetes (Poland) and its phylogenetic position. Acta Geologica Polonica 64, 1–12. https://doi.org/DOI: 10.2478/agp-2014-0001

Muszer, J., Górecka-Nowak, A., Kryza, R., August, C., 2016a. New data on biostratigraphy and chronostratigraphy of the Carboniferous sediments in Sudetes (in Poliosh). XXIII Konferencja Naukowa Sekcji Paleontologicznej Polskiego Towarzystwa Geologicznego, Polskie Towarzystwo Geologiczne, Poznań, 21−23 września 2016, pp. 73–74.

Muszer, J., Królewiecka, K., Strzoda, A., 2016b. Redeposition of the Upper Visean in the Namurian sediments of Sudetes examples from Konradów and Jugów (in Polish). XXIII Konferencja Naukowa Sekcji Paleontologicznej Polskiego Towarzystwa Geologicznego, Polskie Towarzystwo Geologiczne, Poznań, 21−23 września 2016, pp. 75–76.

Narkiewicz, M., 2020. Variscan foreland in Poland revisited: new data and new concepts. Geological Quarterly 64, 377–401.

Narkiewicz, M., 2007. Development and inversion of Devonian and Carboniferous basins in the eastern part of the Variscan foreland (Poland). Geological Quarterly 51, 231–256.

Nemec, W., Porębski, S.J., Teisseyre, A.K., 1982. Explanatory notes to the lithotectonic molasse profile of the Intra-Sudetic Basin, Polish part (Sudety Mts., Carboniferous-Permian), in: Tectonic Regime of Molasse Epochs (Ed. by G. Schwab). Veröff. Zentralinst. Erde, Potsdam, pp. 267–278.

Nemec, W., Porębski, Sz.J., Steel, R.J., 1980. Texture and structure of resedimented conglomerates: examples from Książ Formation (Famennian—Tournaisian), southwestern Poland. Sedimentology 27, 519–538.

Novakova, L., 2015. Tectonic phase separation applied to the Sudetic Marginal Fault Zone (NE part of the Czech Republic). Journal of Mountain Science 12, 251–267.

Oberc, J., 1972. Sudety i obszary przyległe, Budowa Geologiczne Polski, vol. 4. Tektonika, Part 2. Wydawnictwa Geologiczne, Warszawa.

O'Brien, P.J., Kröner, A., Jaeckel, P., Hegner, E., Żelaźniewicz, A., Kryza, R., 1997. Petrological and isotopic studies on Palaeozoic high-pressure granulites, Gory Sowie Mts, Polish Sudetes. Journal of Petrology 38, 433–456. https://doi.org/10.1093/petroj/38.4.433

Pešková, I., Hók, J., Štěpančíková, P., Stemberk, J., Vojtko, R., 2010. Results of stress analysis inferred from fault slip data along the Sudetic Marginal Fault (NE part of Bohemian Massif). Acta Geol Slovaca 2, 11–16.

Porębski, S., 1990. Onset of coarse clastic sedimentation in the Variscan realm of the Sudetes (SW Poland): an example from the upper Devonian-lower Carboniferous Swiebodzice succession. Neues Jahrbuch für Geologie und Paläontologie. Abhandlungen 179, 259–274.

Porębski, S., 1981. Świebodzice Succession (Upper Devonian–lowest Carboniferous; Western Sudetes): a prograding, mass flow dominated fan-delta complex (in Polish with English summary). Geologia Sudetica 21, 101–192.

Rosenbaum, G., Lister, G.S., Duboz, C., 2002. Relative motions of Africa, Iberia and Europe during Alpine orogeny. Tectonophysics 359, 117–129. https://doi.org/10.1016/S0040-1951(02)00442-0

Różycka, M., Jancewicz, K., Migoń, P., Szymanowski, M., 2021. Tectonic versus rock-controlled mountain fronts – Geomorphometric and geostatistical approach (Sowie Mts., Central Europe). Geomorphology 373, 107485. https://doi.org/10.1016/j.geomorph.2020.107485

Sobczyk, A., Szczygieł, J., 2021. Paleostress reconstruction of faults recorded in the Niedźwiedzia Cave (Sudetes): insights into Alpine intraplate tectonic of NE Bohemian Massif. International Journal of Earth Sciences 110, 833–847. https://doi.org/10.1007/s00531-021-01994-1

Solecki, A.T., 2011. Structural development of the epi-Variscan cover in the North Sudetic Synclinorium area (in Polish with English abstract). In: Mezozoik i Kenozoik Dolnego Śląska LXXXI Zjazdu Polskiego Towarzystwo Geologicznego. pp. 19–36.

Solecki, A.T., 1994. Tectonics of the North Sudetic Synclinorium. Acta Universitatis Wratislaviensis 45, 1–59.

Tabaud, A.S., Štípská, P., Mazur, S., Schulmann, K., Míková, J., Wong, J., Sun, M., 2021. Evolution of a Cambro-Ordovician active margin in northern Gondwana: Geochemical and zircon geochronological evidence from the Góry Sowie metasedimentary rocks, Poland. Gondwana Research 90, 1–26. https://doi.org/10.1016/j.gr.2020.10.011

Teisseyre, A.K., 1975. Sedimentology and palaeogeography of the Kulm alluvial fans in the western Intrasudetic Basin (Central

Sudetes, SW Poland) (in Polish with English summary). Geologia Sudetica IX, 7–89.

Teisseyre, H., 1956. Świebodzice Depression as a geological unit (in Polish with English summary). Biuletyn Instytutu Geologicznego, Z badań geologicznych na Dolnym Śląsku 106, 5–60.

Van Breemen, O., Bowes, D., Aftalion, M., Żelaźniewicz, A., 1988. Devonian tectonothermal activity in the Sowie Góry gneissic block, Sudetes, southwestern Poland: evidence from Rb-Sr and U-Pb isotopic studies. Annales Societatis Geologorum Poloniae 58, 3–19.

Voigt, T., Kley, J., Voigt, S., 2021. Dawn and dusk of Late Cretaceous basin inversion in central Europe. Solid Earth 12, 1443–1471. https://doi.org/10.5194/se-12-1443-2021

Wajsprych, B., 1978. Allochthonous paleozoic rocks in the Visean of the Bardzkie Mts. (Sudetes) (in Polish with English summary). Annales Societatis Geologorum Poloniae 48, 99–127.

Żakowa, H., 1966a. Stratigraphic and facial problems of the Lower Carboniferous of the Sudeten on the background of the actual state of research on the development of this formation in Poland ((in Polish with English summary). In: Z Geologii Ziem Zachodnich, Sesja Naukowa Dwudziestolecia Polskich Badań 1945-1965. Wrocław, pp. 185–216.

Żakowa, H., 1966b. Zone *Goniatites crenistria* Phill. in the vicinity of Sokolec and Jugów, at the foot of the Sowie Góry Mountains (Central Sudetes) (in Polish with English summary). Prace Inst. Geol., 43, 1–197.

Żakowa, H., 1960. Horizon *Goniatites crenistria* from Glinno (Sowie Góry, Sudeten Mts.) (in Polish with English summary). Kwartalnik Geologiczny 4, 349–366.

Żakowa, H., Żak, C., 1962. Lower Carboniferous at Kamionki (Sowie Mts. - Lower Silesia) (in Polish with English summary). Biuletyn Instytutu Geologicznego, Z badań geologicznych na Dolnym Śląsku 173, 169–277.

Żelaźniewicz, A., 1990. Deformation and metamorphism in the Góry Sowie gneiss complex, Sudetes, SW Poland. Neues Jahrbuch für Geologie und Paläontologie 179, 129–157.

Żelaźniewicz, A., 1987. Tectonic and metamorphic evolution of the Sowie Góry, Sudtetes Mts., SW Poland (in Polish with English summary). Annales Societatis Geologorum Poloniae 57, 203–348. https://doi.org/PL ISSN 0208-9068

Stop 1 – Walim

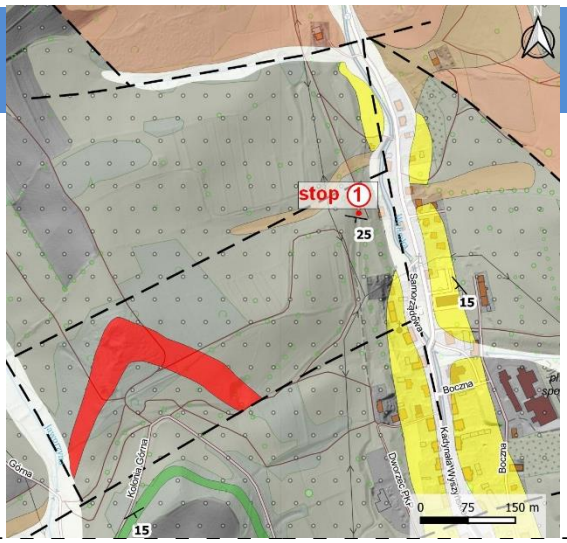

Abandoned railway cut

GPS coordinates: 50° 42' 19.07" N, 16° 26' 10.97" E

Stratigraphy: Walim Formation, lower part (middle – early late Viséan?)
Described problems: Walim Graben: structural geometry and characteristics, syn-tectonic deposition, alluvial fan conglomerate

An abandoned railway cut located in the northeasternmost part of the Walim Graben exposes gneissic conglomerate of the Walim Formation (the lowermost member of the GSM Carboniferous succession; cf. Fig. 2). The continuous part of the outcrop is c. 60 m long and up to 2.5 high and consists of extremely poorly sorted conglomerate dipping 15-25° SSW. The grain framework is typically clast-supported, less often matrix-supported, with clasts ranging in size from pebbles to boulders and matrix composed of medium- to coarse grained lithic sandstone (Fig. 11A). Both grain size distribution and roundness of clasts is bimodal. In general, smaller clasts are angular to subangular, while the largest ones ranging from moderate to well rounded. The largest, well-rounded migmatic gneissic clast observed in an outcrop attains 2.2 m in diameter (Fig.11A). Results of petrographic analyses by Łapot (1986), show that the conglomerate is monomictic and its clasts are dominated by petrographic varieties of gneisses – migmatic and fibrous gneisses, biotite-oligoclase paragneisses, orthogneisses and other metamorphic rocks as well as massive quartz.

Seemingly, the rock does not show evidence of internal organisation and its clast fabric appears to be chaotic (Fig. 11A). The bedding within conglomerates is poorly visible, and is either planar or slightly undulatory. In the basal parts of beds, elongated clasts are locally imbricated (a (p) a (i) fabric). In the upper parts of beds, clasts reveal weak a-axis pseudoimbrication which is parallel to the bedding planes. Indistinct inverse grading is also visible. Measurements of large population of clast long axes (a-axes; n=394) show their preferred orientation (Fig. 11A). Given the average (inferred) orientation of pebbles parallel to the palaeotransport direction, as well as their imbrication, the interpreted inclination of palaeoslope is from NNW to SSE (Mo=342.8°).

The conglomerates of the Walim Formation are interpreted to have formed as deposits of clast-rich, cohesionless subaerial debris flows which occurred in proximal zones of alluvial fans (Fig. 11B). The fans developed along tectonically active, high-relief, WNW-ESE-

oriented(?) fault margins of a wider basin. Petrographic composition of clasts suggests that the Góry Sowie Massif was the source area of the clastic material. Gabbroic pebbles, present in conglomerates of the Walim Graben c. 500 m of the SW from the described outcrop, were probably derived from an area of the present-day Intra-Sudetic Basin, situated W and SW of the Intra-Sudetic Fault (Głuszyca Fault; cf. Fig. 1). Gabbros were drilled there at the base of the Upper Carboniferous deposits (Ihnatowicz, 2001). This suggests a significant episode of palaeogeographic inversion of the Intra-Sudetic area during the late Carboniferous.

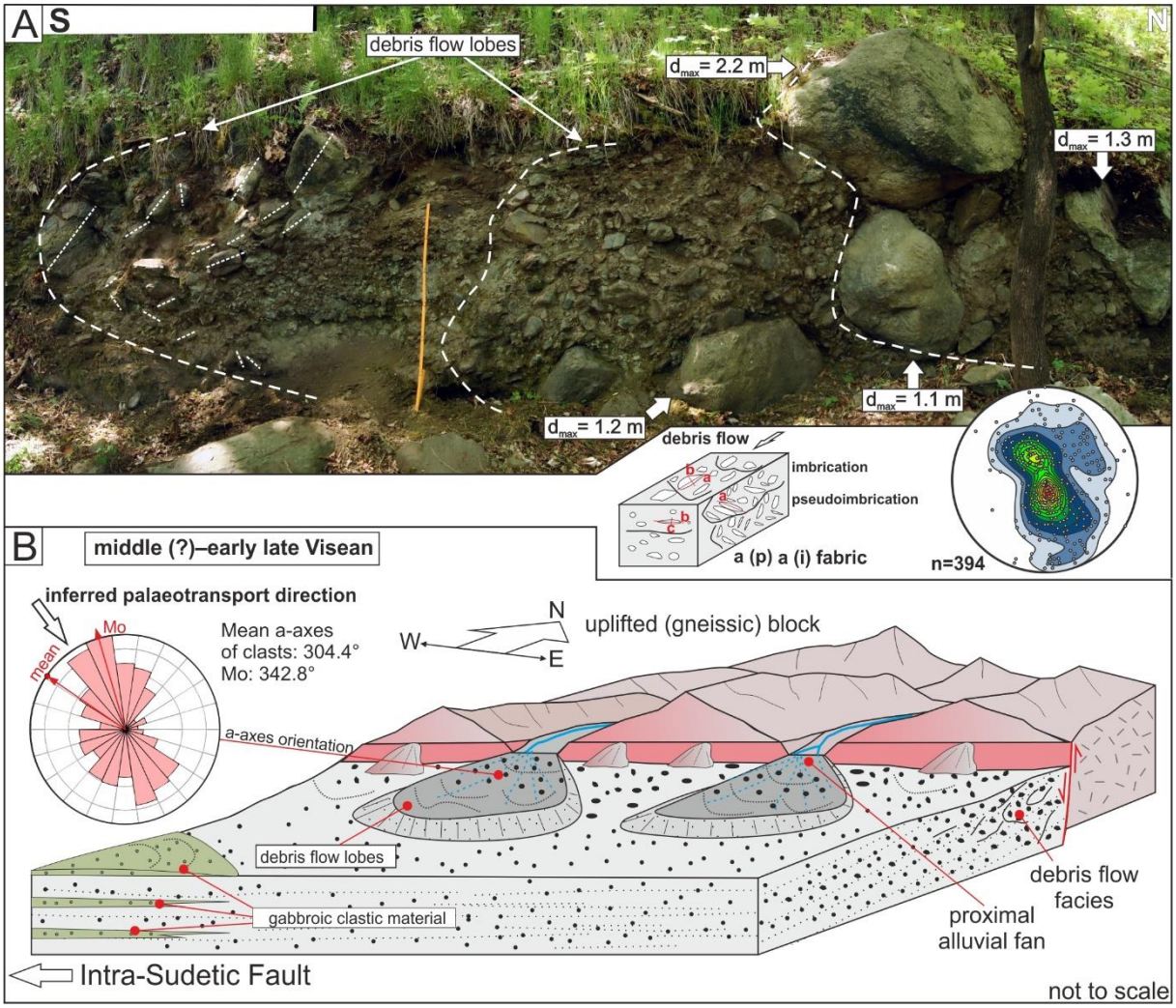

Fig. 11. A. Outcrop of gneissic conglomerates of the Walim Formation in Walim (stop 1). White dashed lines indicate interpreted fronts of debris flow lobes on proximal alluvial fan. Inset blockdiagram shows an idealized alignement of pebbles a-axes during clast-rich, cohesionless subaerial debris flow (inspired and modified after Harms et al., 1975). B – Palaeogeographic reconstruction of the present-day Walim Graben area in the early Carboniferous (middle(?) – early late Viséan). Inset rose diagram shows orientation of long a-axes of pebbles measured in outcrop and interpreted palaeotransport direction.

Stop 2 – Glinno

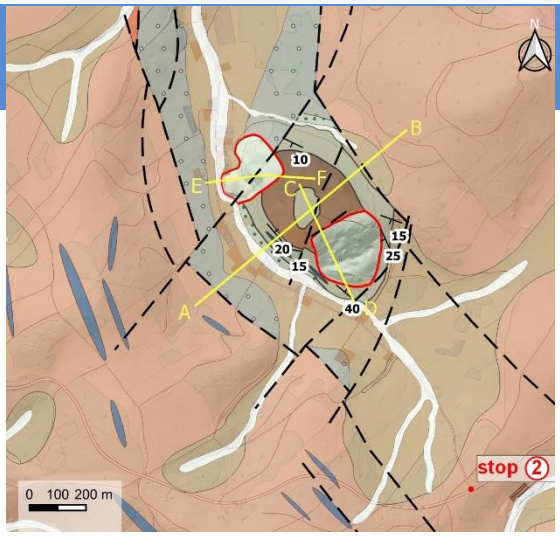

Viewpoint
GPS coordinates: 50° 41' 49.26" N, 16° 29' 27.95" E

Stratigraphy: marine sandstones and mudstones of the Sokolec Formation (Upper Viséan (?)) intruded by upper Carboniferous kersantite

Described problems: Glinno Graben: structural geometry and characteristics, structurally controlled landslides developed on slopes built of sedimentary and igneous rocks

Stop 2 is located at the southern edge of the Glinno Graben (Fig. 12). To the north of the viewpoint, situated on the gneissic bedrock of the Góry Sowie Massif, gneissic conglomerates and sandstones of the Walim Formation are overlain by sandstones and mudstones with limestone intercalations (Żakowa, 1960) of the Sokolec Formation. These strata define an erosional outlier – Ostrzew hill – which is well visible from the viewpoint. In the uppermost part of the flat-topped hill, the Carboniferous sedimentary rocks are intruded by upper Carboniferous (?) kersantite forming a sill-like intrusion (Awdankiewicz, 2007; Grocholski, 1965; Łapot, 1986; Fig. 13; 14A). The hill is capped by sandstones which are the youngest preserved Carboniferous deposit in the Glinno Graben.

Two rotational, bedrock-controlled landslides have been recognized by the present author on the north-western and south-eastern slopes of Ostrzew hill (landslide 1 and landslide 2, respectively in Figs 12, 13). The landslides are hardly accessible and will be not presented during the field trip. The landslides affected densely forested, steep slopes (inclined by 25–33°) over an area of 3.3 and 4.4 ha. Mass movements developed within kersantites and underlying sedimentary rocks of the Sokolec Formation. In the nearly flat-lying kersantite and in the sandstones, two main join sets (J_1 and J_2) were determined (Fig. 14B–D). Structural measurements show that the landslide slip surfaces and detachment developed partly along the joint planes (Kowalski, 2018). The mass movements resulted in transfoming once homogeneous rock into separate blocks, predominantly along nearly vertical joints of J_2 set. A similar displacement mechanism operated in the north-western part of the massif, where orientation of steep J_2 joints in kersantite coincides with the orientation of the main landslide scarp. Lithological and geomechanical contrast between the resistant, rigid kersantites and underlying, strongly fractured sandstones and mudstones was also an important factor that controlled the slope instability and further landslide motion.

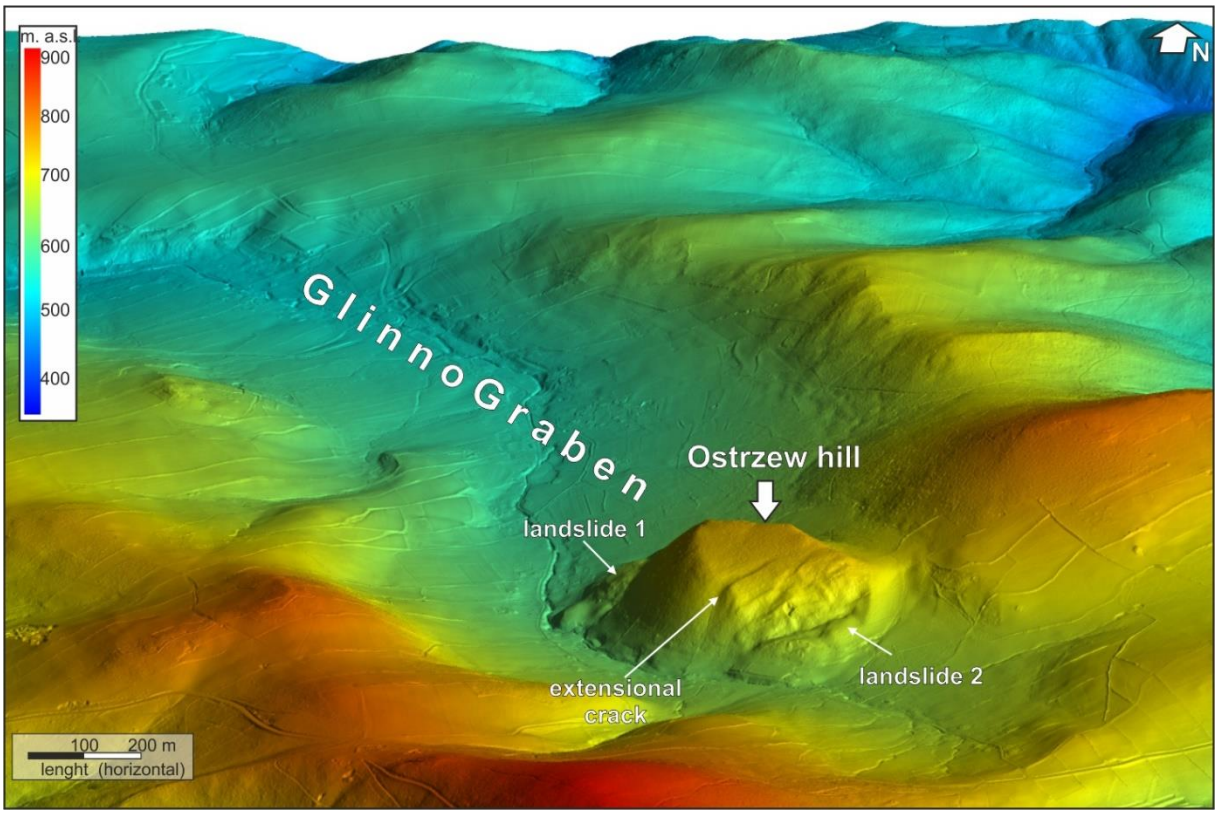

Fig. 12. LiDAR-based three-dimensional model of the southern part of the Glinno Graben. The two landslides described in the text are indicated by arrows. 1.5 x vertical exaggeration.

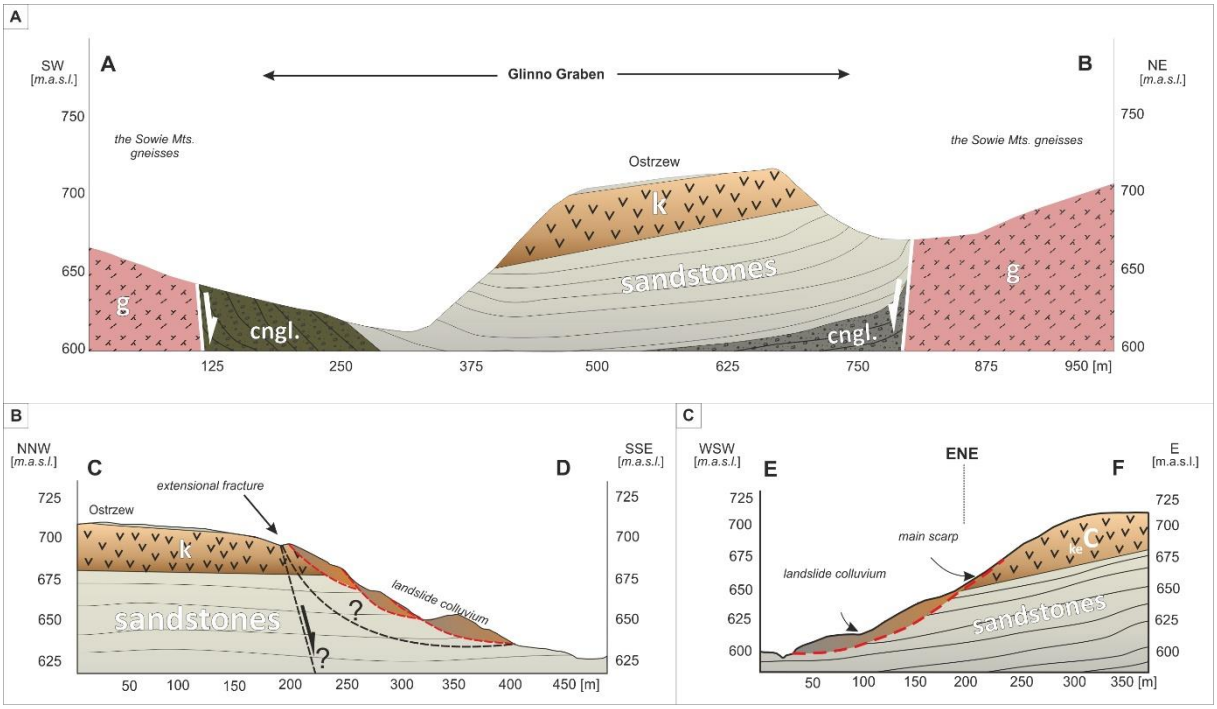

Fig. 13. Geological cross-sections through the Glinno Graben (A) and of the landslides on Ostrzew hill (B). Geological cross sections after Grocholski, 1962, supplemented and modified by the author (Kowalski, 2018). The geology as in Fig. 4.

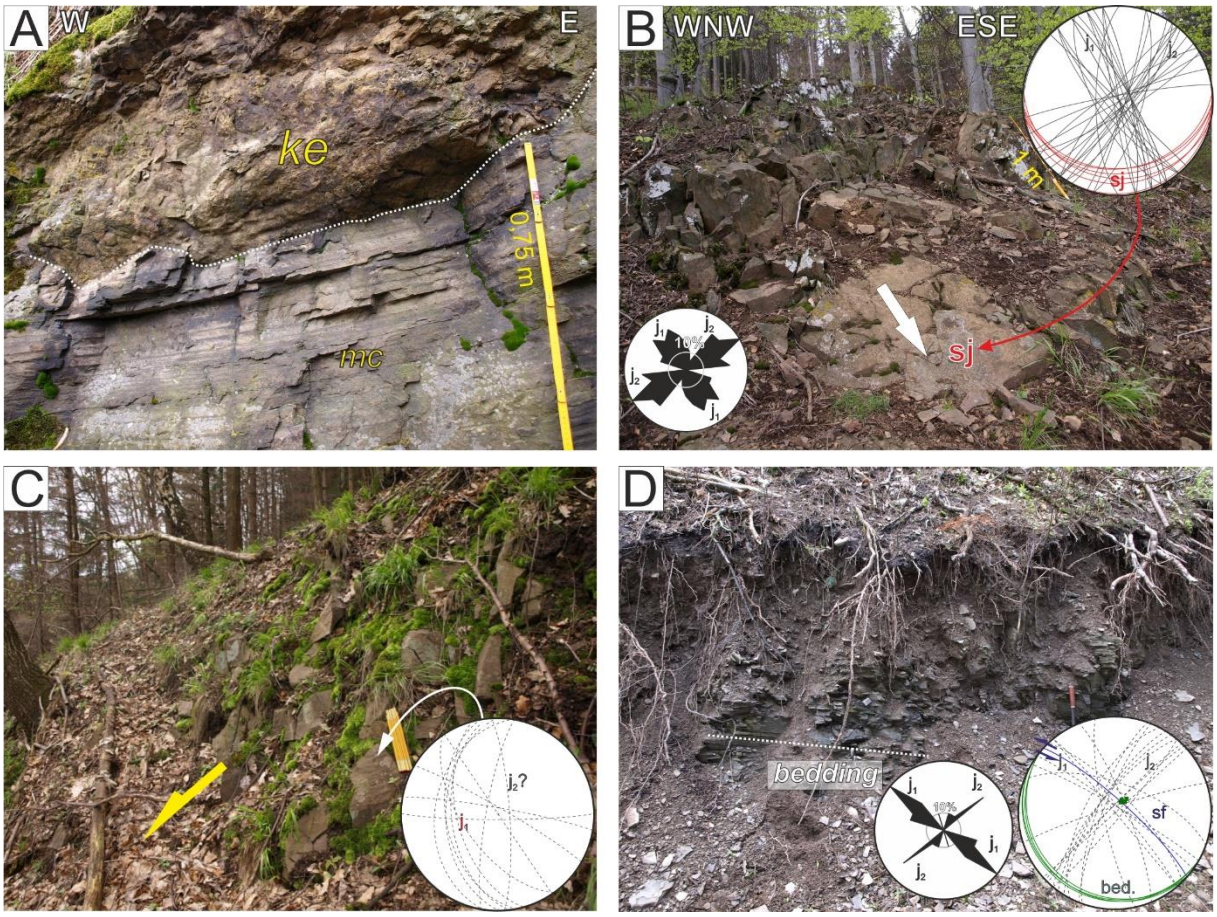

Fig. 14. Landslides on Ostrzew hill. A – sharp contact between kersantite (top) and sandstone of the Sokolec Formation (bottom) within landslide block in the quarry below the summit of Ostrzew hill (south-eastern landslide). B – head scarp of the south-eastern landslide. Stereogram showing two sets of joints: NW-SE/NNW/SSE (j_1) and NE-SW/ENE-WSW (j_2) and set of sheeting joints (sj). Arrow indicates the direction of mass movements on the main scarp of the landslide. C – secondary scarp that cutting the displaced kersantite block within the landslide colluvium of the north-western landslide. Arrow indicates the direction of mass movements on the main scarp of the landslide. D – outcrops of sandstones and mudstones exposed in the lower, western slope of Ostrzew Mt. (*in situ*). Great circle and pole point diagrams showing two sets of joints (j_1, j_2) and bedding planes (bed., green). J_2 set of joints is reactivated by strike-slip faults (sf).

Stop 3 – Kamionki

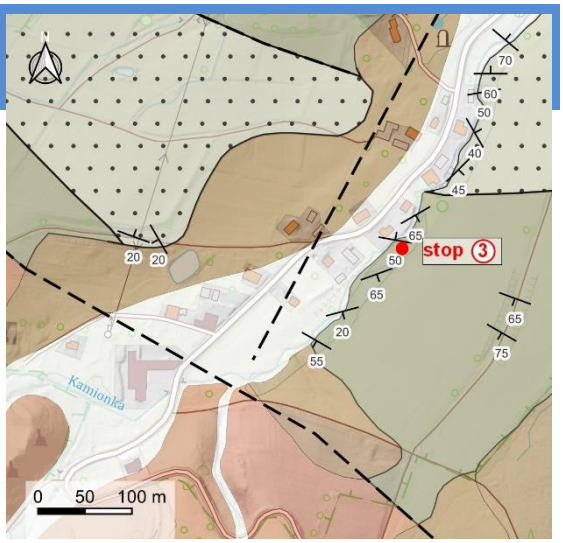

Kamionka stream valley

GPS coordinates: 50° 40' 12.10" N, 16° 32' 27.78" E

Stratigraphy: marine sandstones and mudstones of the Sokolec Formation (Upper Viséan (?))

Described problems: Kamionki Graben: structural geometry and characteristics, late-Variscan folding of the lower Carboniferous strata

In the southernmost part of the Kamionki Graben, in exposures of the Sokolec Formation located along the Kamionka stream valley, minor folds are relatively common. On the valley's eastern slopes these folds display very gentle, open geometry with interlimb angles of 70–110°; Fig. 15A). Towards the north there occur horizontal upright folds, commonly of chevron geometry with angular and sharp hinges, commonly displaying chevron-like profiles (Fig. 15B). They exhibit nearly vertical axial planes and horizontal hinge lines with wavelengths of 1 to 3 m. The asymmetric to moderately-inclined, N-vergent folds with southern limbs dipping gently (up to 15°) to the S, and northern limbs inclined nearly 80° to the S, are also present (Fig. 15C).

The fold axes in the Kamionki Graben trend predominantly W-E to WSW-ENE, suggesting the N-S to NNE-SSW direction of tectonic shortening (Fig. 15D). The hinge zones of the anticlines occasionally contain nearly vertical, planar axial cleavage. Within the northern limbs of asymmetric folds, reverse minor faults dipping up to about 60° toward the NE have been developed. Some reverse faults were also observed (Fig. 15D).

The described fold structures developed most probably during Namurian(?) epoch at the waning stages of the Variscan orogeny. A transpression related to strike-slip (dextral?) displacements may have played an active role in the folding process (Kowalski and Pacanowski, 2024). No mesoscopic folds have been observed in sandstones exposed in the opposite, north-western part of the graben. In this part of the graben a series of NW-SE-trending map-scale folds occur. These folds are attributed here to the Late Cretaceous – early Palaeogene trans-regional tectonic shortening event, which had likely led to reactivation of the main boundary faults of the graben as well as to large-scale, gentle folding of the Carboniferous strata, visible only in map-view (cf. Fig. 8).

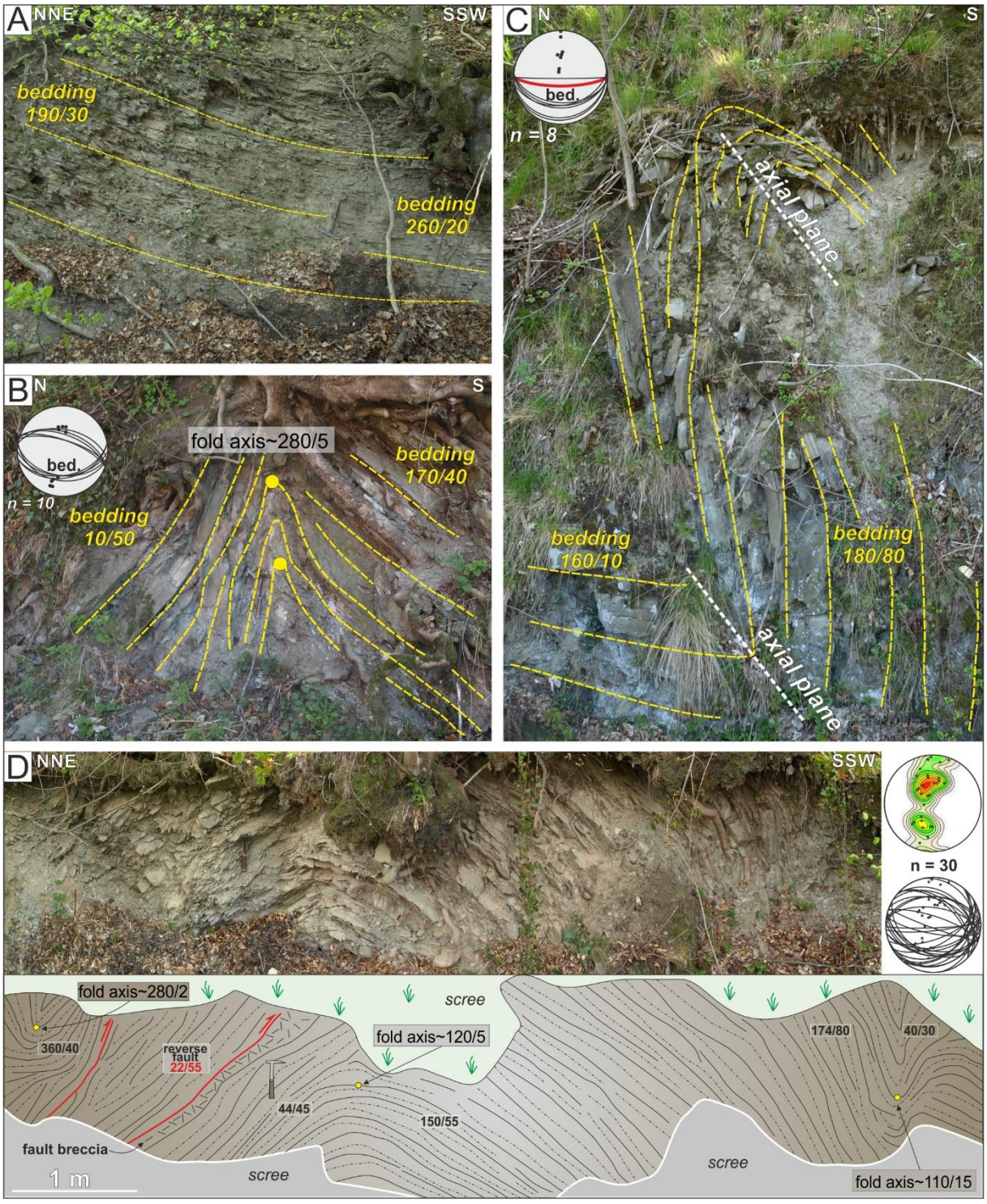

Fig. 15. Mesoscale folds in Carboniferous sandstones exposed in the southernmost part of the Kamionki Graben (see Figure 2 for locations). The bedding attitudes (shown as yellow dashed lines) are described with dip direction/dip angle. Inset stereoplots are showing bedding orientation (bed). A – northern limb of a gentle syncline. B – upright, tight, nearly symmetric anticline with chevron profile, vertical axial plane and horizontal hinge line (stop 4). C – inclined, asymmetric folds affecting sandstone beds with axial plane dipping nearly 60° to the S (red great circle) (stop 4). D – open to tight, E-W to WNW-ESE-trending folds, cut by two minor reverse faults in the NNE part of the stream valley profile.

Stop 4 – Kamionki

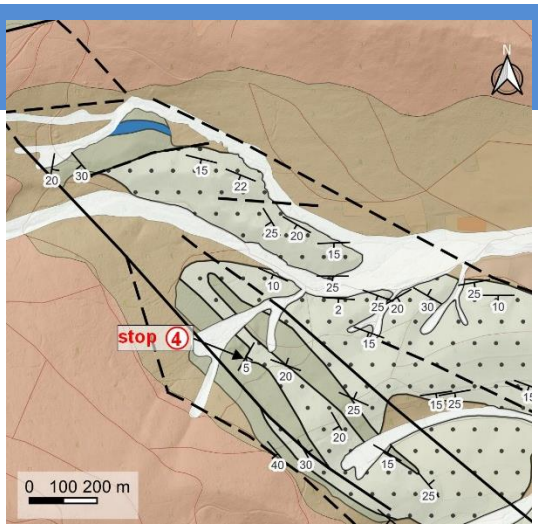

Abandoned quarry

GPS coordinates: 50° 40' 49.51" N, 16° 31' 24.83" E

Stratigraphy: marine sandstones and mudstones of the Sokolec Formation (upper Viséan (?)), conglomerates of the Kamionki Formation (upper Visean – Namurian (?))

Described problems: Kamionki Graben: structural geometry and characteristics, sedimentology of the Carboniferous marine deposits (upper Viséan–Namurian (?))

An abandoned quarry in the northwestern part of the Kamionki Graben, close to the Western Kamionki Fault (main boundary fault of the Kamionki Graben; cf. Fig. 7), exposes the uppermost part of the marine Sokolec Formation and the sedimentary contact with the overlying polymictic conglomerates of the Kamionki Formation (Żakowa and Żak, 1962). The most representative outcrop is situated in the south-eastern wall of the quarry and reveals c. 10 m thick sedimentary succession (Fig. 16A). The marine sandstones dip ca. 5–10° towards the ESE (Fig. 16A). The lower part of the succession consists of medium- to coarse-grained, poorly-sorted lithic sandstones with mm-thick mudstone intercalations. The sandstones are well-bedded and reveal distinct platy parting. Bed thickness ranges from 0.05 to 0.4 m. The lower surfaces of beds are predominantly sharp, with undulatory or flat boundaries displaying abundant erosional structures (both scour and tool marks). They include flutes (Fig. 16B), groove casts (generated probably as a result of dragging of a plant stalks or stems), prod- and bounce marks. Small-scale, S- to SW-vergent slump folds (Fig. 16C), load casts and flame structures are also present in the bottom parts of beds. The sandstones are predominantly structureless (Bouma T_a), normally and inversely-graded or horizontally-laminated (Bouma T_b). Greenish mudstone intraclasts and plant detritus occur sporadically in the lower parts of beds. The upper parts of beds consist predominantly of ripple-cross laminated sandstones (Bouma T_c). They pass upward into structureless mudstones (Bouma T_e), at tops of the composite beds.

Conglomerates constituting the uppermost part of the quarry are typically clast-supported and contain mainly quartz, gneiss, quartzite, lydite, granite, phyllite and greenstone clasts (Łapot, 1986). The lower contact of the conglomerate exposed in the quarry shows soft-sediment deformation structures, including folded slabs of underlying sandstone and deformed clasts of sandstone incorporated into the conglomerate (Fig. 16D).

The sedimentary succession described here is interpreted as deposit of high-density turbidity currents (sandy lithofacies) and subaqueous sediment gravity flows (gravelly lithofacies). Deposition occurred on slopes of fan-

deltas which entered the late Viséan marine basin (embayment? cf. Mastalerz, 1995) from the N and NW.

The sandstones exposed in the quarry contain three conjugate sets of joints designated here as the J_1 to J_3, respectively. Apart from the sets J_1 and J_2 described earlier from the Glinno Graben (Kowalski, 2018), there occur well-defined joints assigned here to set J_3, striking subparallel (N-S) to the graben boundaries (Fig. 16E). In the north-westernmost part of the Kamionki Graben, joints of set J_3 show little evidence of shearing in a dextral strike-slip regime (Fig. 16F).

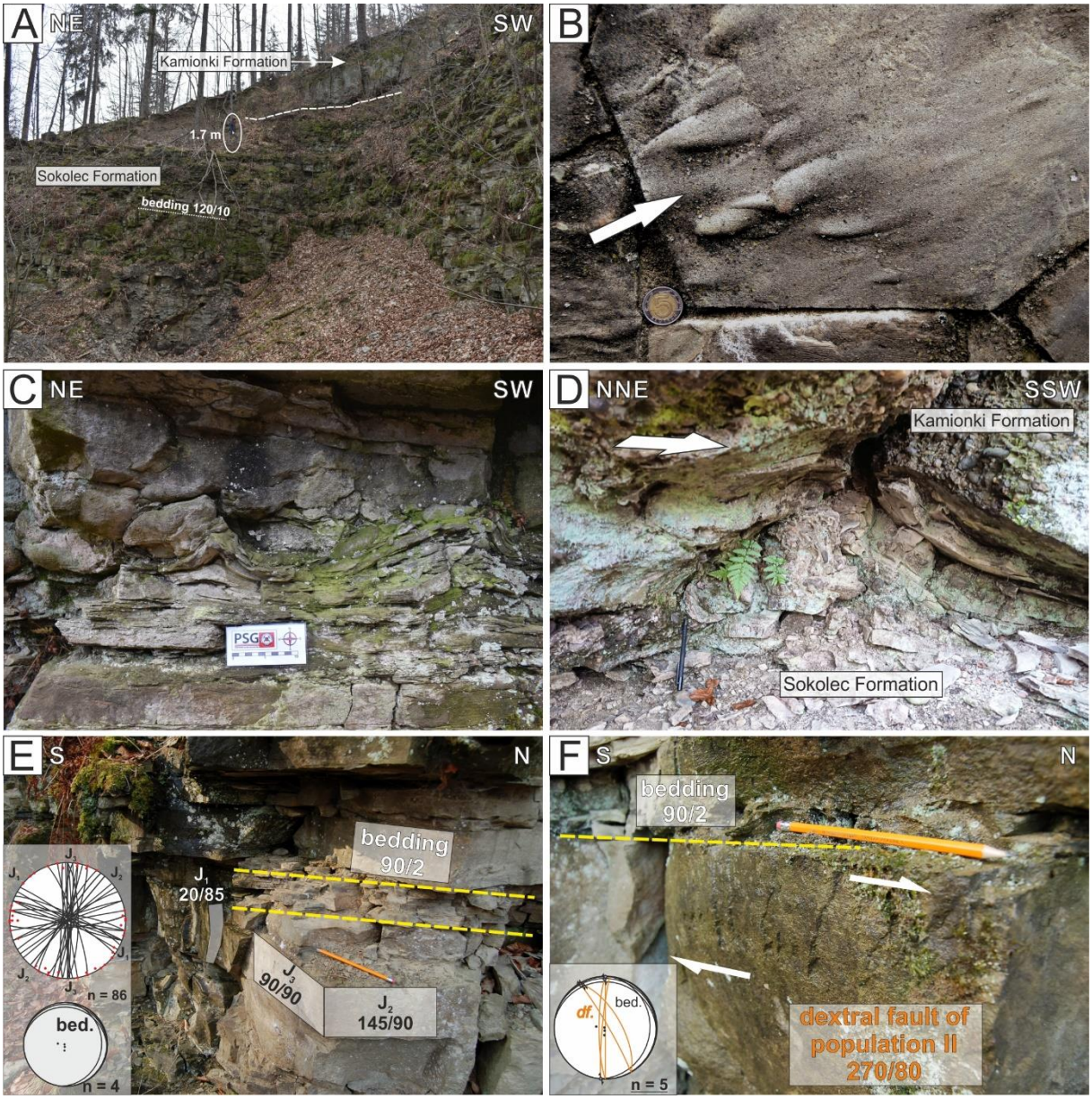

Fig. 16. Main sedimentary and structural features of the Sokolec and Kamionki formations exposed in abandoned quarry (stop 4). A – the south-eastern wall of the quarry with exposure of the uppermost Sokolec Formation and the lowermost Kamionki Formation. B – flute marks on the base of a sandstone bed (slab). The interpreted palaeocurrent direction is marked by arrow. C – small-scale, S- to SW-vergent slump folds within marine sandstone exposed in the quarry. D – folded slab of sandstone of the Sokolec Formation at the base of polymictic conglomerate of the Kamionki Formation. The interpreted palaeocurrent direction is marked by arrow E – three sets of planar, vertical to subvertical bed-confined fractures cutting nearly horizontal sandstones exposed in an abandoned quarry on the footwall of the Western Kamionki Fault. F – Surface of J_3 joint in sandstone, showing evidence of shearing in dextral strike-slip regime (fault population I).

Acknowledgements

The results of cartographic works presented during the field trip was partially funded by the Ministry of the Climate and Environment of Poland from the sources of the National Fund for Environment Protection and Water Management (projects no 22.0201.1901.01.1: "*Prace kartograficzne na 3 arkuszach Szczegółowej Mapy Geologicznej Sudetów 1:25 000: Zagórze Śląskie, Pieszyce, Ostroszowice – etap I*" and 22.1509.2001.00.1: „*Wykonanie sześciu arkuszy Szczegółowej Mapy Geologicznej Sudetów w skali 1:25 000: Walim, Jugów, Ludwikowice Kłodzkie, Nowa Ruda, Szalejów Górny, Jeleniów i Pasterska Górka*"). The author would like to thank Paweł Aleksandrowski, Jacek Szczepański and Marcin Dąbrowski for their critical reading, great help in improving the text and many inspiring suggestions. I also thank Krzysztof Mastalerz for insightful discussions. Joanna Brytan is thanked for providing GIS layer including the Quaternary sediments on Fig. 4.

References

Awdankiewicz, M., 2007. Late Palaeozoic lamprophyres and associated mafic subvolcanic rocks of the Sudetes (SW Poland): petrology, geochemistry and petrogenesis. Geologia Sudetica 39, 11–97.

Grocholski, W., 1965. Objaśnienia do Szczegółowej Mapy Geologicznej Sudetów. Arkusz Walim 1:25 000 (in Polish). Wydawnictwa Geologiczne Warszawa.

Ihnatowicz, A., 2001. Profile głębokich otworów wiertniczych Państwowego Instytutu Geologicznego, Zeszyt 98, Miłków IG-1 (in Polish). Państwowy Instytut Geologiczny, Warszawa.

Kowalski, A., 2018. Osuwiska jako przyczyna błędnych interpretacji budowy geologicznej–przykłady z Sudetów. Biuletyn Państwowego Instytutu Geologicznego 473, 27–48. https://doi.org/10.5604/01.3001.0012.7708

Kowalski, A., Pacanowski, G., 2024. Record of superimposed late- and post-Variscan regional-scale tectonic events at the NE margin of the Bohemian Massif: structural evolution of the Kamionki Graben (SW Poland, Sudetes). In: 20th CETEG Meeting, Srebrna Góra, 24-27.04.2024.

Łapot, W., 1986. Petrography of Carboniferous rocks from the Sowie Mts (Sudetes) (in Polish with English summary). Geologia Sudetica 21, 1–144.

Mastalerz, K., 1995. Deposits of high-density turbidity currents on fan-delta slopes: an example from the upper Visean Szczawno formation, Intrasudetic Basin, Poland. Sedimentary Geology 98, 121–146. https://doi.org/10.1016/0037-0738(95)00030-C

Żakowa, H., 1960. Horizon *Goniatites crenistria* from Glinno (Sowie Góry, Sudeten Mts.) (in Polish with English summary). Kwartalnik Geologiczny 4, 349–366.

Żakowa, H., Żak, C., 1962. Lower Carboniferous at Kamionki (Sowie Mts. - Lower Silesia) (in Polish with English summary). Biuletyn Instytutu Geologicznego, Z badań geologicznych na Dolnym Śląsku 173, 169–277

CONTENTS

Central European Tectonic Studies Groups meetings

20 editions of CETEG 2003–2024

20th	24–27 Apr 2024	Srebrna Góra (Poland)
19th	12–15 Apr 2023	Kazincbarcika (Hungary)
18th	22–25 Sep 2022	Terchová (Slovakia)
17th	24–27 Apr 2019	Rozdrojovice (Czech Republic)
16th	18–21 Apr 2018	Rytro (Poland)
15th	5–8 Apr 2017	Zánka (Hungary)
14th	28 Apr–1 May 2016	Predná Hora (Slovakia)
13th	22–25 Apr 2015	Kadaň (Czech Republic)
12th	23–26 Apr 2014	Lądek-Zdrój (Poland)
11th	24–27 Apr 2013	Várgesztes (Hungary)
10th	2–5 May 2012	Medvedia Hora (Slovakia)
9th	13–17 Apr 2011	Lísek (Czech Republic)
8th	22–25 Apr 2010	Mąchocice Kapitulne (Poland)
7th	13–16 May 2009	Pécs (Hungary)
6th	23–16 Apr 2008	Upohlav (Slovakia)
5th	11–14 Apr 2007	Teplá (Czech Republic)
4th	19–22 Apr 2006	Zakopane (Poland)
3rd	14–17 Apr 2005	Felsötárkány (Hungary)
2nd	22–25 Apr 2004	Lučenec (Slovakia)
1st	24–27 Apr 2003	Hrubá Skála (Czech Republic)

20th Jubilee Meeting of the Central European Tectonic Studies Groups

Book of Abstracts and Field-Trips Guide

Editors: Rafał Sikora, Marcin Olkowicz & Marta Adamuszek

Graphic design: Marta Adamuszek &Rafał Sikora

Cover photo: View of the Bardzkie Mountains (Bardo Basin; Sudetes) and the Paczków Graben (Fore-Sudetic Block) on the south east of Srebrna Góra (Sowie Mountains). Author: Rafał Sikora

Year of the publication: 2024

First edition: 189 pages

ISBN: 978-83-68112-55-9 (online PDF version)

XX CETEG

SREBRNA GÓRA 2024

Polish Geological Society
ISBN: 978-83-68112-55-9